1989

Free radical reactions of organomercurials

De-Liang Guo
Iowa State University

Order Number 9014901

Free radical reactions of organomercurials

Guo, De-Liang, Ph.D.

Iowa State University, 1989

U·M·I
300 N. Zeeb Rd.
Ann Arbor, MI 48106

Free radical reactions of organomercurials

by

De-Liang Guo

A Dissertation Submitted to the

Graduate Faculty in Partial Fulfillment of the

Requirements for the Degree of

DOCTOR OF PHILOSOPHY

Department: Chemistry
Major: Organic Chemistry

Approved:

Signature was redacted for privacy.

In Charge of Major Work

Signature was redacted for privacy.

For the Major Department

Signature was redacted for privacy.

For the Graduate College

Members of the Committee:

Signature was redacted for privacy.

Iowa State University
Ames, Iowa
1989

TABLE OF CONTENTS

LIST OF TABLES

LIST OF FIGURES

GENERAL INTRODUCTION

This dissertation has been divided into three parts. Part I presents data on the chemically induced dynamic nuclear polarization (CIDNP) proton NMR signals during oxidation of organomercurials. Part II presents data on the alkylation of heteroaromatic compounds in photostimulated free radical chain reactions utilizing alkylmercurials. Part III presents data on free radical oxidation-reduction reactions of RHgX with organic compounds.

PART I.

CHEMICALLY INDUCED DYNAMIC NUCLEAR POLARIZATION (CIDNP) OBSERVED DURING OXIDATION OF ORGANOMERCURIALS

CHAPTER 1. INTRODUCTION

In 1967, Bargon, Fischer and Johnsen [1] and independently Ward and Lawler [2] reported a similar phenomena for NMR spectra taken during radical reactions: emission or enhanced absorption or both.

The accidental discovery of nuclear polarization by Ward and Lawler [2] in the reaction of *n*-butyllithium with *n*-butyl bromide provided the first example of the demonstration of radical character by CIDNP in a reaction that had often been considered to be ionic.

CIDNP studies in the reaction of organometallic compounds have been largely limited to those involving group I and II metals (Li,Na,Mg). Reactions of alkyllithiums with alkyl halides reactions of Grignard reagents with alkyl halides, [3] or nitrobenzene [4], and reactions of alkyl iodides with sodium mirrors [5] and of alkyl halides with sodium naphthalene have been reported [6].

CIDNP has been observed in the related oxidation of alkyllithium reagents and Grignard reagents with peroxide [7].

The observation of CIDNP in the thermal decomposition di-*tert*-butyl derivatives of magnesium, zinc and mercury confirmed that these decompositions occur via homolysis [8]. Lehr and Lawler recently reported quantitative CIDNP evidence for the S_H2 reaction of alkyl radicals with a Grignard reagent [9].

Furthermore, CDINP studies have been carried out in the reactions of heavier organometallic compounds, such as the alkylleads. Pair substitution CIDNP effects have been utilized to study S_H2 reactions of benzoyloxyl radicals at the metal centers of group IV (Pb and Sn) and transition-metal alkyls ($MeAuPPh_3$) [10].

CIDNP studies of a few reactions of organic mercury compounds have been reported. Mitchell observed polarization from *tert*-butyl radical pairs (F-pairs) in the decomposition of *tert*-butyl(trialkylstannyl)mercury [11], and Beletskaya et al. found enhanced NMR lines during the reaction of triphenylmethyl bromide with dibenzylmercury or benzylmercuric bromide [12]. CIDNP arising from the thermolysis and photolysis of di-*tert*-butylmercury [8] and from the photolysis of di-*n*-propylmercury, diisopropylmercury, dibenzylmercury in chloroform have been reported by Kanter [13].

Polarizations have been observed in the NMR spectra during reaction of $Pt(PEt_3)_3$ or $Pd(PEt_3)_4$ and isopropyl iodide and in the NMR spectra of the α-chloro organoplatinum (II) complexes formed in the reaction of organoplatinums and chloroform [14].

In 1987, I observed ^1H NMR emission spectra in the reaction of $(CH_3)_3CHgX$ with 2-cyclopentenone in the presence of NaI and $(NH_4)_2S_2O_8$. Furthermore, the CIDNP phenomena appeared in the reactions of RHgX, ArHgCl, R_2Hg, Ar_2Hg, RCOOH and RCHO with the strongly oxidizing $S_2O_8^{2-}$, $AgNO_3/S_2O_8^{2-}$, $NaI/S_2O_8^{2-}$ and $Hg(NO_3)_2$.

The interpretation of the CIDNP signals observed has proved to be useful in several regards:

1. As a probe of S_H2 mechanism in the reaction of RHgX or R_2Hg with radicals.

2. As a probe of ET mechanism in the reaction of RHgX or R_2Hg with oxidizing reagents.

3. As a probe of the mechanism of radical production for organomercuricals.

CHAPTER 2. THEORETICAL CALCULATION OF THE CIDNP EFFECT BY THE CKO METHOD (CLOSS, KAPTEIN, OoSTERHOFF) [15][16]

The Radical-pair Model

Concept of the radical pair

The CIDNP effect is observed in the products of the reactions between two radicals, in which the distance between the two parts where the unpaired electrons are located is greater than in a covalant bond but not so much greater as to remove all interactions, from a radical pair.

$$\overline{(CH_3)_3C\bullet\ \bullet C(CH_3)_3}$$

$$\overline{(CH_3)_3C\bullet\ \bullet SO_4^-}$$

The generation of the disappearance of the radical pair

From a common precursor Thermal dissociations usually give a radical pair in the singlet(S) state, while photochemical dissociations give singlet or triplet(T) states (depending on the rates of dissociation and of the singlet to triplet intersystem crossing of the photoexcited state).

From free radicals A radical pair may be formed by the diffusive encounter of two free radicals each in a non-polarized state. A radical pair formed in this way is called the F state. Recombination products or disproportionation products are obtained from reactions occurring when the radical pair is in an S state. These products will be called cage products or C products. If the electronic state of the radical pair cannot lead to reaction, the two radicals diffuse apart to give two free radicals, but now these radicals may be polarized. These free radicals may encounter another radical and form a new radical pair which can lead to products showing the CIDNP effect. These products will be called escape products or e products. Alternately, the $R_1\bullet$ and $R_2\bullet$ which have escaped with polarization may react with another reagent to form a product which yield a polarized NMR spectrum.

First-order Spectra (CIDNP Intensities)

Kaptein gave a first order expression of CIDNP intensities [17].

$$I_{mn} \sim \frac{1}{2}A_i[\Delta g\beta_e H_0 + \sum_{j\neq i} A_j M_j - \sum_k A_k M_k + A_i(M_i - \frac{1}{2})] \qquad (2.1)$$

I_{mn}: the intensity of the transition $m \rightarrow n$ of nucleus i belonging to fragment a.

$\Delta g = g_a - g_b$,

A: hyperfine coupling constants (hfc),

M: nuclear spin states,

H_0: the applied field,

β_e: Bohr magneton.

The j index refers to radical a and k index to radical b of the radical pair $\overline{a\bullet\bullet b}$.

(If $I_{mn} < 0$, an emission line appears under the baseline of the spectrum obtained experimentally.)

The first term of equation 2.1 gives a net emission (E) or a net absorption (A) according to whether Δg is negative or positive. The second term gives the multiplet effect which arises from coupling of nucleus i (belonging to fragment a) with the other nucleus j (belonging to fragment a or b) of the radicals and it depends on signs of $A_i A_j M_j$. The 'phase' of the multiplet effect (E/A or A/E) depends further on the absolute sign of the coupling constant J_{ij} because this determines whether lines with positive M_j appear at low or high field in the multiplet of i. The third term gives a multiplet effect of opposite phase for coupling of i to a nucleus of radical b. The last term is of no importance in pure first-order spectra, because transitions with $M_i > 1/2$ and $M_i < 1/2$ are degenerate and the effects cancel. However, in spectra exhibiting second-order effects, polarization due to this term appears ($A_n B$ spectra).

Kaptein's Rules

Qualitative features of CIDNP spectra can be described with the signs of two quantities, Γ_{ne} for net effects and Γ_{me} for multiplet effects.

$$\Gamma_{ne} = \mu\varepsilon\Delta g A_i \begin{cases} +, & A \\ -, & E \end{cases} \tag{2.2}$$

$$\Gamma_{me} = \mu\varepsilon A_i A_j J_{ij}\sigma_{ij} \begin{cases} +, & E/A \\ -, & A/E \end{cases} \tag{2.3}$$

In these relations the spectrum of nucleus i of fragment a of the radical pair is considered. A represents a net absorption, E represents a net emission, E/A and A/E

represent a multiplet effect. μ, ε and σ_{ij} are labels indicating precursor multiplicity, c or e product, and presence of i and j in the same or different radicals.

In these expression:

$$\mu = \begin{cases} + & \text{for T and F precursor} \\ - & \text{for S precursor} \end{cases}$$

$$\varepsilon = \begin{cases} + & \text{for c products (coupling or disproportionation)} \\ - & \text{for e products (escape)} \end{cases}$$

$$\sigma_{ij} = \begin{cases} + & \text{when } i \text{ and } j \text{ reside in the same radical} \\ - & \text{when } i \text{ and } j \text{ reside in the different radical} \end{cases}$$

CHAPTER 3. RESULTS AND DISCUSSION

The System, *t*-BuHgCl/$S_2O_8^{2-}$/NaI

The reaction between *tert*-butylmercury chloride, ammonium peroxydisulfate and sodium iodide in d_6-dimethyl sulfoxide (d_6-Me_2SO) at 25 °C takes place rapidly and leads to isobutane and isobutene among other products. The NMR spectrum recorded immediately after addition of ammonium peroxydisulfate to a solution of *t*-BuHgCl and NaI in d_6-Me_2SO shows multiplet A/E polarization (A=enhanced absorption downfield, E=emission upfield) of the signal for the methyl protons of isobutene and isobutane and the methylene protons of isobutylene. The signals of the polarized products can be observed in the spectrum for ca. 10 min. A typical CIDNP spectrum is shown in Figure 3.1. The products, isobutane (methyl δ 0.81) and isobutene (methylene δ 4.61 and methyl δ 1.60), show the A/E multiplet effect expected for geminate disproportionation of *tert*-butyl radicals.

The multiplet polarization of the signals for the protons of isobutene and isobutane is generated in the F-pairs of *tert*-butyl radicals as a result of the disproportionation reaction.

The A/E multiplet polarization is consistent with the Kaptein's rule prediction for the multiplet effect in the products from the reaction of the F-pair. The third

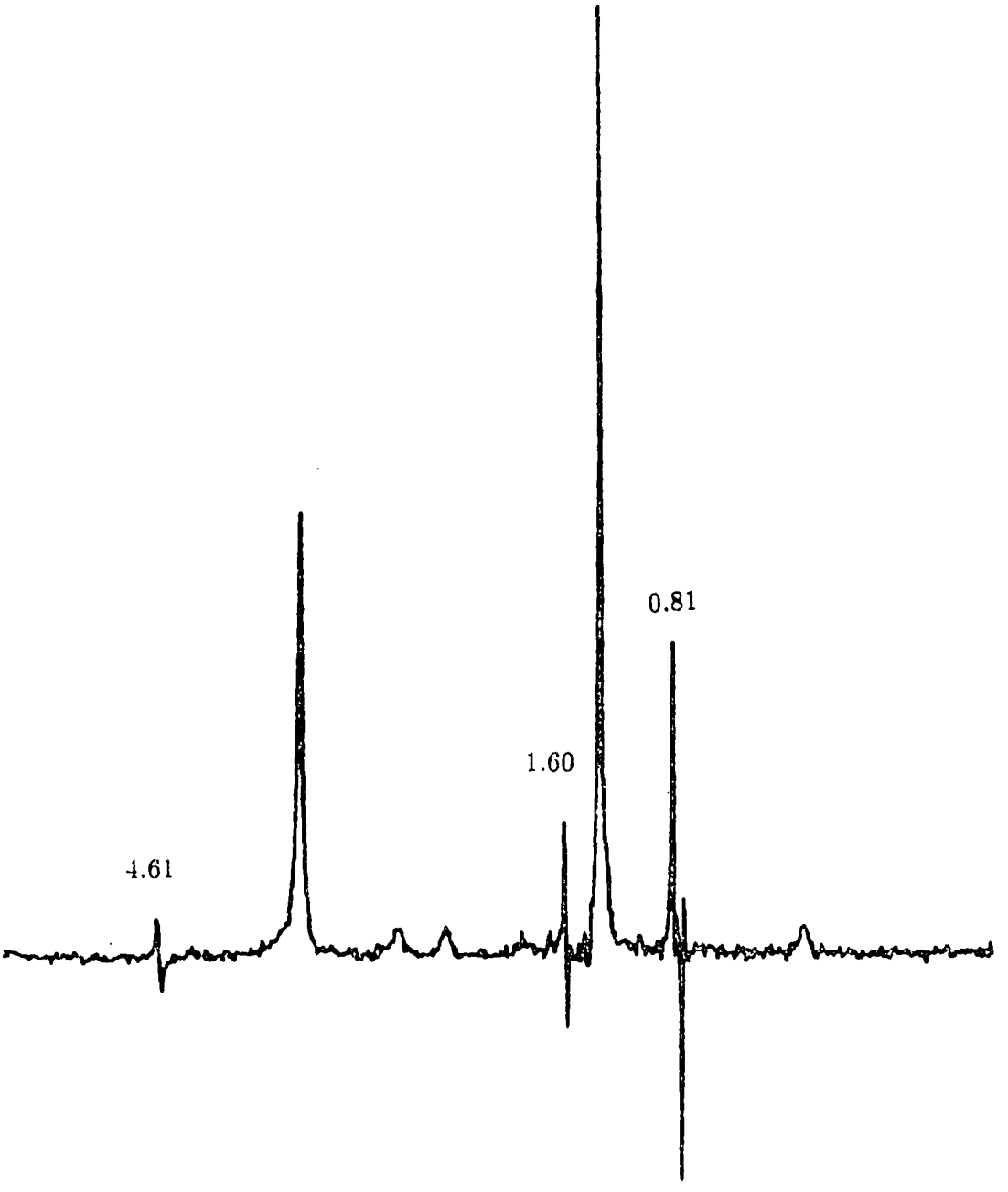

Figure 3.1: CIDNP recorded during the reaction of $(CH_3)_3CHgCl$ and $S_2O_8^{2-}$ in d_6-Me_2SO with NaI at 25 °C.

product from the reaction of the pair of *tert*-butyl radicals is unpolarized hexamethyl ethane. Since the coupling product, $(CH_3)_3CC(CH_3)_3$, has a single line NMR spectrum it cannot exhibit a multiplet effect.

The CKO theory of radical pairs, which explains the CIDNP effect, shows that the polarization phases and the intensities of the polarized signals depend on the electron spin multiplicity of the pair (μ), on the g factors and the hfs constants of the radicals (A), on the type of elementary reactions of the radicals (ε), and on the spin-spin coupling constants (J) and the form of the interacting protons (σ) in the product. If the polarization occurring because of a difference in the g factors is close to zero, the hfs constants of the radicals give rise to multiplet polarization in the spectrum. The theory of radical pairs, formulated as Kaptein's rules for net ($\Gamma_{ne} = \mu\varepsilon\Delta g A_i$) and multiplet ($\Gamma_{me} = \mu\varepsilon A_i A_j J_{ij}\sigma_{ij}$) effects, makes it possible to analyze the polarization phases of the spectrum for the reaction carried out in strong magnetic fields. The hfs constant for the protons of the *tert*-butyl radical is +22.74G, and the g factor is 2.0026. Characteristics of the CKO theory are that net polarization (E or A) arises only from pairs of non-equivalent radicals (Δg effects) and that pairs of equivalent radicals ($\Delta g = 0$) can only give multiple effects.

For the *tert*-butyl radical pair since $\Delta g = 0$, no net polarization occurs in the diffusive disportionation reaction. The hfs constants of the radicals give rise to a multiplet effect in the spectrum. Since the spin-spin coupling constant, J_{ij}, in isobutane is positive and the methine proton came originally from the other radical (i.e., σ_{ij} is negative) and since μ and ε are positive for the case of F precursors and disportionation products, it follows that

$$\Gamma_{me} = + + + + + - = -(A/E)$$

For the methyl and methylene in the isobutene, J_{ij} is negative and the splitting is due to protons on the same fragment, therefore

$$\Gamma_{me} = + + + + - + = -(A/E)$$

No polarization was observed for the singlet NMR spectrum of hexamethylethane due to $\Delta_g = 0$ and $\sum A\Delta_M = 0$ for symmetrical F-pairs.

Furthermore, it can be seen that a second-order multiplet effect is present in the methyl doublet (δ=0.9, 0.97) of isobutane (A/E, E/A), (Figure 3.2) arising from the last term of Keptein's CIDNP intensity Equation 2.1.

The observation of the A/E multiplets for isobutane and isobutene allow certain mechanistic conclusion to be drawn about the $RHgCl/S_2O_8^{2-}/I^-$ system. Of course, the observation of CIDNP proves that *tert*-butyl radicals are formed and that they are produced quite rapidly.

The reaction of ammonium peroxydisulfate with sodium iodide has been suggested to occur in two steps involving the complex, $IS_2O_8^{3-}$ [18].

$$S_2O_8^{2-} + I^- \longrightarrow S_2O_8I^{3-} \qquad \text{slow} \qquad (3.1)$$

$$S_2O_8I^{3-} + I^- \longrightarrow 2SO_4^{2-} + I_2 \qquad \text{fast} \qquad (3.2)$$

Alternatively, Morgan suggested that a one-electron transfer reaction may occur forming iodine atoms and sulfate radical ions [19].

$$S_2O_8^{2-} + I^- \longrightarrow SO_4^{2-} + SO_4^{-\bullet} + I^{\bullet} \qquad (3.3)$$

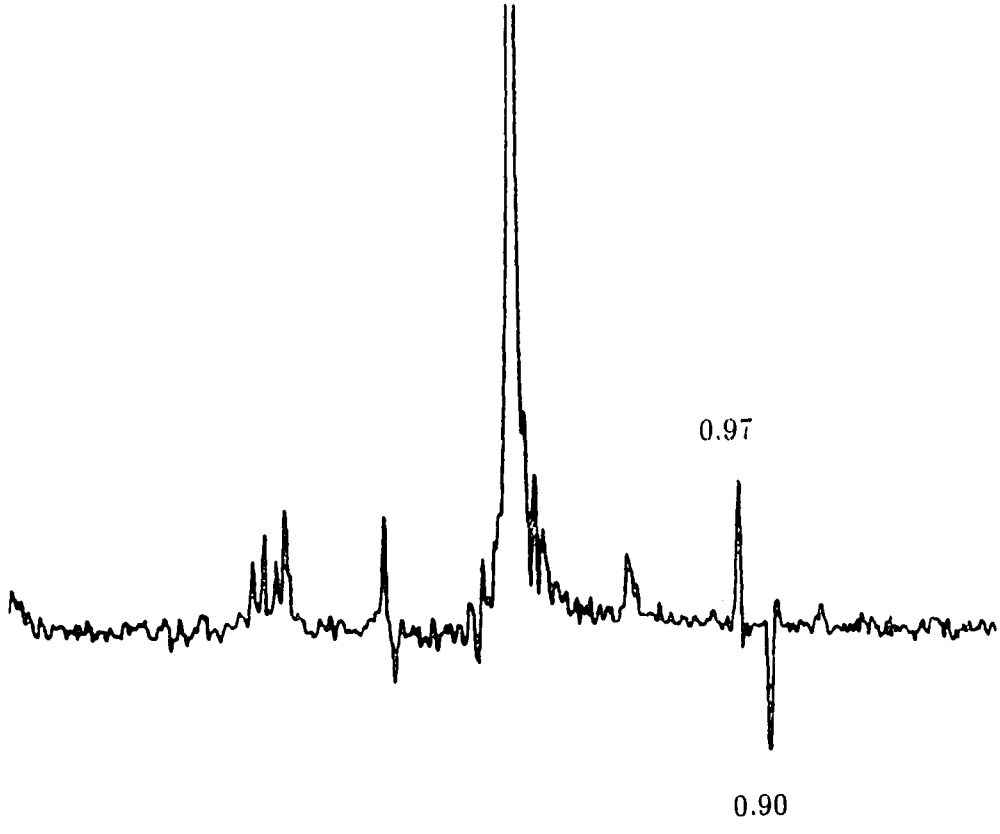

Figure 3.2: The spectrum of second-order multiplet effect in $(CH_3)_3CH^*$

$$SO_4^{-\bullet} + I^- \longrightarrow SO_4^{2-} + I^\bullet \tag{3.4}$$

$$I^\bullet + I^\bullet \longrightarrow I_2 \tag{3.5}$$

Jensen and Rickborn assumed that the alkylmercuric halides react with X_2 to form RX via intermediate [$RHg^\bullet X_2$] [20].

$$RHgX + I_2 \longrightarrow RI + HgI_2 \tag{3.6}$$

$$I^\bullet + RHgX \rightleftharpoons [RHgX_2]^\bullet \longrightarrow R^\bullet + HgXI \tag{3.7}$$

$$R^\bullet + I_2 \longrightarrow RI + I^\bullet \tag{3.8}$$

He pointed out that the electron deficient species $[RHgX_2]^\bullet$ is included as a possible intermediate in the reaction, although there is no direct evidence in support of its existence.

Furthermore, Ingold and Roberts also suggested that a stepwise S_H2 mechanism will often operate involving the reaction of a halogen atom at mercury $[RHgX_2]^\bullet$ [21].

The radical mechanism for the reaction of *tert*-butyl mercury chloride with ammonium peroxydisulfate and sodium iodide can be described by Scheme 1.

Scheme 1

$$S_2O_8^{2-} + I^- \longrightarrow SO_4^{-\bullet} + I^\bullet + SO_4^{2-} \tag{3.9}$$

$$SO_4^{-\bullet} + I^- \longrightarrow SO_4^{2-} + I^\bullet \tag{3.10}$$

$$(CH_3)_3CHgCl + I^\bullet \rightleftharpoons [(CH_3)_3CHg(I)Cl]^\bullet \longrightarrow (CH_3)_3C^\bullet + IHgCl \tag{3.11}$$

$$2\overline{(CH_3)_3C^\bullet}^F \longrightarrow (CH_3)_3CH\ (A/E) + (CH_3)_2 = CH_2\ (A/E) \text{ disproportionation} \tag{3.12}$$

$$2\overline{(CH_3)_3C^{\bullet}}^{F} \longrightarrow (CH_3)_3CC(CH_3)_3 \quad \text{coupling} \tag{3.13}$$

Alternatively, it is possible that the RHgX can coordinate with I^- to form the complexes, $RHgX_2^-$ and $RHgX_3^{2-}$, which are easily oxidized by $S_2O_8^{2-}$ or $SO_4^{-\bullet}$ or $X^{\bullet}$ in the presence of X^-.

$$R\text{-}Hg(X)\text{-}X^- + S_2O_8^{2-} \longrightarrow R^{\bullet} + HgX_2 + SO_4^{-\bullet} + SO_4^{2-} \tag{3.14}$$

$$R\text{-}Hg(X)\text{-}X^- + SO_4^{-\bullet} \longrightarrow R^{\bullet} + HgX_2 + SO_4^{2-} \tag{3.15}$$

$$R\text{-}Hg(X)\text{-}X^- + I^{\bullet} \longrightarrow R^{\bullet} + HgX_2 + I^- \tag{3.16}$$

The System, $RHgX/S_2O_8^{2-}$

Peroxydisulfate ions and sulfate radical ions

The $S_2O_8^{2-}$ ion has been shown by X-ray studies to have the structure in which the four oxygen atoms around each sulfur atom are tetrahedrally arranged.

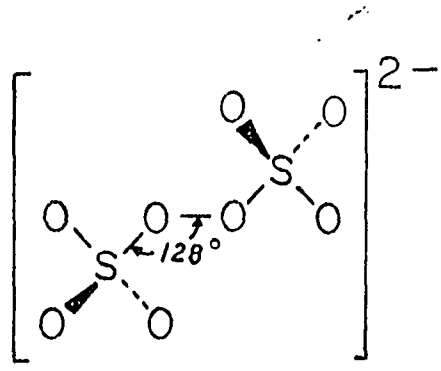

Table 3.1: Thermal decomposition of initiators

Initiator	Half-Lives			
	50 °C	60 °C	70 °C	85 °C
Benzoyl Peroxide(Bz_2O_2)	-	-	7.3 hr	1.4 hr
Propionyl Peroxide	70.9 hr	-	4.5 hr	42 min
Peroxydisulfate($S_2O_8^{2-}$)	191 hr	38.5 hr	8.25 hr	2.1 hr

The peroxydisulfate ion has an oxygen-oxygen linkage similar to those of the organic peroxides. The peroxide linkage of peroxydisulfate is thermally unstable and the peroxydisulfate ion can be homolytically cleaved into two sulfate ion radicals.

$$S_2O_8^{2-} \longrightarrow 2\,SO_4^{-\bullet} \tag{3.17}$$

The rate of the unimolecular decomposition of peroxydisulfate is slower than that of benzoyl peroxide [22] (see Table 3.1). The activation energy for the unimolecular decomposition is 33.5 Kcal/mole [23].

Sulfate radical ion ($SO_4^{-\bullet}$) is a very effective electron transfer oxidizing agent with a redox potential of 3.40 V (NHE) [24]. The highly reactive sulfate radical ion may undergo reactions with various substrates present in the solution. In addition, the one electron oxidation product of the substrate may be an unstable intermediate which may further decompose into new products.

The peroxydisulfate ion undergoes a fission of the weak oxygen-oxygen bond with formation of two sulfate radical ions in d_6-Me_2SO at (40-80) °C which could bring about homolytic displacement of R• radicals from mercury (equation 3.18). An alternative mechanism is electron transfer from RHgX to the $SO_4^{-\bullet}$ followed by

very rapid decomposition of the alkylmercuric halide radical cation (equation 3.19). Diffusive collisions of the R• radicals give F-pairs in which polarization arises showing the A/E type of multiple effect. The coupling of the radicals R• is accompanied by disproportionation, which leads to RH and R(-H). Scheme 2 outlines the mechanism of these reactions.

Scheme 2

$$S_2O_8^{2-} \longrightarrow 2\,SO_4^{-\bullet}$$

$$RHgX + SO_4^{-\bullet} \longrightarrow [RHgSO_4^-X]^\bullet \longrightarrow R^\bullet + XHgSO_4^- \qquad (3.18)$$

$$RHgX + SO_4^{-\bullet} \longrightarrow RHgX^{+\bullet}SO_4^{2-} \longrightarrow R^\bullet + HgX^+ + SO_4^{2-} \qquad (3.19)$$

$$\overline{R\bullet\bullet R}^F \longrightarrow R(-H)(A/E) + RH\,(A/E) \quad \text{disproportionation} \qquad (3.20)$$

$$\overline{R\bullet\bullet R}^F \longrightarrow (R-R) \quad \text{coupling} \qquad (3.21)$$

$$\overline{R\bullet\bullet R}^F \longrightarrow 2\,R\bullet^* \quad \text{escape} \qquad (3.22)$$

As we have seen, net polarization arises only from pairs of inequivalent radicals (Δg effects), and pairs of equivalent radicals can give only multiplet effects. On this basis, the RHgX/$SO_4^{-\bullet}$ systems to be discussed exhibit multiplet effects (A/E) due to the reaction of F-pairs.

$(CH_3)_3CHgCl/(NH_4)_2S_2O_8$

The 90 MHz ^{1}H CIDNP spectrum taken during thermal decomposition of ammonium peroxydisulfate in the presence of *tert*-butylmercury chloride in d_6-dimethyl

sulfoxide (d_6-Me_2SO) at 60 °C is shown in Figure 3.3. Apart from the parent compounds ($(CH_3)_3CHgCl$) all lines show A/E polarization.

The radical character of the reaction can be judged from the appearance of enhanced absorption and emission lines in the NMR spectrum when the reaction is carried out in the spectrometer at 60 °C. Figure 3.4 shows the spectrum recorded immediately after the reagents were mixed at 25 °C. The *tert*-butylmercury chloride exhibits a proton NMR spectrum with a single line at δ 1.37 in d_6-Me_2SO with a doublet symmetrical with respect to the main signal, with components of equal intensity, due to the interaction of the protons with Hg^{199} nuclei (J Hg^{199}-C-C-H^1 = 266 Hz). As the solutions are heated to about 60 °C, the NMR spectra of the products, isobutane (d, δ 0.85) and isobutene (septet, δ 4.61, triplet, δ 1.65) show pure A/E multiplet polarization in Figure 3.3. A weaker A/E polarization of the methine proton of isobutane (decet, δ 1.67) is somewhat obscure and is superimposed on the stronger A/E multiplet polarization of the signals for the methyl protons of isobutene (δ 1.65).

The A/E multiplet polarization of the signals for the protons of isobutene and isobutane is generated from the F-pairs of *tert*-butyl radicals as a result of the disproportionation reaction.

The Kaptein's multiplet effect rule ($\Gamma_{me} = \mu\varepsilon A_i A_j J_{ij} \sigma_{ij}$) applied to isobutane and isobutene would give

$$\Gamma_{me} = + + + + + - = -(A/E) \quad \text{for} \quad (CH_3)_3CH$$

$$\Gamma_{me} = + + + + - + = -(A/E) \quad \text{for isobutene}$$

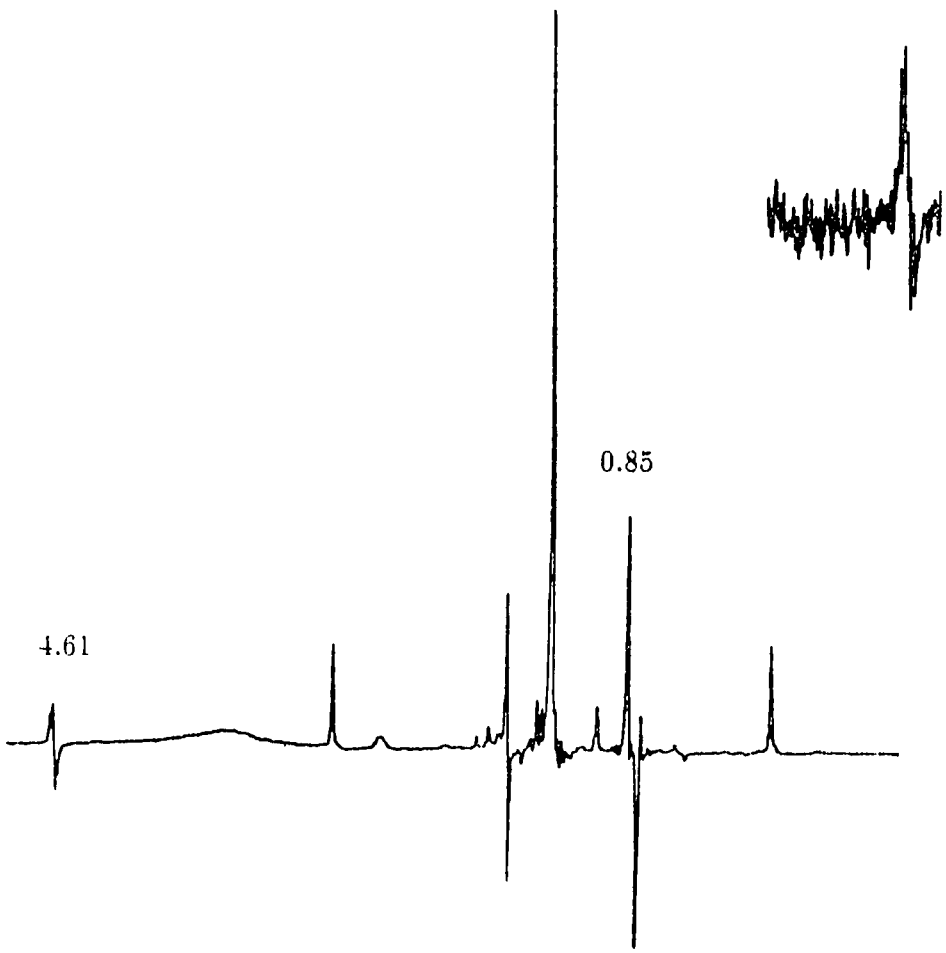

Figure 3.3: CIDNP observed during the reaction of $(CH_3)_3CHgCl$ and $S_2O_8^{2-}$ in d_6-Me_2SO at 60 °C

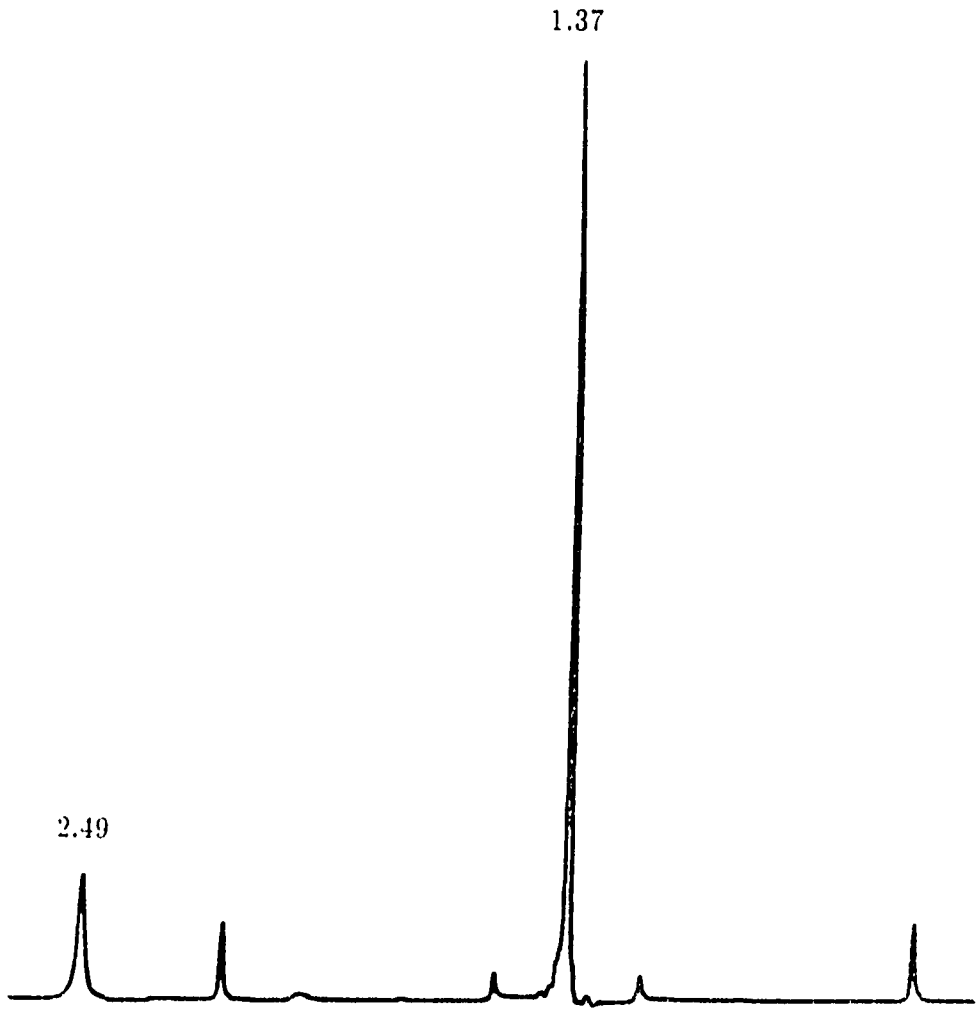

Figure 3.4: The NMR spectrum of $(CH_3)_3CHgCl$ and $S_2O_8^{2-}$ in d_6-Me_2SO at 25 °C

since μ = +(F precursor), ε = +(disproportionation product), A(CH_3)> 0 in the *tert*-butyl radical, J_{ij} = + and σ_{ij} = − for $(CH_3)_3CH$, J_{ij} = − and σ_{ij} = + for isobutene.

The reaction of *tert*-butylmercury chloride with peroxydisulfate ion is assumed to follow Scheme 3.

Scheme 3

$$S_2O_8^{2-} \longrightarrow 2\,SO_4^{-\bullet}$$

$$(CH_3)CHgCl + SO_4^{-\bullet} \longrightarrow (CH_3)_3C^{\bullet} + ClHgSO_4^{-} \quad (3.23)$$

$$\overline{(CH_3)_3C\bullet\ \bullet C(CH_3)_3}^{F} \longrightarrow (CH_3)_3CC(CH_3)_3 \quad \text{coupling} \quad (3.24)$$

$$\overline{(CH_3)_3C\bullet\ \bullet C(CH_3)_3}^{F} \longrightarrow (CH_3)_2C=CH_2 + (CH_3)_3CH \quad \text{disproportionation} \quad (3.25)$$

$$\overline{(CH_3)_3C\bullet\ \bullet C(CH_3)_3}^{F} \longrightarrow (CH_3)_3C\bullet^{*} \quad \text{escape} \quad (3.26)$$

$(CH_3)_2CHHgX/(NH_4)_2S_2O_8$ X=Cl,Br,I

CIDNP was found in the reaction of isopropylmercury halides with ammonium peroxydisulfate in d_6-Me_2SO at (60-80) °C. The CIDNP spectrum is given in Figure 3.5. The spectrum shows enhancements for propane and propene, which contribute to the A/E lines at δ 1.67, 5.67, 4.84 and 0.87, 1.33.

Typical A/E lines at δ 1.67, 5.67, 4.84 and 0.87, 1.33 belong to propene and propane. This indicates that isopropyl radicals generated from bimolecular homolytic substitution or electron transfer (Equation 3.27 or Equation 3.28) form diffusive radical pairs as shown in Scheme 4.

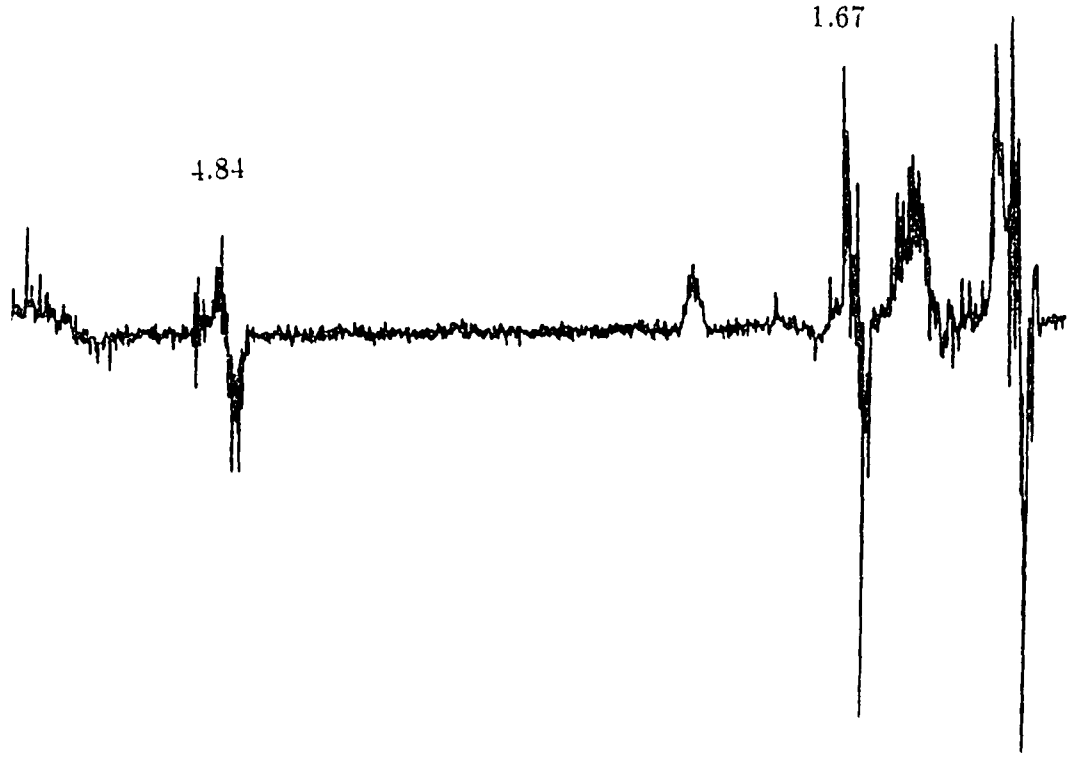

Figure 3.5: CIDNP observed during the reaction of i-$(CH_3)_2CHHgCl$ and $S_2O_8^{2-}$ in d_6-Me_2SO at 80 °C

Scheme 4

$$i\text{-}C_3H_7HgX + SO_4^{-\bullet} \longrightarrow i\text{-}C_3H_7HgXSO_4^{-\bullet} \longrightarrow i\text{-}C_3H_7\bullet + XHgSO_4^- \quad (3.27)$$

$$i\text{-}C_3H_7Hg + SO_4^{-\bullet} \longrightarrow i\text{-}C_3H_7H_7HgX^{+\bullet}SO_4^{2-} \longrightarrow i\text{-}C_3H_7\bullet + XHgSO_4^- \quad (3.28)$$

$$2\overline{i\text{-}C_3H_7\bullet}^F \longrightarrow CH_3CH_2CH_2 \quad (A/E) \; + \; CH_3CH=CH_2 \quad (A/E) \quad (3.29)$$

The A/E multiplet polarization of propene can be explained by Kaptein's rules since $\mu = +$, $\varepsilon = +$, A(CH_3)> 0, A(=C-H)< 0 in the isopropyl radical with

$$J_{ij} = + \quad \text{and} \quad \sigma_{ij} = +.$$

$$\Gamma_{me} = +++--++ = -(A/E) \quad \text{for propene.}$$

$CH_3CH_2HgX/S_2O_8^{2-}$ X=Cl, I

Figure 3.6 shows the CIDNP spectrum obtained during the decomposition of peroxydisulfate in d_6−Me_2SO solution of ethylmercury iodide at 80 °C. Butane (δ=0.87) and ethyl iodide (δ=1.80, 3.146) are major products. A weak ethylene absorption is observed at δ 5.24. An A/E multiplet polarization is observed for butane and E/A for ethyl iodide.

The polarization is a multiplet effect which must originate from a pair with $\Delta g = 0$. The disproportionation products ethane and ethylene both have single line NMR spectra which cannot exhibit a multiplet effect.

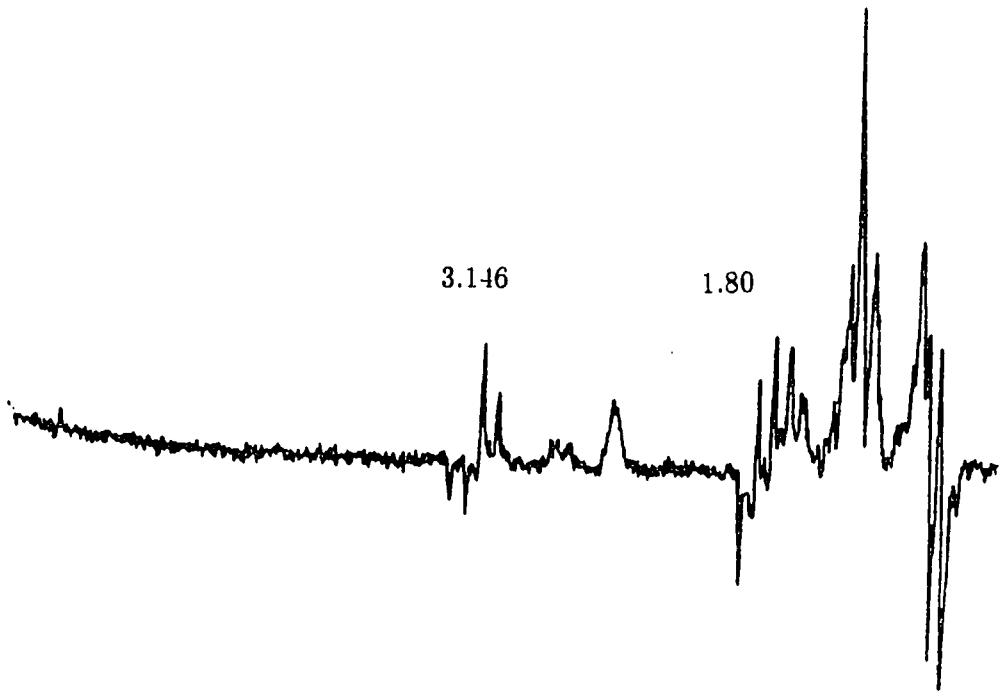

Figure 3.6: CIDNP observed during the reaction of CH_3CH_2HgI and $S_2O_8^{2-}$ in d_6-Me_2SO at 80 °C

The radical coupling product, butane, exhibits a multiplet effect too complicated to fit the simple rules. In the reaction of ethylmercury iodide and ammonium peroxydisulfate, the multiplet phase of the polarization of ethyl iodide is observed to be E/A. The Kaptein's multiplet effect rule applied to ethyl iodide would give

$$\Gamma_{me}(ICH_2CH_3) = + - - + ++ = +(E/A).$$

since μ = +(F precursor), ε = −(escape product). A(CH_2)< 0 and A(CH_3)> 0 in the ethyl radical, J = + and σ = + (the coupled protons come from the same radical).

These polarizations are appropriate for a radical-radical termination and iodide transfer steps, suggesting

$$S_2O_8^{2-} \longrightarrow SO_4^{-\bullet}$$

$$SO_4^{-\bullet} + CH_3CH_2HgI \longrightarrow CH_3CH_2\bullet + IHgSO_4^- \qquad (3.30)$$

$$\overline{CH_3CH_2\bullet\bullet CH_2CH_3}^F \longrightarrow CH_3CH_2CH_2CH_3^* +$$

$$CH_2 = CH_2 + CH_3CH_3 \qquad (3.31)$$

$$\overline{CH_3CH_2\bullet\bullet CH_2CH_3}^F \longrightarrow 2CH_3CH_2\bullet^* \qquad (3.32)$$

$$CH_3CH_2\bullet^* + CH_3CH_2HgI \longrightarrow CH_3CH_2^*I + CH_3CH_2Hg\bullet \qquad (3.33)$$

n-C_4H_9HgCl/ $(NH_4)_2S_2O_8$

Figure 3.7 shows the CIDNP spectrum obtained during the decomposition of $(NH_4)_2S_2O_8$ in presence of n-C_4H_9Cl in d_6-Me_2SO at 80 °C. The A/E multiplet polarization occurs for the products n-butane (δ=0.85) and n-butene (δ=1.68, 4.81,

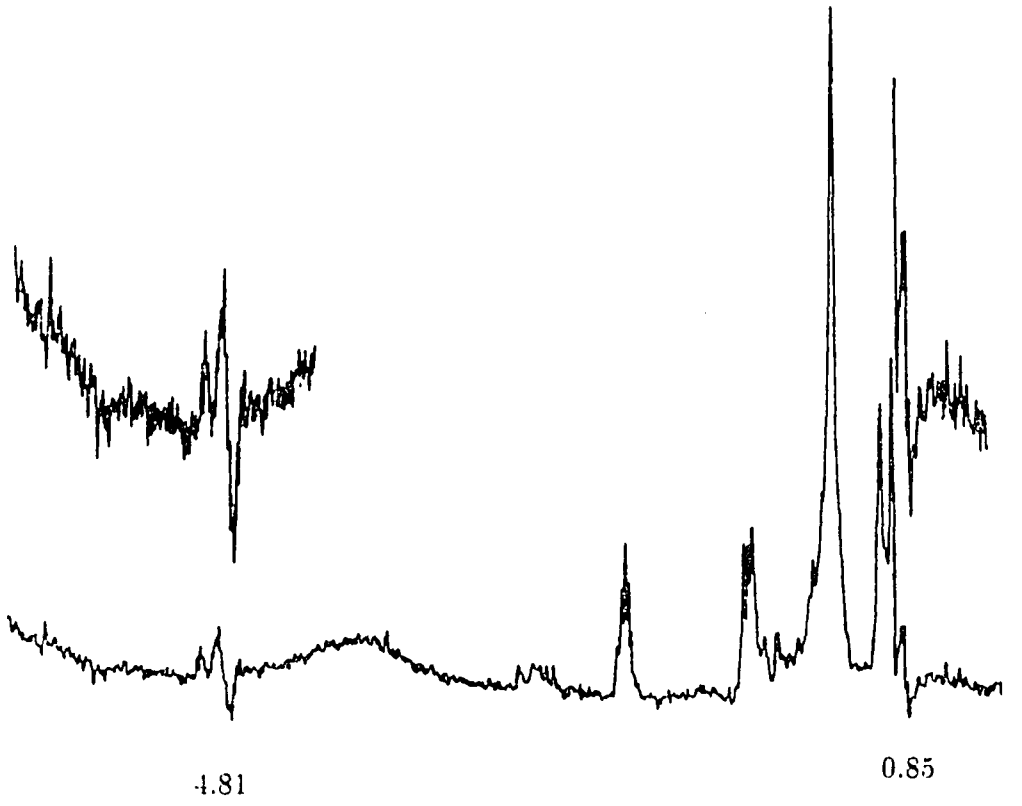

Figure 3.7: CIDNP observed during the reaction of n-C_4H_9HgCl and $S_2O_8^{2-}$ in d_6-Me_2SO at 80 °C

5.5). The A/E multiplet effects originates in the radical F-pair(n-$C_4H_9\bullet$) and the products, butene and butane, result from the disproportionation reaction of this radical pair.

n-$C_6H_{11}HgCl$/ $(NH_4)_2S_2O_8$

Figure 3.8 shows the CIDNP spectrum obtained during the reaction of n-hexyl mercury chloride with peroxydisulfate ion in d_6-Me_2SO at 80 °C. The lines at δ=5.05 (A/E) and δ=5.85 (A/E) belong to vinyl group of n-hexene. These A/E polarization must arise from the radical F-pair (n-$C_6H_{11}\bullet$).

$(CH_3)_3CCH_2CH_2HgCl$/ $(NH_4)_2S_2O_8$

Figure 3.9 shows the CIDNP spectrum during the decomposition of peroxydisulfate ion in the presence of $(CH_3)_3CCH_2CH_2HgCl$ in d_6-Me_2SO at 80 °C. The A/E multiplet polarizations occur for the product $(CH_3)_3CCH{=}CH_2$ (methine δ 4.73; methylene δ 6.65). These multiplet effects arise from the radical F-pair ($(CH_3)_3CCH_2CH_2\bullet$) and are in accord with following reaction.

$$2\overline{(CH_3)_3CCH_2CH_2\bullet} \longrightarrow (CH_3)_3CCH_2CH_2CH_2CH_2C(CH_3)_3 \quad (3.34)$$

$$2\overline{(CH_3)_3CCH_2CH_2\bullet} \longrightarrow (CH_3)_3CCH=CH_2 \ (A/E) \ + \ (CH_3)_3CCH_2CH_3 \quad (3.35)$$

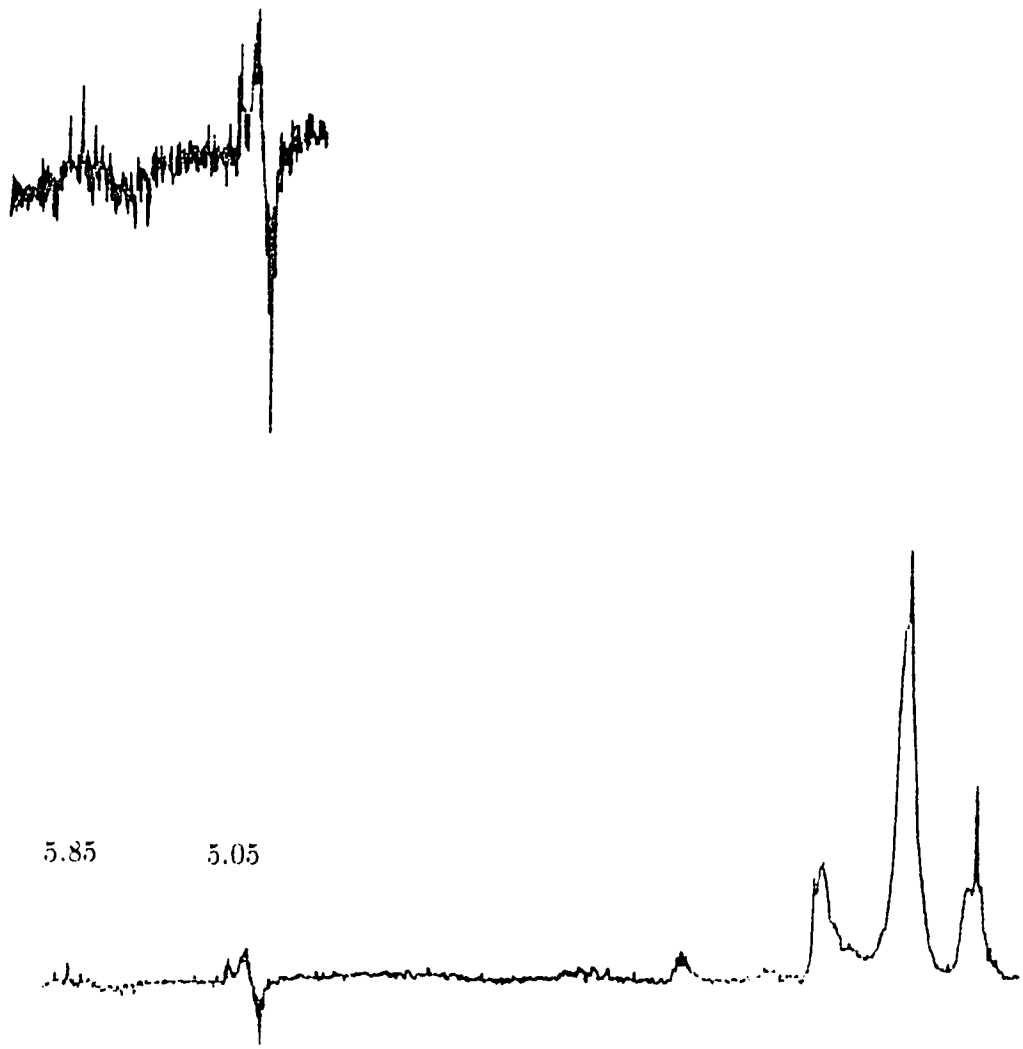

Figure 3.8: CIDNP observed during the reaction of n-$C_6H_{11}HgCl$ and $S_2O_8^{2-}$ in d_6-Me_2SO at 80 °C

Figure 3.9: CIDNP observed during the reaction of $(CH_3)_3CCH_2CH_2HgCl$ and $S_2O_8^{2-}$ in d_6-Me_2SO at 80 °C

2-Methoxycyclohexylmercury chloride/ $S_2O_8^{2-}$

As we have seen, the $RHgX/SO_4^{-\bullet}$ systems exhibit only (A/E) multiplet effects due to the diffusive radical F-pair. It is interesting that an E/A multiplet polarization spectrum was obtained during the reaction of 2-methoxycyclohexylmercury chloride with $S_2O_8^{2-}$ ion in d_6-Me_2SO at 80 °C as shown in Figure 3.10. The NMR spectrum of the olefin proton revealed the pattern of an E/A multiplet effect in the quartet at 5.82 ppm. The weak multiplet effect at 2.2 ppm is superimposed on the spectrum of the parent compound.

Jensen and Rickborn have suggested a free radical mechanism for the hydrocarbon and olefin products obtained on prolonged heating of the bis-2-methoxycyclohexyl mercury as shown in Scheme 5 [20].

Scheme 5

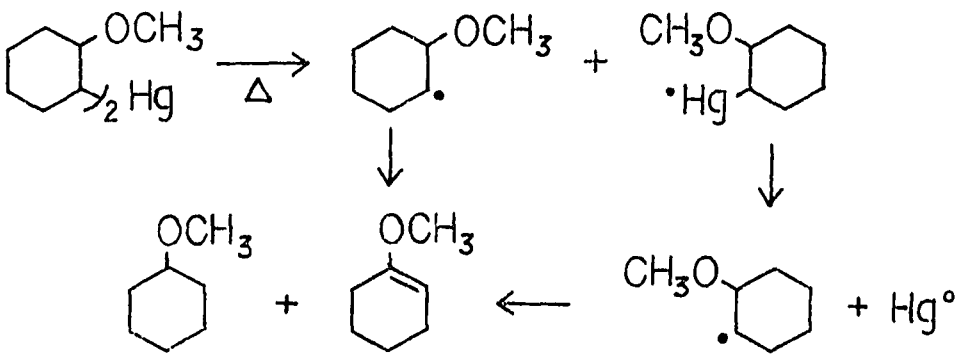

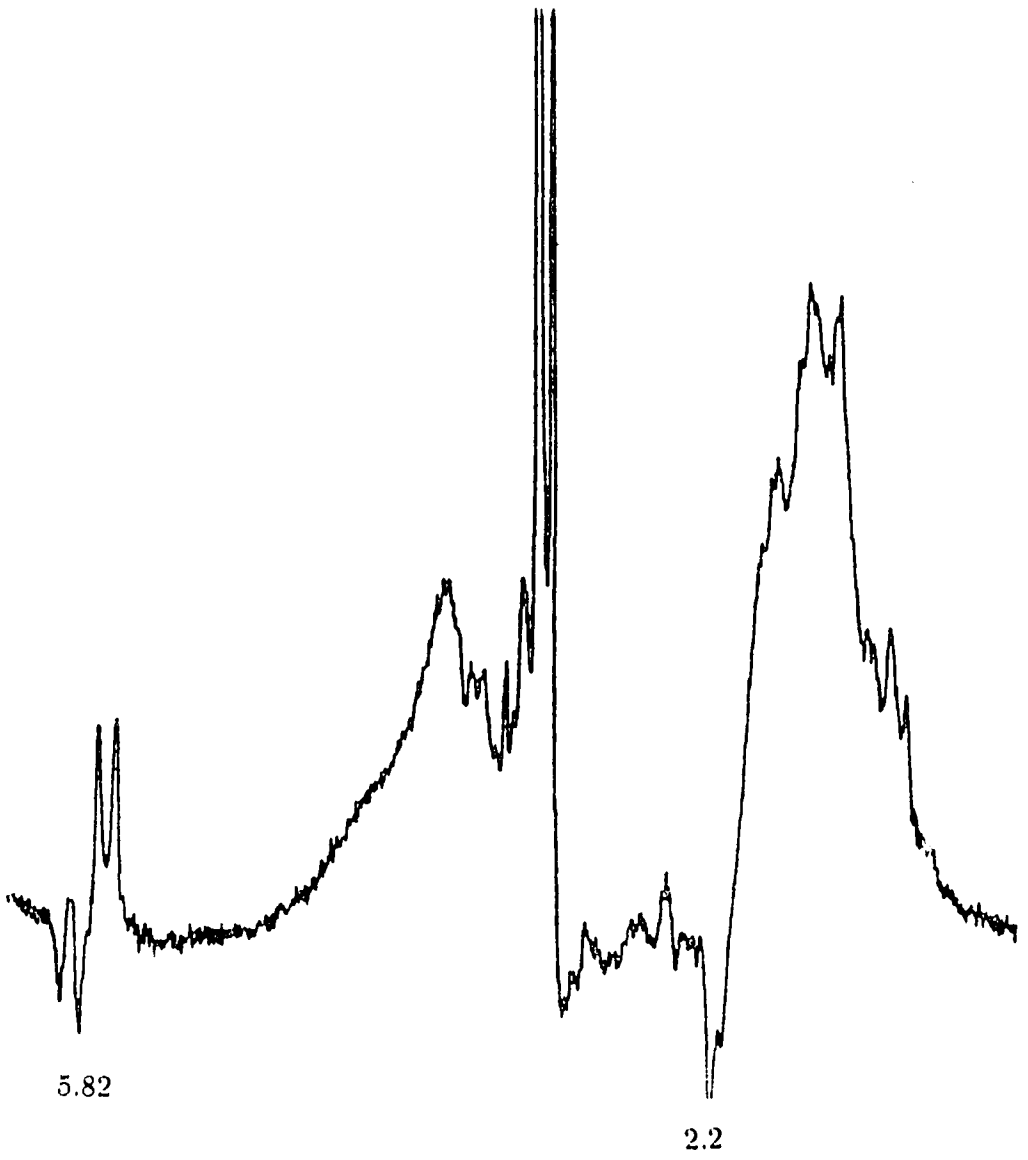

Figure 3.10: CIDNP observed during the reaction of 2-methoxycyclohexyl-mercury chloride and $S_2O_8^{2-}$ in d_6-Me_2SO at 80 °C

In the present investigation of CIDNP, the olefin and hydrocarbon are generated as shown in Scheme 6.

Scheme 6

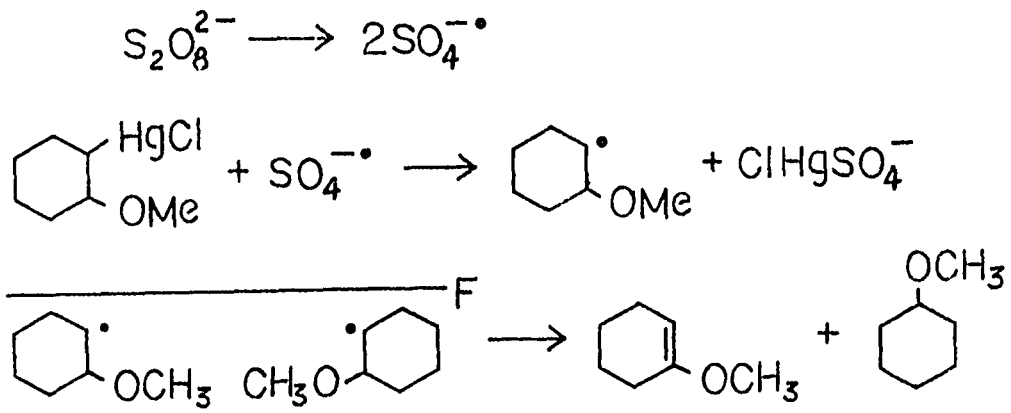

According to Kaptein's rule, ($\Gamma_{me} = \mu\varepsilon A_i A_j J_{ij} \sigma_{ij}$) for the multiplet effect. The parameters μ and ε will both be positive for the products of diffusive encounter between alkyl radicals. The hfs A_i and A_j will be negative for the α protons and positive for the protons of OCH_3 and β protons. The parameter σ_{ij} is defined as being positive when nuclei i and j belong to the same radical. Usually, vicinal coupling constant J_{ij} for alkenes are known to have a positive sign, but here J_{ij} for 2-methoxycyclohexene is negative for the coupling of the methoxy protons with the vinyl proton. Therefore

$$\Gamma_{me} = + + + - - + = +$$

and an E/A multiplet effect is predicted.

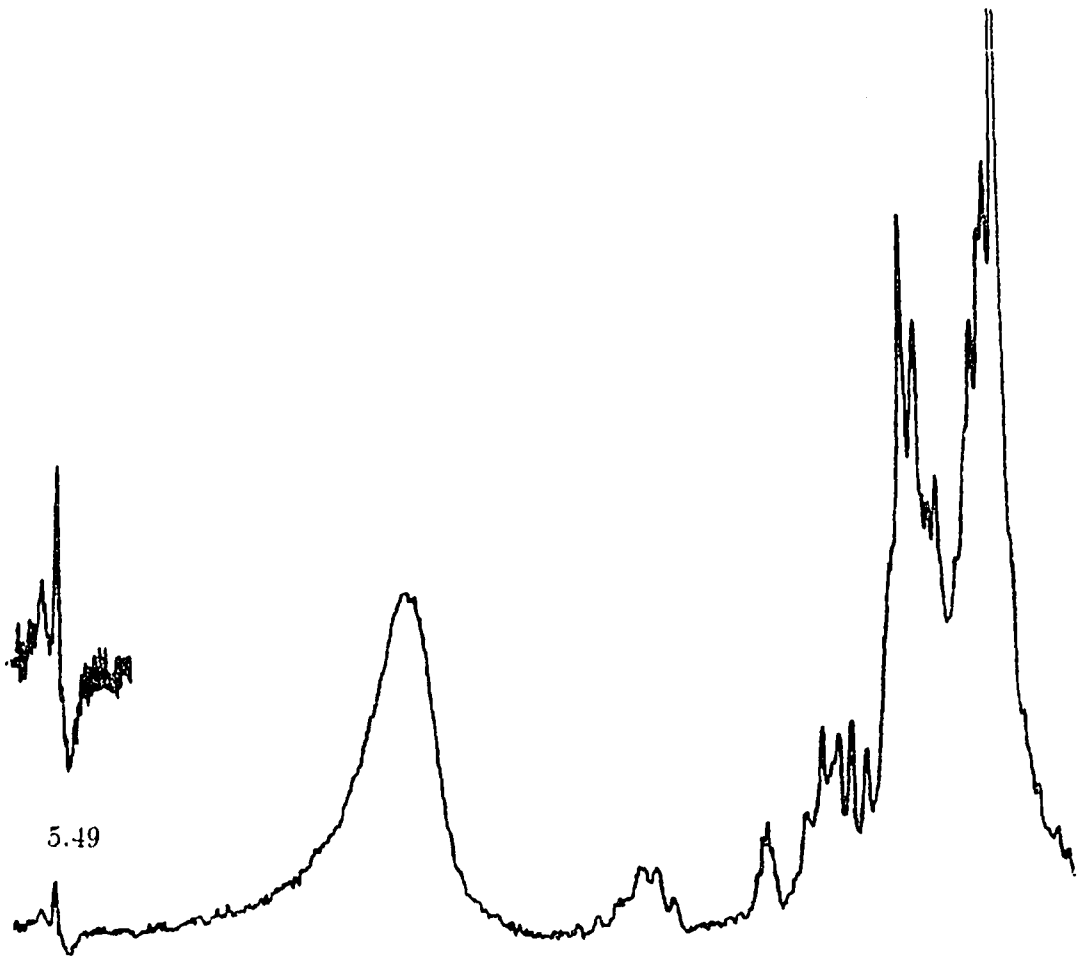

Figure 3.11: CIDNP observed during the reaction of *c*-C_5H_9HgCl and $S_2O_8^{2-}$ in d_6-Me_2SO at 80 °C

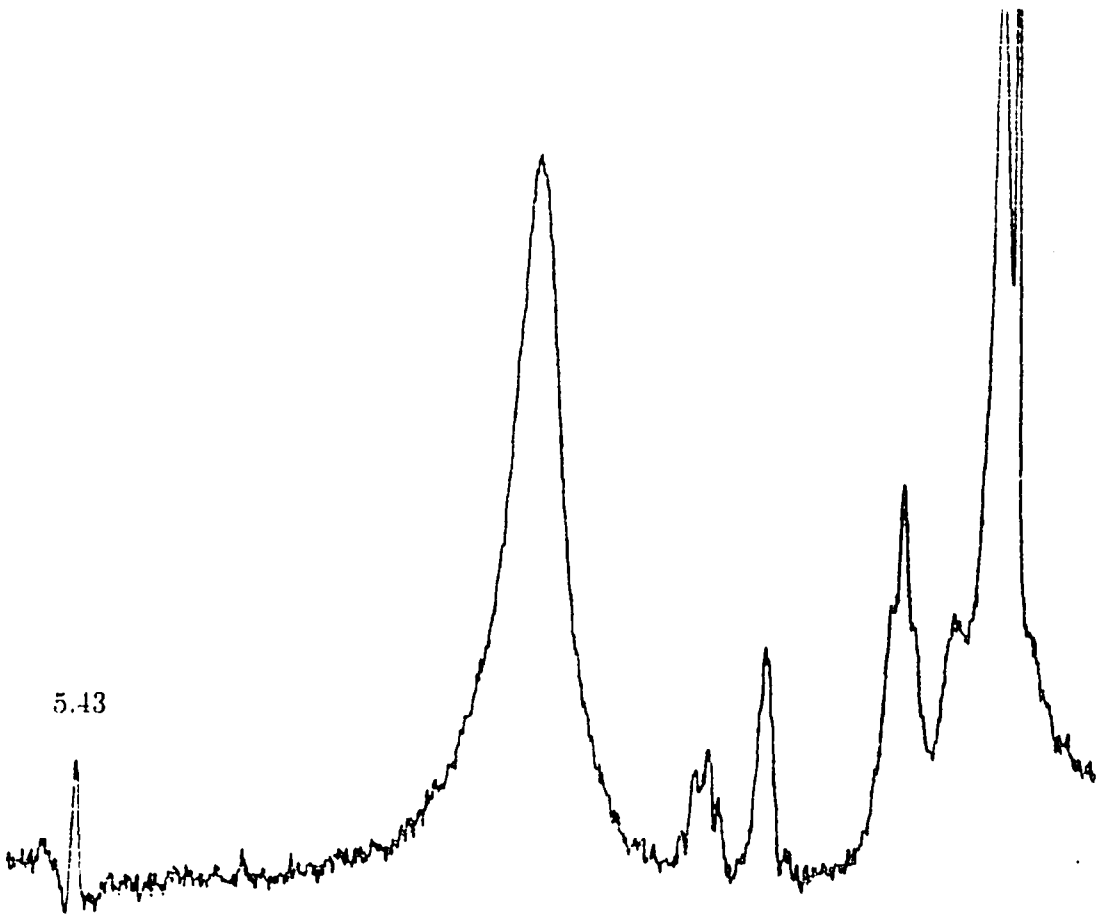

Figure 3.12: CIDNP observed during the reaction of *c*-$C_6H_{11}HgCl$ and $S_2O_8^{2-}$ in d_6-Me_2SO at 80 °C

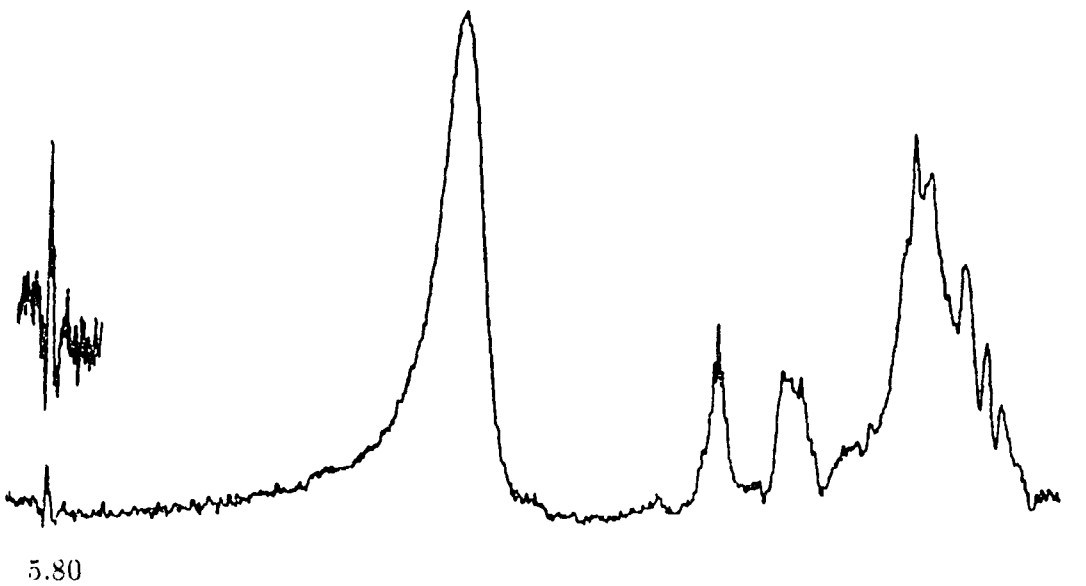

Figure 3.13: CIDNP observed during the reaction of *exo*-2-norbornylmercury chloride and $S_2O_8^{2-}$ in d_6-Me_2SO at 80 °C

$RHgCl/S_2O_8^{2-}$ (R = *c*-C_5H_{11}, *c*-C_6H_{13} and *c*-C_7H_{11})

Weak polarizations were observed when the peroxydisulfate ion reacts with cycloalkylmercury chlorides in d_6-Me_2SO at 80 °C. Figure 3.11 shows the spectrum observed during the reaction of peroxydisulfate and cyclopentylmercury chloide in d_6-Me_2SO at 80 °C. The olefinic protons of cyclopentene are observable at 5.49 ppm, and show an A/E effect. The CIDNP spectrum resulting from the reaction of peroxydisulfate and cyclohexylmercury chloride is shown in Figure 3.12. The product cyclohexene (vinyl proton δ=5.43) shows A/E multiplets. The reaction of peroxydisulfate and norbornylmercury chloride in d_6-Me_2SO at 80 °C results in the CIDNP spectrum shown in Figure 3.13. The A/E multiplet lines at 5.80 ppm belong to olefinic protons of norbornene. Note, however, that some multiplet lines are superimposed on the lines of parent compounds and products. These A/E multiplet polarizations of olefins are a result of disproportionation products from the radical F-pairs.

The System, $R_2Hg/S_2O_8^{2-}$

(*t*-Bu)$_2$Hg/$S_2O_8^{2-}$

The CIDNP spectrum obtained during the reaction of di-*tert*-butylmercury with peroxydisulfate in d_6-Me_2SO at 70 °C is shown in Figure 3.14. The strong E net polarization of methyl and vinyl protons of isobutene is seen at 1.65 ppm and 4.6 ppm. Only pure E net polarization of isobutene is observed, indicating that the radical pairs of sulfate radical ion ($SO_4^{-\bullet}$) and *tert*-butyl radical are formed in diffusive encounters.

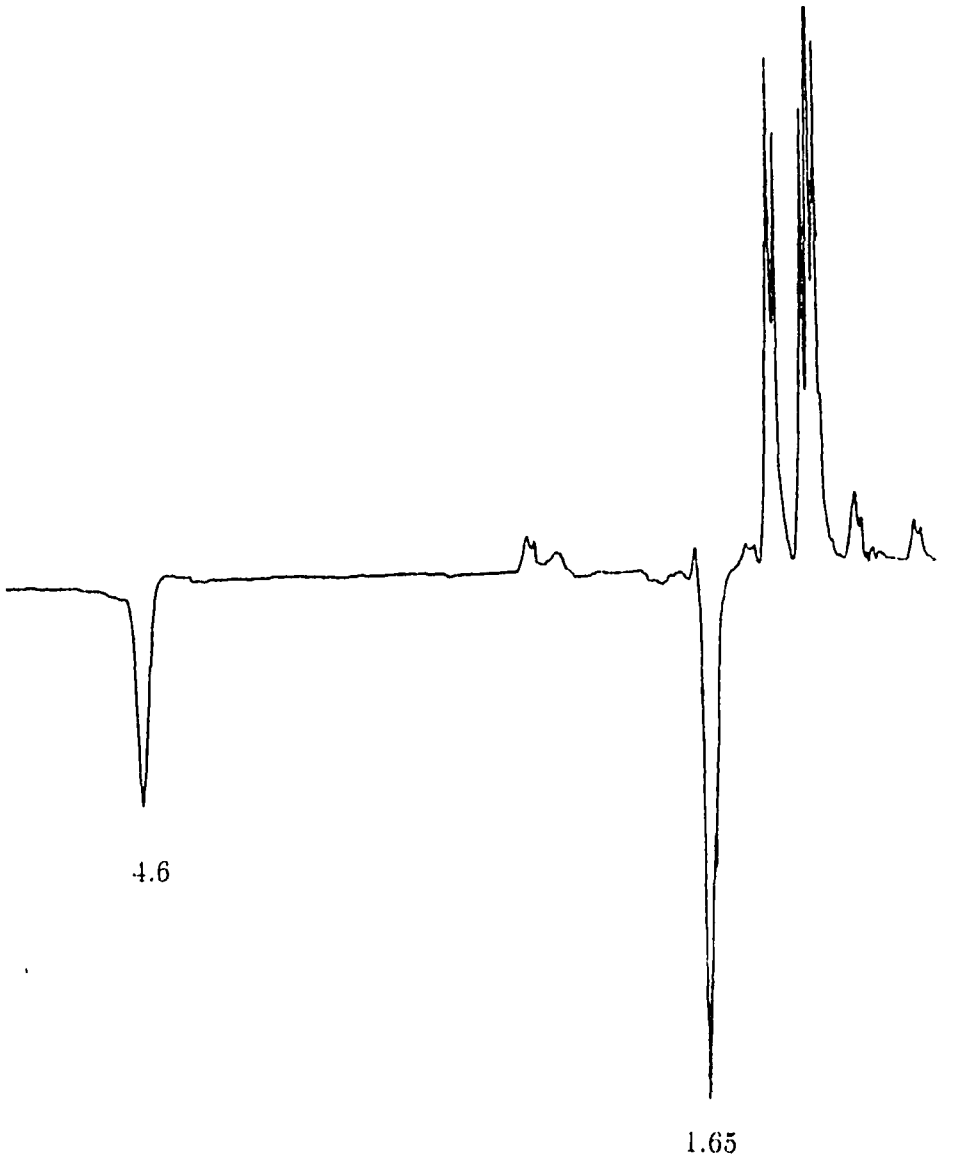

Figure 3.14: CIDNP observed during the reaction of di-*tert*-butylmercury and $S_2O_8^{2-}$ in d_6-Me_2SO at 70 °C

$$(CH_3)_3C^{\bullet} + SO_4^{-\bullet} \longrightarrow \overline{\overline{(CH_3)_3C \bullet \bullet SO_4^-}}^{F}$$
$$\longrightarrow (CH_3)_2C = CH_2 + HSO_4^- \qquad (3.36)$$

The isobutene emission can be explained by Kaptein's rules

$$\Gamma_n = \mu\varepsilon\Delta g A_i = + + -+ = -(E)$$

since μ = +(F precursor), ε = +(disproportionation product) and A(CH_3)> 0 for the *tert*-butyl radical. The g_1-factor of the *tert*-butyl radical (2.0026) is less than the g_2-factor of the sulfate radical ion (2.022), i.e.; $\Delta g = g_1 - g_2 < 0$

The initial step forming *tert*-butyl radicals may involve S_H2 mechanisms in the reaction of di-*tert*-butylmercury with peroxydisulfate ion.

$$S_2O_8^{2-} \longrightarrow 2\,SO_4^{-\bullet}$$

$$SO_4^{-\bullet} + Hg(C(CH_3)_3)_2 \longrightarrow (CH_3)_3CHgSO_4^- + \bullet C(CH_3)_3 \qquad (3.37)$$

Alternatively, the di-*tert*-butylmercury may be cleaved by peroxydisulfate ion, via electron transfer.

$$(CH_3)_3CHgC(CH_3)_3 + S_2O_8^{2-} \longrightarrow [((CH_3)_3C)_2HgS_2O_8^{2-}] \qquad (3.38)$$

$$[((CH_3)_3C)_2Hg^{+\bullet}S_2O_8^{2-\bullet}] \longrightarrow (CH_3)_3CHg^+ + \bullet C(CH_3)_3 + SO_4^{-\bullet} + SO_4^{2-} \qquad (3.39)$$

The *tert*-butyl radicals can form *tert*-butyl/*tert*-butyl radical pairs or *tert*-butyl/sulfate radical ion pairs.

$$\overline{(CH_3)_3C\bullet\bullet C(CH_3)_3}^{F} \longrightarrow (CH_3)_2C=CH_2^*(A/E) + (CH_3)_3CH^* \quad (A/E) \tag{3.40}$$

$$\overline{(CH_3)_3C\bullet\bullet SO_4^-}^{F} \longrightarrow (CH_3^*)_3C=CH_2 + HSO_4^- \tag{3.41}$$

$$\overline{(CH_3)_3C\bullet\bullet SO_4^-}^{F} \longrightarrow (CH_3)_3C^{+*} + SO_4^{2-} \tag{3.42}$$

$$(CH_3)_3C^{+*} \longrightarrow (CH_3)_2C=CH_2^* + H^+ \tag{3.43}$$

On the basis of the E polarization, the S_H2 or ET path must predominate in the reaction.

$Et_2Hg/(NH_4)_2S_2O_8^{2-}$

Figure 3.15 shows the CIDNP spectrum obtained during the reaction of diethylmercury with peroxydisulfate ion in d_6-Me_2SO at 80 °C. The A/E multiplet polarization observed at $\delta = 0.85$ belong to the methyl protons of butane. The A/E multiplet results from the radical F-pair (2Et•). On the basis of these results, the following free-radical paths can be assumed (Scheme 7).

Scheme 7

$$S_2O_8^{2-} \longrightarrow 2SO_4^{-\bullet}$$

$$SO_4^{-\bullet} + (CH_3CH_2)_2Hg \longrightarrow CH_3CH_2^{\bullet} + CH_3CH_2HgSO_4^- \tag{3.44}$$

$$CH_3CH_2HgSO_4^- + SO_4^{-\bullet} \longrightarrow CH_3CH_2\bullet + Hg(SO_4)_2 \tag{3.45}$$

$$2\overline{CH_3CH_2\bullet}^{F} \longrightarrow CH_3CH_2CH_2CH_3 + CH_2=CH_2 + CH_3CH_3 \tag{3.46}$$

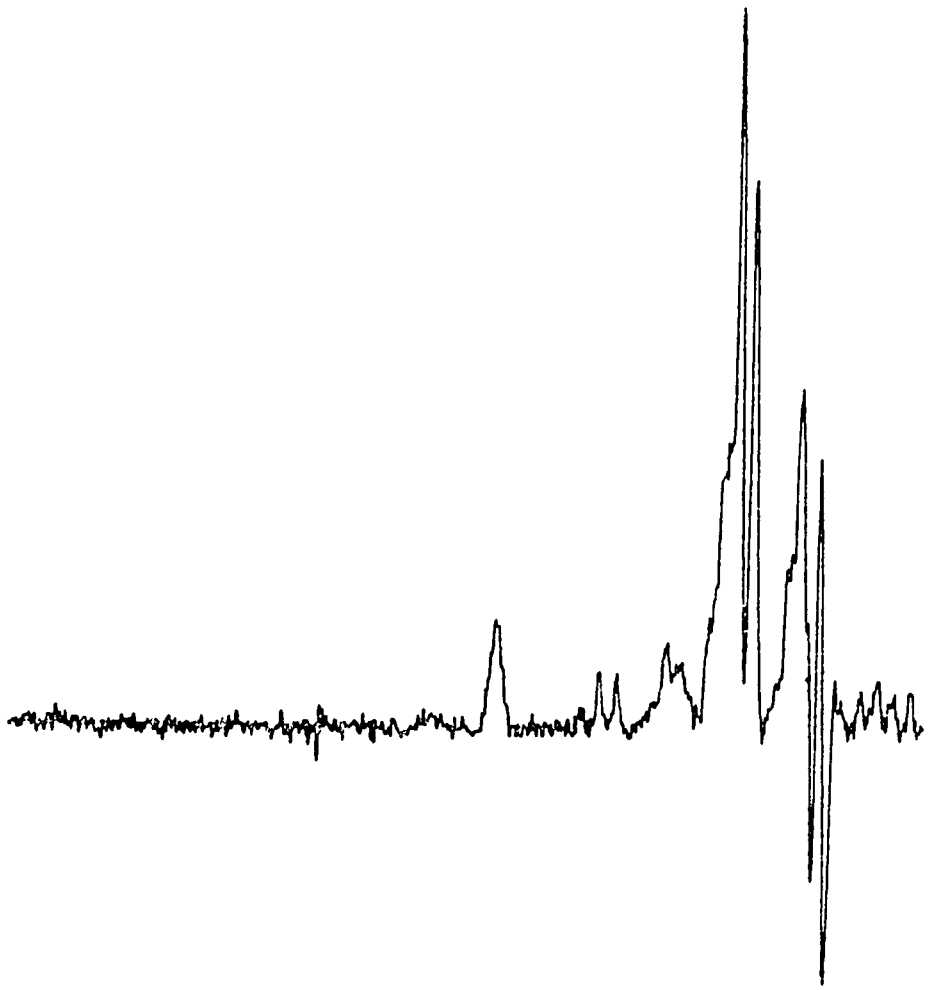

Figure 3.15: CIDNP observed during the reaction of Et_2Hg and $S_2O_8^{2-}$ in d_6-Me_2SO at 80 °C

The reaction of diethylmercury with sulfate ion forming ethyl radical may occur via an S_H2 process or electron transfer following by very fast cleavage of the diethylmercury radical cation.

$$(CH_3CH_2)_2Hg + SO_4^{-\bullet} \longrightarrow [(CH_3CH_2)_2HgSO_4^-]^\bullet \longrightarrow CH_3CH_2\bullet + CH_3CH_2HgSO_4^- \quad (3.47)$$

$$(CH_3CH_2)_2Hg + SO_4^{-\bullet} \longrightarrow [(CH_3CH_2)_2]Hg^{+\bullet} + SO_4^{2-} \longrightarrow CH_3CH_2\bullet + CH_3CH_2HgSO_4^- \quad (3.48)$$

$$(CH_3CH_2)_2Hg + SO_4^{-\bullet} \longrightarrow HSO_4^- + CH_2 = CH_2 + \bullet HgCH_2CH_3 \longrightarrow Hg + \bullet CH_2CH_3 \quad (3.49)$$

No CIDNP was observed during the reaction of di-*tert*-butylmercury with $S_2O_8^{2-}$ in d_6-Me_2SO at 80 °C.

$PhSHgC(CH_3)_3/S_2O_8^{2-}$

The NMR spectrum of $PhSHgC(CH_3)_3$ in d_6-Me_2SO is shown in Figure 3.16 at 25 °C. The signals at δ 1.37 and δ 7.28, 7.13, 7.06 are assigned to the *tert*-butyl protons and phenyl protons of $PhSHgC(CH_3)_3$, respectively. Figure 3.17 shows the CIDNP spectrum obtained during the reaction of $PhSHgC(CH_3)_3$ with $S_2O_8^{2-}$ in d_6-Me_2SO at 80 °C. The doublet for the methyl protons of isobutane (δ = 0.85) as well as the septet of the vinyl protons (δ = 4.64) and the triplet of the methyl protons (δ = 1.68) of isobutene show a pure A/E multiplet polarization. A slight A/E polarization of the methine proton of isobutane is indicated at 1.6 ppm.

These polarization contributed by radical F-pair ($(CH_3)_3C^\bullet$) are in accord with

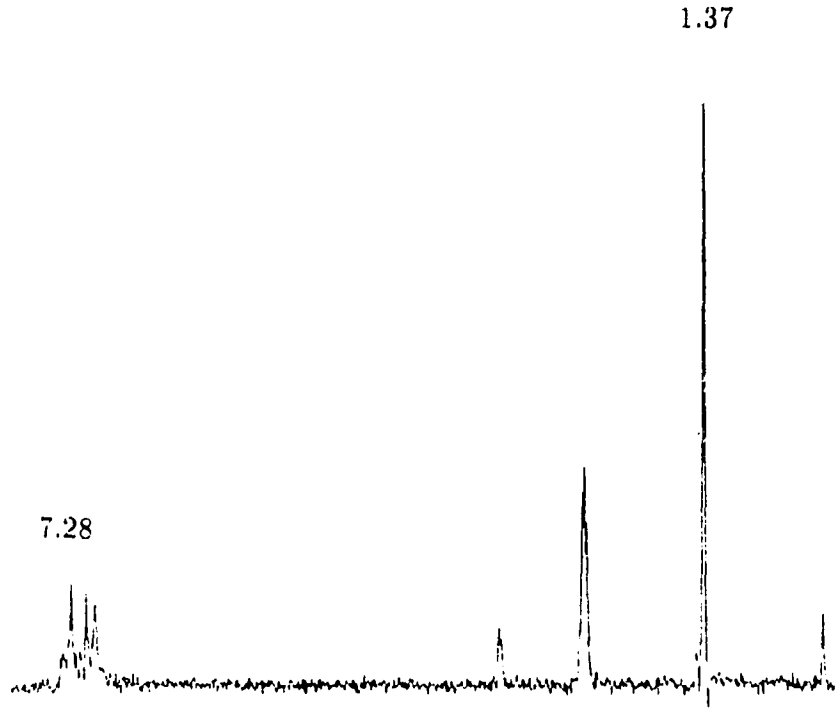

Figure 3.16: NMR spectrum of $PhSHgC(CH_3)_3$ in d_6-Me_2SO at 25 °C

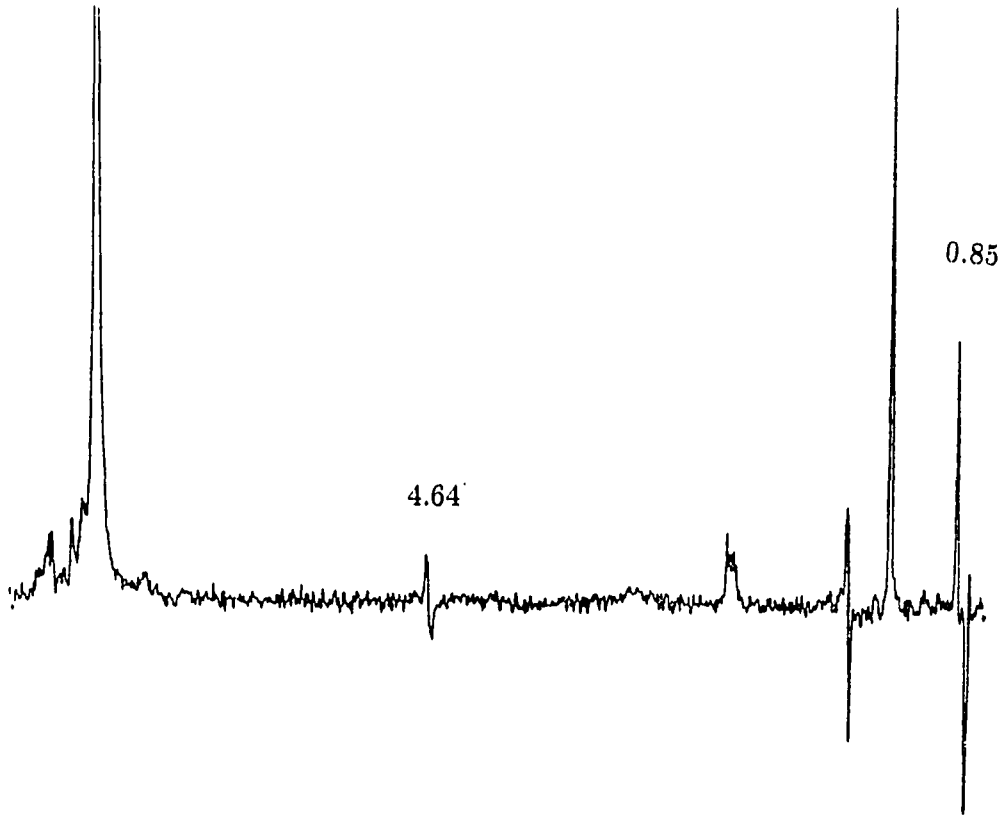

Figure 3.17: CIDNP observed during the reaction of $PhSHgC(CH_3)_3$ and $S_2O_8^{2-}$ in d_6-Me_2SO at 80 °C

Scheme 8.

Scheme 8

$$S_2O_8^{2-} \longrightarrow 2SO_4^{-\bullet}$$

$$SO_4^{-\bullet} + (CH_3)_3HgSPh \longrightarrow (CH_3)_3C\bullet + PhSHgSO_4^- \qquad (3.50)$$

$$2\overbrace{(CH_3)_3C\bullet}^{F} \longrightarrow (CH_3)_2C = CH_2 \ \ (A/E) + HC(CH_3)_3 \ \ (A/E) \qquad (3.51)$$

The System, $RHgCl/S_2O_8^{2-}/RI$

$MeHgCl/S_2O_8^{2-}/RI$

No CIDNP spectra occur in the reaction of MeHgCl with peroxydisulfate in d_6-Me_2SO at 80 °C, but in the presence of ethyl iodide, the multiplet polarization spectra shown in Figure 3.18 were observed. The signals at $\delta = 0.76$ and $\delta = 2.20$ are assigned to the methyl protons of MeHgCl and MeI respectively. A symmetrical doublet with respect to the main signal ($\delta = 0.48, 2.0$) is due to the interaction of the protons with Hg^{199} nuclei.

The E/A polarization of ethyl iodide is indicated at 1.83 ppm (methyl) and 3.20 ppm (methylene). An A/E polarization occurs for butane (methyl $\delta = 0.85$, methylene $\delta = 1.27$). These multiplet effects obtained from the ethyl radical F-pair ($Et^\bullet$) are in accord with Scheme 9.

Scheme 9

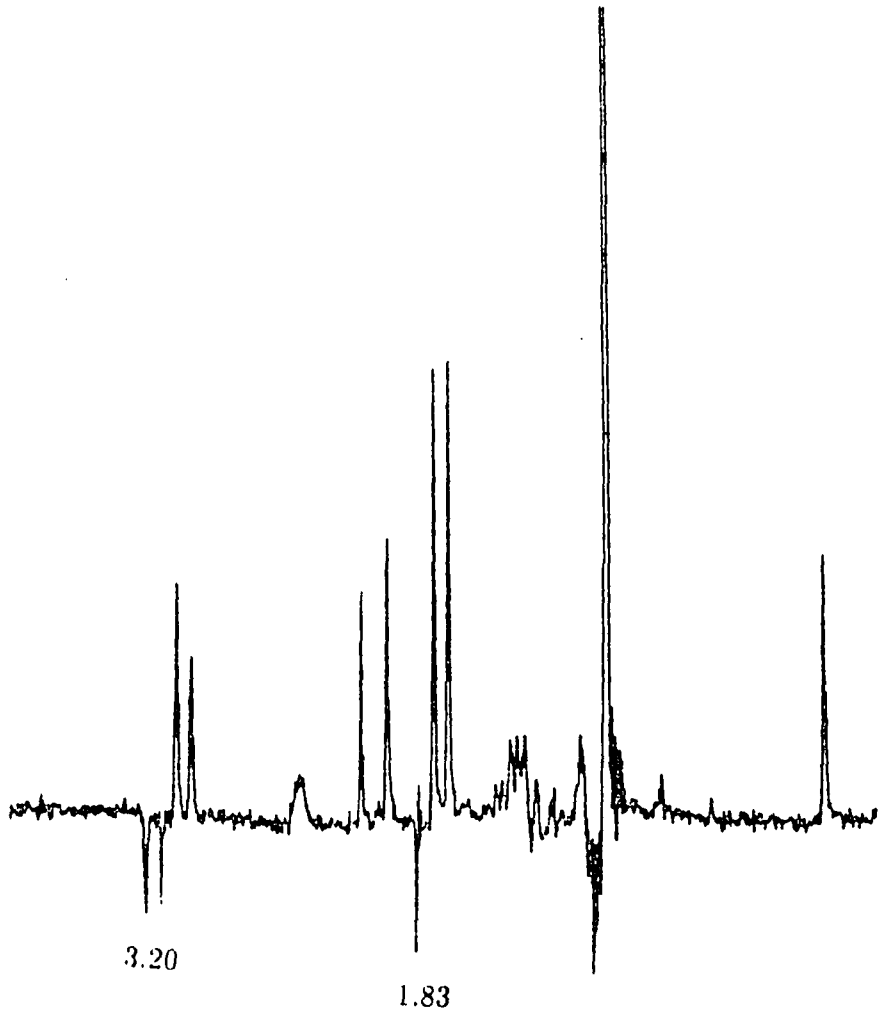

Figure 3.18: CIDNP recorded during the reaction of MeHgCl and $S_2O_8^{2-}$ in d_6-Me_2SO with CH_3CH_2I at 80 °C

$$S_2O_8^{2-} \longrightarrow 2SO_4^{-\bullet}$$

$$CH_3HgCl + SO_4^{-\bullet} \longrightarrow CH_3\bullet + ClHgSO_4^- \quad (3.52)$$

$$CH_3\bullet + CH_3CH_2I \longrightarrow CH_3CH_2\bullet + CH_3I \quad (3.53)$$

$$\overline{CH_3CH_2\bullet\bullet CH_2CH_3}^F \longrightarrow CH_3CH_2CH_2CH_3 \ (A/E) \quad (3.54)$$

$$CH_3CH_2^*\bullet + CH_3I \longrightarrow CH_3CH_2I \ (E/A) + CH_3\bullet \quad (3.55)$$

However, in the presence of isopropyl iodide, only the A/E multiplet polarization of propene and propane are observed at δ = 0.86 (methyl), 1.30 (methylene) and 1.6 (methyl), 4.88, 6.04 (vinyl) and no polarization of isopropyl iodide occurs. (the reaction analogous to Equation 3.55 is not important with i-Pr$^\bullet$). However, with PrI, polarization was observed (Figure 3.19).

$Cl_3CHgCl/S_2O_8^{2-}/RI$

Figure 3.20 shows the CIDNP spectrum obtained when trichloromethylmercury chloride reacts with peroxydisulfate ion in the presence of ethyl iodide in d_6-Me_2SO at 80 °C.

Enhanced absorption (A) and emission (E) occur for the products chloroform (δ = 8.25 E) and 1,1,1-trichloropropane (CH_3 δ = 1.22 E; CH_2 δ = 2.76 A). These polarization patterns are completely in accord with Equation 3.59 of Scheme 10.

Scheme 10

$$S_2O_8^{2-} \longrightarrow 2SO_4^{-\bullet}$$

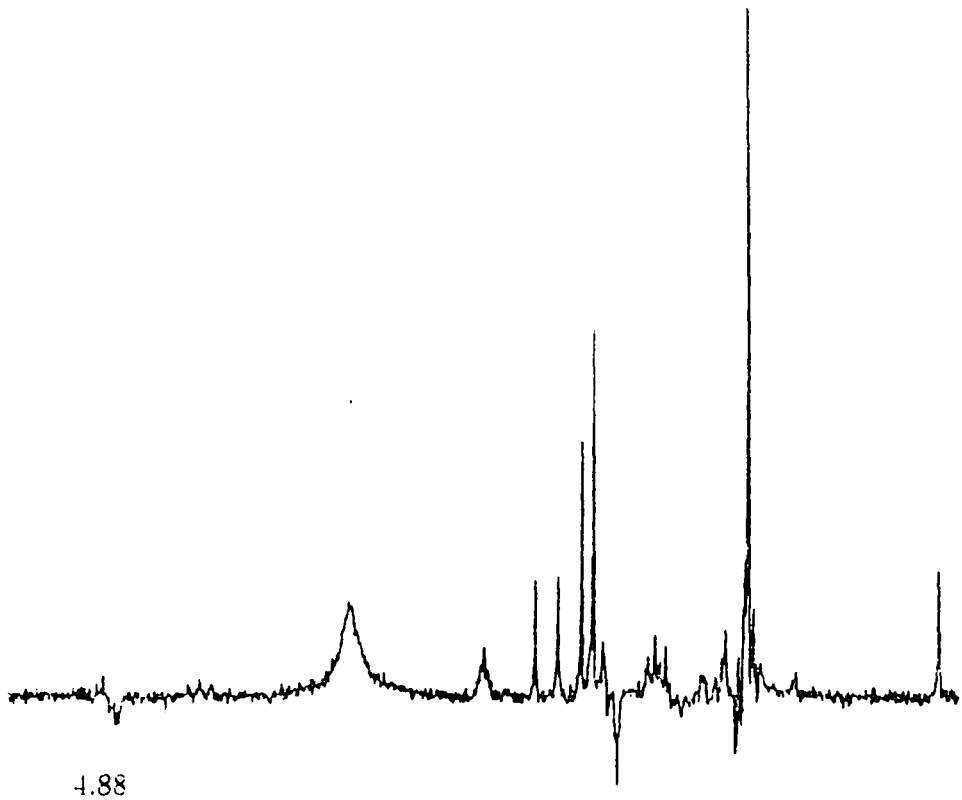

Figure 3.19: CIDNP recorded during the reaction of MeHgCl and $S_2O_8^{2-}$ in d_6-Me_2SO with $(CH_3)_2CHI$ at 80 °C

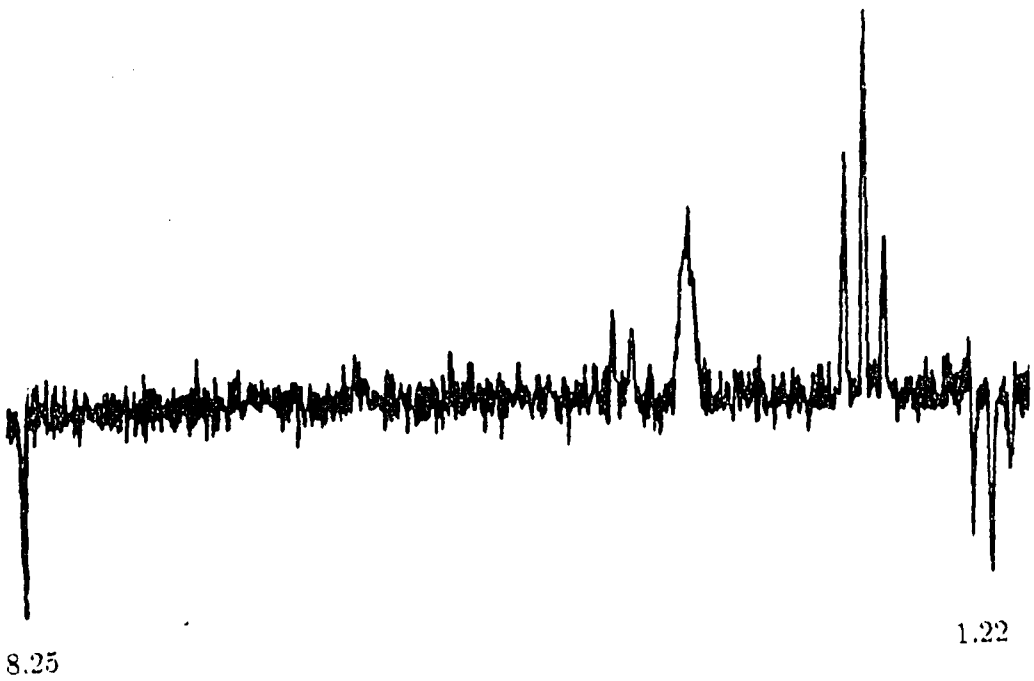

Figure 3.20: CIDNP recorded during the reaction of Cl_3CHgCl and $S_2O_8^{2-}$ in d_6-Me_2SO with CH_3CH_2I at 80 °C

$$SO_4^{-\bullet} + Cl_3CHgCl \longrightarrow Cl_3C\bullet + ClHgSO_4^- \quad (3.56)$$

$$\overline{Cl_3C\bullet\bullet CCl_3} \longrightarrow \bullet CCl_3^* \quad (3.57)$$

$$\bullet CCl_3^* + CH_3CH_2I \longrightarrow CH_3CH_2\bullet + Cl_3CI \quad (3.58)$$

$$\overline{CH_3CH_2\bullet\bullet Cl_3C}^F \longrightarrow CHCl_3 + CH_2 = CH_2 + CH_3CH_2CCl_3 \quad (3.59)$$

The net polarization of trichloropropane and chloroform can be explained by Kaptein's rule:

$$\Gamma_n = \mu\varepsilon\Delta g A_i$$

$$\Gamma_n(CH_3) = ++-+ = -(E)$$

$$\Gamma_n(CH_2) = ++-- = +(A)$$

$$\Gamma_n(CHCl_3) = ++-+ = -(E)$$

μ = +(F precursor), ε = + (disproportionation product),

$\Delta g = g$(ethyl)$-g$(trichloromethyl)= 2.0026 − 2.0091 < 0,

and A(CH_3)> O, A(CH_2)< 0 for the ethyl radical.

c-$C_3H_5HgBr/S_2O_8^{2-}$/RI

Polarized spectra were encountered during the reaction of cyclopropylmercury bromide with peroxydisulfate ion in presence of ethyl iodide in d_6-Me_2SO at 80 °C (Figure 3.21). The multiplet effect (A/E+E) may belong to butane. The weak E/A polarization of ethyl iodide at δ = 3.27 and δ = 1.86 is due to escape of polarized ethyl radicals from the radical pair.

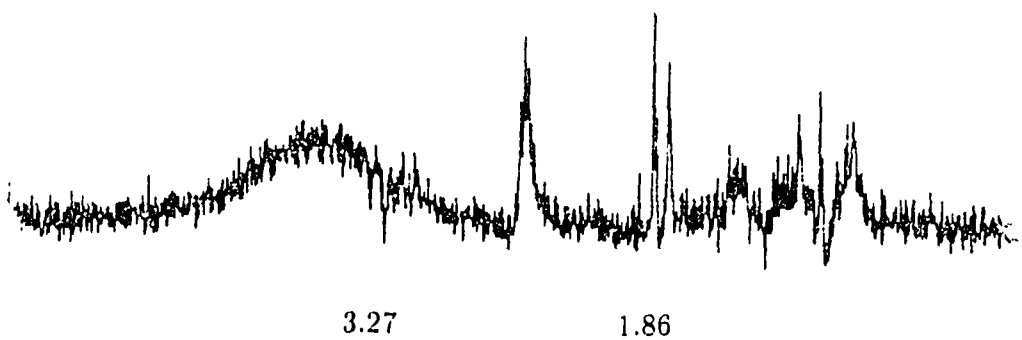

Figure 3.21: CIDNP recorded during the reaction of *c*-C_3H_5HgCl and $S_2O_8^{2-}$ in d_6-Me_2SO with CH_3CH_2HgI at 80 °C

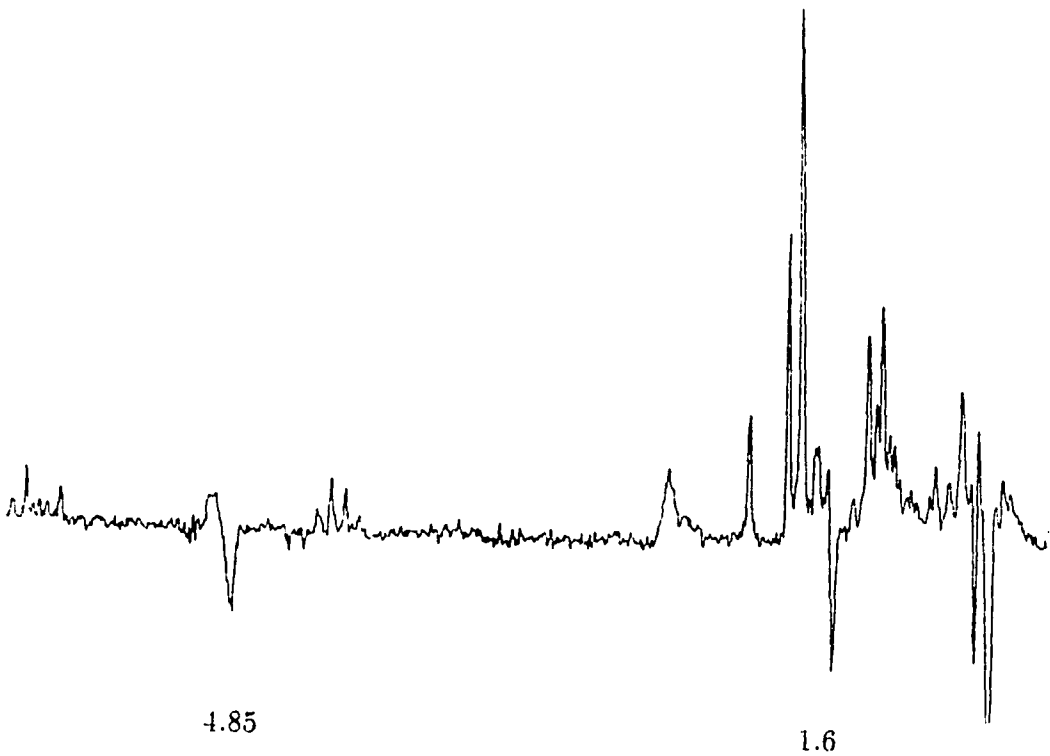

Figure 3.22: CIDNP recorded during the reaction of *c*-C_3H_5HgCl and $S_2O_8^{2-}$ in d_6-Me_2SO with $(CH_3)_2CHI$ at 80 °C

Figure 3.22 shows the CIDNP spectrum during the reaction of cyclopropylmercury bromide with peroxydisulfate ion in presence of isopropyl iodide in d_6-Me_2SO at 80 °C. The A/E + E multiplet polarizations are observed for propene (δ=1.6, 4.85 and 5.85). The E/A multiplets observed at δ = 1.84 and 4.86 belong to isopropyl iodide. The strong multiplets (E + A/E) at δ = 0.76 and 0.85 have not been assigned. Perhaps these lines belong to propane. These polarizations result from the radical F-pairs, $\overline{(CH_3)_2CH\bullet\bullet HC(CH_3)_2}^F$, $\overline{(CH_3)_2CH\bullet\bullet c\text{-}C_3H_5}^F$. These polarizations are in accord with the reactions of Scheme 11

Scheme 11

$$S_2O_8^{2-} \longrightarrow 2SO_4^{-\bullet}$$

$$SO_4^{-\bullet} + c\text{-}C_3H_5HgBr \longrightarrow c\text{-}C_3H_5\bullet + BrHgSO_4^- \quad (3.60)$$

$$c\text{-}C_3H_5\bullet + (CH_3)_2CHI \longrightarrow c\text{-}C_3H_5I + (CH_3)_2CH\bullet \quad (3.61)$$

$$\overline{(CH_3)_2CH\bullet\bullet HC(CH_3)_2}^F \longrightarrow CH_3CH=CH_2 + CH_3CHCH_3 \quad (3.62)$$

$$\overline{c\text{-}C_3H_5\bullet\bullet CH(CH_3)_2}^F \longrightarrow c\text{-}C_3H_4 + CH_3CH_2CH_3 \quad (3.63)$$

$$\overline{c\text{-}C_3H_5\bullet\bullet CH(CH_3)_2}^F \longrightarrow c\text{-}C_3H_6 + CH_3CH=CH_3 \quad (3.64)$$

$$\overline{c\text{-}C_3H_5\bullet\bullet CH(CH_3)_2}^F \longrightarrow c\text{-}C_3H_5CH(CH_3)_2 \quad (3.65)$$

$$\overline{(CH_3)_2CH\bullet\bullet c\text{-}C_3H_5}^F + (CH_3)_2CHI \longrightarrow (CH_3)_2CH^*I \text{ or } c\text{-}C_3H_5^*I + (CH_3)_2CH\bullet \text{ or } c-C_3H_5\bullet \quad (3.66)$$

The net effect rule applied to propane and propene would give

$$\Gamma_{(C\underline{H}_3CH_2CH_3)} = ++-+ = -(E)$$

$$\Gamma_{(C\underline{H}_3CH{=}CH_2)} = ++-+ = -(E)$$

Since for

$$\overline{c\text{-}C_3H_5 \bullet\bullet HC(CH_3)_3}^F$$

$\mu = +$(F precursor), $\varepsilon = +$(disproportionation), $A(CH_3) > 0$

in the isopropyl radical and

$\Delta g = g(i\text{-Pr}\bullet) - g(c\text{-}C_3H_5\bullet) = 2.0026 - 2.0028 < 0.$

For escape of cyclopropyl radical from the cage a net polarization of emission is predicted for the cyclopropyl iodide.

$$\Gamma_{ne} = +-++ = -(E)$$

.

$ClHgCH_2CHO/S_2O_8^{2-}/CH_3CH_2I$

No CIDNP was observed during the reaction of $ClHgCH_2CHO$ with $S_2O_8^{2-}$ in d_6-Me_2SO at 80 °C. However, the NMR spectrum recorded immediately after addition of ethyl iodide to a solution of $ClHgCH_2CHO$ and $S_2O_8^{2-}$ in d_6-Me_2SO showed in Figure 3.23. E/A polarization for the ethyl iodide is shown at 3.19 ppm and 1.80 ppm. There are a number of E lines at 0.87, 2.36, 3.60 and 4.09 ppm that have not been assigned. We suggest that these lines belong to coupling and/or disproportionation products of radical pair $\overline{CH_3CH_2\bullet \bullet CH_2CHO}^F$ (Scheme 12)

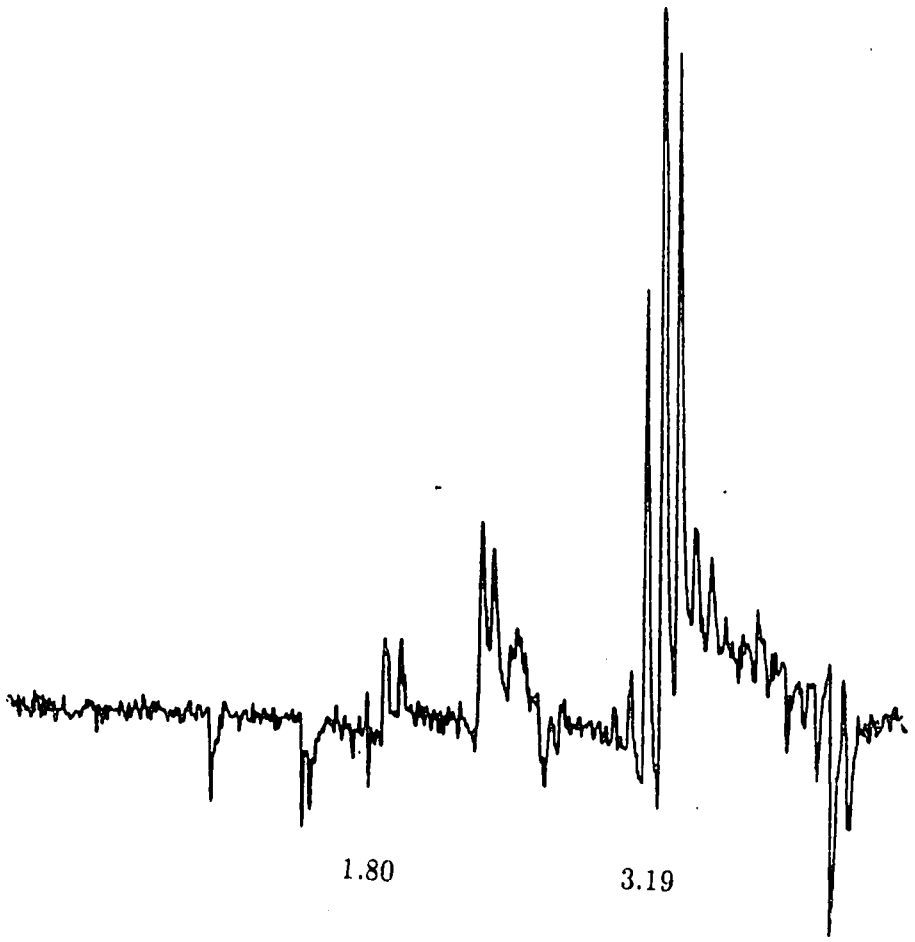

Figure 3.23: CIDNP recorded during the reaction of ClHgCHO and $S_2O_8^{2-}$ in d_6-Me_2SO with CH_3CH_2I at 80 °C

Scheme 12

$$S_2O_8^{2-} \longrightarrow 2SO_4^{-\bullet}$$

$$SO_4^{-\bullet} + ClHgCH_2CHO \longrightarrow ClHgSO_4^- + \bullet CH_2CHO \quad (3.67)$$

$$CH_3CH_2I + \bullet CH_2CHO \longrightarrow CH_3CH_2\bullet + ICH_2CHO \quad (3.68)$$

$$2\overline{CH_3CH_2\bullet}^F \longrightarrow CH_2CH_2 + CH_3CH_3 + CH_3CH_2CH_2CH_3 \quad (A/E) \quad (3.69)$$

$$CH_3CH_2^*\bullet + CH_3CH_2I \longrightarrow CH_3CH_2^*I \quad (E/A) \quad (3.70)$$

$$\overline{CH_3CH_2\bullet\bullet CH_2CHO}^F \longrightarrow CH_2CH_2 + CH_3CHO + CH_3CH_2CH_2CHO \quad (3.71)$$

$$\overline{CH_2=CHO\bullet\bullet CH_2CH_3}^F \longrightarrow CH_2=CHOCH_2CH_3 \quad (3.72)$$

The E effects for all protons would result from free radical encounters (F type). Kaptein's net rule for the emission line of butyraldehyde would give

$$\Gamma_{ne}(-CH_3) = ++-+ = -(E) \quad \delta = 0.86$$

$$\Gamma_{ne}(-CH_2-) = ++-- = +(A) \quad \delta = 1.54$$

$$\Gamma_{ne}(-CH_2-CHO) = +++- = -(E) \quad \delta = 2.35$$

Since $\mu = +$(F precursor), $\varepsilon = +$(coupling product),

$\Delta g = g(CH_3CH_2\bullet) - g(\bullet CH_2CHO) < 0$, $A(CH_3) > 0$, and

$A(CH_2) < 0$ for ethyl radical and

$A(CH_2) < 0$ for the radical $\bullet CH_2CHO$.

The System, $R_2Hg/S_2O_8^{2-}/RI$

$Ph_2Hg/S_2O_8^{2-}/RI$

The reactions of diphenylmercury with peroxydisulafate ion in the presence of alkyl iodides such as ethyl iodide, isopropyl iodide and propyl iodide give rise to E/A polarization. Figure 3.24 shows the spectrum obtained during the reaction of diphenylmercury with peroxydisulfate ion in the presence of ethyl iodide in d_6-Me_2SO at 80 °C. The NMR spectra of the products, butane (δ 0.84, 1.2) and ethyl iodide (δ 1.75, 3.18) show pure A/E and E/A multiplet polarization, respectively. Figure 3.25 shows the spectrum obtained from a reaction between diphenylmercury and peroxydisulfate ion in presence of isopropyl iodide. The A/E multiplets of propane and propene are seen at δ 0.78, 1.30 and 1.60, 4.90, 5.16.

The CIDNP spectrum resulting from the reaction of diphenylmercury with peroxydisulfate ion in the presence of propyl iodide is shown in Figure 3.26. The products propane (methyl δ 0.81), propene (vinyl methylene, δ 4.86) and propyl iodide (α-methylene, δ 3.12) show A/E, A/E and E/A multiplets respectively.

As we have seen, the reaction of alkylmercurials with peroxydisulfate ion give rise to A/E multiplets for alkene and alkane and E/A multiplets for alkyl iodide due to the coupling and/or disproportionation and escape of the diffusive radical pair. The following mechanism of the reaction would accord with the A/E and E/A multiplet polarization for diffusion pair $\overline{R\bullet \ \bullet R}^F$.

Scheme 13

$$S_2O_8^{2-} \longrightarrow SO_4^{-\bullet}$$

Figure 3.24: CIDNP recorded during the reaction of Ph_2Hg and $S_2O_8^{2-}$ in d_6-Me_2SO with CH_3CH_2I at 80 °C

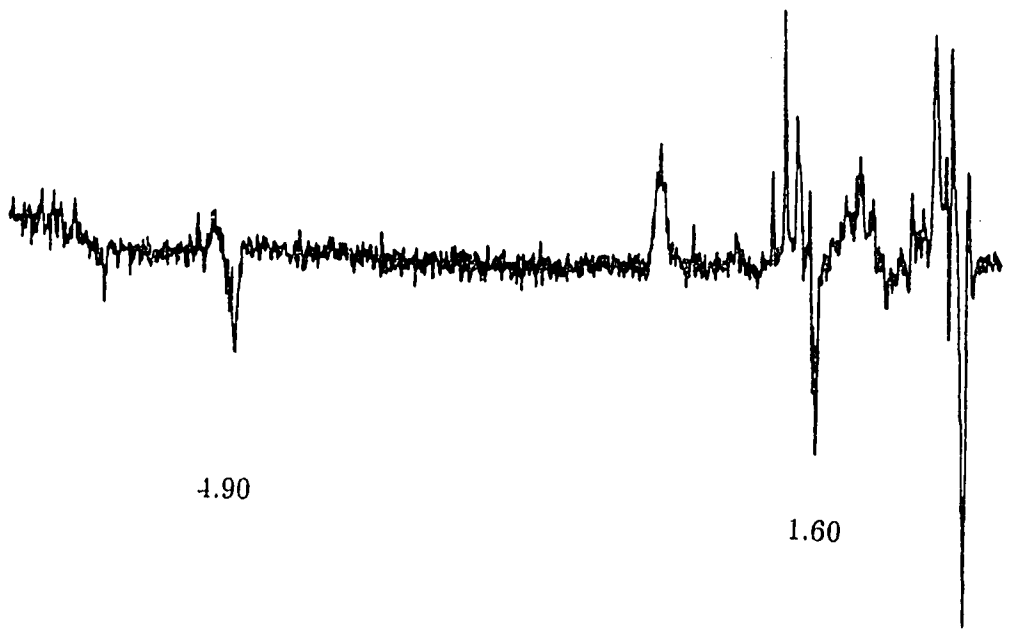

Figure 3.25: CIDNP recorded during the reaction of Ph_2Hg and $S_2O_8^{2-}$ in d_6-Me_2SO with $(CH_3)_2CHI$ at 80 °C

Figure 3.26: CIDNP recorded during the reaction of Ph_2Hg and $S_2O_8^{2-}$ in d_6-Me_2SO with $CH_3CH_2CH_2I$ at 80 °C

$$Ph_2Hg + SO_4^{-\bullet} \longrightarrow Ph\bullet + PhHgSO_4^- \quad (3.73)$$

$$Ph\bullet + RI \longrightarrow PhI + R\bullet \quad (3.74)$$

$$\overline{R\bullet\bullet R}^F \longrightarrow R(\text{-}H) + RH + R\text{-}R \quad (3.75)$$

$$\overline{R\bullet\bullet R}^F \longrightarrow 2\,R^*\bullet \quad (3.76)$$

$$\Gamma_{me} = + + + - ++ = -(A/E)$$

$$R^*\bullet + RI \longrightarrow R^*I + R\bullet \quad (3.77)$$

$$\Gamma_{me} = + - + - ++ = +(E/A)$$

The sulfate radical ion $SO_4^{-\bullet}$ generated from the dissociation of peroxydisulfate ion reacts rapidly with diphenylmercury to form the phenyl radical via S_H2 or ET.

$$SO_4^{-\bullet} + Ph_2Hg \longrightarrow [Ph_2HgSO_4^-]\bullet \longrightarrow Ph\bullet + PhHgSO_4^- \quad (3.78)$$

$$SO_4^{-\bullet} + Ph_2Hg \longrightarrow SO_4^{2-} + Ph_2Hg^{+\bullet} \longrightarrow Ph\bullet + PhHg^+ \quad (3.79)$$

Figure 3.27 shows the multiplet polarization obtained during the reaction of diphenylmercury with peroxydisulfate ion in presence of butyl iodide. The weak A/E multiplet of 1-butene is seen at δ 4.86 and the E/A multiplet of butyl iodide is observed clearly at δ 3.24 ($CH_3CH_2CH{=}C\underline{H}_2$ and $CH_3CH_2CH_2C\underline{H}_2I$, respectively).

$((EtO)_2PO)_2Hg/S_2O_8^{2-}/EtI$

No CIDNP spectrum was observed during the reaction of $((EtO)_2PO)_2Hg$ with $S_2O_8^{2-}$ in d_6-Me_2SO at 80 °C. However, in presence of EtI, multiplet polarization

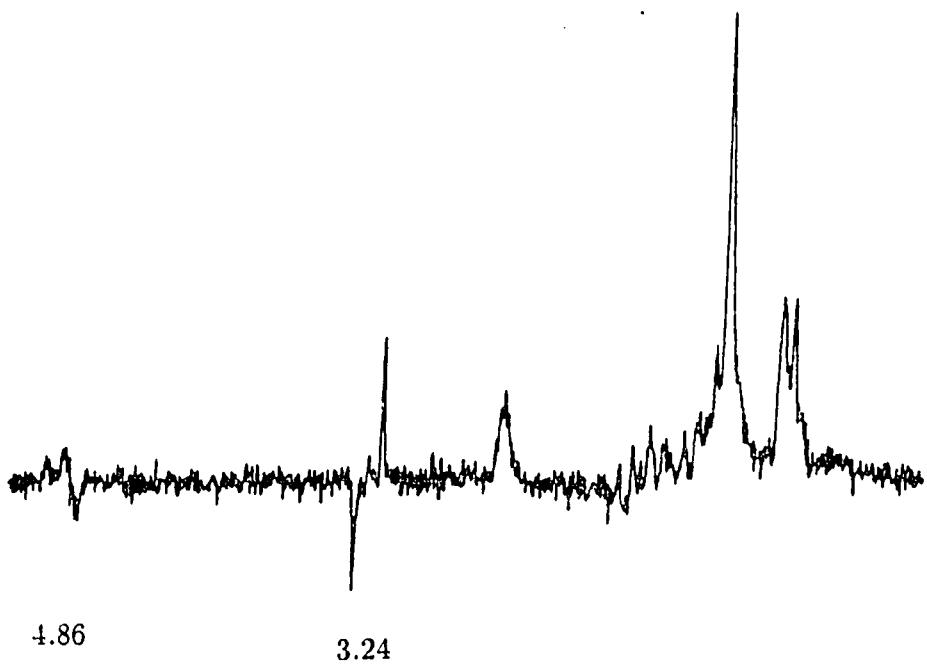

Figure 3.27: CIDNP recorded during the reaction of Ph_2Hg and $S_2O_8^{2-}$ in d_6-Me_2SO with $CH_3CH_2CH_2CH_2I$ at 80 °C

spectrum are observed. The signals at δ =1.18 (CH_3) and δ =3.88 (CH_2) are assigned to the ethyl of $((EtO)_2PO)_2Hg$. An E/A polarization of the ethyl iodide is shown at 3.22 ppm (CH_2) and 1.88 ppm (CH_3). The A/E multiplet belongs to butane (CH_3 δ=0.85). With *i*-PrI, A/E multiplet effects of propane (methyl δ 0.81) and propene (vinyl methylene δ 4.88) are also observed. These polarization are in accordance with Scheme 14.

Scheme 14

$$S_2O_8^{2-} \longrightarrow 2SO_4^{-\bullet}$$

$$((EtO)_2PO)_2Hg + SO_4^{-\bullet} \longrightarrow (EtO)_2P^{\bullet}O + (EtO)_2POHgSO_4^{-} \quad (3.80)$$

$$(EtO)_2P^{\bullet}O + RI \longrightarrow (EtO)_2POI + R\bullet \quad (3.81)$$

$$R = Et, \quad i\text{-}pr$$

$$R\bullet + R\bullet \longrightarrow \overline{R\bullet\bullet R}^F \longrightarrow R\text{-}R^* + R(H)^* + R(\text{-}H)^* \quad (3.82)$$

$$\overline{R\bullet\bullet R}^F + RI \longrightarrow R^*I + R\bullet \quad (3.83)$$

$$2(EtO)_2P^{\bullet}O \longrightarrow (EtO)_2P\text{-}P(OEt)_2 \quad (3.84)$$

$(PhCOCH_2)_2Hg/S_2O_8^{2-}$ / $(CH_3)_2CHI$

Polarized spectra were encountered during the reaction of $(PhCOCH_2)_2Hg$ with peroxydisulfate ion in the presence of isopropyl iodide in d_6-Me_2SO at 80 °C. There are a number of E lines at 0.87, 1.61, 2.53, 4.50 and 4.86 ppm that have not been assigned. We suggest that these lines belong to coupling and/or disproportionation products of the radical pair $\overline{PhCOCH_2\bullet\bullet CH(CH_3)_2}^F$.

These net polarizations can be explained by Kaptein's rules.

$$\overline{PhCOCH_2\bullet\bullet CH(CH_2)_2}^F + (CH_3)_2CHI \longrightarrow PhCOCH_2I\,(A) + (CH_3)_2CHI^* + (CH_2)CH\bullet$$

$\mu = +, \quad \varepsilon = -,$

$\Gamma_{ne} = + - +- = +(A)$ for $PhCOC\underline{H}_2I,$

$\Gamma_{ne} = + - -+ = +(A)$ for $(C\underline{H}_3)_2CHI,$

$\Gamma_{ne} = + - -- = -(E)$ for $(CH_3)_2C\underline{H}I,$

$$\overline{PhCOCH_2\bullet\bullet CH(CH_2)_2}^F \longrightarrow PhCOCH_3 + CH_3CH{=}CH_2 + PhCOCH_2CH_2(CH_3)_2$$

$\mu = +, \quad \varepsilon = +,$

$\Gamma_n = + + -+ = -(E)$ for $PhCOC\underline{H}_3,$

$\Gamma_n = + + -+ = -(E)$ for $C\underline{H}_3CH{=}CH_2,$

$\Gamma_n = + + -- = +(A)$ for $CH_2\text{-}C\underline{H}{=}CH_2,$

$\Gamma_n = + + -+ = -(E)$ for $PhCOCH_2CH_2(C\underline{H}_3)_2,$

$\Gamma_n = + + -- = +(A)$ for $PhCOCH_2C\underline{H}(CH_3)_2,$

$\Gamma_n = + + +- = -(E)$ for $PhCOC\underline{H}_2CH(CH_3)_2.$

The System, $RHgNO_3/(NH_4)_2S_2O_8/AgNO_3$

Despite the relatively high oxidation potential for the half-reaction (Equation 3.85) many oxidations by peroxydisulfate do not proceed at a convenient

rate at ambient temperatures.

$$S_2O_8^{2-}(aq.) + 2e \longrightarrow 2SO_4^{2-}(aq.) \tag{3.85}$$

$$E^\circ = 2.1V$$

Many oxidations by $S_2O_8^{2-}$ involve a rate-limiting homolysis given by Equation 3.86 which has an activation energy of approximately 30 kcal/mole.

$$S_2O_8^{2-} \longrightarrow 2SO_4^{-\bullet} \tag{3.86}$$

The decomposition of the peroxydisulfate ion, however, is accelerated by silver and other metal ions.

$$Ag^+ + S_2O_8^{2-} \longrightarrow Ag^{2+} + SO_4^{2-} + SO_4^{-\bullet} \tag{3.87}$$

$$Ag^+ + SO_4^{-\bullet} \longrightarrow Ag^{2+} + SO_4^{2-} \tag{3.88}$$

Silver(II) species are among the most powerful oxidants (E°=1.98V) available for organic and inorganic reactions [25], e.g., Equation 3.89.

$$RCO_2H + Ag^{2+} \longrightarrow RCOO\bullet + Ag^+ + H^+ \tag{3.89}$$

In aqueous solutions, Ag^{2+} is viable only in highly acidic media in which it is in equilibrium with Ag^{3+}.

$$2Ag^{2+} \rightleftharpoons Ag^+ + Ag^{3+} \tag{3.90}$$

$(CH_3)_2CHHgNO_3$/ $(NH_4)_2S_2O_8$/$AgNO_3$

The NMR spectrum of $(CH_3)_2CH\,HgNO_3$ in d_6-Me_2SO is shown in Figure 3.28. The signals at δ= 1.30 and 2.48 are assigned to the methyl protons and the methine protons of isopropylmercury nitrate. Satellites (Hg^{199}-C-C-H) are observed at

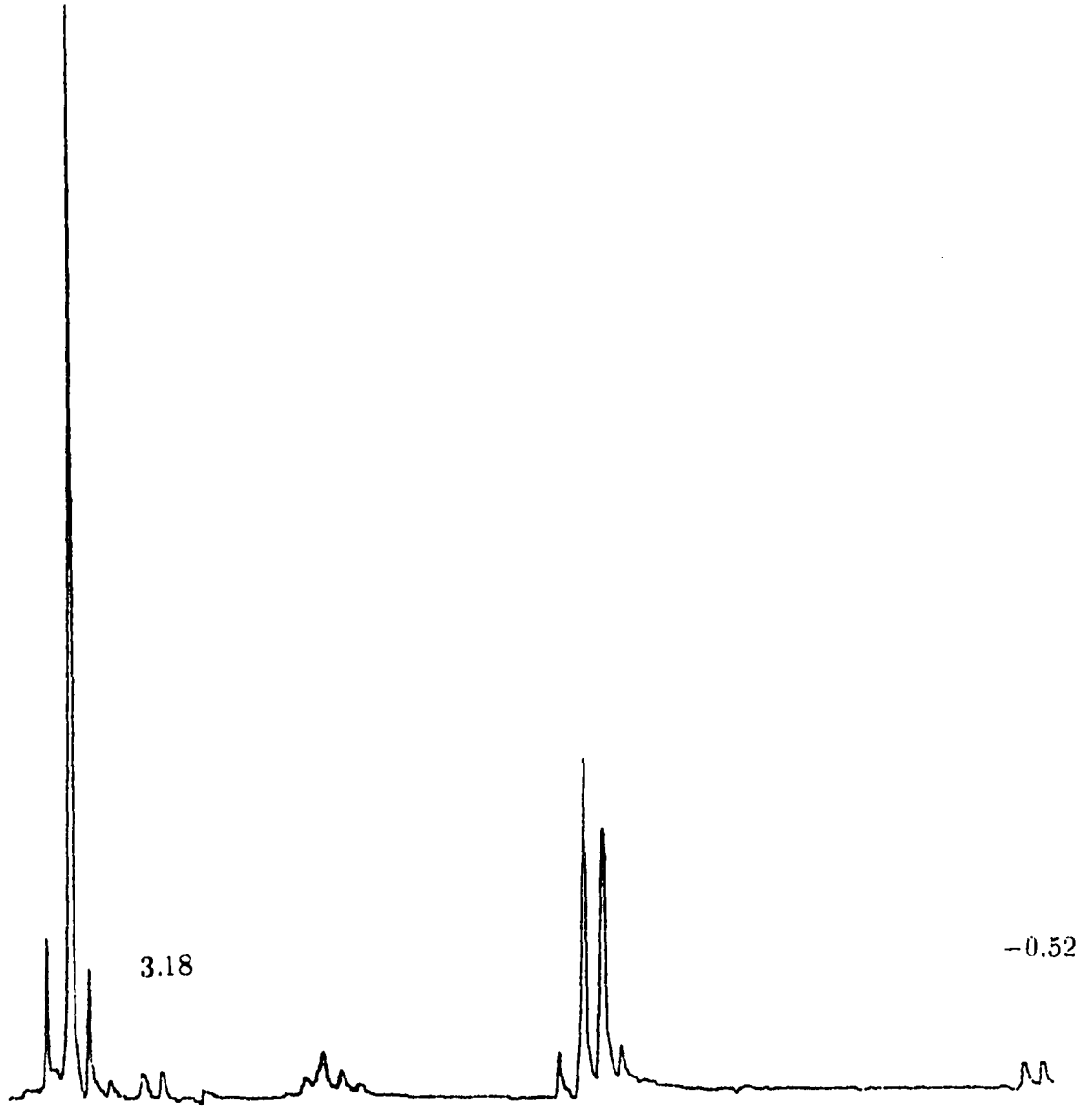

Figure 3.28: The NMR spectrum of $(CH_3)_2CHHgNO_3$ and $S_2O_8^{2-}$ in d_6-Me_2SO at 25 °C

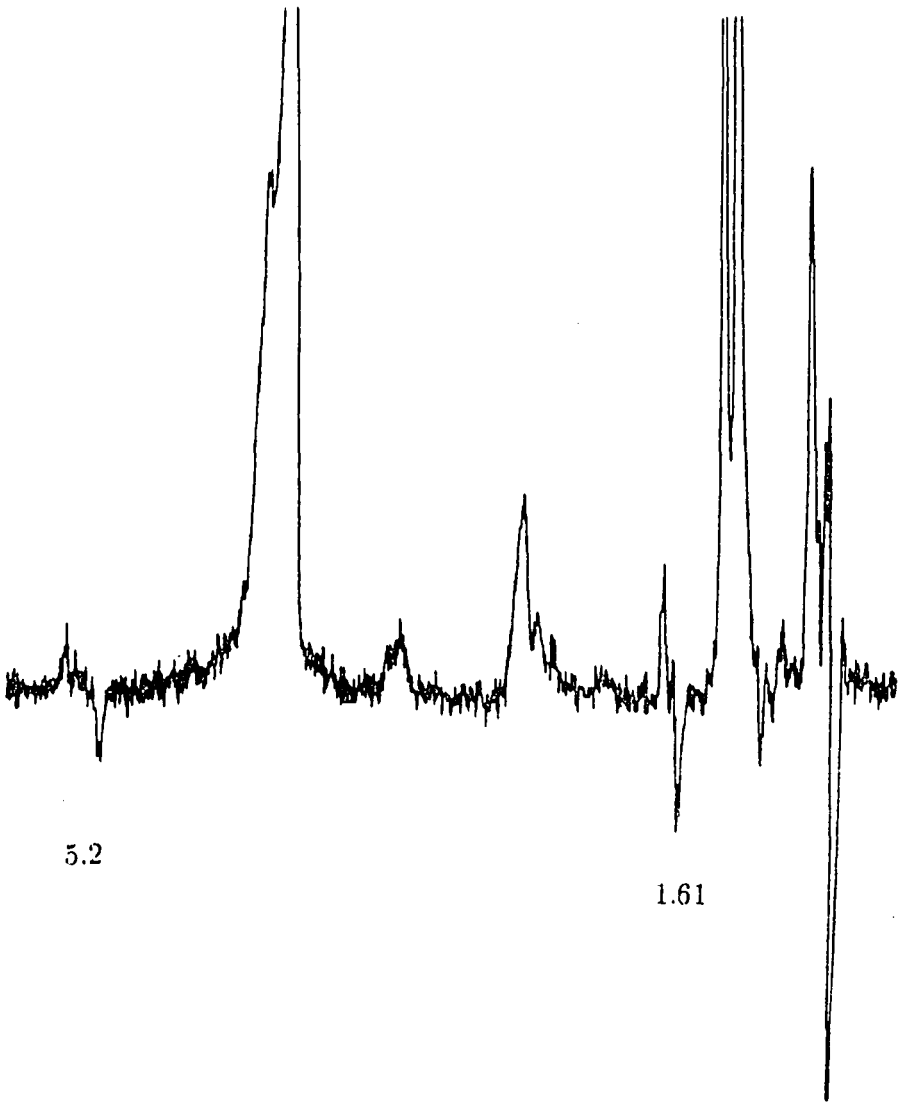

Figure 3.29: CIDNP recorded during the reaction of $(CH_3)_2CHHgNO_3$ and $S_2O_8^{2-}$ in d_6-Me_2SO with $AgNO_3$ at 25 °C

$\delta = -0.52$ and $\delta = 3.18$. When the $AgNO_3$ was added to $(CH_3)_2CHHgNO_3/S_2O_8^{2-}$ solution at 25 °C, pure A/E multiplet polarization was immediately observed as shown in Figure 3.29. The polarizations of propane (CH_3 δ=0.75, CH_2 δ=1.16) and propene (CH_3 δ=1.61, -CH_2=CH_2 δ=5.2, 6.2) result from radical pair reaction of 2 $(CH_3)_2CH\bullet$.

These polarization patterns are completely in accord with Equation 3.96 of Scheme 15.

Scheme 15

$$S_2O_8^{2-} + Ag^+ \longrightarrow SO_4^{2+} + SO_4^{-\bullet} + Ag^{2+} \quad (3.91)$$

$$SO_4^{-\bullet} + Ag^+ \longrightarrow SO_4^{2+} + Ag^{2+} \quad (3.92)$$

$$(CH_3)_2CHHg^+NO_3^- \rightleftharpoons (CH_3)_2CHHg^+ + NO_3^- \quad (3.93)$$

$$(CH_3)_2CHHg^+ + Ag^{2+} \longrightarrow (CH_3)_2CH^\bullet + Hg^{2+} + Ag^+ \quad (3.94)$$

$$(CH_3)_2CHHg^+ + SO_4^{-\bullet} \longrightarrow (CH_3)_2CH^\bullet + Hg^{2+} + SO_4^{2-} \quad (3.95)$$

$$\overline{(CH_3)_2CH\bullet\ \bullet HC(CH_3)_2}^F \longrightarrow CH_3CH{=}CH_2\ (A/E) + CH_3CH_2CH_3\ (A/E) \quad (3.96)$$

$CH_3CH_2HgNO_3/(NH_4)_2S_2O_8/AgNO_3$

The NMR spectrum of $CH_3CH_2HgNO_3$ in d_6-Me_2SO is shown in Figure 3.30. The lines at δ = 1.21 (CH_3) and δ = 1.80 (CH_2) belong to $CH_3CH_2HgNO_3$. A CIDNP spectrum is obtained from the reaction of $CH_3CH_2HgNO_3$ with $(NH_4)_2S_2O_8$ in presence of $AgNO_3$ in d_6-Me_2SO at 25 °C (Figure 3.31). A pure A/E multiplet polarization at δ = 0.83 (CH_3) belongs to butane. The A/E multiplet effect is

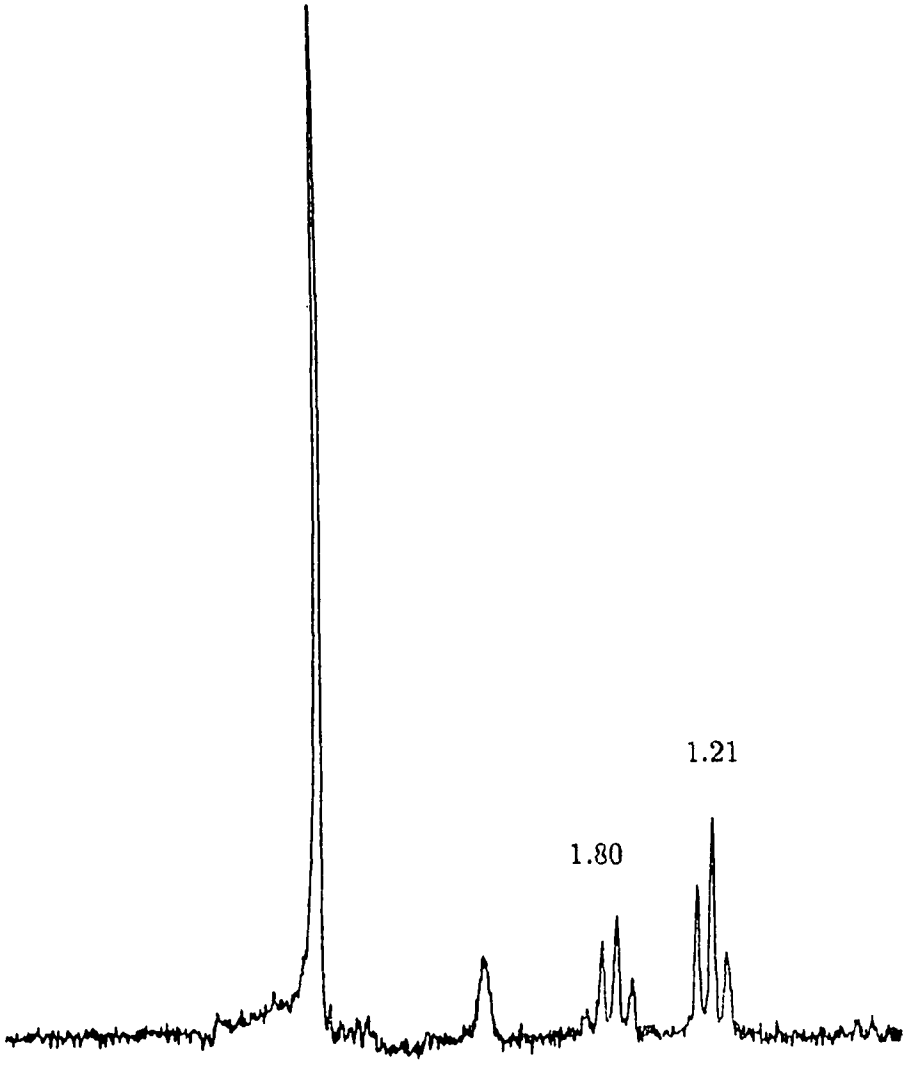

Figure 3.30: The NMR spectrum of $CH_3CH_2HgNO_3$ in d_6-Me_2SO at 25 °C

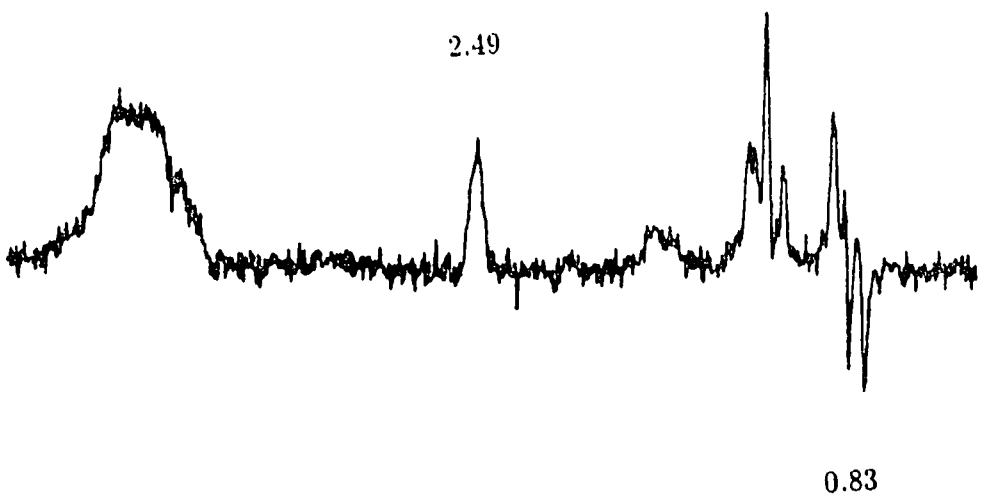

Figure 3.31: CIDNP recorded during the reaction of $CH_3CH_2HgNO_3$ and $S_2O_8^{2-}$ in d_6-Me_2SO with $AgNO_3$ at 25 °C

contributed by the F-pairs of ethyl radicals and the products (butane) is due the coupling of the radical pair.

$$2\overline{CH_3CH_2\bullet}^F \longrightarrow CH_2{=}CH_2 + CH_3CH_3 + CH_3CH_2CH_2CH_3^* \ (A/E) \quad (3.97)$$

$(CH_3)_3CHgSPh/\ (NH_4)_2S_2O_8/AgNO_3$

The NMR spectrum of $(CH_3)_3HgSPh$ in d_6-Me_2SO is shown in Figure 3.32. The signal at $\delta = 1.39$ is assigned to $(C\underline{H}_3)_3C$-. A symmetrical doublet with respect to the main signal at $\delta = -0.019$ and $\delta = 2.80$ with components of equal intensity is due to the interaction of the protons with the Hg^{199} nuclei. A CIDNP spectrum is obtained during the reaction of $(CH_3)_3CHgSPh$ with $(NH_4)_2S_2O_8$ in the presence of $AgNO_3$ in d_6-Me_2SO at 25 °C (Figure 3.33).

The methyl protons of isobutane ($\delta = 0.81$) as well as the methyl protons ($\delta = 1.60$) and the vinyl protons ($\delta = 4.59$) of isobutene show a pure A/E multiplet polarization which are completely in accord with Equation 3.101 of Scheme 16.

Scheme 16

$$S_2O_8^{2-} + Ag^+ \longrightarrow S_2O_4^{-\bullet} + Ag^{2+} + SO_4^{2-} \quad (3.98)$$

$$SO_4^{-\bullet} + Ag^+ \longrightarrow SO_4^{2-} + Ag^{2+} \quad (3.99)$$

$$(CH_3)_3CHgSPh + Ag^{2+} \longrightarrow (CH_3)_3C\bullet + HgSPh^+ + Ag^+ \quad (3.100)$$

$$2\overline{(CH_3)_3C\bullet}^F \longrightarrow (CH_3)_2{=}CH_2\ (A/E) + (CH_3)_3CH\ (A/E) \quad (3.101)$$

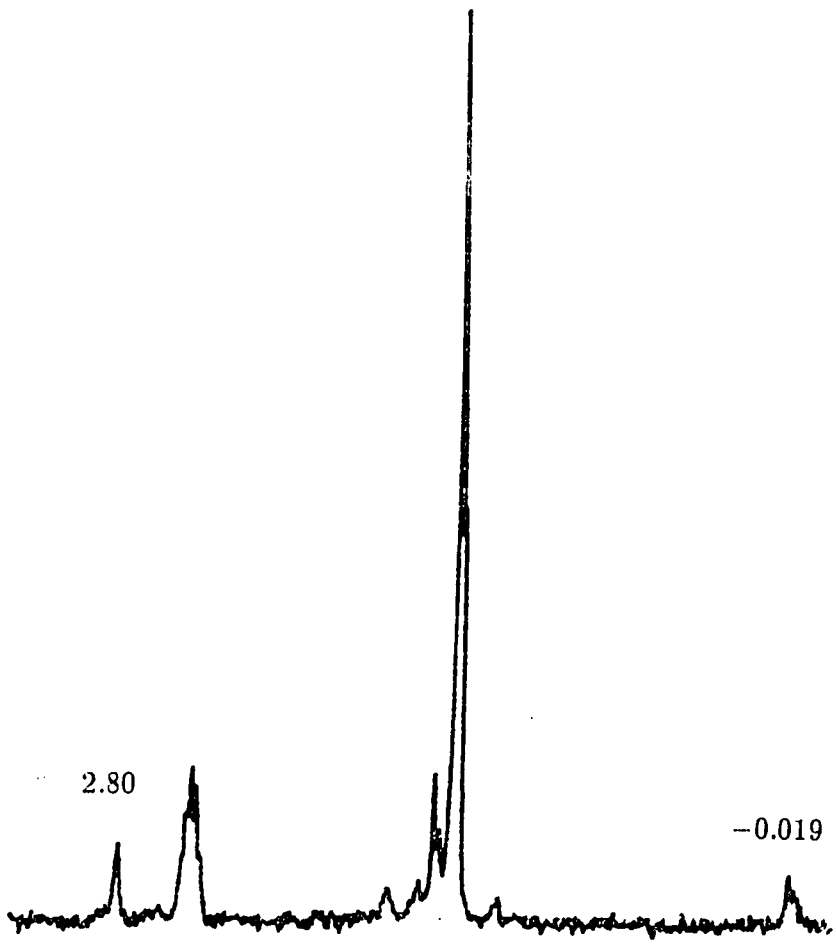

Figure 3.32: The NMR spectrum of $(CH_3)_3CHgSPh$ in d_6-Me_2SO at 25 °C

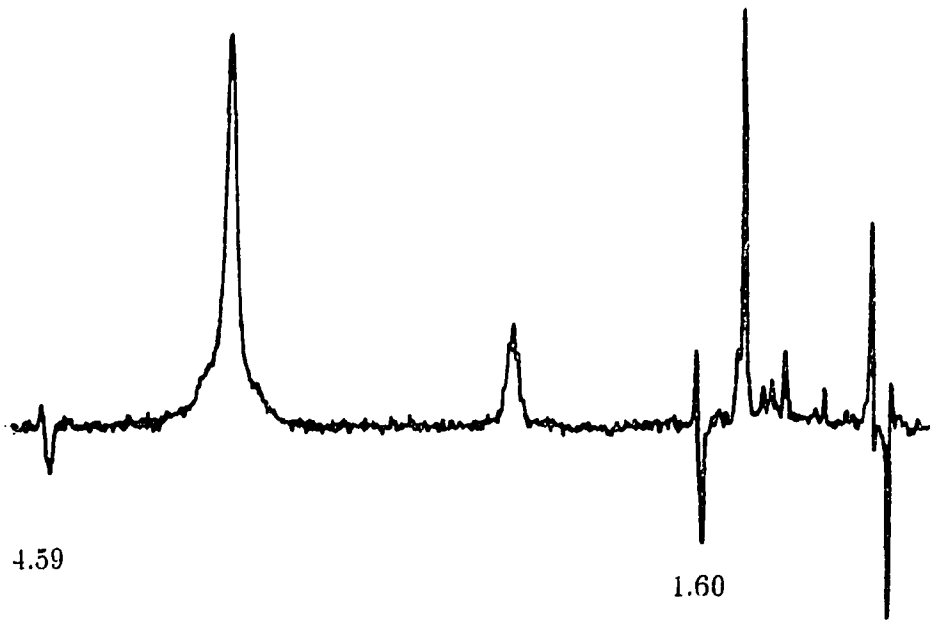

Figure 3.33: CIDNP recorded during the reaction of $(CH_3)_3CHgSPh$ and $S_2O_8^{2-}$ in d_6-Me_2SO with $AgNO_3$ at 25 °C

$((CH_3)_3C)_2Hg/Hg(NO_3)_2$

Charman and co-workers reported that the reaction of dialkylmercury with $HgCl_2$, $Hg(OAc)_2$ and $Hg(NO_3)_2$ are ionic [26].

$$R_2Hg + HgX_2 \rightleftharpoons 2RHgX \tag{3.102}$$

$$R = s\text{-}butyl$$

The rate constant follows the order

$$Hg(NO_3)_2 > Hg(OAc)_2 > HgCl_2$$

They confirm that comproportionation reaction between the salts HgX_2 and the dialkylmercury R_2Hg, and the reverse, disproportionation between two molecules RHgX, all proceed by a configuration-retaining, bimolecular, electrophilic mechanism of substitution, S_E2.

A typical net-effect CIDNP spectrum was obtained in the reaction of di-*tert*-butylmercury with $Hg(NO_3)_2$ in d_6 -Me_2SO at 25 °C is shown in Figure 3.34. There are two E lines at 4.637 ppm (vinyl) and 1.673 ppm (methyl) belonging to isobutene. No isobutane is observed from the NMR spectra. It is impossible that the net-effect polarization is contributed by $\overline{(CH_3)_3C\bullet\ \bullet C(CH_3)}^F$. However, the E effect could result from $\overline{(CH_3)C\bullet\ \bullet NO_3}^F$.

The hfs constant for the protons of the *tert*-butyl radical is +22.74G, and the *g*-factor of $NO_3^\bullet$ is 2.018. According to the Kaptein rule

$$\Gamma_{ne} = \mu\varepsilon\Delta g A_i = + + - + = -$$

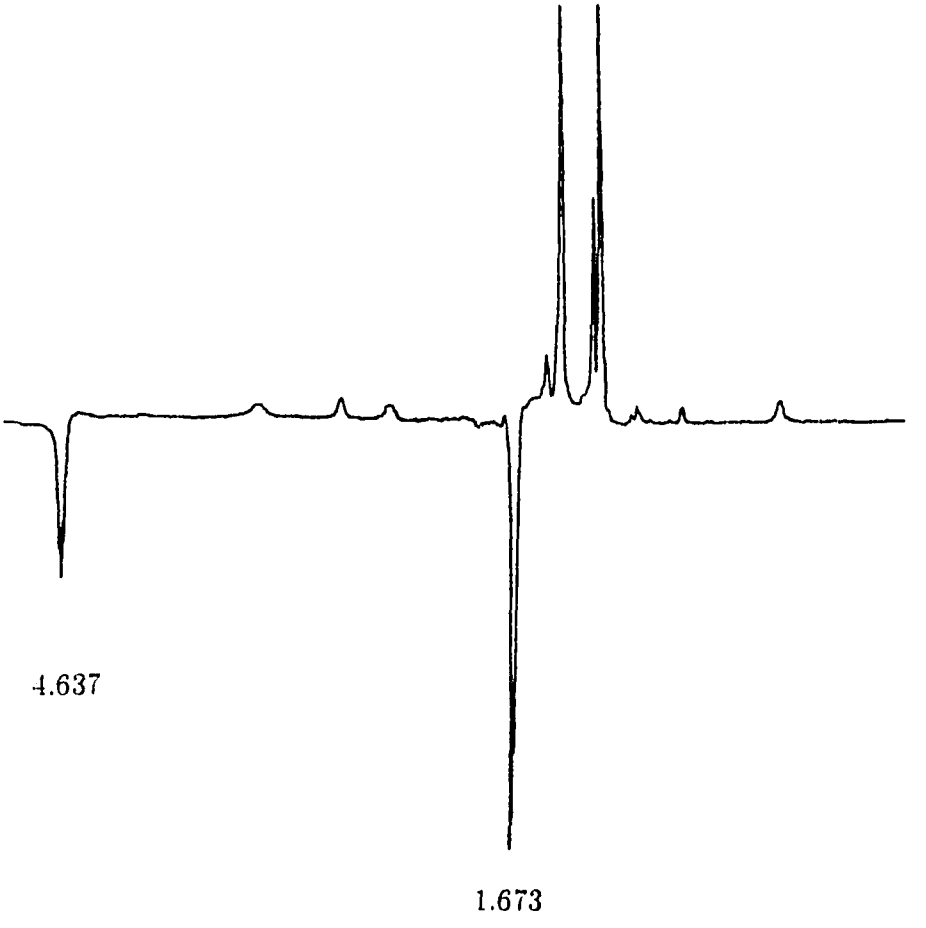

Figure 3.34: CIDNP observed during the reaction of $((CH_3)_3C)_2Hg$ and $Hg(NO_3)_2$ in d_6-Me_2SO at 25 °C

for E net effect. With the aid of Kaptein's rules and the radical parameters $g(\bullet NO_3) > g((CH_3)_3C\bullet)$ the observed E net polarization can be explained by nuclear spin dependent singlet-triplet transition in the pair $\overline{(CH_3)_3C\bullet\ \bullet NO_3}^F$.

The di-*tert*-butylmercury is an electron donor with a low IP, 7.57 eV and $Hg(NO_3)_2$ is an electron acceptor with high IP, over 11.37 eV ($HgCl_2$). The reaction between di-*tert*-butylmercury and mercury nitrate is accompanied by transfer of an electron from the organomercurial to mercury nitrate. Thus transfer should lead to a radical pair of the di-*tert*-butylmercury radical cation and the mercuric nitrate radical anion. Then, diffusion collision between $(CH_3)_3C\bullet$ and $NO_3^\bullet$ forms F radical pairs. Scheme 17 outlines the mechanism of these reactions.

Scheme 17

$$t\text{-}Bu_2Hg + Hg(NO_3)_2 \longrightarrow [t\text{-}Bu_2Hg^{+\bullet}Hg(NO_3)^{-\bullet}] \longrightarrow t\text{-}BuHg^+ + t\text{-}Bu^\bullet + Hg + NO_3^- + NO_3^\bullet \quad (3.103)$$

$$\overline{t\text{-}Bu\ \bullet\ \bullet NO_3}^F \longrightarrow H_2C{=}C(CH_3)_2 + HNO_3 \quad (3.104)$$

$$\overline{t\text{-}Bu\ \bullet\ \bullet NO_3}^F \longrightarrow (CH_3)_3CONO_2 \quad \text{coupling} \quad (3.105)$$

$$\overline{t\text{-}Bu\ \bullet\ \bullet NO_3}^F \longrightarrow NO_3 + t\text{-}Bu^{+*} \longrightarrow CH_2{=}C(CH_3)_2 + H^+ \quad (3.106)$$

Furthermore, the comproportionation of radical pairs may lead to equal amounts of isobutene and HNO_3. Alternatively, since *t*-Bu$^\bullet$ also is an electron donor with E°_{ox}, 0.72 V and $NO_3^\bullet$ is electron acceptor with E°_{ox}, 1.88 V, the electron transfer from *t*-Bu$^\bullet$ to $NO_3^\bullet$ could occur followed by very fast deprotonation of *t*-Bu$^+$.

The System, $Ph_3Sb/(NH_4)_2S_2O_8/(CH_3)_2CHI$

Figure 3.35 shows the CIDNP spectrum obtained during the reaction of triphenylantimony with peroxydisulfate ion in the presence of isopropyl iodide in d_6-Me_2SO at 80 °C. The strong A/E multiplet polarizations occur for the products propane (CH_3, 0.82 ppm; CH_2, 1.20 ppm) and propene (CH_3, 1.62 ppm; $=CH_2$, 4.9 ppm; $-C\underline{H}=CH_2$, 5.63 ppm). Weak E/A multiplets are observed at 4.42 ppm (CH_2) and 1.85 ppm (CH_3). These polarizations are in accord with the reactions of Scheme 18.

Scheme 18

$$S_2O_8^{2-} \longrightarrow 2SO_4^{-\bullet}$$

$$SO_4^{-\bullet} + Ph_3Sb \longrightarrow Ph\bullet + Ph_2SbSO_4^- \qquad (3.107)$$

$$Ph\bullet + (CH_3)_2CHI \longrightarrow PhI + (CH_3)_2CH\bullet \qquad (3.108)$$

$$2\overline{(CH_3)_2CH\bullet}^F \longrightarrow (CH_3)_2CH_2(A/E) + CH_3CH=CH_2(A/E) \qquad (3.109)$$

$$2\overline{(CH_3)_2CH\bullet}^F + (CH_3)_2CHI \longrightarrow (CH_3)_2CH\bullet + (CH_3)_2CHI^* \quad (E/A) \qquad (3.110)$$

The reaction triphenylantimony with sulfate radical ion forming phenyl radical may be via S_H2 or electron transfer process followed by very fast cleavage of the triphenylantimony radical cation.

$$SO_4^{-\bullet} + Ph_3Sb \longrightarrow [Ph_3SbSO_4^-]^\bullet \longrightarrow Ph\bullet + Ph_2SbSO_4^- \qquad (3.111)$$

Figure 3.35: CIDNP recorded during the reaction of Ph_3Sb and $S_2O_8^{2-}$ in d_6-Me_2SO with $(CH_3)_2CHI$ at 80 °C

$$SO_4^{-\bullet} + Ph_3Sb \longrightarrow Ph_3Sb^{+\bullet}SO_4^{2-} \longrightarrow Ph\bullet + Ph_2SbSO_4^- \qquad (3.112)$$

No strong CIDNP spectra occur during the reaction of $(NH_4)_2S_2O_8$ with Ph_3P, Ph_3AS, Ph_3Bi and Ph_4Sn in presence of $(CH_3)_2CHI$ or EtI in d_6-Me_2SO.

The System, RCOOH/$S_2O_8^{2-}$

The oxidation of carboxylic acids, equation 3.113 is a useful source of alkyl radical. Decarboxylation is exothermic by about 15 Kcal/mole, although it becomes less with increasing S character in the alkyl-carbonyl bond. The decarboxylation carried out electrochemically is known as the Kolbe oxidation when alkyl dimers are found.

$$RCO_2H \longrightarrow RCO_2\bullet + H^+ + e \qquad (3.113)$$

$$RCO_2\bullet \longrightarrow R\bullet + CO_2 \qquad (3.114)$$

A number of metal oxidants such as lead(IV), silver(II), manganese(IV), cobalt (III), thallium(II) and cerium(IV) are also capable of effecting decarboxylation. Silver(II) is particularly effective in the decarboxylation of acids.

$$RCO_2H + Ag^{2+} \longrightarrow RCO_2\bullet + H^+ + Ag^+ \qquad (3.115)$$

An outer-sphere process may be involved. The efficient generation of alkyl radicals has been utilized in the homolytic alkylation of a variety of heteroaromatic bases in acidic media [27].

The 1°-alkyl radicals have been detected by using ESR but *tert*-butyl and isopropyl radicals are not detected in the RCOOH/$S_2O_8^{2-}$ system. Davies et al. suggest that this is probably a result of their rapid oxidation by $S_2O_8^{2-}$ to relatively stable carbocations [28].

$$R^{\bullet} + S_2O_8^{2-} \longrightarrow R^{+} + SO_4^{-\bullet} + SO_4^{2-} \qquad (3.116)$$

Fortunately, CIDNP was observed during the reaction of $S_2O_8^{2-}$ with RCOOH, $(RCOO)_2Hg$ or RCOOHg in d_6-Me_2SO at 60-80 °C or in presence of Ag^{+} at 25 °C.

$(CH_3)_3CCOOH$ / $S_2O_8^{2-}$

The NMR spectrum of the reaction of $S_2O_8^{2-}$ with $(CH_3)_3CCOOH$ in d_6-Me_2SO is shown in Figure 3.36 at 80 °C. The signal at 1.095 ppm is assigned to the *tert*-butyl protons of $(CH_3)_3CCOOH$. The triplet of the methyl protons (1.64 ppm) (Figure 3.37) and the septet of the vinyl protons (4.73 ppm) of isobutene (Figure 3.38) shows a pure E net polarization.

The net effect phasing of isobutene can be explained by Kaptein's rules:

$$\overline{(CH_3)_3C \bullet\bullet SO_4^{-}}^{F}$$

$$\Gamma_{ne} = \mu\varepsilon\Delta g A_i = + + -+ = -(E)$$

Since $\mu = +$ (F precursor), $\varepsilon = +$ (disproportionation product),

$\Delta g = g(t\text{-butyl}) - g(\text{sulfate}) = 2.0026 - 2.022 < 0$, and

$A_i = +$ for *t*-butyl radical.

These polarization patterns are in accord with Equation 3.117 and Equation 3.118 of Scheme 19.

Scheme 19

$$S_2O_8^{2-} \longrightarrow 2SO_4^{-\bullet}$$

Figure 3.36: CIDNP recorded during the reaction of $(CH_3)_3CCOOH$ and $S_2O_8^{2-}$ in d_6-Me_2SO at 80 °C

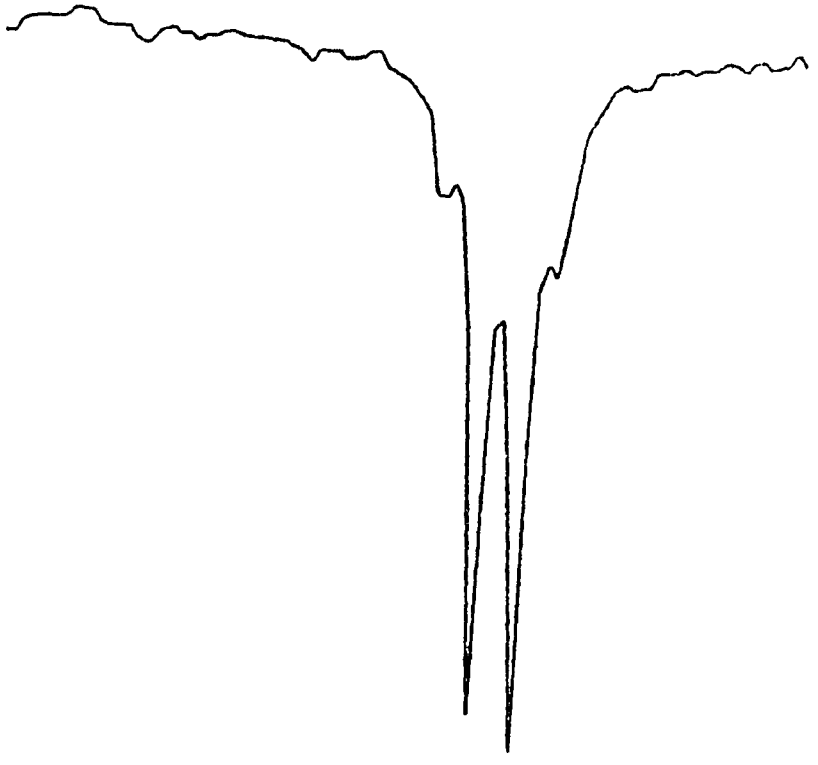

Figure 3.37: The triplet (E) of the methyl protons of isobutene

Figure 3.38: The septet (E) of the vinyl protons of isobutene

$$(CH_3)_3COOH + SO_4^{-\bullet} \longrightarrow (CH_3)_3CCOO^{\bullet} + HSO_4^- \quad (3.117)$$

$$((CH_3)_3CCOO^{\bullet} \longrightarrow (CH_3)_3C^{\bullet} + CO_2 \quad (3.118)$$

$$(CH_3)_3C^{\bullet} + SO_4^{-\bullet} \longrightarrow \overline{(CH_3)_3C \bullet\bullet SO_4^-}^F \quad (3.119)$$

$$\overline{(CH_3)_3C \bullet\bullet SO_4^-}^F \longrightarrow (CH_3)_2C = CH_2 + HSO_4^- \quad (3.120)$$

$$\overline{(CH_3)_3C \bullet\bullet SO_4^-}^F \longrightarrow SO_4^{2-} + (CH_3)_3C^+ \longrightarrow$$

$$(CH_3)_2C = CH_2 + H^+ \quad (3.121)$$

$$(CH_3)_3C \bullet + S_2O_8^{2-} \longrightarrow (CH_3)_3C^+ + SO_4^{2-} + SO_4^{-\bullet} \quad (3.122)$$

It is interested that the E net polarization of isobutene is strong evidence that *t*-butyl radical is oxidized by sulfate radical forming isobutene and that this reaction is too fast to allow the *t*-butyl radical to be detected by ESR.

$(CH_3)_2CHCOOH/S_2O_8^{2-}$

Figure 3.39 shows the CIDNP spectrum obtained during the decomposition of $(CH_3)_2CHOOH$ in presence of $S_2O_8^{2-}$ in d_6-Me_2SO at 80 °C. After 2 min, emission (E) and enhanced absorption (A) occur for the products isobutene (CH_3, δ 1.62, $=C=CH_2$, δ 4.88, E; -C<u>H</u>$=CH_2$, δ 5.92, A) and $CH_3CH_2CH_3$ (CH_2, δ 1.20, E + A/E, CH_3, δ 0.83, A + A/E). The net effects must arise from the isopropyl-sulfate radical pair. The Kaptein net effect rule applied to propene obtained from isopropyl-sulfate radical F-pair would give

$$\Gamma_{ne} = \mu\varepsilon\Delta A_i$$

$$\Gamma_{ne}(CH_3) = + + -+ = -(E)$$

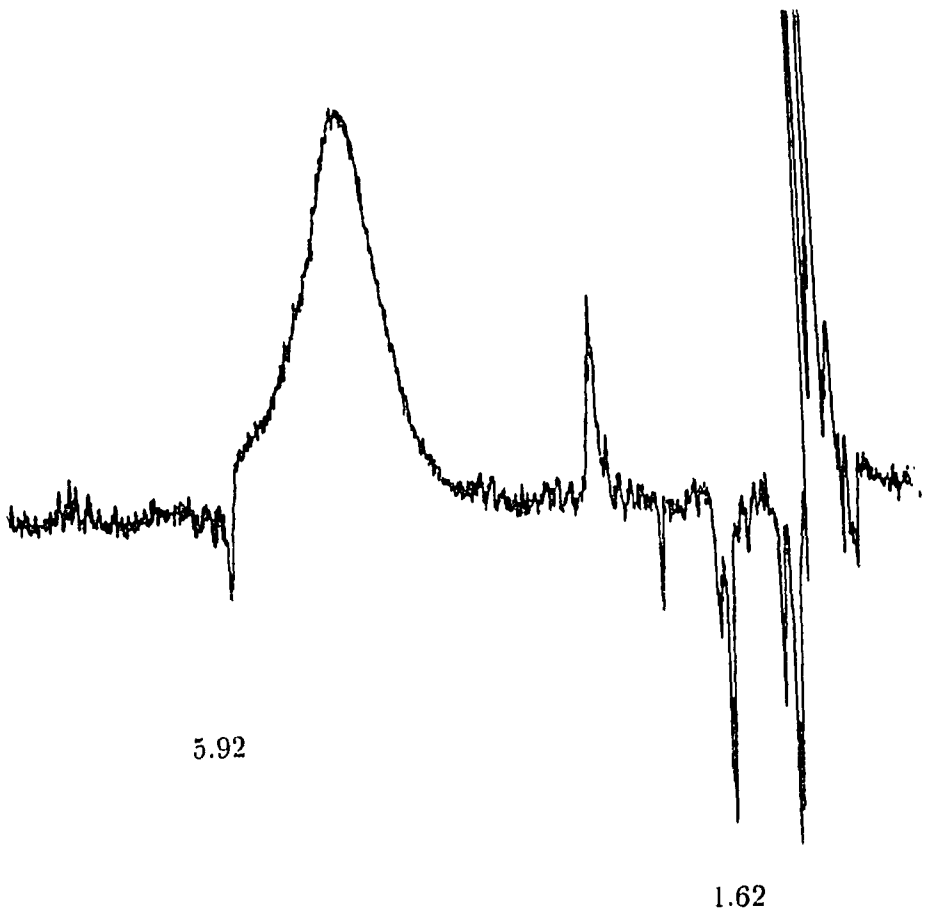

Figure 3.39: CIDNP observed during the reaction of $(CH_3)_2CHCOOH$ and $S_2O_8^{2-}$ in d_6-Me_2SO at 80 °C

$$\Gamma_{ne}(=CH_2) = + + -+ = -(E)$$

$$\Gamma_{ne}(-CH=C) = + + -- = +(A)$$

since $\mu = +$ (F precursor), $\varepsilon = +$ (disproportionation product), $\Delta g = g$(isopropyl) $-g$(sulfate)= 2.0026 − 2.022 < 0, $A(CH_3) > 0$ and $A(=CH) < 0$ for the isopropyl radical.

If isopropyl radical escaped from the isopropyl-sulfate radical F-pair the polarization can be explained by Scheme 20.

Scheme 20

$$S_2O_8^{2-} \longrightarrow 2SO_4^{-}$$

$$SO_4^{-\bullet} + (CH_3)_2CHCOOH \longrightarrow SO_4^{2-} + (CH_3)_2CHCOO\bullet \quad (3.123)$$

$$(CH_3)_2CHCOO\bullet \longrightarrow (CH_3)_2CH\bullet + CO_2 \quad (3.124)$$

$$2\overline{(CH_3)_2CH\bullet}^{F} \longrightarrow CH_3CH=CH_2\ (A/E) + CH_3CH_2CH_3\ (A/E) \quad (3.125)$$

$$\overline{(CH_3)_2CH\bullet\bullet SO_4^{-}}^{F} \longrightarrow CH_3CH=CH_2^{*} + HSO_4^{-} \quad (3.126)$$

$$\overline{(CH_3)_2CH\bullet\bullet SO_4^{-}}^{F} + (CH_3)_2CHCOOH \longrightarrow$$

$$(CH_3)_2CH_2^{*} + \bullet C(CH_3)_2COOH + HSO_4^{-} \quad (3.127)$$

The $(CH_3)_2CH\bullet^*$ which escaped from the isopropyl-sulfate radical F-pair would give a net effect according to Kaptein rules:

$$\Gamma_{ne} = \mu\varepsilon\Delta A_i$$

$$\Gamma_{ne} = + - -- = -(E)$$

$$\Gamma_{ne} = + - -+ = +(A)$$

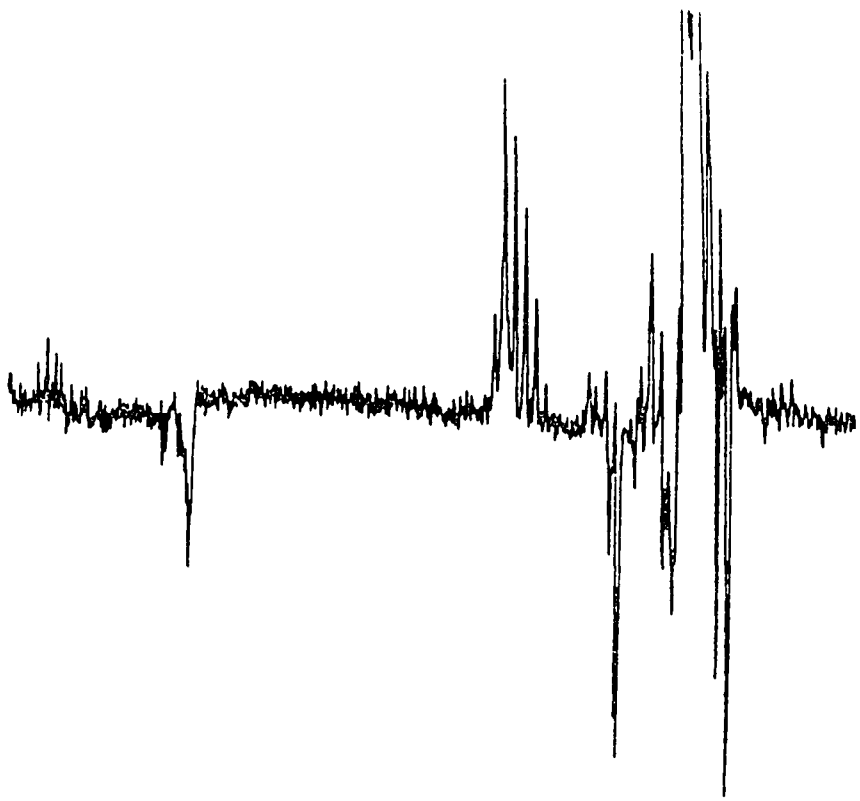

Figure 3.40: CIDNP observed during the reaction of $(CH_3)_2CHCOOH$ and $S_2O_8^{2-}$ in d_6-Me_2SO at 80 °C (5 min)

Figure 3.40 shows the A/E multiplet polarization of propane obtained during further reaction (5 mins). The net polarization of propane disappears and A/E polarization appears. These polarization patterns are completely in accord with Equation 3.125 of Scheme 20.

Further evidence is obtained from the reaction of $(CH_3)_2CHOOH$ with $S_2O_8^{2-}$ in presence of Ag^+ at room temperature as described in the following section.

$(CH_3)_2CHOOH/S_2O_8^{2-}/AgNO_3$

In Figure 3.41 is shown the NMR spectrum obtained when the reaction of the $(CH_3)_2CHOOH$ with peroxydisulfate ion in presence of $AgNO_3$ in d_6-Me_2SO at room temperature. The observed polarizations are for propane (CH_3, δ 0.79, A/E and CH_2, δ 4.88, E + A/E; -CH=, δ 5.92, E + A/E). It is interesting that the net effect of propene become E + A/E and apparently only the multiplet effect is observed for propane. These polarization patterns are contributed by the radical pairs of $\overline{(CH_3)_2CH \bullet\bullet SO_4^-}^F$ and $\overline{(CH_3)_2CH \bullet\bullet HC(CH_3)_2}^F$.

Scheme 21

$$S_2O_8^{2-} + Ag^+ \longrightarrow SO_4^{-\bullet} + Ag^{2+} + SO_4^{2-}$$

$$SO_4^{-\bullet} + Ag^+ \longrightarrow Ag^{2+} + SO_4^{2-}$$

$$(CH_3)_2CHCOOH + Ag^{2+} \longrightarrow (CH_3)_2CHCO_2^{\bullet} + H^+ + Ag^+ \qquad (3.128)$$

$$(CH_3)_2CHCOO^{\bullet} \longrightarrow (CH_3)_2CH^{\bullet} + CO_2 \qquad (3.129)$$

$$\overline{(CH_3)_2CH \bullet\bullet HC(CH_3)_2}^F \longrightarrow CH_3CH = CH_2 + CH_3CH_2CH_3$$

$$\overline{(CH_3)_2CH \bullet\bullet SO_4^-}^F \longrightarrow CH_3CH = CH_2 + HSO_4^-$$

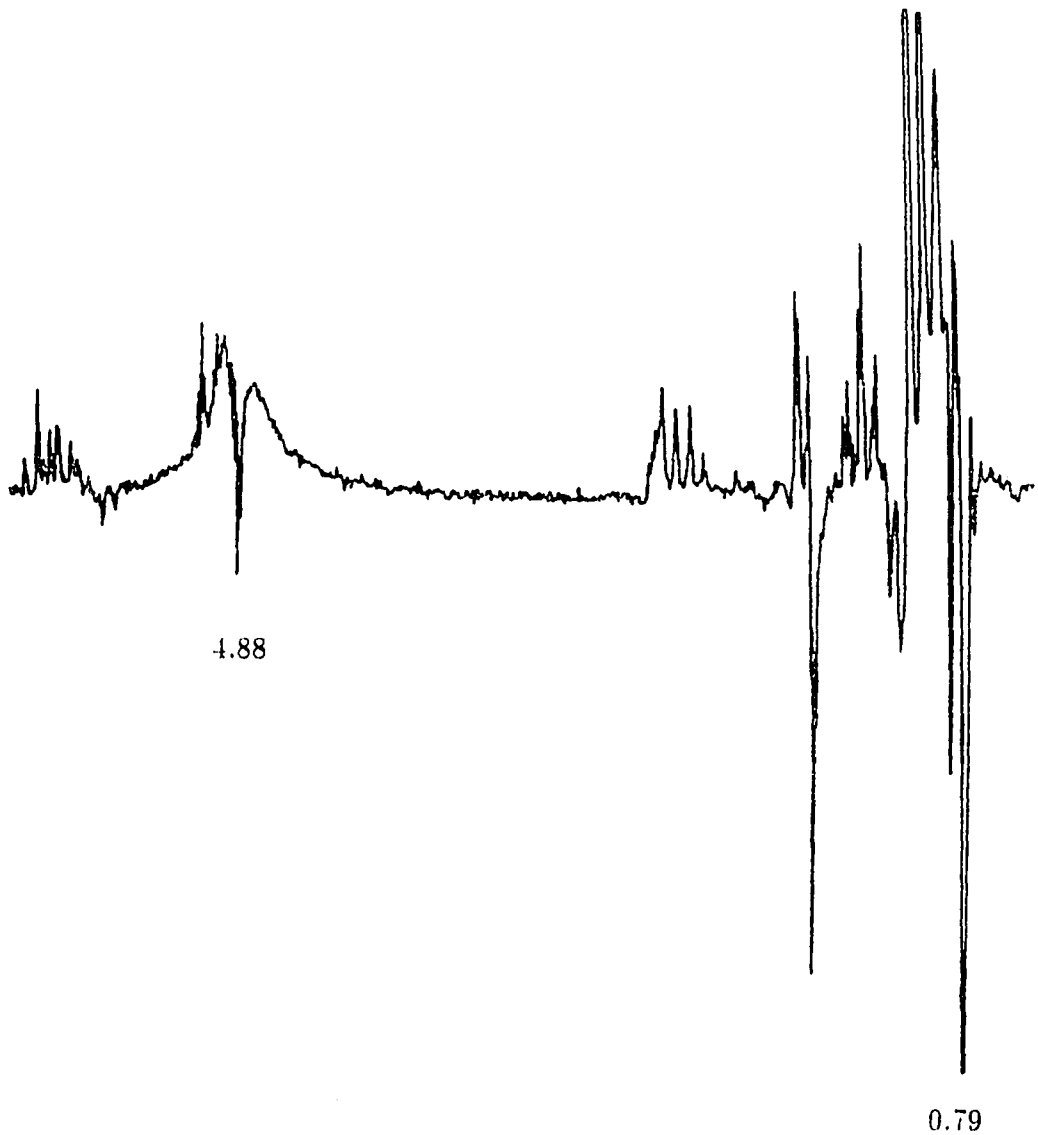

Figure 3.41: CIDNP recorded during the reaction of $(CH_3)_2CHCOOH$ and $S_2O_8^{2-}$ in d_6-Me_2SO with $AgNO_3$ at 25 °C

These polarization patterns also show that the concentration of the sulfate radical ions is less than that of isopropyl radicals. In other words, in the presence of Ag^+, the reactions of $(CH_3)_2CHOOH$ with $SO_4^{-\bullet}$ can generate a large amount of the radical $(CH_3)_2CH^\bullet$ which can be used for radical processes. CIDNP can be a useful tool for the probe of radical sources for free radical reactions.

A weak polarized ^{13}C spectrum was observed during the reaction of trimethylacetic acid with peroxydisulfate in d_6-Me_2SO at 80 °C.

The spectrum exhibits an emission peak detectable in Fourier transform pulse ^{13}C NMR and is shown after adding $AgNO_3$ to the d_6-Me_2SO solution of trimethylacetic acid and peroxysulfate ion at 25 °C (Figure 3.42).

The ^{13}C NMR spectrum of trimethylacetic acid is shown in Figure 3.43 in d_6-Me_2SO at 80 °C. The signals at δ=27.0, 38.8 and 179.3 belong to the C_3, C_2, and C_1 carbon atoms of trimethylacetic acid respectively [29], (Table 3.2).

The emission peak at δ=141.7 is assigned to C_2 of 2-methylpropene. The observed ^{13}C polarization arises from the disproportionation of the radical pair $\overline{(CH_3)_3C\bullet\bullet SO_4^-}^F$.

$$\overline{(CH_3)_3C\bullet\bullet SO_4^-}^F \longrightarrow (CH_3)_2^*C=CH_2 + HSO_4^-$$

$$\overline{(CH_3)_3C\bullet\bullet SO_4^-}^F \longrightarrow (CH_3)_3C^*\bullet$$

The CKO theory can be used to rationalize the ^{13}C results, since ^{13}C is a spin 1/2 nuclei. Since heteronuclear decoupling was used in the ^{13}C experiments, only the net polarization effect is observable. Hence Kaptein's net rule can be used for

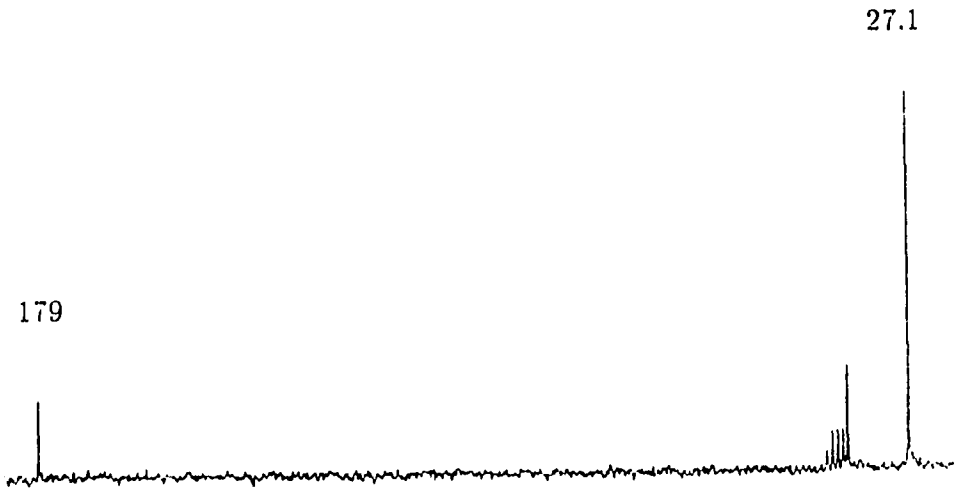

Figure 3.42: ^{13}C CIDNP recorded during the reaction of $(CH_3)_3COOH$ and $S_2O_8^{2-}$ in d_6-Me_2SO with $AgNO_3$ at 25 °C

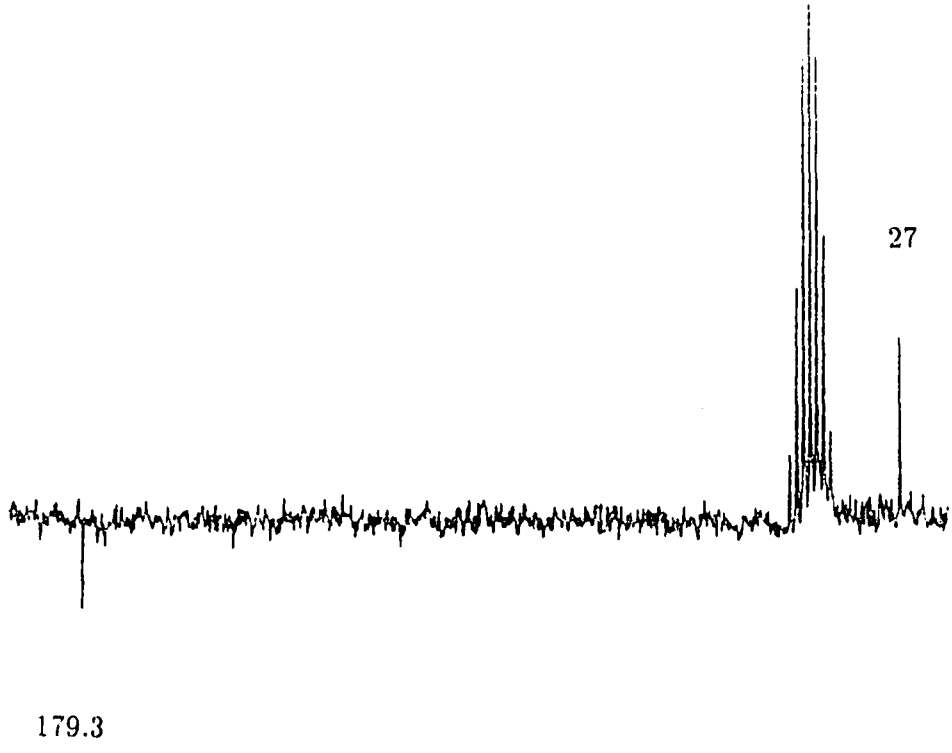

Figure 3.43: ^{13}C NMR spectrum of trimethylacetic acid

Table 3.2: ^{13}C NMR δ value obtained during the reaction of $(CH_3)_3CCOOH$ and $S_2O_8^{2-}/Ag^+$

	$(\underline{C}H_3)_2SO$	$\underline{C}_6H_6$	$(CH_3)_3CCOOH$			$(CH_3)_2\underline{C}=CH_2$
	^{13}C ppm	^{13}C ppm	C_1 ppm	C_2 ppm	C_3 ppm	^{13}C ppm
Experiment	39.8	128.3	179	38.8	27.1	141.7
Literature	40	128.5	185	38.7	27.1	141.8

determining the sign of the net polarization.

$$\Gamma_{ne} = \mu\varepsilon\Delta g A$$

$$\Gamma_{ne} = + + -+$$

Since $\mu = +$ (F precursor), $\varepsilon = +$ (disproportionation),

$\Delta g = g((CH_3)_3C^{\bullet}) - g(SO_4^{-\bullet}) < 0$,

and $A^C = +49.5$ Gauss for *tert*-butyl radical.

The System, $(CH_3)_3CCHO/S_2O_8^{2-}$

Figure 3.44 shows the CIDNP spectrum obtained during the reaction of trimethylacetaldehyde ($(CH_3)_3CCHO$) with peroxydisulfate ion in d_6-Me_2SO at 80 °C. The signal at $\delta = 1.00$ is assigned to the *tert*-butyl protons of trimethylacetaldehyde. The doublet of the methyl protons of isobutane (δ 0.82, A/E) as well as the septet of the vinyl protons (δ 4.62, E) and the triplet of the methyl protons (δ 1.65, E) of isobutene are observed. An A/E polarization of the methine proton of isobutane is indicated at $\delta = 1.6$.

Figure 3.44: CIDNP observed during the reaction of $(CH_3)_3CHO$ and $S_2O_8^{2-}$ in d_6-Me_2SO at 80 °C

The net effects of polarization for isobutene must arise from the *tert*-butyl-sulfate radical pair and the A/E multiplet of the isobutane from the *tert*-butyl radical pairs.

$$\overline{(CH_3)_3C\bullet\bullet SO_4^-}^F \longrightarrow (CH_3)_2C=CH_2 + HSO_4^-$$

$$\overline{(CH_3)_3C\bullet\bullet C(CH_3)_3}^F \longrightarrow (CH_3)_2C=CH_2 + (CH_3)_3CH\ (A/E) + (CH_3)_3CC(CH_3) \quad (3.130)$$

According to Kaptein's net rule,

$$\Gamma_{ne} = \mu\varepsilon\Delta g A_i$$

$$\Gamma_{ne} = ++-+ = -E$$

since $\mu = (+)$, $\varepsilon = +$, $\Delta g = -$, $A_i = +$. The reaction of trimethylacetaldehyde with peroxydisulfate based upon the observed CIDNP is shown in Scheme 22.

Scheme 22

$$S_2O_8^{2-} \longrightarrow 2SO_4^{-\bullet}$$

$$SO_4^{-\bullet} + (CH_3)_3CCHO \longrightarrow HSO_4^- + (CH_3)_3CC^\bullet O \quad (3.131)$$

$$(CH_3)_3CC^\bullet O \longrightarrow (CH_3)_3C + CO \quad (3.132)$$

$$\overline{(CH_3)_3C\bullet\bullet SO_4^-}^F \longrightarrow (CH_3)_2C=CH_2 + HSO_4^- \quad (3.133)$$

$$\overline{(CH_3)_3C\bullet\bullet C(CH_3)_3}^F \longrightarrow (CH_3)_2C=CH_2 + (CH_3)_3CH + (CH_3)_3CC(CH_3)_3 \quad (3.134)$$

$$RC^\bullet O + S_2O_8^{2-} \longrightarrow RC^+O + SO_4^{2-} + SO_4^{-\bullet} \quad (3.135)$$

The Equation 3.131 and Equation 3.132 have been suggested by Huyser. However Equation 3.134 is not important because of the fast oxidation of $(CH_3)_3C\bullet$ by $SO_4^{-\bullet}$.

The System, $(CH_3)_3CCHO/S_2O_8^{2-}/AgNO_3$

Figure 3.45 shows the CIDNP spectrum obtained during the reaction of trimethlacetaldehyde with peroxydisulfate in presence of silver nitrate in d_6-Me_2SO at 25 °C. The polarization is a pure E net polarization for the isobutene observed (methyl, δ 1.64; vinyl, δ 4.61). Obviously, the net effects must arise from the radical pair $\overline{(CH_3)_3C\bullet\bullet SO_4^{-\bullet}}^F$.

The A/E multiplets of isobutane and isobutene which do not appear, indicate a difference between the $(CH_3)_3CHO$ and $(CH_3)_3CCOOH$ reacting in presence of Ag^+. Equation 3.139 is of little importance in the aldehyde system.

On the basis of these results, the following free radical paths can be assigned.

Scheme 23

$$S_2O_8^{2-} + Ag^+ \longrightarrow SO_4^{-\bullet} + SO_4^{2-} + Ag^{2+}$$

$$SO_4^{-\bullet} + (CH_3)_3CCHO \longrightarrow (CH_3)_3CC=O + HSO_4^-$$

$$(CH_3)_3CCO \longrightarrow (CH_3)_3C^\bullet + CO$$

$$(CH_3)_3CCHO + Ag^{2+} \longrightarrow (CH_3)_3CCHO^{+\bullet} + Ag^+ \qquad (3.136)$$

$$(CH_3)_3CCHO^{+\bullet} \longrightarrow H^+ + (CH_3)_3CCO \qquad (3.137)$$

$$\overline{(CH_3)_3C\bullet\bullet SO_4^-}^F \longrightarrow (CH_3)_2C=CH_2^* + SO_4^{2-} \qquad (3.138)$$

$$(CH_3)_3C\bullet + (CH_3)_3C\bullet \longrightarrow (CH_3)_2C=CH_2 + (CH_3)_3CH \qquad (3.139)$$

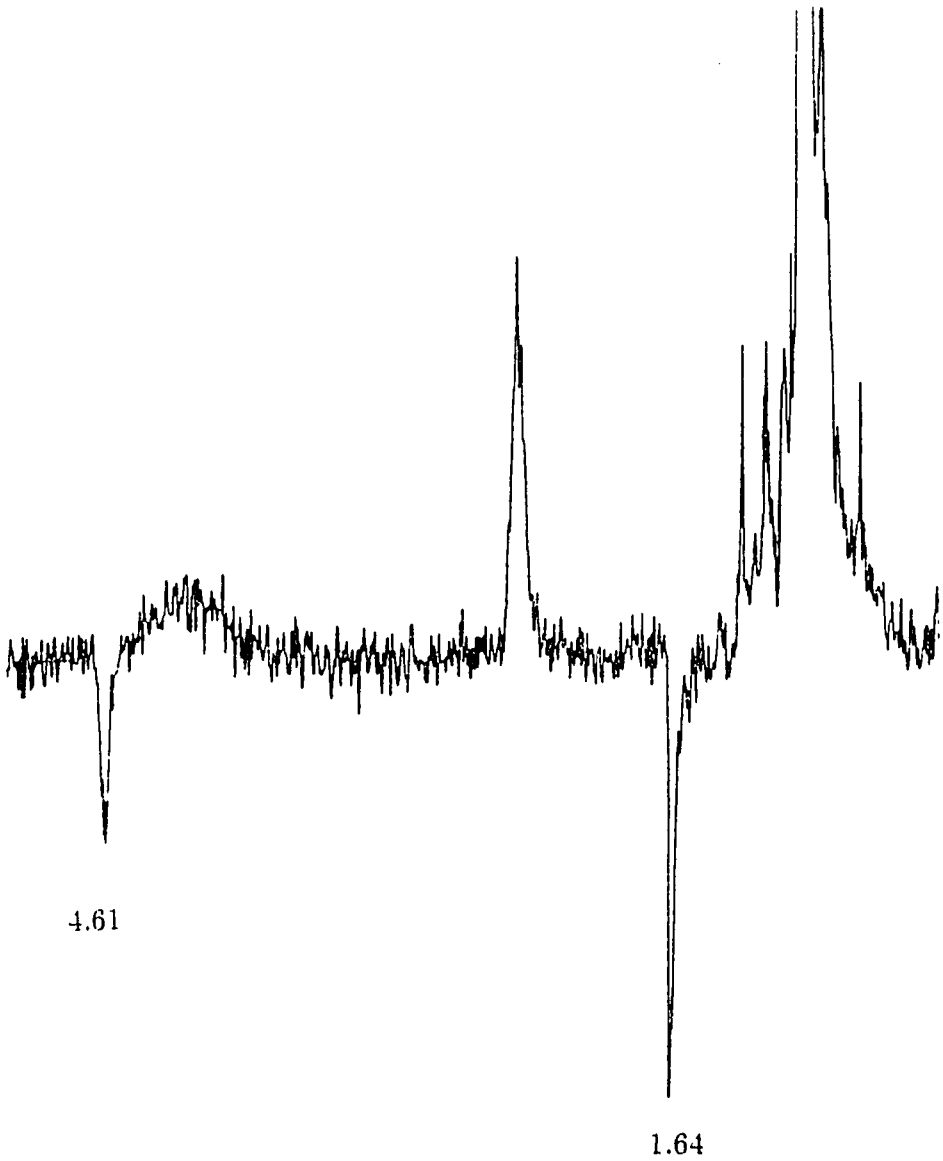

Figure 3.45: CIDNP recorded during the reaction of $(CH_3)_3CHO$ and $S_2O_8^{2-}$ in d_6-Me_2SO with $AgNO_3$ at 25 °C

CHAPTER 4. CONCLUSION

Chemically induced nuclear polarization (CIDNP) spectra observed during the reaction of $(CH_3)_3CHgCl$ or $(CH_3)_2CHHgCl$ with $S_2O_8^{2-}$ and NaI in d_6-Me_2SO at 25 °C show multiplet effect polarization (A/E) for the coupling and disproportionation products of $(CH_3)C\bullet$ or $(CH_3)_2CH\bullet$. These radicals result from S_H2 attack of $I\bullet$ at the metal center of RHgX. During the thermolysis at 60 – 80 °C of $S_2O_8^{2-}$ in d_6-Me_2SO containing RHgX, strong CIDNP multiplet signals (A/E) for RH, R(−H) and R-R were observed from the diffusive encounter of primary, secondary, or tertiary alkyl radicals generated by electron transfer from RHgX to $SO_4^{-\bullet}$. CIDNP spectra taken during the thermal decomposition of $S_2O_8^{2-}$ in d_6-Me_2SO solutions containing either RHgX, R'_2Hg or Ph_3Sb and R"I show multiplet effect polarization for R"I(E/A) and for the coupling and disproportionation products of R"• (A/E). CIDNP spectra obtained during the reaction of $((CH_3)_3C)_2Hg$ and $S_2O_8^{2-}$ show net effect (E) polarization for $(CH_3)_2C{=}CH_2$ from the pair of $(CH_3)_3C\bullet$ and $SO_4^{-\bullet}$. This reaction involves electron transfer from the $((CH_3)_3C)_2Hg$ to $S_2O_8^{2-}$ and from $(CH_3)_3C\bullet$ to $SO_4^{-\bullet}$.

Strong CIDNP multiplet signals (A/E) for RH and R(−H) were observed from the diffusive encounter of primary, secondary or tertiary alkyl radicals during the reaction of $RHgNO_3$ or *t*-BuHgSPh with $S_2O_8^{2-}$ and Ag^+ at 25 °C. The alkylmer-

curials in this case undergo electron transfer with Ag^{2+} and/or $SO_4^{-\bullet}$. CIDNP net effect polarized signals (E) for R(−H) were observed from the diffusive radical pairs of $(CH_3)_3C\bullet$ and $NO_3\bullet$ generated by electron transfer from $((CH_3)_3C)_2Hg$ to $Hg(NO_3)_2$ at 25 °C.

During the reaction of carboxylic acid such as $(CH_3)_3CCOOH$ or $(CH_3)_2CHCOOH$, or of $(CH_3)_3CCHO$ with $S_2O_8^{2-}$ in the absence or presence of Ag^+, CIDNP signals (E and A/E) were observed from the radical pairs $\overline{R\bullet\bullet SO_4}^F$ and diffusive radical pairs, $\overline{R\bullet\bullet R}^F$. These pairs were generated by the reaction of RCOOH or $(CH_3)_3CCHO$ with SO_4^{-}, followed by the cleavage of RCOO• or $RC^{\bullet}{=}O$ to yield R•.

CHAPTER 5. EXPERIMENTAL

The CIDNP experiments were conducted on a JEOL FX-90Q (90 MHz) spectrometer by the addition of $(NH_4)_2S_2O_8$ or $K_2S_2O_8$ (15–20 mg) to 0.5 mL of a 0.2–0.5 M solution of RHgX in presence or absence of NaI in d_6-Me_2SO under argon in an NMR tube placed in the gap of the magnet of the spectrometer at 25 °C or 80 °C. The chemical shifts are given in ppm relative to Me_2SO as internal standard (δ 2.49).

PART II.

PHOTOSTIMULATED FREE-RADICAL CHAIN REACTIONS OF ALKYLMERCURIALS WITH HETEROAROMATIC COMPOUNDS

CHAPTER 1. INTRODUCTION

Alkylmercury halides are convenient sources of free alkyl radicals in chain reaction. Alkylation of organic compounds has been observed upon reactions of RHgX with metal hydrides or by a photo-initiated chain reaction with RHgX alone. The reduction of alkylmercury halides by metal hydrides, such as sodium borohydride or lithium aluminum hydride, has been proposed to be a free radical chain process involving an intermediate RHgH. Giese [30] has extensively studied the formation of carbon-carbon bonds by addition of free radicals, generated from alkylmercury halides and sodium borohydride, to election deficient olefins (π) via a chain mechanism involving intermediates RHgH and RHg•.

Scheme 24

$$RHgX + NaBH_4 \longrightarrow RHgH + NaX + BH_3$$

$$RHgH \longrightarrow R\bullet + \bullet HgH$$

$$R\bullet + \pi \longrightarrow R\pi\bullet$$

$$R\pi\bullet + RHgH \longrightarrow R\pi H + RHg\bullet$$

$$RHg\bullet \longrightarrow R\bullet + Hg$$

Russell, Hershberger and Owens [31] have found that reaction of alkylmercury

halides with salts of aliphatic nitro compounds (A^-) yield tertiary nitro compounds, mercury metal, and the halide salt. The reaction was originally formulated as an $S_{RN}1$ process involving RHg• which decomposes to R• and Hg (Scheme 25).

Scheme 25

$$RHgX \longrightarrow R\bullet + \bullet HgX$$

$$R\bullet + A^- \longrightarrow RA^{-\bullet}$$

$$RA^{-\bullet} + RHgX \longrightarrow RA + RHg\bullet + X^-$$

$$RHg\bullet \longrightarrow R\bullet + Hg$$

Obviously, the reaction of RHgH with Rπ• is an S_H2 process and the reaction of RHgX with $RA^{-\bullet}$ is an electron transfer process. Both of these reactions may involve RHg• which can easily decompose into the alkyl radical and mercury metal.

To develop free-radical chain reactions involving carbon-carbon bond formation with RHgX as the source of the radical was this investigator's task. The only example of this reaction was the reaction of alkylmercury halides with the nitronate anions in 1982.

The carbon-carbon bond formation by the reaction of RHgX with some heteroaromatic compound, such as pyridine and quinoline, is reasonable since the C-Hg bond energy of RHgX [32] is less than C-C bond energy of organic compounds [33]. A simple calculation of the reaction enthalpy would predict feasibility for the reaction of RHgX with pyridine.

This calculation has not included the heat which would be evolved from the reaction between pyridine and hydrogen chloride. Obviously, the reaction is exothermic

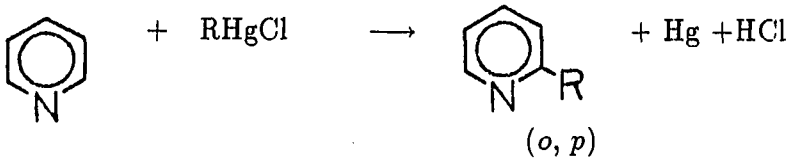

B.D.E. (kcal/mol)		B.D.E. (kcal/mol)	
C-H = 103		C-C = 99	
Hg-C = 50		H-Cl = 103	
Hg-Cl = 23			
Δ H =176	−	202	= −26 kcal/mol

and should be favorable. A possible reaction mechanism is shown in scheme 26.

Scheme 26

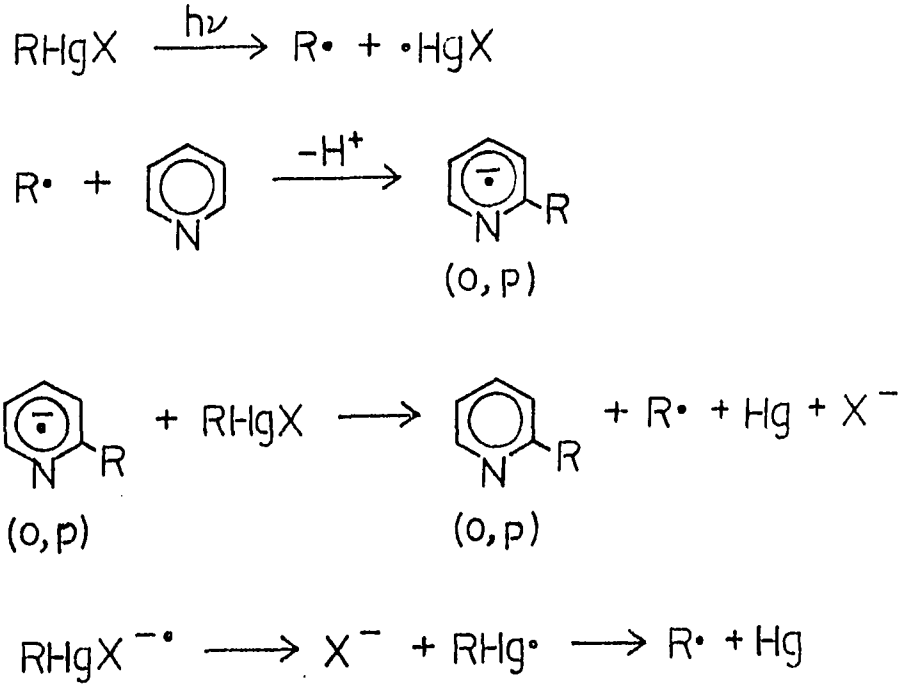

We supposed that an alkylpyridine radical anion might be formed by the addition of R• to pyridine followed by the loss of a proton. A chain reaction could propagate by the transfer of an election to an organomercury halide molecule to form X^- and RHg• which splits into R and Hg. Such a process seemed reasonable, since the reduction potential of pyridine is -2.62 V (DMF) [34] and RHgCl is $-(0.2 - 0.6)$ V vs SCE in DMF [35].

Pyridine, quinoline, N,N,N'N'-tetramethyl-*p*-phenylenediamine, isoquinoline and benzothiazole were found to undergo photostimulated ring substitution with a variety of alkylmercury halides in high yields. Ring substitution of other heteroaromatic compounds such as pyrazine and N,N-dialkylanilines were observed in low yield.

CHAPTER 2. RESULTS AND DISCUSSION

Reactions of RHgX with Pyridine

Results, some of which have been published in preliminary form [36] are tabulated in Table 2.1. In a typical reaction, mercury metal was observed to be formed quantitatively as a drop and the 2- and 4-alkylpyridines were formed in high yield. Small amounts of disubstituted products were also obtained.

The experimental procedure is particularly simple and the conditions are mild. Yields are good and the selectively of the attack is completely in position 2 and 4 of the pyridine ring for secondary and tertiary alkylmercury halides. Small amounts of 3-substituted products were also observed in the reaction of primary alkylmercury halides with pyridines.

Evidence for a Free Radical Chain Process

Typical inhibitors of chain reactions are O_2, *m*-dinitrobenzene and di-*tert*-butyl nitroxide. Another diagnostic feature of a chain reaction is that it can be initiated by light. Presumably a species capable of entering the cycle is generated photochemically.

In a normal reaction, mercury metal was observed to precipitate from pyridine solution after a few minutes of sunlamp irradiation when helium purged solution

Table 2.1: Photostimulated reactions of RHgCl with pyridine

R	% Hg	% RC_5H_4N[a]	*o/p*
C_2H_5	66	64(N)	2.0
n-C_4H_9	82	66(I)	2.4
n-C_6H_{13}	83	50(N)	
$Me_3CCH_2CH_2$		64(N)	2.5
Me_3CCH_2		54(N)	1.9
c-$C_5H_9CH_2$	93	77(N)	1.9
i-C_3H_7		72(N)	1.6
c-C_6H_{11}	90	69(I)	3.1
2-norbornyl	95	90(I)	4.1
Me_3C	98	94(N)	1.4

[a]Reaction of 1 mmol of RHgCl in 10 ml of pyridine for 20 h at 40 °C; irradiation by a 275-W sunlamp ~ 20 cm from pyrex reaction flask. N, by ^1H NMR; I, isolated.

was employed. When sunlamp irradiation was not employed and all light was excluded from the reaction tube with an aluminum foil wrapping, essentially no mercury metal or substituted pyridines were observed. Furthermore, the reaction of cyclohexylmercury chloride with pyridine or pyridinum ion was initially inhibited by O_2, 5 mole % di-*tert*-butylnitroxide or 10 mole % *m*-dinitrobenzene (0.5-3.5h.) and was severally retarded by radical traps such as anthracene or N,N,N',N'-tetramethyl-*p*-phenylenediamine. Oxygen, nitroxide and *m*-dintrobenzene inhibition as well as light initiation are consistent with a chain reaction mechanism.

Firm evidence that substituted product is the offspring of the organomercury-derived radical was provided by the 5-hexenyl rearrangement, a probe which has found extensive application in mechanistic studies [37]. The radical rearrangement

from 5-hexenyl to cyclopentylmethyl is diagnostic for the radical.

Reaction of 5-hexenylmercury chloride with pyridine produced essentially all cyclized product (*o*-and *p*-cyclopentylcarbinylpyridines) as expected for a chain reaction involving R• (Scheme 27).

Scheme 27

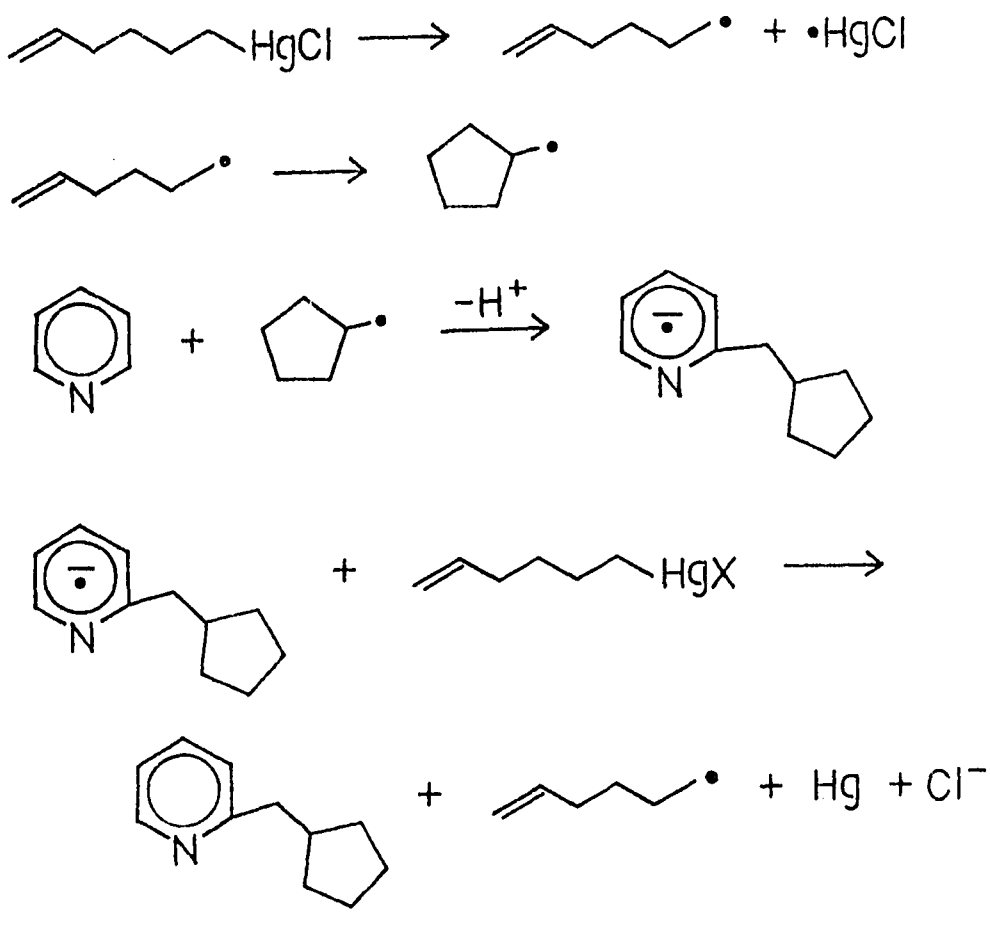

The structure of the observed products were verified by comparison of ^{1}H NMR, MS and GLC data with authentic samples prepared by reaction of pyridine with

cyclopentylmethylmercury chlorides.

The unimolecular rate constant for cyclizations of radical has been estimated to be 10^5 s^{-1} at 40 °C [38] [39]. The rate constant for reaction of 1-hexenyl radical with pyridine cannot be greater than 10^3 M^{-1} s^{-1}.

Determination of the Kinetic Chain Length of the Reaction between *t*-BuHgCl and γ-picoline

The kinetic chain length (K.C.L.) [40] can be defined as the rate of appearance of products divided by the rate of radical formation by initiation.

$$K.C.L. = \frac{\text{rate of appearance of products}}{\text{rate of radical formation by initiation}}$$

The rate of appearance of products was obtained from the slope of the curve at the beginning of the reaction (determined by use of a tangent meter) as shown in Figure 2.1. The rate of radical formation by initiation was calculation from the concentration of di-*tert*-butyl nitroxide (DTBN) and the time needed to consume all of the DTBN which can also be determined from Figure 2.1.

From Figure 2.1:

Rate of appearance of products=0.008 M/min.

Rate of radical formation by initiation=0.0024 M/12 min.

$$K.C.L. = \frac{0.008\text{M}}{0.0024\text{M}/12min} = 40$$

The reaction of *tert*-butylmercury chloride and γ-picoline is definitely a chain process. The short chain length may reflect that some step in the chain sequence is endothermic even though the thermochemistry predicts that the overall reaction

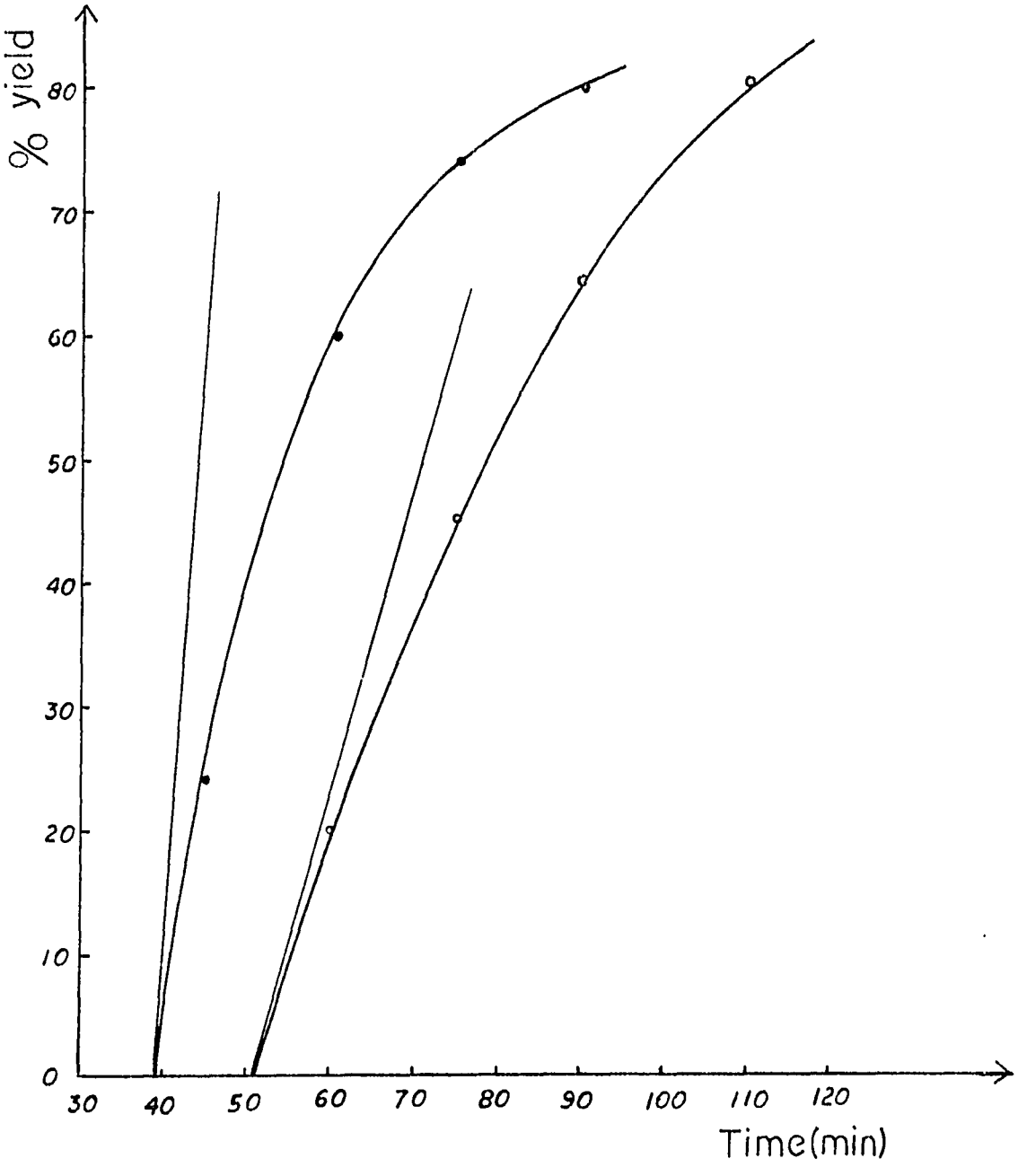

Figure 2.1: Formation of product vs time for the reaction of t-BuHgCl and γ-picoline

should be favorable. Kinetic chain length are, of course, a function of radical and substrate concentration as well as the rate constant for competing propagation and termination reactions.

Reactions of RHgX with Substituted Pyridines

Reactions of *tert*-butyl radical with 4-substituted pyridines

The substrate selectivity is strongly affected by the presence of substituents. Generally, with t-Bu$^{\bullet}$, 4-substituted pyridines gave a single monosubstituted product and no problem of regioselectivity is involved. Thus in 4-substituted pyridines the substitution exclusively occurs in position 2 and the effect of the substituents is very striking with a selective radical such as the *tert*-butyl radical. With t-BuHgCl reaction of pyridines with irradiation by a sunlamp gave the following products (substituent, product, %); 4-Me, 2-t-Bu, 87; 4-Et, 2-t-Bu, 68; 4-$CONH_2$, 2-t-Bu, 55; 4-Ph, 2-t-Bu, 60; 4-benzyl, 2-t-Bu, 40.

However, the reaction of *tert*-butylmercury chloride with 4-cyanopyridine when irradiated by the sunlamp for five days produced only 33% of a 4:1 mixture (by GLC) of 2-and 3-*tert*-butyl-4-cyanopyridine. Citterio et al. [41] reported only one product, 2-*tert*-butyl-4-cyanopyridine, was observed from the *tert*-butylation of protonated 3-cyanopyridine. This suggests that in the present case, t-Bu• attacks the unprotonated 4-cyanopyridine or a weak complex such as NCPy—Hg(t-Bu)Cl or PyCN—Hg(t-Bu)Cl.

Reactions of *tert*-butyl radical with 3-substituted pyridines

The high sensitivity to steric effects was clearly shown by the results obtained. With all the substituents investigated only the 6 position was attacked. Toward *t*-Bu• the 2 and 4 positions, ortho to the substituent, are not attacked because of steric hindrance. With *tert*-butylmercury chloride, the reaction of 3-substituted pyridines gave the following products (substituent, product, %); 3-Me, 6-*t*-Bu,90; 3-Et, 6-*t*-Bu, 88; 3-Ph, 6-*t*-Bu, 60; 3-COOMe, 6-*t*-Bu, 74; 5-$CONHCH_3$, 6-*t*-Bu,87.

However, the reaction of 3-cyanopyridine with *tert*-butylmercury chloride gave 60% of a 1.43:1 mixture of 6- and 4-*tert*-butyl-3-cyanopyridine and a small amount of the 2-*tert*-butyl-cyanopyridine. With protonated 3-cyanopyridine, it gave 95% of 6-*tert*-3-cyanopyridine [42].

The effect of the substituents in 3-substituted pyridines, which results in high regioselectivity for *t*-Bu• attack, is less pronounced for 1° and 2° alkyl radical attack. Toward the less sterically demanding *c*-C_5H_{11}•, the reaction of 3-substituted pyridines gave three substitution products. For example the reaction of 3-picoline with *c*-$C_5H_{11}HgCl$ produced three isomers. The relative ratio of 6-/2-/4- substitution production is 5.4/3.8/2.6. With *t*-Bu• only position 6 is substantially attacked in a reaction which is exceptionally sensitive to steric effects.

Reactions of *tert*-butyl radical with 2-substituted pyridines

The *tert*-butylations of 2-substituted pyridines gave a mixture of 2,4- and 2,6-pyridine derivatives. With *tert*-BuHgCl reaction of pyridine with irradiation by a of sunlamp gave the following products (substituent, product, %); 2-Me, mixture of

4 and 6-*t*-Bu, 90; 2-Ph, 2.2:1 mixture 6-*t*-Bu and 4-*t*-Bu, 69; 2-Cl, 1.3:1 mixture of 6-and 4-*t*-Bu, 85. Reactions were not observed with 2-methoxy- or 2-fluoropyridines.

Reactions of *tert*-BuHgCl with phenylpyridines

The reactions of *tert*-BuHgCl with phenylpyridines gave the following products (substituent, product, %); 4-Ph, 2-*t*-Bu, 60; 3-Ph, 6-*t*-Bu, 60; 2-Ph, 2.2:1 mixture 6-*t*-Bu and 4-*t*-Bu, 69. No substitution products in the benzene ring were observed. This indicates that *tert*-butyl radical will only react with the pyridine ring at the available nuclear positions to yield the corresponding substitution products. According to experiments by Minisci et al. [42], no reaction occurs between *tert*-butyl radical and pyridine (unprotonated) or benzene. Toward $CH_3\bullet$, the ratio of rate constants for attach on pyridine and benzene is 3:1 [43]. On the basis of these results, it seems likely that the pyridine ring is activated by coordination with RHgX to form a complex which can undergo a chain process with *t*-BuHgCl. The pyridine-RHgCl complex has a partial positive charge in the pyridine ring and undergoes facile reaction with free radicals similar to the reactions of pyridinium ions.

Reactions of Cyclopentylmercury Chloride with Pyridine and Anthracene

The reaction of cyclopentylmercury chloride with pyridine in the presence of anthracene was inhibited by the anthracene. The mercury metal precipitation was retarded and the reaction time needed to alkylate the pyridine was increased to 20 h. The main reaction products were 2-and 4-cyclopentylpyridines and a small amount of the disubstituted pyridines. Only trace amounts of cyclopentylanthracene were

detected by GCMS. The ratio of 2- and 4- substituted pyridines to substituted anthracene was about 58:1 by GLC. Pyridine or PyHg(R)Cl appears to be much more reactive than anthracene toward cyclopentyl radical. However, toward $CH_3\bullet$, the ratio of rate constants for attack on anthracene and pyridine is 275:1 [43]. Alternatively, the electron transfer reaction from the stable intermediate radical of anthracene to RHgX may not occur but this should result in anthracene derived products.

Reactions of RHgX with Protonated or Unprotonated Heteroaromatic Compounds

tert-Butylmercury chloride reacts with pyridinium, 4-methylpyridinium and quinolinium trifluoracetate in Me_2SO with irradiation by a sunlamp to form the corresponding *tert*-butyl derivatives in high yield and in a short time (Table 2.2). It is evident that the addition of *tert*-butyl radical to protonated pyridine and quinoline is faster than with the unprotonated heteroaromatic compounds.

No substitution occurs between $PhCH_2HgCl$ and pyridine upon irradiation with a sunlamp. However, in the presence of trifloroacetic acid, benzylpyridine and bibenzyl are observed after a reaction photostimulated by a sunlamp. It is interesting that only 2-benzylpyridine was observed in the reaction of benzylmercuryl choride (0.12 M) with protonated pyridine (0.5 M) and that the ratio of bibenzyl to 2-benzylpyridine is 1.5 : 1 which leads to rate constant for the attack of benzyl radical upon the protonated pyridine of 3.8×10^5 $M^{-1}s^{-1}$[36], since the reaction of addition of benzyl radical to $PhCH_2HgCl$ has a rate constant of 2.4×10^6 $M^{-1}s^{-1}$. However, in the Minisci reaction with the benzyl radical no substitution was observed

Table 2.2: Reactions of RHgCl with protonated pyridine, 4-picoline and lepidine

Substrates	RHgX	% Products[a]	Byproducts	% Hg
Pyridine	*t*-BuHgX	80		85
α-Picoline	*t*-BuHgX	78		75
Lepidine	*t*-BuHgX	97	-[b]	135
Pyridine	$PhCH_2HgCl$	2-Benzylpyridine	$PhCH_2CH_2Ph$	(1:1.5)[c]

[a] A mixture of *t*-BuHgCl (0.1 mmol) and protonated heteroaromatic compounds (0.2 mmol) in 5 mL of Me_2SO was irradiated by sunlamp for 10 h.
[b] 2,6-Di-*tert*-butyllepidine to bibenzyl.
[c] The ratio of 2-benzylpyridine to bibenzyl.

with protonated pyridine and bibenzyl was the only reaction product [42].

With RHgCl, heteroaromatic base gave the following products (RHgX, base, product, %); *t*-BuHgCl, 4-methylquinoline, 2-*tert*-butyl-4-methylquinoline, 93; *t*-BuHgCl, bezothiazole, 2-*tert*-butylbenzothiazole, 70; 2-norbornylmercury chloride, 4-methyl-quinoline, 2-norbornyl-4-methylquinoline, 70; *c*-$C_6H_{11}HgCl$, isoquinoline, 2-cyclo-hexyl isoquinoline, 90; *c*-$C_6H_{11}HgCl$, benzothiazole, 2-cyclohexyl benzothiazole 69 (Table 2.3). Reactions of *t*-BuHgCl were not observed with acridine, isoquinoline and quinaldine because of steric hindrance after addition of *t*-Bu• to these heteroaromatic compounds.

Table 2.3: Reactions of RHgCl with benzothiazole, isoquinoline and lepidine (substrates)

Substrates	RHgX	% Products[a]
Benzothiazole	*t*-BuHgX	70
	c-C_6H_{11}HgCl	69
Isoquinoline	*c*-C_6H_{11}HgCl	90
Lepidine	*t*-BuHgX	93
	2-norbornyl mercury chloride	70

[a]A mixture of RHgCl (0.1 mmol) and heteroaromatic compounds (1.0 mmol) in 5 mL of Me_2SO was irradiated by sunlamp for 10 h.

Regioselectivity and Reactivity

Table 2.1 summarizes the observed ortho/para ratios for the reaction between alkylmercury chlorides and pyridine with irradiation by a sunlamp. The tertiary and secondary alkylmercury chlorides only afforded ortho and para substituted products but the primary alkylmercury chlorides also give the meta-isomers in small amounts. All of reaction formed small amounts of disubstituted derivatives.

In Table 2.4 the effect of solvent and temperature on the ortho/para ratio for the reaction of *t*-BuHgCl with pyridine is shown. The ratio of ortho/para isomers in benzene, hexamethylphosphoric triamide, dimethylformamide, tetrahydrofuran and neat pyridine are 3.10 : 1, 2.67 : 1, 2.64 : 1, 1.70 : 1 and 1.40 : 1 respectively. The ratio of ortho/para isomers increased with decreasing temperature. The ratio at

Table 2.4: The solvent effect on the regioselectivity of the 2- and 4- position in pyridine

Solvent	o/p (35 °C)[a]
THF	1.70
Pyridine	1.85 (3.0, 0 °C)
DMF	2.64
HMPA	2.67
Benzene	3.10

[a] A mixture of *t*-BuHgCl (0.3 mmol) and pyridine (1.0 mmol) in solvent (5 mL) was irradiated by sunlamp for 10 h.

35 °C was 1.4 : 1, but it become 3 : 1 at 0 °C in pyridine as solvent.

The effects of the acidity on the ratio of ortho/para substitution products is reported in Table 2.5. The ratio of o/p isomers is less in the presence of trifluromethansulfonic acid (0.7:1) than in the presence of trifluroacetic acid (1:1).

The reactions may involve attack of R• upon PyH^+ or Py—Hg(R)Cl as well as C_5H_5N. PyH^+ is much more reactive than Py toward *t*-Bu• [44] since the strongly nucleophilic radical, *t*-Bu• prefers to add to the more electron deficient pyridine-ring (PyH^+ > Py-Hg(R)Cl > Py). However, recently Minisci et al. have reported that with the most nucleophilic radicals (*t*-Bu•, α-THF•) no substitution was observed with unprotonated pyridine in the solvents such as water, benzene, acetonitrile, Me_2SO, THF [44].

If the Minisci et al. negative experiments are dependable for the attack of *t*-Bu•

Table 2.5: The acidity effect on the regioselectivity of the 2- and 4-position in pyridine

Acidity[a]	Unprotonated	CF_3COOH	CF_3SO_3H
o/p	1.4	1.0	0.7

[a] A mixture of *t*-BuHgCl (0.1 mmol) and protonated pyridine (0.3 mmol) in 5 mL of Me_2SO was irradiated by sunlamp for 10 h.

upon pyridine, *tert*-butyl radical generated from *t*-BuHgCl, may react with other species which exist in pyridine solutions of *t*-BuHgCl. In the initial stages of the reaction between *t*-BuHgCl and pyridine or 4-methylpyridine, no protonated pyridines are present. Thus, the species which react with *tert*-butyl radical may be complexes between C_5H_5N and RHgCl, Py—Hg(R)Cl. The reaction of $BuHgNO_3$ with pyridine or 4-methylpridine to form 1:1 adducts, 3-coordinated $PyHg(R)NO_3$ in benzene solution and the 2-coordinated complex, $PyHgPy^+$ in acetone, acetonitrile and water has been reported by Graddon and Mondal [45]. The nature of solvent and the temperature may affect the equilibrium between 3-coordinate (molecular) and 2-coordinate (ionic) complexes in solution.

$$Py + t\text{-}BuHgCl \rightleftharpoons Py—Hg(t\text{-}Bu)Cl \rightleftharpoons PyHg(t\text{-}Bu)^+Cl^-$$

The Py—Hg(R)X and Py-HgR^+X^- should be more reactive than Py toward *t*-Bu•. For the reaction of primary alkylmercury chloride with pyridine or 4-methylpyridine, primary alkyl radical can attack either Py—Hg(R)Cl or pyridine, since toward *n*-Bu•, 4-methylpyridine has a rate constant $k = 1.5 \times 10^3\ M^{-1}s^{-1}$ at 78 °C [45].

These results are well interpreted in terms of frontier orbital interactions [46]

between the single occupied molecular orbital of the radical (SOMO) and either the highest occupied molecular orbital (HOMO) or the lowest unoccupied molecular orbital (LUMO) of the substrate involving pyridine, Py—Hg(R)Cl and $PyHgH^{+}Cl^{-}$.

The nucleophilic-type SOMO-LUMO interaction (2 orbitals - 1 electron) is always stabilizing. The energetic effect $\Delta E(PMO)$ associated with this interaction is proportional to the square of the overlap integral between the 2 orbitals and inversely proportional to the energy difference, $\Delta\varepsilon$ (SOMO-LUMO) before the interaction

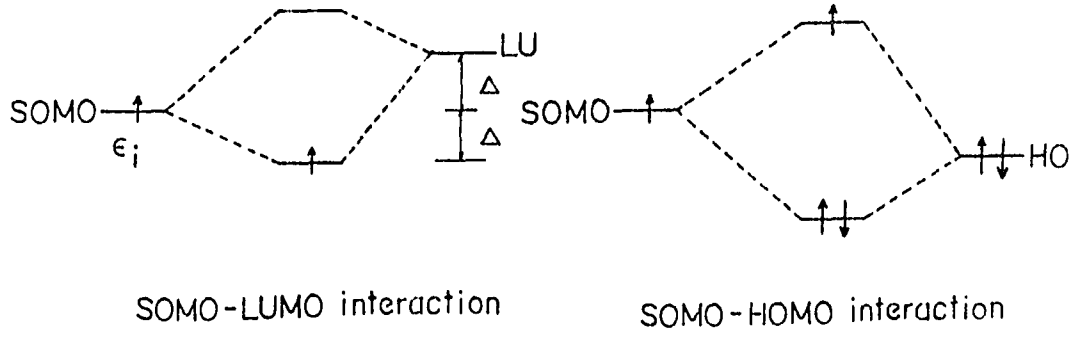

$$\Delta E(PMO) = \frac{S_{ij}^2(\varepsilon_j - H_{ij}/S_{ij})^2}{\varepsilon_i - \varepsilon_j}$$

i = SOMO, j = LUMO,

ε = orbital energy,

S_{ij} = overlap integral,

H_{ij} = matrix element.

In view of PMO theory, the frontier orbital interaction is controlled by two factors, the energy gap ($\Delta\varepsilon$) and the overlap integral (S_{ij}). The smaller the difference $\Delta\varepsilon = \varepsilon_i - \varepsilon_j$, that is to say the higher the SOMO energy level, the stronger the SOMO-LUMO interaction and the stronger the nucleophilic reactivity of the radical.

The HOMO-SOMO interaction is a three electron two orbital interaction. The lowest orbital is stabilized (here the HOMO) and the highest is destabilized. By this interaction the radical behaves as an electrophilic species. To a first approximation, when the overlap is neglected, both interactions are stabilizing. If we take into account the overlap, the interaction LUMO-SOMO is always stabilizing, but the interaction HOMO-SOMO can become destabilizing, specially when the overlap increases and when the difference of energy $\varepsilon_i - \varepsilon_j$ is important.

The 'experimentally adjusted' energies obtained according to the procedure described by Arnaud et al. [47] are reported in Table 2.6 and illustrated in Figure 2.2.

The difference of reactivity of *t*-Bu• and *n*-Bu• towards the substrates, pyridine, Py—Hg(*t*-Bu)Cl and PyH^+ seem to be best explained by LUMO-SOMO and HOMO-SOMO interactions. The strong nucleophilic radical *t*-Bu• has the highest energy which interacts strongly with the LUMO of the PyH^+ and not nearly so well with the LUMO of Py, MePy and C_6H_6. The reactivity of *t*-Bu• toward the substrates increases according to the sequence PyH^+ >> Py-H—Cl=Py-Hg^+(*t*-Bu) >> Py~MePy~C_6H_6. We can see that the difference of reactivity between benzene and pyridine toward *t*-Bu• is not very important because when going from benzene to pyridine the LUMO-SOMO interaction is similar ($\varepsilon_j - \varepsilon_i$). The values of the energy gap

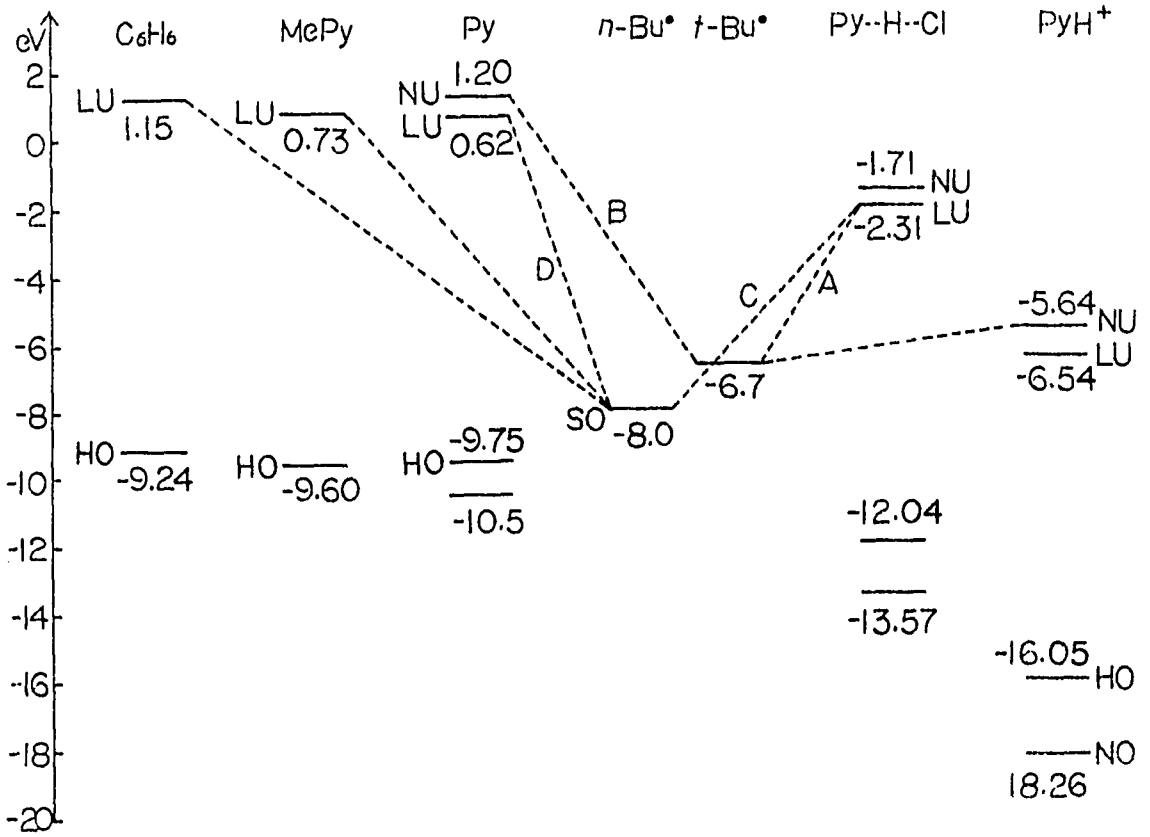

Figure 2.2: Interaction diagram for the SOMO of *t*-Bu• and *n*-Bu• with the frontier orbitals of C_6H_5, MePy, Py, Py-Hg(R)Cl and PyH^+

Table 2.6: 'Adjusted' unperturbed molecular orbital energies (eV) used in the interaction energy calculation

Reactants orbitals energy	NOMO	HOMO	LUMO	NUMO	SOMO
4-MePy	-10.05[a]	-9.60[a]	+0.73[a]	+1.27[a]	
4-MePyH$^+$	-16.58[a]	-15.78[a]	-6.82[a]	-6.44[a]	
Py	-10.50[b]	-9.75[b]	+0.62[c]	+1.20[c]	
PyH$^+$	-18.26[d]	-16.05[d]	-6.54[d]	-5.64[d]	
Py—HCl	-13.57[d]	-12.04[d]	-2.13[d]	-1.71[d]	
Ph•					-8.1[b]
t-Bu•					-6.7[b]
n-Bu•					-8.0[b]

[a]Ref. [47].

[b]From ionization potential: pyridine [48], phenyl [48], *tert*-butyl radical [49].

[c]From electron affinity of pyridine [50].

[d]From adjusted values of pyridine MO corrected by the quantity E(PyH$^+$)-E(Py) [51].

are so big that no reaction occurs between *tert*-butyl radical and benzene or pyridine [44]. Thus we can suppose that the *t*-Bu• may largely attack Py—Hg(*t*-Bu)Cl.

The *n*-butyl radical has the lowest energy SOMO and hence the difference between the interactions C and D on Figure 2.2 is not so great as for the corresponding interactions (A and B) of the *tert*-butyl radical. In this situation, the LUMO-SOMO interaction is weak and the HOMO-SOMO interaction should be important. The difference of reactivity between pyridine and Py—Hg(R)X is not very important because when going from pyridine to Py—Hg(R)X the LUMO-SOMO interaction is increased but at the same time the HOMO-SOMO interaction is decreased by the same order of magnitude. In addition, pyridine as solvent has a high concentration ca 12 M. Thus, the low selectivity primary alkyl radical would attack both pyridine and Py—Hg(R)Cl resulting in a small amount of the meta-substituted product.

The rearomatization of the radical adduct (1) involves a proton transfer and an electron transfer from strongly nucleophilic radicals of the pyridinyl type (2) to RHgX.

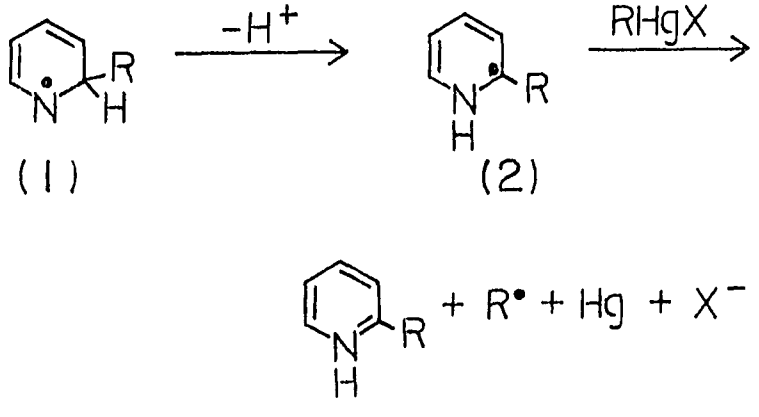

The reactivity of the reaction increases by increasing the nucleophilic character of the radical (**2**) which is generally associated with an increased stability and electron transfer ability (oxidizability) of the radical (**2**). The sequence of the radical stability may be $3^{\circ} > 2^{\circ} > 1^{\circ}$ for radical (**2**). The *t*-Bu radical adduct (**1**) may more easily undergo a 1,2 proton shift and an electron transfer reaction than the *n*-Bu radical adduct (**1**). The *t*-Bu substituted radical (**2**) is a capto-dative radical with a high energy SOMO which interacts more strongly than low energy SOMO of the *n*-Bu substituted radical with LUMO of RHgX. Thus, the reaction of *t*-BuHgCl with pyridine may occur, even though the addition of *t*-Bu• to Py is unfavorable, because the rearomatization is more favorable.

tert-Butylmercury chloride reacts rapidly with pyridine, but very slowly with 4-cyanopyridine (which requires a 5 day irradiation period for significant reaction) even though 4-cyanopyridine should be much more reactive than pyridine toward *t*-Bu•. Possibly the rate of electron transfer from the intermediate radical to RHgX is slow for the 4-cyano derivative. This results are well interpreted in terms of orbital interaction theory.

The intermediate radicals for alkyl-substituted pyridines have a higher energy HOMO compared to the intermediate 4-cyanopyridine radical. The intermediate radicals of alkyl substituted pyridines have a relatively high energy SOMO while the intermediate radical from 4-cyanopyridine is conjugated to the cyano group and will have a lower energy SOMO. The orbital interaction A can be more effective than B. Thus RHgX can be reduced by the intermediate adduct radical of pyridine faster than by the intermediate adduct radical of 4-cyanopyridine. Thus, total overall rate

of reaction of *t*-BuHgCl with pyridine is faster than with 4-cyanopyridine.

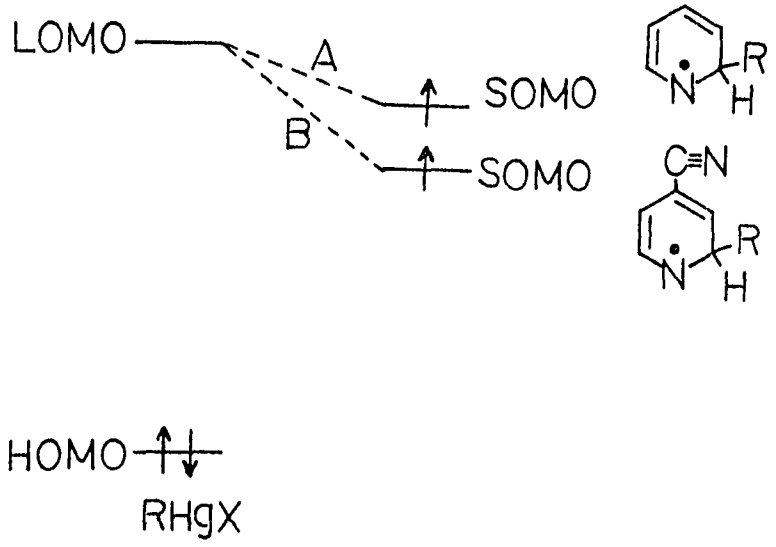

Reactions of Alkylmercury Chlorides with (*s*)-(−)-Nicotine

The synthesis of nicotine analogues is important not only in the assessment of structure-reactivity relationships but also in the development of radio immunoassays (RIA) for tobacco alkaloids.

Seeman et al. reported [52] that optically active 6-alkylnicotines can produced by the addition of alkyl radicals to (*s*)-(−)-nicotine using the Minisci alkylation procedure. However, the yield of optically active product is below 42%. We have had

Table 2.7: 6-Alkylnicotines prepared from the reaction of RHgCl with (*s*)-(−) nicotine with sunlamp irradiation

Alkyl HgCl	% Product	% Hg	$[\alpha]_D^{20}(CH_2Cl_2)$
tert-Bu	94[a], 54[b]	92	-141 °C(*c* 0.087)
exo-2-Norbornyl	80[a]	80	

[a] A mixture of (*s*)-(−) nicotine (0.24 g), TFA (0.1 mL) and *t*-BuHgCl (0.3 g) in 2 mL of Me_2SO was irradiated by sunlamp for 32 h. Yields by GLC.

[b] Isolated yield.

success in the reaction alkylmercury chlorides with (*s*)-(−)-nicotine with irradiation by a sunlamp to give the optically active products in higher yields (Table 2.7).

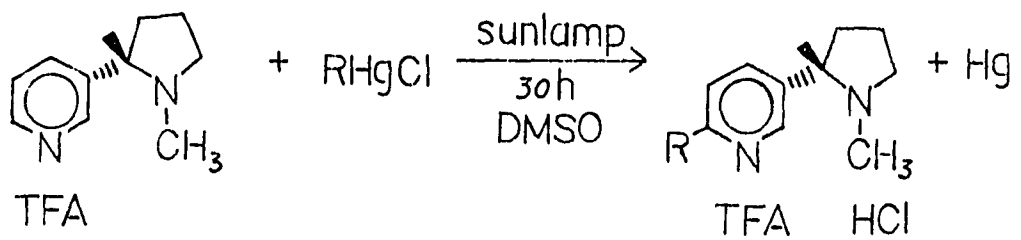

This method had several advantages including:

1. one step procedure;

2. high optical activity of product;

3. regioselectivity for *tert*-butyl and norbonyl radicals.

Solvomercuration-pyridination

Solvomercuration was discovered by Kucherov in 1892 [53] and developed by Hofman and Sand in 1900 [54]. This reaction has become an extremely valuable tool for the functionalization of olefins. Alkenes react with HgX_2 in presence of solvents to give solvomercurials (Equation 2.1).

$$C{=}C + HgX_2 + YH \longrightarrow YC\text{-}CHgX \qquad (2.1)$$

$$X : OAc, CF_3CO_2, NO_3, SO_4^-,$$

$$Y : OH, OR, HNR.$$

The solovomercuration-demercuration of alkenes (Equation 2.1 and Equation 2.2) is probably the most important synthetic method employing intermediate organomercurials [55]. The use of solvomercuration-demercuration as a general synthetic tool is due largely to Brown et al. [56] [57].

$$YC\text{-}CHgX + NaBH_4 \longrightarrow YC\text{-}CH \qquad (2.2)$$

Formation of C-C bonds is an important synthetic procedure in organic chemistry. We have succeeded in a one pot two-stage process of solvomercuration-pyridination which is convenient, takes place under mild conditions, and gives good yields. The alkene is added at room temperature to a methanol solution of mercuric trifluoroacetate. This reaction is generally complete within 15 minutes. The olefin

solvomercuration products need not be isolated. Addition of excess pyridine (Py) and sunlamp irradiation to initiate the chain process leads to the formation of a drop of elemental mercury and the alkylated pyridine (Scheme 28).

Scheme 28

$$C{=}C + Hg(CF_3COO)_2 + ROH \longrightarrow$$
$$ROC\text{-}CHgO_2CCF_3 + Py \xrightarrow{h\nu} Py\text{-}C\text{-}COR$$

The solvomercuration-pyridination process can make complicated pyridine derivatives in a one pot reaction. The long chain alkylpyridine derivatives may be used as surface active agents.

The general approach to synthesis of oxymercurials is straightforward and normally involves the reaction of mercuric acetate directly with the olefin in a suitable, usually aqueous or alcoholic, medium. The reaction is generally assumed to be complete when a sample of the reaction mixture fails to produce a yellow precipitate of mercuric oxide on basification.

Methoxy-mercuration of cyclohexene has been well studied and the kinetically formed product is *trans*-1-acetoxymercuri-2-methoxycyclohexene.

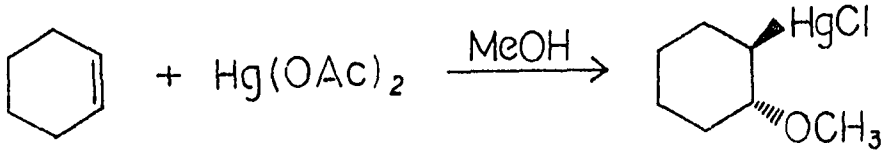

Initially the organomercurical was isolated and then reacted with pyridine. How-

Table 2.8: Alkylpyridines formed by the reaction of an alkene with $Hg(OAc)_2$ followed by reaction with C_5H_5N with sunlamp irradiation

Alkene	Solvent	RC_5H_4N[a]	% Yield[b]	*o*/*p*(GC)
Cyclohexene	H_2O/THF	-[c]	36 (I)	1.8
Cyclohexene	CH_3OH	-[d]	56 (I)	2.3
cis-*cis*-1,5 Cyclooctadine	CH_3OH	-[e]	20 (I)	2

[a]Reaction of 20 mmol of alkene and 20 mmol of $Hg(OAc)_2$ in 20 mL of MeOH. After 1 h, 8 mL of pyridine was added and the mixture irradiated with a sunlamp for 40 h.
[b](I), isolated; GC by GLC.
[c]*o*- and *p*-(2-hydroxycyclohexyl)pyridine.
[d]*o*- and *p*-(2-methoxycyclohexyl)pyridine.
[e]*o*- and *p*-(*cis*-2-*exo*-methoxy-6-*exo*-bicyclo[3,3,0]octyl)pyridine.

ever, we have found that there is no particular disadvantage in carrying out the pyridination stage in situ without isolating the methoxymercurial. Methoxymercuration-pyridination of cyclohexene provided 56% of isolated *o*-and *p*-(2-methoxycyclohexyl) pyridine (Table 2.8). Hydroxymercuration-pyridination of cyclohexene afforded 36% of isolated *o*- and *p*-(2-hydroxycyclohexyl)pyridine.

A more rapid reaction and higher yield was observed using trifluroacetate, instead of mercury acetate. The mercury was recovered as a drop of elemental mercury in high yield (see Table 2.9). The reaction of the olefin with mercury trifluroacetate in the presence of methanol gave the methoxy mercuration product and trifluoracetic

acid which would protonate the pyridine to form the pyridinium ion (Scheme 29).

Scheme 29

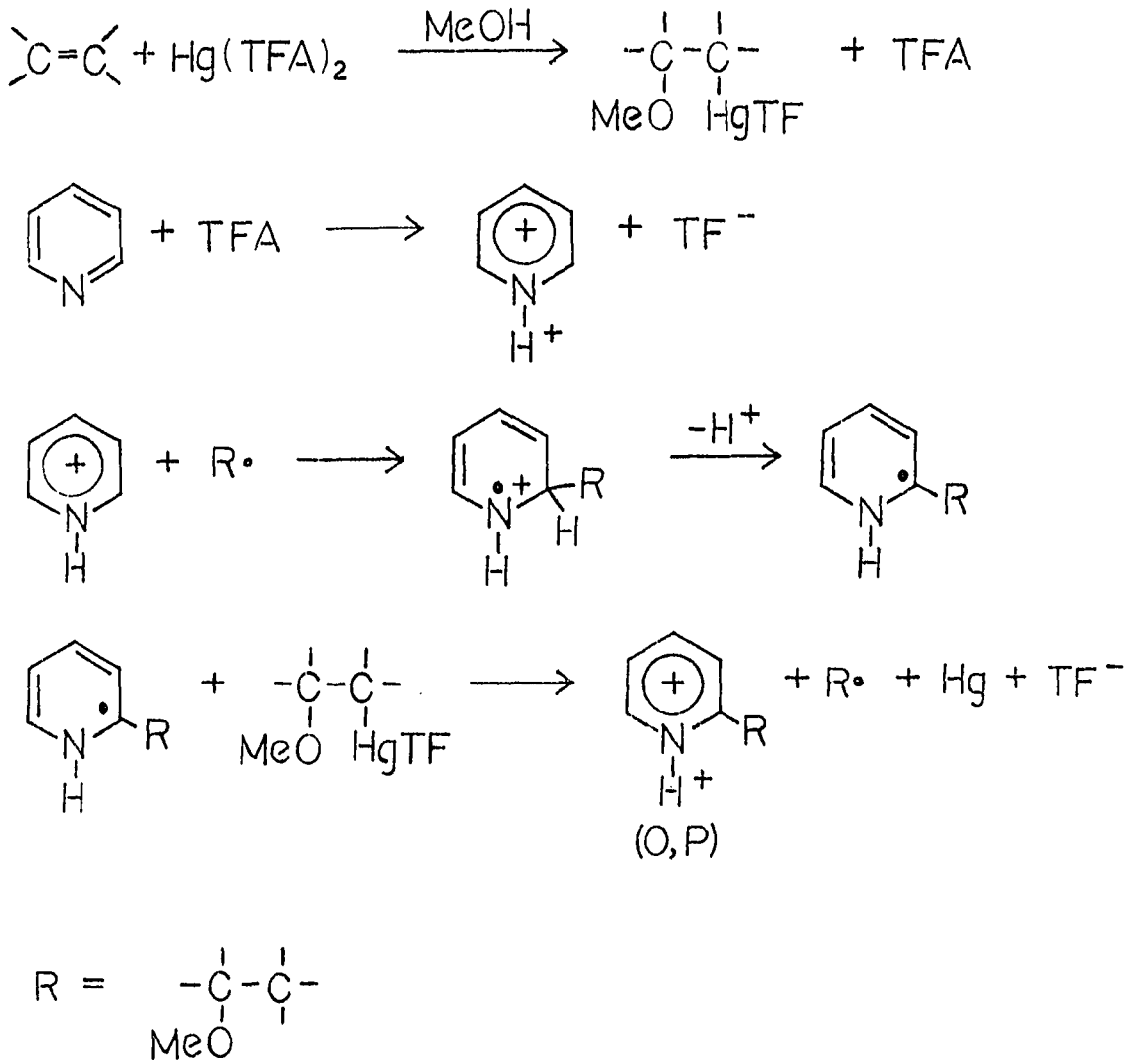

Transannular reactions have been observed in the free radical reaction of cyclootane derivatives [58], [59]. Benzoyl peroxide addition of chloroform to *cis,cis*-1,5-

Table 2.9: Alkylpyridines formed by the reaction of an alkene with $Hg(TFA)_2$ and MeOH followed by reaction with C_5H_5N with sunlamp irradiation

Alkene	% Hg	R	% RC_5H_4N[a]	*o/p*
C_2H_4	92	$CH_2CH_2OCH_3$	73	2.0
$CH_3C_2H_3$	87	$CH_2CH(CH_3)OCH_3$	76	2.5
$C_2H_5C_2H_3$	92	$CH_2CH(C_2H_5)OCH_3$	78	2.5
n-$C_4H_9C_2H_3$	91	$CH_2CH(n\text{-}C_4H_9)OCH_3$	80	2.7
t-$C_4H_9C_2H_3$	80	$CH_2CH(t\text{-}C_4H_9)OCH_3$	67	2.8
$CH_3CH{=}CHCH_3$	90	$CH(CH_3)CH(CH_3)OCH_3$	81	1.9
c-C_6H_{10}	97	2-methoxycyclohexyl	86	2.2
norbornene	91	*exo*-3-methoxy-2-norbornyl	78	3.0

[a]Reaction of 10 mmol of alkene and 10 mmol of $Hg(O_2CCF_3)_2$ in 10 mL of MeOH. After 10 min, 8mL of C_5H_5N was added and the mixture irradiated with a sunlamp for 8 h. Yields by GLC.

cyclooctadiene yields the bicyclic saturated addition product in 37 % yield [60]. The conformational aspects of the eight-membered ring system are such that the radical site can be in the proximity of the unsaturated linkage across the ring.

We have found that methoxymercuration of *cis,cis*-1,5-cyclooctadiene with mercury acetate and methanol produces 5-methoxy-6-acetoxymercuriocyclooctene, which undergoes a photostimulated reaction with pyridine yielding 20% of a 2:1 mixture (by GLC) of *o*- and *p*-(2-methoxy-6-bicyclo[3,3,0]-octyl)pyridine(Table 2.8).

The absence of olefinic protons was confirmed by the ^{1}H NMR spectrum which showed protons for an ortho monosubstituted pyridine at δ 8.537(1H pyridine-α), 7.582(1H pyridine-γ), 7.160(1H pyridine-β_1), 7.095(1H pyridine-β_2), and protons of the methoxy group at 3.239 ppm. No olefinic protons was observed at 5-6 ppm. The IR spectrum of the compound did not have bands at 3000-3050 cm^{-1} (=CH-).

The mechanism and stereochemistry of the methoxymercuration of *cis,cis*-1,5-cyclooctadiene followed by photoreaction with pyridine is shown in Scheme 30.

Scheme 30

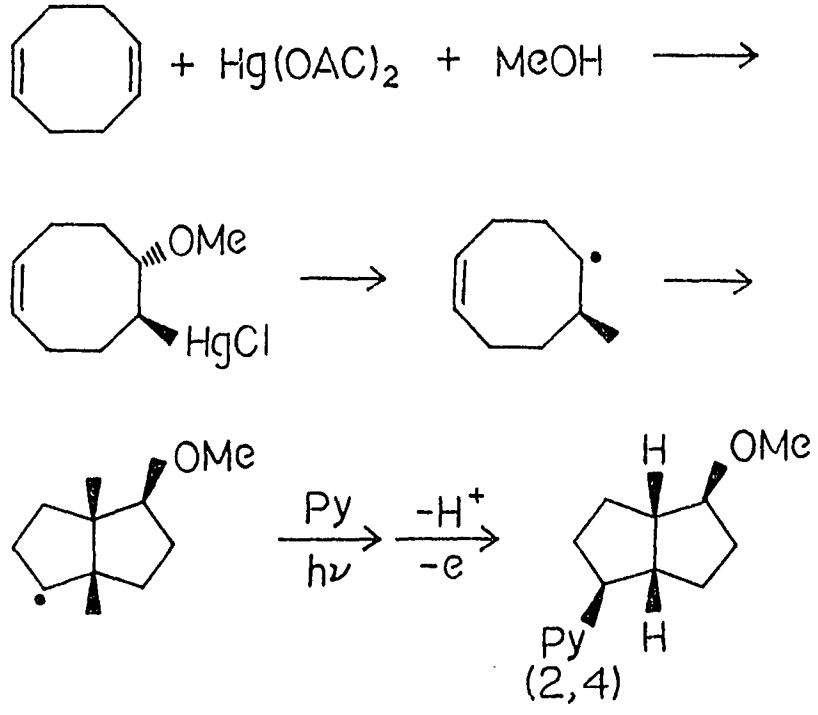

Methoxymercuration of *cis,cis* 1,5-cyclooctadiene with mercury acetate and

methanol produced *trans*-5-methoxy-6-acetoxymercuriocyclooctene which can decomposed photochemically into the 2-methoxy-5-cyclooctenyl radical. This radical can undergo a transannular reaction to form the bicyclic radical which reacts with pyridine to form the products.

The products are probably pure stereoisomeric compounds, because methoxymercuration is stereoselective. In addition, the only reasonable position for reaction of the bicyclootyl radical is 6-*exo* because of the prohibitive steric hindrance on the 6-*endo* side of bicyclooctane. The steric argument suggests that the methoxy and pyridine substituents are in a cis-exo arrangement.

Reaction of 5-*exo*-Methoxy-3-*exo*-nortricyclylmercury Chloride with Pyridine or Quinoline

The norbornenyl-nortricyclyl radical rearrangement has been studied by organic chemists [61][62]. The opening and closing of the cylopropane ring during the rearrangement of the nortricyclyl radical to the norbornenyl radical has been estimated to have a similar rate constants. The reverse ring-closing reaction has a rate constant of approximately 4 x 10^7 sec^{-1} at 20 °C [63]. The EPR data obtained at −130 °C suggest that $k_1 \geq 10\ k_{-1}$ while at -10 °C the tin hydride reduction experiments give $k_{-1} = 1.26\ k_1$ [64].

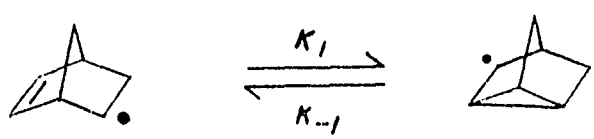

The reaction of 3-acetoxynorborn-5-en-2-ylmercury chloride or 5-acetoxy-3-nortri-cyclylmercury chloride with sodium borohydride in THF to form three acetates, 2- *exo*-acetoxynorborn-5-ene, 7-*anti*-acetoxynorborn-2-ene and 3-acetoxy-nortricyclene in the ratio 8 : 35 : 57 has been reported [65]. Strong evidence in favor of a radical mechanism for the reaction of RHgX with borohydride has been provided [66].

We hoped to use that the norbornenyl-nortricyclyl radical rearrangement as a timing device to probe chain transfer reaction of RHgX with pyridine. The reaction of 5-methoxy-3-nortricyclylmercury chloride with pyridine with irradiation by a sunlamp affords eight substituted isomers with MW 201 involving relative peak intensities of 41 : 5 : 4 : 20 : 10 : 3 : 1 : 7 (by GLC). These compounds will be referred to as isomers 1-8, respectively. The first isomer which is one of the major products has been isolated and identified to be 2-*exo*-(7-*anti*-methoxynorborn-5-en-2-yl)pyridine (**6**) by using TLC and ^{1}H, ^{13}C NMR, GCIR and MS. The fourth isomer was also isolated and assigned to 2-(5-*exo*-methoxy-3-*exo*-nortricyclyl)pyridine (**7**).

The fifth and the eighth isomers were isolated and identified as 4-(*exo*-7-*syn*-methoxynorbon-5-en-2-yl)pyridine (**6**) and 4-*exo*-(5-*exo*-methoxy-3-*exo*-notricyclyl)-pyridine (**7**). Analysis by GCIR confirmed that isomers, No. 1-4 and No. 5-8, were 2- and 4- substituted pyridines, respectively. The total yields of products and mercury metal were 77 % and 94 % respectively. On the base of these results, the following scheme is proposed.

Scheme 31

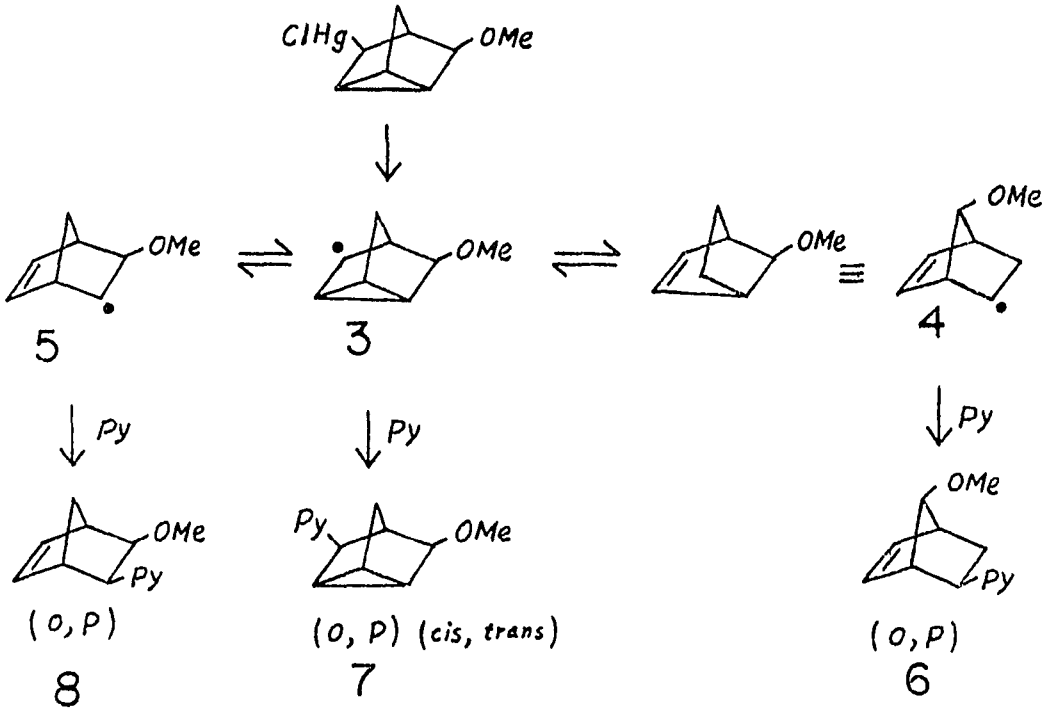

A 5-*exo*-methoxynortricyclyl radical (**3**) first formed from the photodecomposition of 5-*exo*-methoxy-3-nortricyclylmercury chloride underwent the nortricyclyl-norbornenyl radical rearrangement to yield 5- and 7-methoxynorbornenyl radicals (**4** and **5**). These radicals react with pyridine to give the corresponding ortho and para products as a 0.52:1 mixture of (**7**) and (**6**). The addition of the (**3**), (**4**) and (**5**) radicals to pyridine must be a sufficiently slow process to allow the (**5**) $\rightleftharpoons$ (**3**) $\rightleftharpoons$ (**4**) $\rightleftharpoons$ equilibrium to occur. Perhaps radical (**4**) may be more reactive than radical (**3**) toward pyridine since (**6**) is the major product.

The reaction of 5-methoxy-3-nortricyclylmercury chloride with 4-methylquinoline produced 5 substituted products. The total yields of products and mercury metal were 60% (by GLC) and 70%. The relative GC peak intensities of the 5 products were 4.2 : 3.1 : 3.3 : 0.84 : 11.4. These products will be referred to as isomers 1-5, respectively. The major product is No. 5 which has been isolated and identified to be 4-methyl-2-(5-*exo*-methoxy -3-*exo*-nortricyclyl)quinoline.

The No. 1 product was also isolated and identified as 4-methyl-2-(7-*syn*-methoxynorborn-5-en-2-yl)quinoline. The ^{1}H NMR spectrum of this rearrangement product showed an X-A-B-Y olefinic system at δ=6.295 and 6.124 and an ortho substituted quinoline ring at δ=8.040, 7.928, 7.643, 7.471, 7.388. The signal of the 7-proton of the norbornene system is α to a methoxy group and appears at δ=3.702 as a poorly resolved multiplet. The protons of the methoxy group observed at δ=2.888 show a dramatic shift due to interaction between the methoxy group and the quinoline ring. The signal of the 2-proton (α to the quniolinyl group) appears at δ = 2.972 as a well resolved quartet with the expected patterns for H-2-*endo*.

The sterochemistry of the No. 1 product was further confirmed by spin decoupling experiments. For the *exo*-adduct irradiation at the frequency of the bridgehead 1-proton at δ=3.312 did not effect the H-2 signal but did effect the H-7 signal.

This confirmed that H-2 was *endo* and therefore the quinoline group was *exo*. When the frequency of H-2 at δ=2.972 was irradiated, the H-3*exo* and H-3*endo* signals at δ=2.480 and 1.833 were reduced to a doublet of doublets and a doublet. This confirmed that H-2 is *endo* and therefore the quinoline is *exo*.

We have seen that the reaction of 5-methoxy-3-nortricyclylmercury chloride with

pyridine gave a 0.52:1 mixture of 5-*exo*-methoxy-3-*exo*-nortricyclyl and 7-*anti*-methoxy-norbon-5-en-2-yl derivative. However, lepidine gave a 2.13 : 1 mixture of these isomers. This indicates that quinoline is probably more reactive than pyridine toward (**3**), (**4**) and (**5**). Another interpretation is that radical (**3**) is more reactive (**4**) toward lepidine because of steric hindrance in the addition of radical (**4**) to lepidine. Even though the nortricyclyl-norbornenyl radical rearrangement is fast (k=10^7 $M^{-1}s^{-1}$) it is reversible and one of the radicals could be preferentially trapped by the lepidine.

Reaction of RHgX with N,N,N',N'-tetramethyl-p-phenylene-diamine

N,N,N',N'-tetramethyl-*p*-phenylenediamine (TMPDA) has low oxidation potential of 0.25 V (NHE) [67]. Thus, oxidation can occur readily with a wide variety of oxidizing agents, such as peroxides, lead dioxide, and air in alkaline solution. The paramagnetic salt (Wurster blue) formed by oxidation of TMPDA is an intermediate between TMPDA and the quinoid dication [68].

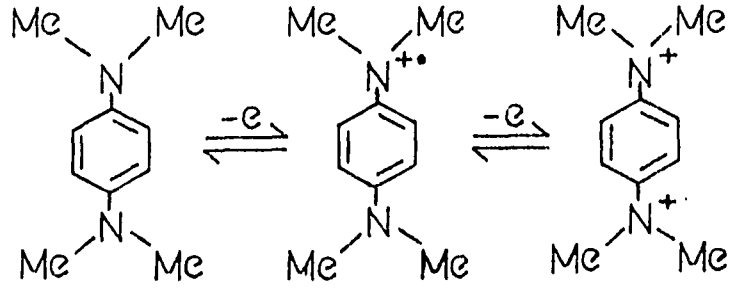

The ESR spectrum of Wurster blue has been measured and is rich in hyperfine splitting due to coupling of the unpaired electron with the nuclei of the atoms at the different positions.

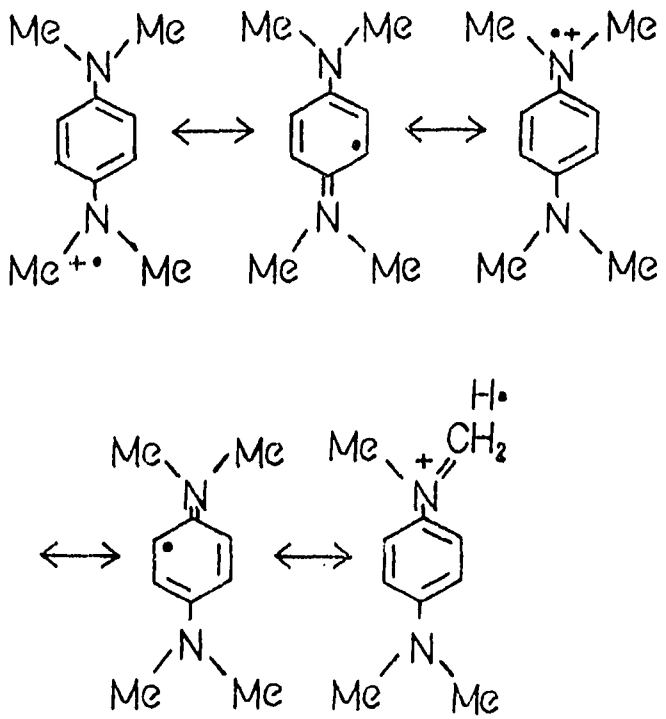

TMPDA has been much studied as a charge-transfer donor since it is one of the few donors which is stable enough in the radical cation form for all degrees of charge transfer to be observed [69]:

$$D + A \rightleftharpoons [D - A] \rightleftharpoons [D^{+\bullet}A^{-\bullet}] \rightleftharpoons D^{+\bullet} + A^{-\bullet}$$

TMPDA has been extensively studied as an antioxidant and anti-ozonant for hydrocarbons, rubber, etc. The scavenging process involves Wurster's blue formed via an initial radical complex [70].

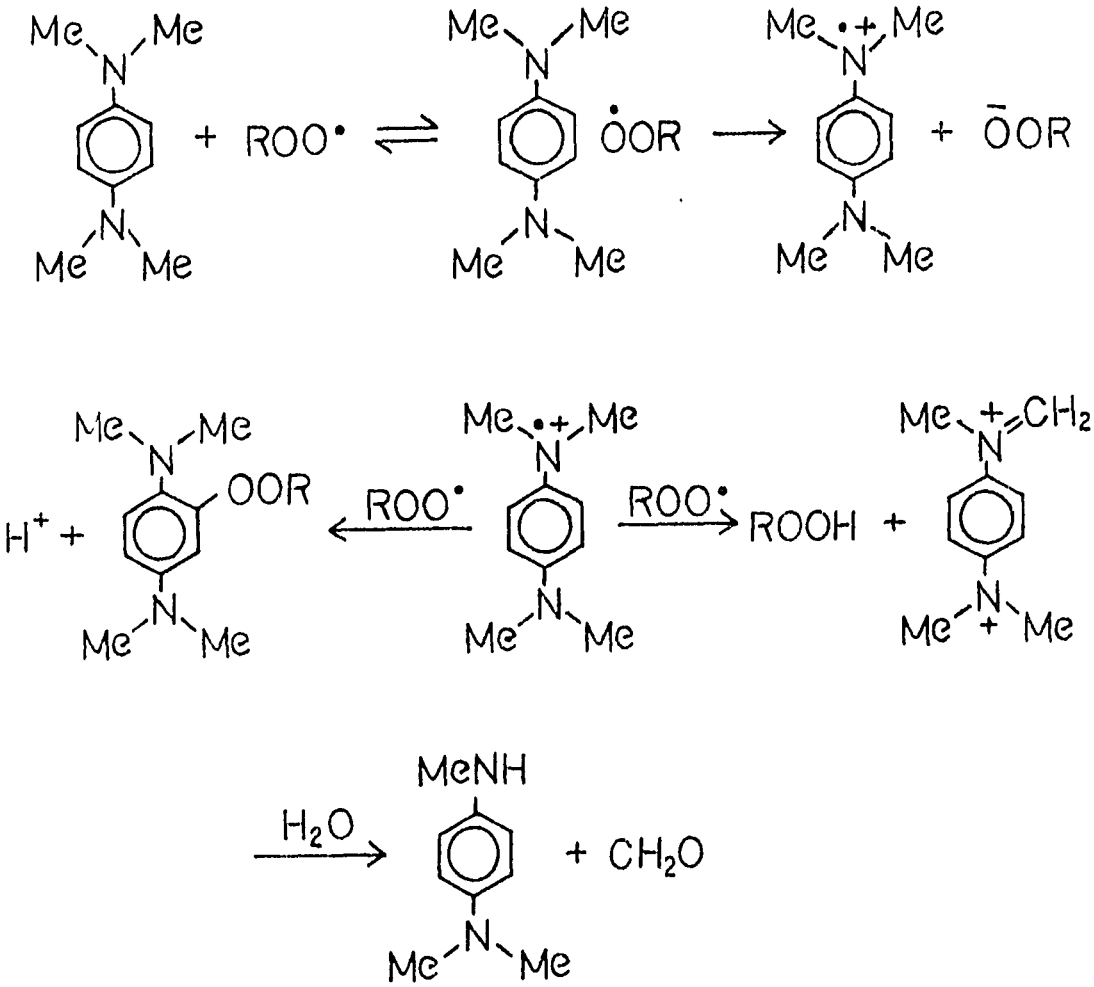

However, the reaction of TMPDA with alkyl radicals has not been reported. We

have shown that alkylmercury halides have dual character in that they can be oxidized or reduced by strong oxidants or reductants. An alkyl radical, mercury metal and halide ion would result from the one electron reduction of an organomercury halide. In the presence of TMPDA an adduct radical might be formed which could propagate a reaction chain by transferring an electron to an organomercury halide. The initial radical may be generated by the photodecomposition of RHgX.

A blue color and an ESR signal were immediately observed upon the addition of benzylmercury chloride to a Me_2SO solution of TMPDA at 25 °C. The *g*-value of ESR signal is near that of DPPH (Figure 2.3).

The NMR peak of TMPDA become broadened and disappeared when the reaction was irradiated for about 0.5 h. After the precipitation of mercury metal was complete, the NMR spectrum become normal and the methyl peak of TMPDA appeared again. The observed ESR and NMR phenomena are due to electron transfer from the charge transfer complex.

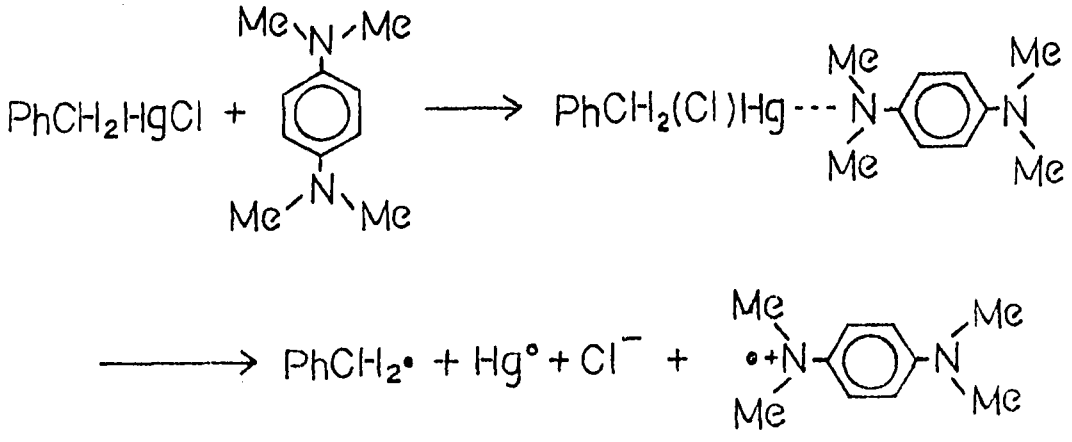

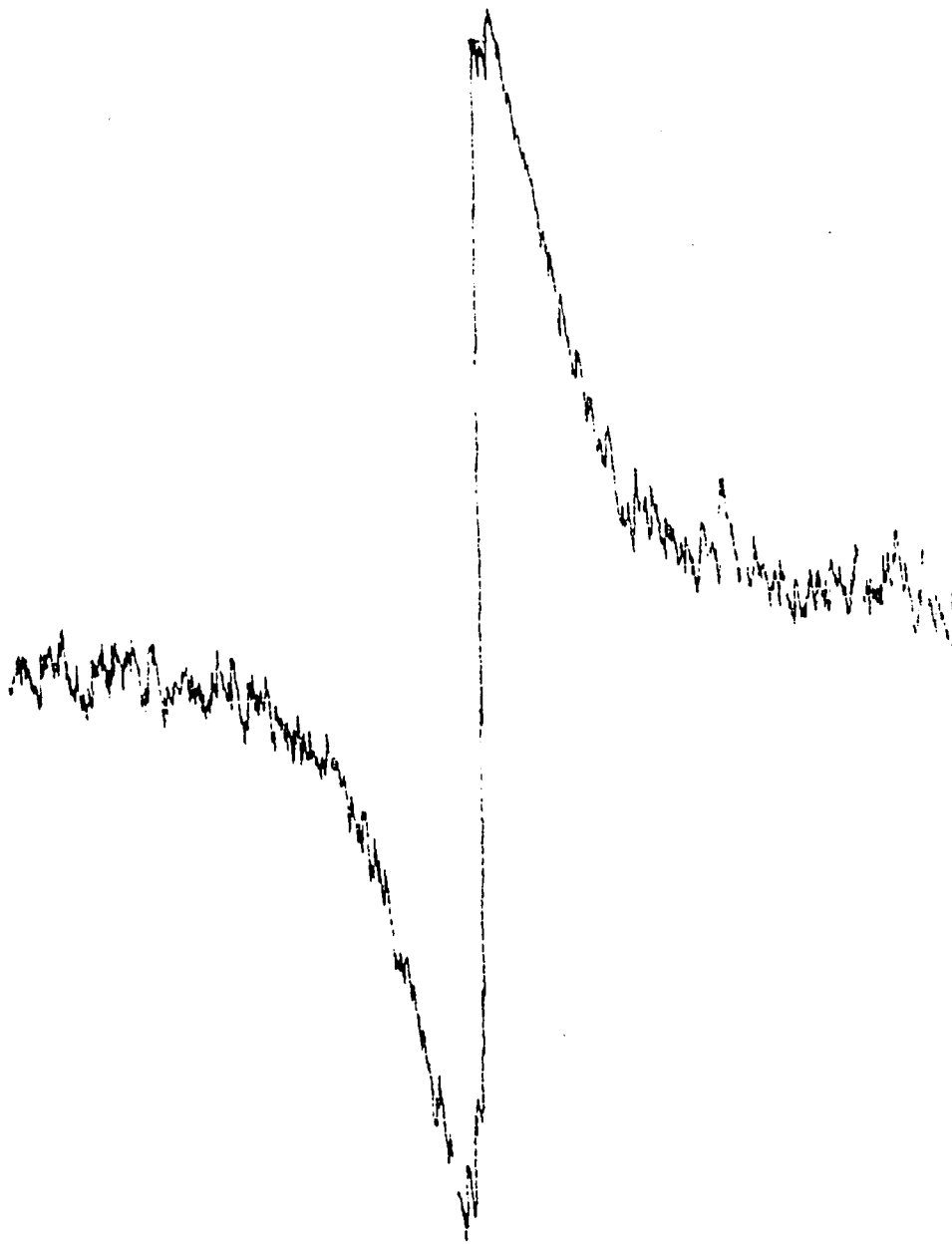

Figure 2.3: ESR spectrum recorded during the reaction of benzylmercury chloride and TMPDA in Me_2SO at 25 °C

Steric effects clearly play an important role in the reactively of alkylmercury halide toward TMPDA. *tert*-Butylmercury chloride, a very labile organomercurial, was unreactive towards the TMPDA. No blue color or the formation of mercury metal were observed during the addition of TMPDA or after irradiation about 40 h by sunlamp or UV(350 nm). Because TMPDA has bulky groups ($N(CH_3)_2$), the reaction of TMPDA apparently fails with the *tert*-butyl radical. However, the reactions of TMPDA with planar benzyl and allyl radicals generated from benzyl and allylmercury chloride gave rise to the alkylated products in high yield, even though benzyl, allyl and *tert*-butyl radicals are all strongly nucleophilic radicals.

Benzylmercury chloride reacted with TMPDA to afford the corresponding benzyl derivative in an isolated yield of 70% and mercury metal in an isolated yield of 90% under sunlamp irradiation for 20-40 h. A small amount of bibenzyl and the dibenzyl derivative of TMPDA were also observed (Table 2.10).

When sunlamp irradiation was not employed and all light excluded from the reaction tube with an aluminum foil wrapping, only 7% (GLC) of the alkylated product was obtained. Light was required to initiate the reaction and the reaction was retarded by O_2, *p*-dinitrobenzene and di-*tert*-butylnitroxide. The reaction of allylmercuryl chloride with TMPDA found the allyl derivative in 70% yield (by GLC) and a small amount of the diallyl derivative.

The reaction of cyclopentyl, cyclohexyl and cyclopentylmethyl mercury chloride with TMPDA afforded the corresponding products in 40-60% yield (by GLC) and some of the corresponding alkyl substituted N,N-dimethylaniline. Diethoxyphosphinylmercury chloride [$(C_2H_5O)_2P(O)HgCl$] gave the diethoxyphosphinyl deriva-

Table 2.10: Photostimulated reactions of RHgCl with TMPDA

RHgX	% R-TMPDA[a]	% Hg	% RDMA[b]
t-BuHgCl	NR		
CH_2=CH-CH_2-CH_2-CH_2-HgCl	–[c]	–	
CH_2=CH-CH_2-CH_2-HgCl	40(GC)		30(GC)
CH_2=CH-CH_2-HgI	70(GC)		0
$PhCH_2HgCl$	70(I) 80(GC)	90	7[d]
c-$C_5H_9CH_2HgCl$	–	85	
c-C_5H_9HgCl	60	70	
$(EtO)_2HgCl$	20		

[a]TMPDA (6.6 mmol) and RHgCl (6.5 mmol) in 40 mL Me_2SO were irradiated by sunlamp for 40 h.; GC by GLC; I, isolate.

[b]RDMA, alkyl substituted N,N- dimethlylaniline.

[c]A mixture of the 5-hexenyl and cyclopentylcarbinyl products in the ratio of 0.33:1.

[d]$PhCH_2CH_2Ph$(7 %).

tive of TMPDA in low yield (20%). Only a small amount of product was observed from the reaction between isopropylmercury chloride and TMPDA. No reaction occurred between methyl, phenyl or vinylmercury chloride and TMPDA.

Reaction of 0.2 M 5-hexenylmercury chloride with one equivalent of TMPDA formed a mixture of the 5-hexenyl and cyclopentylcarbinyl products in the ratio of 0.33 : 1. Thus the rate constant of the addition of 5-hexenyl radical to TMPDA is ca $10^6 s^{-1} M^{-1}$. Other side products were a mixture of 5-hexenyl and cyclopentylcarbinyl substituted N,N-dimethylaniline.

Alkylmercury halides undergo a free radical aromatic substitution reaction with TMPDA. Addition of $R^\bullet$ to TMPDA produces the easily oxidized adduct radical which undergoes dissociative transfer with RHgX to regenerate $R^\bullet$ as shown in Scheme 32.

Scheme 32

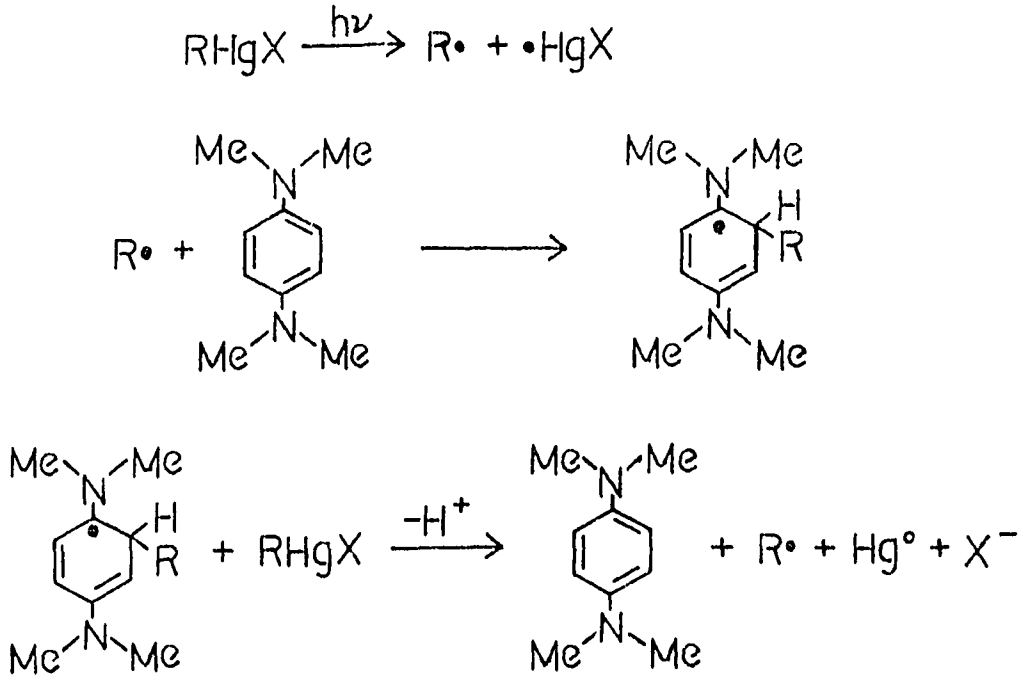

CHAPTER 3. CONCLUSION

Pyridines, quinolines, isoquinolines, benzothiazole, pyrazine, N,N,N',N'-tetramethyl-p-phemylenediamine or N,N-dialkylanilines underwent a photostimulated free radical chain reaction with alkylmercury halides or carboxylates, yielding ring alkylated substitution products.

Alkene mercuration products ($R^1CH(Y)CH(R^2)HgX$ with Y=HO, RO, CH_3CONH; X=Cl, CH_3CO_2, CF_3CO_2) can be used without isolation for the alkylation reaction.

CHAPTER 4. EXPERIMENTAL

General Considerations

^{1}H NMR spectra were recorded on a Nicolet NT 300 (300 MHz) NMR spectrometer, a JEOL FX-90Q (90 MHz) spectrometer and a Varian EM 360 (60 MHz). ^{1}H decoupling and ^{13}C NMR spectra were also determined on the NT 300 instrument. Infrared spectra (IR) were determined on a Beckman 4250 spectrophotometer. Infrared spectra (GCIR) were obtained on an IBM IR/98 spectrometer. Mass spectra (GCMS) are recorded on a Finnegan 4000 spectrometer. High resolution mass spectra (MS) were recorded on an AEI MS 902 mass spectrometer. Analytical gas chromatograph (GLC) was performed on a Varian 3700 gas chromatograph equipped with a Hewlett-Packard 3390 A integrator. Melting points were determined on a Fisher-Johns melting point apparatus and are uncorrected. ESR spectra were obtained on a Varian E-3 spectrometer.

GLC yields were determined by use of internal standards (naphthalene or biphenyl). ^{1}H NMR yields were determined by integration with a known amount of an internal standard (dibromomethane or acetonitrile).

Dimethyl sulfoxide (Me_2SO), dimethylformamide (DMF) and hexamethylphosphoramide (HMPA) were distilled from calcium hydride and stored over 4A molecular

sieves under nitrogen. Tetrahydrofuran (THF) was distilled from lithium aluminum hydride before use and stored over 4A molecular sieves under nitrogen. Davidson 4A molecular sieves were activated by drying in vacuo at 230 °C for 16 h. Deuterated dimethyl sulfoxide was dried with activated 4A molecular sieves and purged with argon to remove traces of oxygen.

Literature procedures [71] [72] were employed for the preparations of *tert*-butylmercury chloride, benzylmercury chloride, ethylmercury chloride, *n*-butylmercury nitrate, allylmercury chloride, cyclohexylmercury chloride, 5-hexenylmercury chloride, isopropylmercury chloride and 5-methoxy-3-nortricyclylmercury chloride.

Samples of cyclopentylmethylmercury chloride, neopentylmercury chloride, and *exo*-norbonylmercury chloride were supplied by J. W. Hershberger.

^{1}H NMR of Mono-alkylated Pyridines

The ^{1}H NMR of pyridine derivatives is complicated because of the coupling between the α, β, and γ protons. For γ-alkylated pyridines, the α and β hydrogens appear as doublets. For α-alkylated pyridines the remaining α-hydrogen atom is a doublet at the lowest field ($\delta \sim 8.5$), the γ hydrogen is found at intermediate fields ($\delta \sim 7.6$), usually as a triplet of doublets, while the β-hydrogens are at highest field ($\delta \sim 7.1$) as a multiplet which often looks like a triplet but may will be overlapping multiplets. β-Alkylated pyridines in general display at low field ($\delta \sim 7.2$) overlapping singlets and doublets for the α hydrogen and at higher field a complex multiplet for the β and γ hydrogen atoms of the ABX system. In the following section apparent coupling constant are reported for alkylated pyridines but only the J value for the α

proton (observed at the lowest field) can be considered as a true coupling constant reflecting the coupling between α and β protons.

Reaction of Cyclohexylmercury Chloride with Pyridine

Cyclohexylmercury chloride (6.32 g) was added to 6.32 g of pyridine in 40 mL of Me_2SO in a Pyrex tube with a rubber septum. The Pyrex reaction tube was irradiated with a 275 W General Electric fluorescent sunlamp placed about 20 cm away. Without external cooling the temperature of the reaction was about 40-45 °C. After 5-10 min, mercury metal began to precipitate. The reaction was irradiated a total of 20 h. Beads of mercury formed at the bottom of the tube. The pyridine solution was decanted from the mercury metal (3.6 g, 90% yield) and added to 10 mL of 0.1 M KOH, extracted with Et_2O, and the ether solution was washed twice with 10 ml of H_2O. The dried ether solution was evaporated and Kugelrohr distilled to give 2.05 g (64%) of a 3.1 : 1 mixture (by GLC) of 2- and 4-cyclohexylpyridines, bp 80-90 °C (5 torr).

The 2- and 4-cyclohexylpyridines are readily distinguished by GCMS. The 2-cyclohexylpyridine has a pronounced M^+-H peak (160) while 4-cyclohexylpyridine gives mainly M^+ (161) (Table 4.1).

The 2-cyclohexylpyridine was isolated on a TLC plate using hexane-ethyl acetate as eluent and analyzed by ^{1} NMR.

^{1}H NMR (300 Hz, $CDCl_3$) δ 1.20-1.59 (m, 5H), 1.717-1.969 (m, 5H), 2.734 (tt, J=14, 7.1 Hz, 1H), 7.142 (ddd, apparent J=11.0, 6.0, 0.8 Hz, 1H, pyridine-β_2), 7.150 (d, J=6.9 Hz, 1H, pyridine-β_1), 7.594 (d, J=7.7, 1.8 Hz, 1H, pyridine-γ), 8.523 (dd,

Table 4.1: GCMS data for the products of the photostimulated reaction between RHgX and pyridine

R	*o*-RC_5H_5N *m/e* (relative intensity)	*p*-RC_5H_5N *m/e* (relative intensity)
t-C_4H_9	135(M^+, 21), 134(M^+−H, 31), 120(100), 104(5), 93(30), 80(8.4), 79(19.7), 78(10), 65(4), 58(5), 52(74)	135(M^+, 39), 120(100), 104(4) 92(57), 80(5.5), 79(6.4), 78(58), 77(8), 65(11), 59(2), 51(13.4)
c-C_5H_9	147(M^+, 11), 146(M^+−H, 9), 130(3), 119(31), 118(30), 106(100), 80(4), 79(14), 78(11), 65(6), 51(14)	147(M^+, 100), 132(8), 119(43), 118(55), 106(74), 105(84), 104(19), 93(24), 92(15), 91(24), 79(11), 78(21), 65(20), 51(31)
c-C_6H_{11}	161(M^+, 34), 160(M^+−H, 19), 146(5.4),132(63), 120(12), 119(8), 118(18), 117(22), 106(100), 93(38.4), 80(8.6), 79(20), 78(16), 65(9), 59(2), 51(16)	161(M^+, 88), 146(16), 132(28), 118(32), 105(100), 93(55), 80(13.4), 79(124), 79(12.4), 77(17), 65(24), 51(31)

Table 4.1 (Continued)

2-norbornyl	173(M^+, 4), 172(M^+−H, 1.2), 158(2), 144(37), 132(8.8), 130(11.6), 119(6.7), 118(6), 117(14), 106(100), 93(9), 79(12), 78(12), 77(6), 72(2), 67(5), 65(6), 59(2), 51(9)	173(M^+, 29), 158(1), 144(7), 130(14), 117(12), 106(100), 93(30), 81(10), 80(6), 79(8), 78(10), 77(10), 67(29), 58(1), 51(15)
i-C_3H_7	121(M^+, 21.5), 120(M^+−H, 26), 106(100), 93(22), 79(21), 78(23), 65(3), 59(2), 51(9)	121(M^+, 58), 120(M^+−H, 14), 106(100), 93(3), 92(3), 79(13), 78(15), 77(17), 59(1), 52(11), 51(23)
n-C_4H_9	135(M+, 2), 134(M^+−H, 4), 120(12), 106(29), 93(100), 78(16), 65(17), 51(25)	135(M^+, 29), 106(8), 93(100), 78(7), 77(8), 65(17), 51(23).
n-C_6H_{13}	163(M^+, 4), 162(M^+−H, 3.8), 148(4), 134(5), 120(19), 106(25), 93(100), 78(9), 65(9), 51(9)	163(M^+,18), 162(M^+−H, 4), 148(5), 134(8), 120(5), 106(12), 93(100), 79(8), 78(8), 77(8), 65(12), 51(8)

Table 4.1 (Continued)

n-$C_{12}H_{25}$	247(M^+, 0.9), 246(M^+−H, 0.4), 232(2), 218(0.4), 204(0.7), 190(0.5), 176(0.8), 162(1.8), 148(2.3), 134(2.2), 120(10.8), 106(22.6), 93(100), 78(2.6), 65(2.5), 55(2.5)	247(M^+, 3), 246(M^+−H, 1), 232(1), 218(2), 204(4), 190(2), 176(2), 162(3), 148(4), 134(1), 120(6), 106(100), 93(46), 80(2.6), 79(1.7), 78(5), 77(2.4), 65(7), 55(7)
Me_3CCH_2	148(M^+−H, 0.2), 134(9.5), 118(2.5), 106(0.7), 93(100), 78(2.7), 65(5.7), 64(1), 57(4), 51(3.8)	149(M^+, 9.3), 134(12.3), 118(2.4), 106(3.1), 93(100), 78(1.8), 77(2.2), 65(9.5), 57(41)
$Me_3CCH_2CH_2$	162(M^+−H, 2.7), 148(46), 134(7.8), 120(6.2), 106(100), 93(30), 78(10), 65(14), 57(1.4)	163(M^+, 54), 148(22), 130(1.2), 117(3.2), 107(88), 92(65), 79(12.4), 71(5.4), 65(22.7), 57(100), 51(9)
c-$C_5H_9CH_2$	160(M^+−H, 10), 146(5), 132(11), 118(10), 106(9), 93(100), 78(8), 65(14), 51(9)	161(M^+, 25), 144(2), 132(4), 130(4), 118(8), 105(5), 93(100), 77(5), 69(25), 65(11), 51(8)

J=5.7, 0.7 Hz, 1H, pyridine-α).

Reaction of *exo*-2-Norbornylmercury Chloride with Pyridine

exo-2-norbornylmercury chloride (3 g) in 10 mL of pyridine at 30-35 °C was deoxygenated by a helium stream and irradiated by a 275-W sunlamp about 20 cm from the Pyrex tube. Mercury metal precipitated from the solution after an induction period of 5-10 min. After 24 h, the pyridine solution was added to 10 mL of 0.1 M KOH, extracted with Et_2O, and the ether solution was washed twice with 10 mL of H_2O. The dried ether solution was evaporated and Kugelrohr distilled to give 1.40 g (90%) of a 4.1 : 1 mixture (by GLC) of 2- and 4-(*exo*-2-norbornyl) pyridines, bp 125-145 °C (0.1 torr).

The 2-(*exo*-2-norbornyl) pyridine was isolated on a TLC plate using hexane-ethyl acetate as eluent and analyzed by ^{1}H NMR.

^{1}H NMR ($CDCl_3$): δ 1.122 (d, J=9.38 Hz, 1H, 3-*endo*), 1.246 (t, J=8.8 Hz, 1H, 5-*endo*), 1.351 (t, J=8.8 Hz, 1H, 6-*endo*), 1.450-1.610 (m, 3H), 1.664 (td, J=10.4, 1.6 Hz ,1H), 1.875-1.970 (m, 1H), 2.370 (s, $1H_4$, bridged), 2.399 (s, $1H_1$, bridged), 2.380 (m, $\sim$ t or dd, $J \simeq$ 8.4 Hz, $1H_2$), 6.999 (m, $\sim$ t,apparent J=6.7 Hz, 1H, pyridine-β_2), 7.119 (d, J=7.9 Hz, 1H, pyridine-β_1), 7.511 (td, J=7.7, 1.5 Hz, 1H, pyridine-γ), 8.474 (d, J=4.4 Hz, 1H, pyridine-α).

HRMS for 2-(*exo*-2-norbornyl)pyridine was m/e 173.12073 (required for $C_{12}H_{15}N$, 173.12045).

Reaction of *n*-Butylmercury Chloride with Pyridine

n-Butylmercury chloride (3 g) was added to 10 mL of pyridine in a Pyrex tube equipped with a rubber septum. The solution were deoxygenated by a stream of helium bubbles for 15 min and then was irradiated with a 275 W sunlamp positioned approximately 20 cm from the Pyrex tube, which maintained the reaction temperature at 40-45 °C. Mercury metal precipitated from solution after an induction period of 5-10 min and the reaction appeared complete after 24 h. The pyridine solution was decanted from the mercury metal (1.63 g, 80% yield) and added to 10 mL of 10% aqueous potassium hydroxide solution. The product was extracted with Et_2O. The ether solution was washed twice with 10 mL of water and dried over anhydrous sodium sulfate. The dried ether solution was evaporated and Kugelrohr distilled to give 0.89 g (66%) of a 2.4 : 1 mixture (by GLC) of 2- and 4-*n*-butylpyridines, bp 60-75 °C (5 mm).

Reaction of Cyclopentylmethylmercury Chloride with Pyridine

Cyclopentylmethylmercury chloride (1.08 g) in 10 mL of pyridine was deoxygenated by a helium stream and irradiated by a 275 W sunlamp 20 cm from the Pyrex tube to afford 0.63 g (93%) of Hg and 0.45 g (77% by NMR) of crude product.

The 2-cyclopentylmethylpyridine was isolated on a TLC plate using hexane-ethylacetate (1:1) as the eluent. The ^{1}H NMR data were obtained for the 2-derivative. ^{1}H NMR ($CDCl_3$) δ 1.10-1.25 (m,2H), 1.42-1.72 (m,7H), 2.220 (septet, J=7.5 Hz, 1H), 2.746 (d, J=7.5 Hz, 2H), 7.043 ($\sim$ td, apparent J=7.1, 1.4 Hz, 1H, pyridine-β_1), 7.52 (td, J=7.7, 1.8 Hz, 1H pyridine-γ), 8.478 (d, J=4.18 Hz, 1H, pyridine-α).

Reaction of β-Acetaminocyclohexylmercury Chloride with Pyridine

β-Acetaminocyclohexylmercury chloride (3.0 g) in 19 mL of pyridine at 30-35 °C was deoxygenated by a helium stream and irradiated by a 275 W sunlamp 20 cm from the Pyrex tube. Mercury metal precipitated from the solution after an induction period of 5-10 min. After 24 h, beads of mercury formed at the bottom of the tube. The pyridine solution was decanted from the mercury metal (1.51 g, 94%) and added to 10 mL of 10% aqueous potassium hydroxide solution. The mixture was extracted with Et_2O. The ether solution was washed twice with 10 mL of water and dried over anhydrous sodium sulfate. The dried ether solution was evaporated and Kugelrohr distilled to give 1.22 g (70%) of a mixture (by GLC) of 2- and 4-(2-acetaminocyclohexyl)pyridines, bp 160-180 °C (1 torr).

The products were isolated product on a TLC plate using ethylacetate-hexane (1:1) solvent as the eluent. The first isolated product was analyzed by ^1H NMR, IR and MS and found to be the 2-derivative and the second isolated product was identified as the 4-derivative. The following data were obtained.

The 2-derivative had ^1H NMR (60 Hz, $CDCl_3$) δ 1.20-2.30 (m, 8H), 2.4-2.9 (m, 1H), 1.7 (s, 3H), 3.6-4.4 (m, 1H), 6.0 (d, J=7 Hz, 1H, NH), 6.95-7.35 (m, 2H, pyridine-β), 7.4-7.8(m, 1H, pyridine-γ), 8.47 (dd, J=4, 2 Hz, 1H, pyridine-α); IR, 3083 (m), 3021 (w), 2494 (s), 2875 (m), 1720 (vs), 1598 (m), 1500 (s), 14800 (m), 1440 (m), 1376 (m), 1320 (w), 1300 (w), 1260 (m), 1240 (m), 950 (w), 780 (w), 750 (m); HRMS, m/e calculated for $C_{13}H_{18}N_2O$, 218.14192, measured 218.14164, error −1.3 ppm; GCMS m/e (relative intensity) 218 (1.5), 203 (2), 175 (7.7), 159 (100), 146 (4.4), 132 (18.7), 120 (7.3), 106 (68.7), 93.1 (36.1), 77.0 (5.2), 65 (6.5), 56.1 (28.2).

The 4-derivative had GCMS m/e (relative intensity) 218 (4.6), 175 (14), 159 (41.3), 130 (14.3), 118 (9.3), 10.6 (100), 93 (20.7), 78 (10), 65 (4.3), 56 (5.2), 51(4.7); IR: 3083 (m), 3042 (w), 3000 (w), 2949 (s), 2880 (m), 1720 (vs), 1600 (m), 1562 (m), 1500 (s), 1460 (m), 1408 (w), 1375 (m), 1304 (w), 1260 (m), 1230 (m), 1140 (m), 810 (m).

Oxymercuration-pyridination of Cyclohexene

Cyclohexene (1.64 g) was added with magnetic stirring to a solution containing 6.36 g $Hg(OAc)_2$ in 80 mL of THF: H_2O (1:1). After 1 h, 8 mL of pyridine was added. The solution was deoxygenated by a stream of helium bubbles for 15 min, then irradiated with the 275 W sunlamp. After 24 h, the solution was decanted from the mercury metal (2.94 g, 73% yield) and added to 10 mL of 0.1 M potassium hydroxide. After ether extraction the ether solution was washed twice with 10 mL of H_2O. The dried ether solution was evaporated and Kugelrohr distilled to give 1.24 g (36%) of a mixture (by GLC) of 2- and 4-(2-hydroxylcyclohexyl)pyridines, bp 120-135 °C (1 torr).

The products were isolated on a TLC plate using ethylacetate-hexane (1:1) solvent as the eluent. The first eluted product was analyzed by ^1H NMR and MS (Table 4.2) as 2-(2-hydroxylcyclohexyl)pyridine and the second eluted product was identified as 4-(2-hydroxylcyclohexyl)pyridine. The following data were obtained.

2-(2-Hydroxylcyclohexyl)pyridine had ^1H NMR (300 MHz, $CDCl_3$) δ 1.23-1.69 (m, 5H), 1.73-1.90 (m, 3H), 1.93-2.38 (m, 2H), 2.60-2.80 (m, 1H), 3.892 (m, 1H), 7.15 ($\sim$t, apparent J=7.7Hz, 1H, pyridine-β_2), 7.238 (d, J=8.0 Hz, 1H, pyridine-β_1),

7.657 (td, J=7.8, 1.8 Hz, 1H, pyridine-γ), 8.519(d, J=4.1 Hz, 1H, pyridine-α).

4-(2-Hydroxylcyclohexyl)pyridine had ^{1}H NMR (300 MHz, $CDCl_3$) δ 1.14-1.63 (m, 4H), 1.63-1.97 (m, 3H), 1.97-2.26 (m, 2H), 2.450 (td, J=3.38 Hz, 1H), 3.696 (td, J=10.11, 5.15 Hz, 1H), 7.168 (dd, J=5.69, 1.31 Hz, 1H), 7.168 (2d, J=5.69, 1.31 Hz, 1H, pyridine-β), 8.466 (dd, J=4.62, 1.4 Hz, 1H, pyridine-α); HRMS for 4-(2-hydroxylcyclohexyl)-pyridine was m/e 177.11509 (required for $C_{11}H_{15}NO$, 177.11537). Error=−1.6 ppm.

Methoxymercuration-pyridination of Cyclohexene

Cyclohexene (1.64 g) was added with magnetic stirring to a solution containing 6.4 g $Hg(OAc)_2$ in 20 mL of MeOH. After 1 h, 8 mL of pyridine was added. The solution was deoxygenated by a stream of helium bubbles for 15 min and then irradiated with the 275 W sunlamp. After 40 h, the solution was decanted from the mercury metal (3.0 g, 75% yield) and added 10 mL of 10 % KOH solution. After ether extraction the ether solution was washed twice with 10 mL of H_2O. The dried ether solution was evaporated and Kugelrohr distilled to give 2.1 g (56%) of a mixture (by GLC) of o- and p-(2-methoxylcyclohexyl)pyridines, bp 95-115 °C (2 torr). A more rapid reaction and higher yield was observed using $Hg(O_2CCF_3)_2$.

Methoxymercuration-pyridination of *cis,cis*-1,5-Cycloctadiene

cis,cis-1,5-Cycloctadiene (2.2 g) was added with magnetic stirring to a solution containing 6.4 g $Hg(OAc)_2$ in 20 mL of MeOH. After 1 h, 8 mL of pyridine was added. The solution was deoxygenated by a stream of helium bubbles for 15 min, and then

irradiated with the 275 W sunlamp. After 40 h, the solution was decanted from the mercury metal and added 10 mL of 10 % KOH solution. After ether extraction the ether solution was washed twice with 10 mL of H_2O. The dried ether solution was evaporated and Kugelrohr distilled to give 0.9 g (20%) of a mixture (by GLC) of *o*- and *p*-(2-methoxy-6-bicyclo[3,3,0]-octyl)pyridines, bp 100-120 °C (1 mm).

The products were isolated product on a TLC plate using ethylacetate-hexane (1:1) solvent as the eluent. The first eluted product was analyzed by ^1H NMR, IR and MS as the 2-derivative and the second eluted product was identified as the 4-derivative. The following data were obtained.

The ortho derivative had ^1H NMR (60 Hz, $CDCl_3$) δ 1.0-2.2 (m, 8H), 2.4-3.0 (m, 3H), 3.35 (s, 3H, OCH_3), 3.6-3.34 (m, 1H), 6.9-7.4 (m, 2H, pyridine-β), 7.4-7.8 (m, 1H, pyridine-γ), 8.6 (dd, J=8, Hz, 1H, pyridine-α); GCIR, 3025 (vw), 3003 (vw), 2958 (vs), 2875 (m), 2792 (w), 1600 (m) 1475 (m), 1450 (w), 1225 (w), 1100 (m), 745 (m); GCMS, *m/e* (relative intensity) 217 (M^+, 9), 202 (30), 186 (16), 185 (16), 144 (100), 106 (48), 93 (29), 79 (19).

The para derivative had ^1H NMR (60 Hz, $CDCl_3$) δ 1.0-2.2 (m, 8H), 2.4-3.0 (m, 3H), 3.35 (s, 3H, OCH_3), 3.5-3.7 (m, 1H), 7.15 (d, J=8, Hz, 2H, pyridine-β), 8.50 (d, J=8, Hz, 2H, pyridine-α); GCIR, 3005 (vw), 3000 (vw), 2958 (vs), 2875 (m), 2792 (w), 1600 (m) 1460 (w), 1375 (w), 1225 (w), 1100 (m), 805 (vw); GCMS, *m/e* (relative intensity) 217 (M^+, 5), 202 (6), 185 (57), 144 (100), 106 (17), 79 (13).

Table 4.2: GCMS for alkylpyridines formed by the reaction from alkene with $Hg(TFA)_2$ / MeOH followed by the photostimulated reaction with pyridine

R	*o*-RC_5H_5N	*p*-RC_5H_5N
$CH_2CH_2OCH_3$	136(M^+−H, 1.4), 122(100), 106(24),94(24), 93(32), 79(14), 78(15), 65(15), 51(22)	137(M^+, 100), 122(6), 107(23), 93(11), 78(10), 77(10), 65(18), 51(31)
$CH_2CH(CH_3)OCH_3$	150(M^+−H, 0.5), 136(34), 120(13), 93(100), 79(3), 78(5), 65(9), 59(80)	136(M^+−Me, 3.6), 93(84), 79(1), 77(1), 59(100)
$CH_2CH(CH_2CH_3)OCH_3$	150(M^+−H, 28), 136(20), 121(12), 106(5), 93(100), 73(77)	165(M^+, 1), 136(8), 121(4), 107(3), 93(95), 78(2.5), 77(2.3), 73(100), 65(14)
$CH_2CH(n\text{-}C_4H_9)OCH_3$	192(M^+−H, 0.6), 178(23), 162(6), 136(18), 101(33), 93(100), 79(3), 78(5.7), 69(80), 65(10)	193(M^+, 0.9), 178(0.3), 162(1.3), 136(19), 120(6), 107(7), 101(53), 93(100), 79(1.9), 78(3.3), 77(3), 69(93), 59(11)

Table 4.2 (Continued)

$CH_3CH(t\text{-}C_4H_9)OCH_3$	193(M^+, 1.7), 192(M^+−H, 3), 178(27), 136(100), 121(28), 93(26), 78(9), 69(69)	193(M^+, 38), 136(62), 120(10), 107(10), 101(100), 93(13), 78(38), 77(3.6), 69(67)
2-methoxycyclohexyl	177(M^+, 0.4), i76(M^+−H, 1.74), 159(5), 149(14), 130(6), 120(8.5), 106(100), 93(19.6), 80(13), 78(13) 65(6), 52(7)	177(M^+, 1), 176(M^+−H, 0.8), 149(17), 130(10),120(6), 106(100), 93(32), 78(8), 65(8), 51(10)
exo-3-methoxy-2-norbornyl	203(M^+, 2.4), 188(100), 172(8.4), 160(25), 144(15), 117(26), 106(19), 93(25), 79(12), 78(14), 71(13), 65(16), 51(12)	203(M^+, 52), 188(10), 171(45), 156(28), 143(24), 130(31), 117(22), 111(17), 106(57), 85(30), 79(35), 71(100), 65(34), 55(27)

Reaction of Benzylmercury Chloride with N,N,N',N'-Tetramethyl-p-phenylenediamine

Benzylmercury chloride (2.15 g) was dissolved in a solution of N,N,N',N'-tetramethyl-*p*-phenylenediame (1.09 g) in 40 mL Me_2SO. The reaction solution was deoxygenated by a helium stream and irradiated by a 275 W sunlamp 20 cm from the Pyrex tube. The blue solution turned yellow and mercury metal precipitated from the solution after an induction period of 10 min. After 40 h, the Me_2SO solution was added to 10 mL 0.1 M potassium hydroxide solution, extracted with Et_2O, and the ether solution was washed twice with 10 mL of H_2O and dried over anhydrous magnesium sulfate. The dried ether solution was evaporated and Kugelrohr distilled to give 1.19 g (70 %) of the benzyl derivative bp 125-145 °C (0.01 torr).

The product had ^1H NMR (300 MHz $CDCl_3$) δ 2.568 (s, 6H $NC\underline{H}_3$), 2.781 (s, 6H $NC\underline{H}_3$'), 4.082 (s, 2H), 6.485 (d, J=2.86 Hz 1H), 6.595 (dd, J=2.92, 8.67 Hz, 1H), 7.075 (d, J=8.79 Hz, 1H), 7.201 (s, 5H); HRMS, m/e calculated for $C_{17}H_{22}N_2$ 254.17830, found 254.17741, error -3.5 ppm; GCMS, m/e (relative intensity) 254 (100), 239 (60), 223 (10), 211 (8), 194 (18), 180 (8), 165 (15), 146 (20), 135 (20), 127 (8), 118 (18), 111 (18), 104 (10), 91 (30), 80 (20), 65 (8).

General Procedure for the Photostimulated Reactions of RHgCl with Pyridine or Heteroaromatic Compounds

RHgCl (1.0 g) in 10 mL of pyridine at room temperature was deoxgrenated by a helium stream and irradiated by a 275 W sunlamp 20 cm from the Pyrex tube. After 10-24 h, beads of mercury formed at the bottom of the tube. The pyridine

solution was decanted from the mercury metal and added 10 mL of 10% aqueous KOH solution. The mixture was extracted with ether. The solution was washed twice with 10 mL of water and dried over anhydrous sodium sulfate. The dried ether solution was evaporated and the oily residue was analyzed by GLC and GCMS. The products were isolated on a TLC plate using ethylacetate-hexane (1:1) solvent as the eluent and the isolated product was analyzed by ^{1}H NMR and HRMS.

RHgX (0.2 mmol) and the heteroaromatic compound (0.4-0.6 mmol) in 5 mL Me_2SO were irradiated by sunlamp for 10-24 h. After the irradiation, the reaction mixture was worked up and analyzed by usual procedure. Table 4.3 and Table 4.4 present ^{1}H NMR and GCMS data of the substitution products.

Reaction of 5-*exo*-Methoxy-3-*exo*-nortricyclylmercury Chloride with Pyridine

5-*exo*-Methoxy-3-*exo*-nortricyclylmercury chloride (3.0 g) in 10 mL of pyridine at 30-35 °C was deoxygenated by a helium stream and irradiated by a 275 W sunlamp 20 cm from the Pyrex tube. Mercury metal precipitated from the solution after an induction period of 5-10 min. After 24 h, beads of mercury formed at the bottom of the tube. The pyridine solution was decanted from the mercury metal (1.53 g, 92%) and added 10 mL of 10% aqueous potassium hydroxide solution. The mixture was extracted with Et_2O. The ether solution was washed twice with 10 mL of water and dried over anhydrous sodium sulfate. The dried ether solution was evaporated and Kugelrohr distilled to give 1.27 g (77%) of a mixture (by GLC) of 2- and 4-(*exo*-7-*syn*-methoxynorborn-5-en-2-yl)pyridine, and 2- and 4-(5-*exo*-methoxy-3-*exo*-

Table 4.3: ^{1}H NMR data for the products of the photostimulated reaction between *t*-BuHgCl and substituted pyridines

Products (disubstituted pyridine)	^{1}H NMR (300 Hz, $CDCl_3$)
3-C(O)NHCH$_3$, 6-*t*-Bu-	1.248(s,9H), 2.868(d, J=4.7 Hz, 3H), 7.253(d, J=8.1 Hz, 1H, pyridine-β), 7.525(s, 1H, NH), 7.967(dd, J=8.47, 2.1 Hz, 1H, pyridine-γ), 8.876(d, J=1.5 Hz, 1H, pyridine-α).
3-Et, 6-*t*-Bu-	1.235(t, J=7.6 Hz, 3H), 1.356(3, 9H), 2.615(q, J=7.6 Hz, 2H), 7.249(d, J=8.1 Hz, 1H, pyridine-β), 7.429(dd, J=8, 2.1 Hz, pyridine-γ), 8.408($\sim$s, 1H, pyridine-α).
3-Ph, 6-*t*-Bu-	1.411(s, 9H), 7.487-7.252(m, 5H, ph), 7.570(dt, J=8.0, 1.52 Hz, 1H, pyridine-β), 7.787(dd, J=2.4, 8.26 Hz, 1H, pyridine-γ), 8.797(d, J=2.1 Hz, 1H, pyridine-α).
3-C(O)OCH$_3$, 6-*t*-Bu-	1.345(s, 9H), 3.895(s, 3H), 7.376(d, J=8.2 Hz, 1H, pyridine-β), 8.163(dd, J=9.3, 2.3 Hz, 1H, pyridine-γ), 9.114(d, J=2.3 Hz, 1H, pyridine-α).
2-Cl, 6-*t*-Bu-	1.345(s, 9H), 7.107(d, J=8.4 Hz, 1H, pyridine-β), 7.225(d, J=6.4 Hz, 1H, pyridine-β), 7.547(d, J=7.8 Hz, 1H, pyridine-γ).

Table 4.3 (Continued)

Products (disubstituted pyridine)	^{1}H NMR (300 Hz, $CDCl_3$)
2-Ph, 6-*t*-Bu-	1.448(s, 9H), 7.280(dd, J=7.2, 0.7 Hz, 1H, pyridine-β), 7.38-7.50(m, 3H, Ph), 7.563(d, J=7.6 Hz, 1H, pyridine-β), 7.61-7.72(m, 2H, Ph), 8.116(d, J=7.1 Hz, 1H, pyridine-γ).
2-Cl, 4-*t*-Bu-	1.363(s, 9H), 7.254(dd, J=1.4 Hz, 1H, pyridine-β_2), 7.349(d, J=1.0 Hz, 1H, pyridine-β_1), 8.335(d, J=5.35 Hz, 1H, pyridine-α).
4-Et, 2-*t*-Bu-	1.244(t, J=7.6 Hz, 3H), 1.365(s, 9H), 2.627(q, J=7.6 Hz, 2H), 6.927(dd, J=4.9, 1.2 Hz, 1H, pyridine-β_2), 7.159($\sim$s, 1H, pyridine-β_1), 8.446(d, J=5.0 Hz, 1H, pyridine-α).
4-Ph, 2-*t*-Bu-	1.426(s,9H), 7.276(dd, J=5.0, 1.6 Hz, 1H, pyridine-β_2), 7.40-7.49(m, 3H, Ph), 7.536(s, 1H, pyridine-β_1), 7.58-7.62(m, 2H, Ph), 8.60(d, J=5.0 Hz, 1H, pyridine-γ).
4-C(O)NH_2, 2-*t*-Bu-	1.363(s, 9H), 6.842(s, 1H, NH), 6.975(s,1H, NH), 7.419(dd, J=4.9, 1.5 Hz, 1H, pyridine-β_2), 7.740(d, J=0.8 Hz, 1H, pyridine-β_1), 8.654(d, J=5.8 Hz, 1H, pyridine-β_1).

Table 4.4: GCMS and HRMS data for the products of the photostimulated reaction between *t*-BuHgCl and substituted pyridines

Products	*m*/e(Relative intensity)	Caculated	Measured	Error
2-*t*-Bu-5-C(O)N(H)CH_3-Py	192(M^+, 26), 191(M^+−H, 28), 178(12), 177(100), 150(41), 91(10), 78(12), 58(10), 51(10).	192.12598	192.12627	−1.5
2-*t*-Bu, 5-Et-Py	163(M^+, 30), 162(M^+−H, 45) 148(100), 133(14), 121(39), 107(14), 77(7), 65(6).	162.12827 ($C_{11}H_{16}$ M^+−H)	162.12796	−1.9
2-*t*-Bu, 5-Ph-Py	211(M^+, 28), 210(M^+−H, 27), 196(100), 180(6), 169(95), 155(18), 127(21), 115(9), 98(17), 77(22), 51(18).	210.12827 ($C_{15}H_{16}N$ M^+−H)	210.12833	+0.3
2-*t*-Bu, 5-C(O)OCH_3-Py	193(M^+, 14), 192(M^+−H, 20), 178(100), 151(29), 118(11), 78(11), 59(8.6), 65(6), 51(13).	193.11028 $C_{11}H_{15}NO_2$	193.11044	+0.8

Table 4.4 (Continued)

Products	m/e (relative intensity)	Calculated	Measured	Error
2-*t*-Bu, 6-Ph-Py	211(M^+, 211), 210(M^+-H, 35), 196(100), 170(10), 169(72), 155(24), 154(25), 128(13), 127(20), 117(8), 102(10), 98(15), 91(20), 84(10), 78(12), 77(28), 65(9), 51(23).	210.12744	210.12828	+4.0
2-*t*-Bu, 4-Et-Py		163.13610 ($C_{11}H_{17}N$)	163.13618	+0.5
2-*t*-Bu, 4-Ph-Py	211(M^+, 37), 210(M^+-H, 36), 197(14.8), 196(100), 169(39), 155(20), 127(15), 77(10), 51(8).	210.12828 ($C_{15}H_{16}N$ M^+-H)	210.12866	+1.8
2-*t*-Bu, 4-C(O)NH_2 -Py	178(M^+, 19), 177(M^+-H, 21), 163(100), 136(25), 122(11), 104(3), 91(9), 78(16), 51(22).	($C_{10}H_{14}N_2O$)	178.11045	−1.0
2-*t*-Bu (*s*)-(−)-nicotine	218(M^+, 6) 217(M^+-H, 5) 189(5), 161(3), 133(8), 84(100).			

nortricyclyl)pyridine, bp 75-110 °C (0.1 torr).

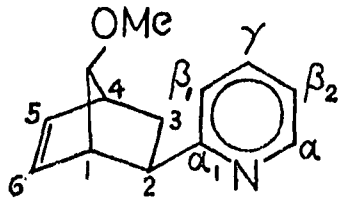

2-(*exo*-7-*syn*-Methoxynorborn-5-en-2-yl)pyridine gave:

(1) ^{1}H NMR (300 MHz, $CDCl_3$), δ 8.517 (dd, 1H$_\alpha$, J=3.38, 0.8 Hz), 7.570 (td, 1H$_\gamma$, J=8.56, 1.79 Hz), 7.389 (d, 1H$_{\beta 1}$, J=8.202 Hz), 7.038 (~t, 1H$_{\beta 2}$, ~J=6.5 Hz), 6.242 (~dd, 1H$_6$, J=3.58, 2.90 Hz), 6.096 (~dd, 1H$_5$, J=3.58, 2.90 Hz), 3.40-3.50 (m, 1H$_7$), 2.872 (s, 4H$_{(2,MeO)}$), 2.901 (s, 1H$_1$), 2.818 (s, 1H$_4$), 2.25-2.40 (m, 1H$_{3_{exo}}$), 1.724 (~t, 1H$_{3_{endo}}$, J=9.2 Hz).

(2) GCIR 3081 (s), 2996 (vs), 2920 (s), 2700 (m), 1590 (s), 1470 (m), 1430 (m), 1360 (w), 1280 (w), 1200 (m), 1150 (m), 1120 (vs), 1000 (w), 795 (m), 750 (m).

(3) RHMS m/e Calculated for $C_{13}H_{15}NO$ 201.11537, measured 201.11554, error +0.8 ppm.

(4) GCMS m/e (relative intensity) 201 (M^+, 22), 186 (76), 170 (41), 168 (60), 156 (47), 143 (16), 130 (69), 123 (14), 117 (78), 108 (22), 106 (22), 93 (42), 79 (100), 65 (33), 53 (56), 51 (58).

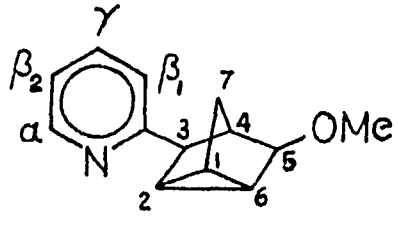

2-(5-*exo*-Methoxy-3-*exo*-nortricyclyl)pyridine gave:

(1) ^{1}H NMR (300 MHz, $CDCl_3$), δ 8.536 (d, $1H_\alpha$, J=4.46 Hz), 7.614 (td, $1H_\gamma$, J=7.69, 1.77 Hz), 7.229 (d, $1H_{\beta 2}$, J=7.82 Hz), 7.114 (~dd, $1H_{\beta 1}$, ~J=7.31, 4.67 Hz), 3.652 (s, $1H_3$), 3.325 (s, $1H_{MeO}$, 3.025 (s, $1H_5$), 2.395 (s, $1H_4$), 1.627 (d, $1H_6$, J=11.78 Hz), 1.572 (d, $1H_2$, J=5.32 Hz), 1.520 (t, $1H_7$, J=5.23 Hz), 1.431 (t, $1H_7$, J=5.34 Hz), 1.109 (d, $1H_1$, J=10.75 Hz).

(2) GCIR 3085 (m), 3000 (m), 2920 (m), 2840 (m), 1590 (s), 1470 (m), 1435 (m), 1360 (m), 1310 (w), 1250 (m), 1120 (vs), 1040 (w), 995 (w), 810 (m), 785 (m).

(3) GCMS m/e (relative intensity) 201 (M^+, 30), 186 (74), 168 (100), 156 (37), 143 (31), 130 (75), 117 (94), 104 (8), 93 (26), 78 (49), 65 (30), 51 (49).

Reaction of 5-*exo*-Methoxy-3-*exo*-nortricyclylmercury Chloride with Lepidine

5-*exo*-Methoxy-3-*exo*-nortricyclylmercury chloride (1.0 g) and 1 mL of lepidine in Me_2SO (3 mL) at 30-35 °C was deoxygenated by a helium stream and irradiated by a 275 W sunlamp 20 cm from the Pyrex tube. Mercury metal precipitated from the solution after an induction period of 5-10 min. After 24 h, beads of mercury formed at the bottom of the tube. The solution was decanted from the mercury metal (0.39 g, 70%) and added to 5 mL of 10% aqueous potassium hydroxide solution. The mixture was extracted with Et_2O. The ether solution was washed twice with 10 mL of water and dried over anhydrous sodium sulfate. Workup provided 60 % (by GLC) of a mixture of 4-methyl-2-(7-*syn*-methoxynorborn-5-en-2-yl)quinoline, 4-methyl-2-(5-*exo*-methoxy-3-*exo*-nortricyclyl)quinoline and other isomers.

4-Methyl-2-(7-*syn*-methoxynorborn-5-en-2-yl)quinoline gave:

(1) ^{1}H NMR (300 MHz, $CDCl_3$), δ 8.040 (d, $1H_{14}$, J=8.37 Hz), 7.928 (d, $1H_{11}$, J=7.31 Hz), 7.643 (t, $1H_{13}$, J=7.07 Hz), 7.471 (t, $1H_{12}$, J=7.07 Hz), 7.388 (s, $1H_9$), 6.295 (~dd, $1H_6$, J=5.8, 2.9 Hz), 6.124 (~dd, $1H_5$, J=5.8, 2.9 Hz), 3.69–3.71 (m, $1H_7$), 3.312 (s, $1H_1$), 2.972 (q, $1H_2$, J=7.8, 3.9 Hz), 2.888 (s, $3H_{18}$), 2.877 (s, $1H_4$), 2.671 (s, $3H_{17}$), 2.480 (~dd, $1H_{3_{exo}}$, J=10.4, 5.0 Hz), 1.833 (~dd, $1H_{3_{end}}$, J=10.88, 9.32 Hz).

(2) ^{13}C NMR (300 MHz, $CDCl_3$), 164.0 (s, C_8), 147.5 (s, C_{15}), 143.0 (s, C_{10}), 135.6 (d, C_6, J=170 Hz), 134.7 (d, C_5, J=168 Hz), 129.4 (dd, C_{14}, J=158, 8.2 Hz), 128.5 (dd, C_{13}, J=158, 8 Hz), 126.5 (s, C_{16}), 125.1 (dd, C_{12}, J=161, 10 Hz), 123.4 (dd, C_{11}, J=161, 10 Hz), 121.7 (dd, C_9, J=161, 4 Hz), 91.6 (d, C_7, J=150 Hz), 55.6 (q, C_{18}, J=142 Hz),47.6 (d, C_2, J=150 Hz), 46.3 (d, C_1, J=135 Hz), 44.9 (t, C_3, J=153 Hz), 28.3 (t, C_4, J=136 Hz), 18.7 (q, C_{17}, J=127 Hz).

(3) GCIR 3080 (s), 2998 (vs), 2900 (s), 2800 (m), 1605 (s), 1560 (m), 1510 (m), 1460 (m), 1350 (m), 1200 (m),1120 (vs), 1000 (w), 860 (w), 760 (s).

(4) GCMS m/e (relative intensity) 265 (M^+, 41), 250 (40), 234 (30), 220 (24), 204 (7), 194 (38), 181 (48), 172 (52), 169 (37), 157 (29.6), 143 (100), 128 (9), 115 (64), 103 (16), 102 (14.5), 96 (22), 77 (25), 65 (16), 63 (17).

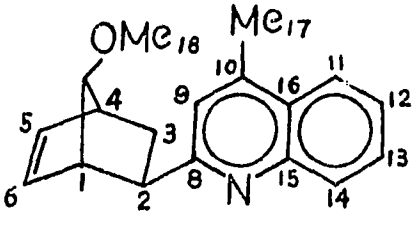

4-Methyl-2-(5-*exo*-methoxy-3-*exo*-nortricyclyl)quinoline gave:

(1) ^{1}H NMR (300 MHZ, $CDCl_3$), δ 8.039 (d, $1H_{14}$, 8.52 Hz), 7.957 (d, $1H_{11}$, J=8,15 Hz), 7.677 (t, $1H_{13}$, J=8.14 Hz), 7.505 (t, $1H_{12}$, J=8.0 Hz), 7.246 (s, $1H_9$), 3.713 (s, $1H_5$), 3.42 (s, $3H_{18}$), 3.163 (s, $1H_3$), 2.703 (s, $3H_{17}$), 2.685 (s, 1H), 2.513 (s, H_4), 1.706 (t, 1H, J=.17 Hz), 1.666 (d, 1H, J=13.66 Hz), 1.594 (t, $1H_7$, J=5.03 Hz), 1.472 (t, $1H_7$, J=5.34 Hz), 1.221 (d, $1H_1$, J=10.75 Hz).

(2) ^{13}C NMR ($CDCl_3$), δ 161.5 (C_8), 147.6 (C_{15}), 129.4 (C_{14}), 129.0 (C_{13}), 125.5 (C_{16}), 123.5 (C_{11}), 120.8 (C_9), 86.1 (C_5), 56.5 (C_{18}), 48.9 (C_3), 38.2 (C_4), 26.0 (C_7), 18.8 (C_{17}), 16.4 (C_2), 16.2 (C_6), 11.9 (C_1).

(3) GCIR 3080 (m), 2998 (m), 2940 (m), 2880 (m), 2680 (m), 1605 (s), 1560 (w), 1510 (w), 1450 (w), 1410 (w), 1370 (m), 1210 (w), 1200 (m), 1040 (w), 810 (m), 760 (s).

(4) GCMS m/e (relative intensity) 265 (M^+, 71), 250 (80), 234 (41), 220 (35), 207 (15.8), 194 (8), 181 (74), 167 (13), 157 (42), 143 (50), 128 (15), 116 (100), 115 (96), 108 (41), 103 (33), 97 (21), 91 (44), 77 (54), 65 (38), 51 (38).

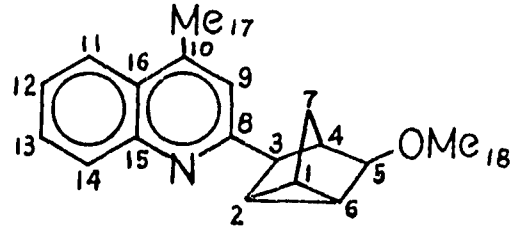

PART III.

FREE-RADICAL OXIDATION-REDUCTION REACTIONS OF RHgX WITH ORGANIC UNSATURATED COMPOUNDS

CHAPTER 1. INTRODUCTION

Free radical reactions of organomercuials have acquired great interest in the past decade due to the importance of radical reactions for carbon-carbon bond formation in organic synthesis [73]. Generally, the radicals can be formed by using thermal, photochemical [74] or chemical-reduction (hydride) of RHgX [75]. Chemical-oxidation methods for forming radicals from RHgX have been reported in a few papers [76]. The oxidation of organomercury compounds by means of mercury(II) salts ($Hg(NO_3)_2$), constitutes a method for the substitution of a mercury atom by a nucleophile, but the proposed radical mechanism for this process is not clear.

The use of other metallic salts (Fe(III), Ru(III), or Ir(IV)) for the generation of radicals starting from R_2Hg have been studied by Kochi and co-workers [77]. Mercury halides and dialkylmercurials have IP's of 11.37 eV and 7.57-9.30 eV respectively. HgX_2 is an oxidatant which has been used for the oxidation of a wide variety of organic compounds and R_2Hg is a reductant which can be oxidized by an oxidizing agent. Having a dual character (IP$\sim$ 9.5-10 eV) [78], RHgX can be reduced by $NaBH_4$ to yield RHgH or oxidized by a strong oxidizing agent, such as, $S_2O_8^{2-}$ or Ag^{2+} to form $RHgX^{+\bullet}$ which rapidly decomposed into R$\bullet$ and HgX^+.

We have found that strong CIDNP multiplet signals (A/E) for RH, R(-H) and R-R can be observed from the diffusive encounter of primary, secondary, or tertiary

alkyl radicals in the reaction of RHgX or R_2Hg and $S_2O_8^{2-}$ with I^- or Ag^+ at 25 °C. This indicates that RHgX or R_2Hg reacts readily with acceptor radicals, such as $SO_4^{-\bullet}$, I•, or Ag^{2+} to form R•. Obviously, the strong A/E multiplet polarizations also indicate that these reactions are good sources of the radicals. We proposed that in the presence of π heteroaromatic or olefinic compounds, a stable adduct radical or radical anion might form and propagate a reaction chain by transferring an electron to $S_2O_8^{2-}$ or Ag^{2+}, or $SO_4^{-\bullet}$ to form corresponding substitution or addition products.

Scheme 33

$$S_2O_8^{2-} + I^-(Ag^+) \longrightarrow SO_4^{-\bullet} + I^\bullet(Ag^{2+}) + SO_4^{2-}$$

$$RHgX + SO_4^{-\bullet}(or I^\bullet) \longrightarrow R\bullet + HgXSO_4^-(or HgXI)$$

$$RHgX + Ag^{2+} \longrightarrow R\bullet + Ag^+ + HgX^+$$

$$R\bullet + \pi \longrightarrow R\text{-}\pi\bullet$$

$$R\text{-}\pi\bullet + S_2O_8^{2-} \longrightarrow R\text{-}\pi(-H) + SO_4^{-\bullet} + HSO_4^-$$

$$R\text{-}\pi\bullet + Ag^{2+} \longrightarrow R\text{-}\pi(-H) + H^+ + Ag^+$$

$$R\text{-}\pi\bullet + I^- \longrightarrow R\text{-}\pi^- + I\bullet$$

A chain-transfer reaction with the RHgX, a reaction in which the Rπ• is converted to Rπ(-H) or RπHgX, will occur if the $S_2O_8^{2-}/I^-$ or $S_2O_8^{2-}/Ag^+$ system is used as an initiator.

$$R\pi\bullet + RHgX \longrightarrow R\pi^+ + R\bullet + Hg + X^-$$

$$R\pi\bullet + RHgX \longrightarrow R\pi HgX + R\bullet$$

We found that the $S_2O_8^{2-}$ also can initiate the $S_{RN}1$ reaction of RHgX with A^-.

$$S_2O_8^{2-} + A^- \longrightarrow SO_4^{-\bullet} + A\bullet + SO_4^{2-}$$

$$A\bullet + RHgX \longrightarrow R\bullet + HgXA$$

$$R\bullet + A^- \longrightarrow RA^{-\bullet}$$

$$RA^{-\bullet} + RHgX \longrightarrow RA + R\bullet + Hg + X^-$$

It is interesting that some reactions of RHgX with π compounds in the presence of the oxidation-reduction system can occur, but no reaction occurs in absence of the oxidation-reduction system, since RHgX is a moderate oxidizing which cannot oxidize R-$\pi\bullet$ to R-π^+.

Finally, these reaction could be related with the Minisci reaction, the Giese reaction and the Meerwein reaction.

CHAPTER 2. RESULTS AND DISCUSSION

Evidence of $RHgX^{+\bullet}$ from RHgX Mass Spectra

The mass spectrometric behavior of a variety of diaryl- and dialkylmercurials, aromatic and aliphatic mercury chlorides has been studied by Bryant and Kinstle [79]. Recently, electron impact mass spectrometry was used to investigate the fragmentation of alkylmercury halides [80].

Here we report on the parent ions ($RHgX^{+\bullet}$) and fragmentation studies of RHgX (R=Me, Et, i-Pr, Bu, *t*-Bu, *c*-C_3H_5, CH_2=$CH(CH_2)_4$, $PhCH_2$, Ph, CF_3, CCl_3, and X=Cl or Br, I). Table 2.1 shows the relative intensities of the $RHgX^{+\bullet}$, RHg^+, Hg^+, R^+ and $C_2H_4HgX^+$ ions in the spectra of RHgX. The stability sequences of the parent ion ($RHgX^{+\bullet}$) are MeHgCl > PhHgCl > EtHgI > Ph_2Hg ≅ CF_3HgCl > EtHgCl > $PhCH_2HgCl$ > *i*-PrHgCl > BuHgCl > CCl_3HgCl > *c*-C_3H_5HgBr > $(Me)_3CHgCl$.

The parent ion of $(Me)_3CHgCl$ has been identified by accurate mass spectrometry as $(Me)_3CHg^{202}Cl^{39}$ (measured m/z 294.00892, calculated m/z 294.00987).

Scheme 34 summarizes the fragmentation behavior of an alkylmercury chloride. At 70 eV, compounds give parent ions of moderate or low intensity with base peaks due to the R^+.

Table 2.1: Relative intensities (%) of ion peaks in RHgX mass spectra

RHgX	$RHgX^{+\bullet}$	C_2H_4HgX	HgX^+	RHg^+	Hg^+	R^+
MeHgCl	23.7		5.8	11	9.6	100
EtHgCl	6.4		5.7	6.2	6.3	100
EtHgBr[a]	11.4		10.9	10.6	12.3	53.5
EtHgI	12.55		8.6	8		100
i-PrHgCl	1.3		1.42		1.8	100
i-PrHgBr[a]	1.4	0.2	5.1	1.5	6.6	76.6
i-PrHgI[a]	0.8	0.3	0.7			
BuHgCl	1.24	13.7	2.5	13.7		100
BuHgBr[a]	0.8	3.6	3.2	0.2	6.4	
CH_2=$CH(CH_2)_4HgCl$	0.76	0.86	0.37		3.7	56
c-C_3H_5HgBr	0.21		1.15	0.08	1.16	100
c-$C_5H_{11}HgCl$	0.26		0.54	6.39		100
$(Me)_3CHgCl$	0.086		0.7		1.3	100
CF_3HgCl	11.1		21.8	2.5	53.5	100
$PhCH_2HgCl$	3.21		0.4			100
PhHgCl	18.7		2.5	4.3	2	100
Ph_2Hg	11.1			14.9	0.02	100
$C_5H_{11}HgBr$[a]	1.4	6.6	3.2	0.6	4.4	82.2
$C_5H_{11}HgI$[a]	0.3	0.2	0.3			
Me_3CCH_2HgBr[a]	7.9		1.2	1.5	3.1	87.5
$C_5H_9CH_2HgBr$[a]	0.2	0.1	3.2		3.1	91.5
CCl_3HgCl	0.68		8.3	9.8	28	100

[a]Ref. [80].

Scheme 34

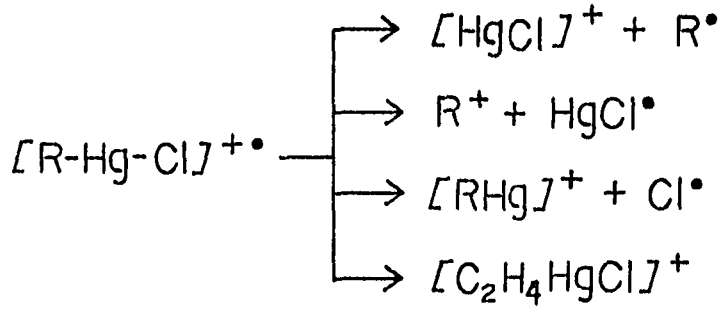

Evidence of R•

The alkyl radicals generated by the reaction of RHgX, R_2Hg with $S_2O_8^{2-}/Ag^+$ or $S_2O_8^{2-}/I^-$ were probed by the use of CIDNP and spin-trapping experiments.

The strong CIDNP multiplet signals (A/E) for RH, R(-H) and R-R can be observed from the diffusive encounter of primary, secondary or tertiary alkyl radicals in the reaction of RHgX or R_2Hg and $S_2O_8^{2-}$ with I^- or Ag^+ at 25 °C (Part I). Formation of *t*-Bu• can be measured by spin trapping with the 2-methyl-2-nitrosopropane. Electron spin resonance (ESR) studies were carried out to probe for paramagnetic intermediates formed in the reactions of RHgX with $S_2O_8^{2-}$. The spin adduct of *t*-Bu• and *t*-BuNO was successfully detected in Me_2SO during reaction of $(Me)_3CHgCl$ with $S_2O_8^{2-}$. The ESR spectrum of the adduct consisted of the pronounced 1:1:1 nitrogen triplet (A_N =16 G) which is identical with that of di-*t*-butyl nitroxide (Figure 2.1).

$$2(Me)_3CHgCl + S_2O_8^{2-} \longrightarrow 2(Me)_3C\bullet + 2HgClSO_4^{-\bullet}$$

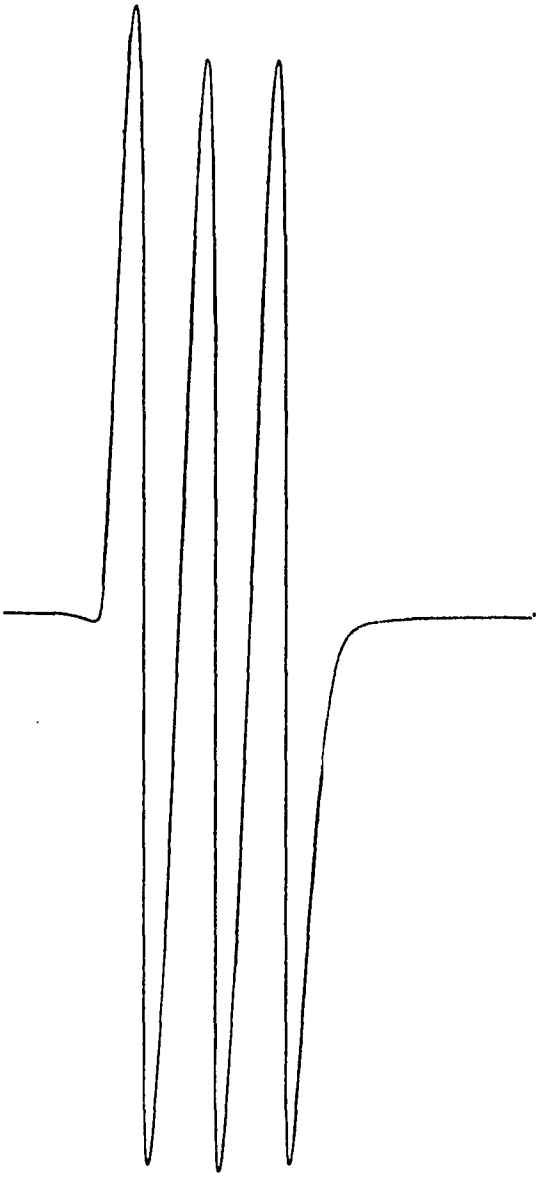

Figure 2.1: The ESR spectrum of the spin adduct of t-Bu• to nitroso*tert*-butane during the reaction of t-BuHgCl with $S_2O_8^{2-}$ in Me_2SO

$$(Me_3)_3C\bullet + t\text{-}BuNO \longrightarrow (t\text{-}Bu)_2NO\bullet$$

Calculations of Electron Transfer Rates from *t*-BuHgCl to $SO_4^{-\bullet}$ by the Marcus Equations

Unfortunately, the $E^\circ(RHgX/RHgX^{+\bullet})$ has not been reported. Attempts to measure directly the reversible oxidation potentials of the alkylmetals in acetronitrile solutions by either cyclic voltammetry or *ac* polarography were unsuccessful, since the voltammograms were irreversible [81]. Evaluation of oxidation potentials of the alkylmercurials (R_2Hg) were obtained from the Marcus equation by Fukuzumi et al. [82]. In general, ionization potentials have often been correlated with electrochemical oxidation potentials. The oxidation potentials ($E^\circ_{RM} + W_pF$) of R_2Hg are linear with the ionization potentials as shown in Figure 2.2. This leads to the equation:

$$E^\circ_{RM} + W_P/F = 0.558IP - 3.5$$

Taking IP = 9.5 eV for *t*-BuHgCl leads to E°(*t*-BuHgCl/*t*-BuHgCl$^{+\bullet}$) =~1.8 V. The sulfate radical ion ($SO_4^{-\bullet}$) is one of the strongest oxidants known. Its standard potential is calculated to be 2.52 V vs NHE by Eberson [83]. However, with this E° value it is impossible to fit the reaction of $SO_4^{-\bullet}$ with benzene involving a rate constant ca. 10^8 $M^{-1}s^{-1}$. In order to fit the data to the Marcus equation, Eberson assumed that $E^\circ(SO_4^{-\bullet}/SO_4^{2-})$ is around 3.1 V.

It is interesting that the $E^\circ(SO_4^{-\bullet}/SO_4^{2-})$ has been obtained by Memming in 1969 [24]. He pointed out that the persulfate ion is a two-electron oxidant which reacts in two steps:

$$S_2O_8^{2-} + 2e \longrightarrow 2SO_4^{2-} \qquad E^\circ = +2.0V$$

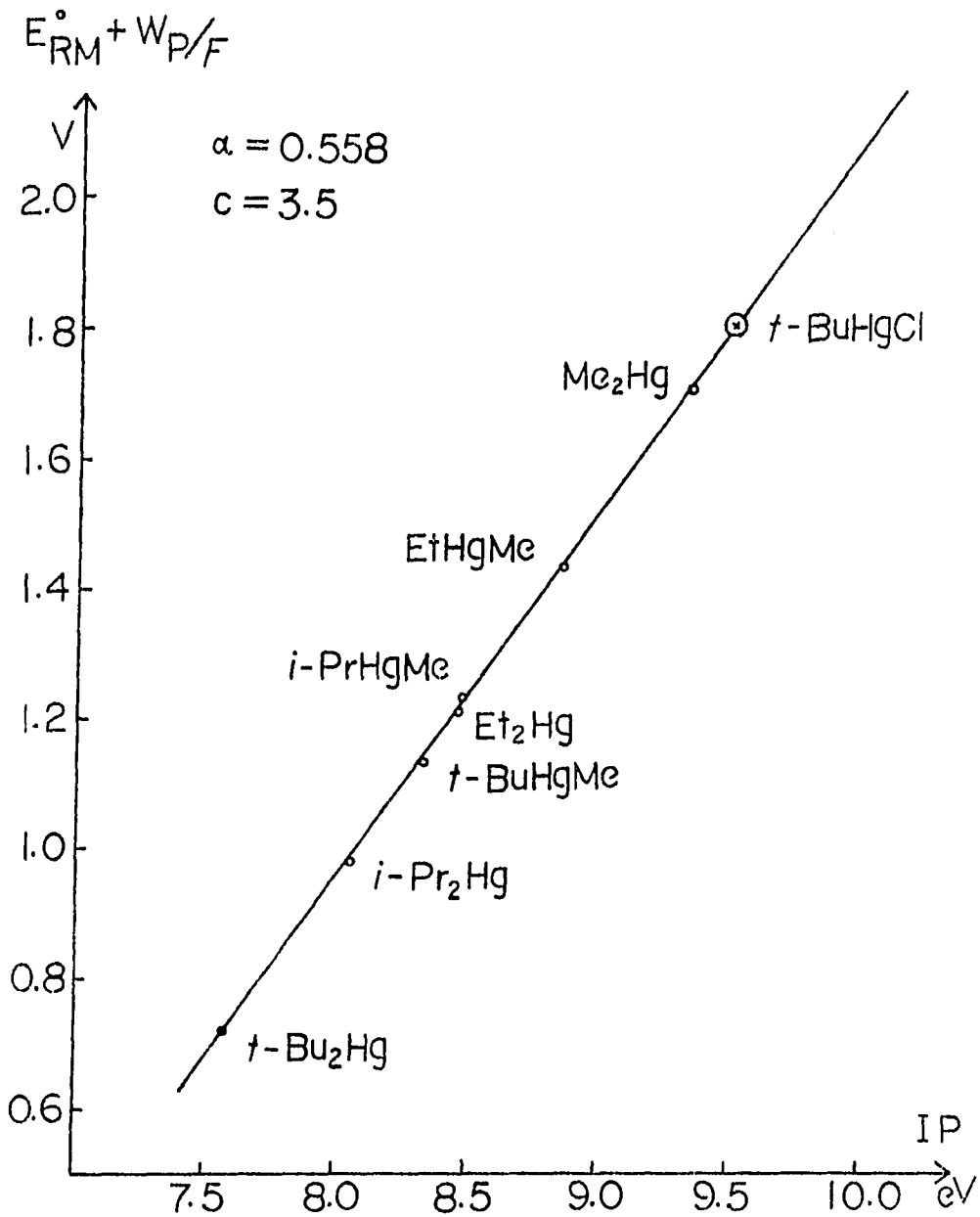

Figure 2.2: Linear correlation of oxidation potentials and ionization IP of alkylmetals (the point for *t*-BuHgCl is based on IP only)

$$S_2O_8^{2-} + e^- \longrightarrow SO_4^{2-} + SO_4^- \qquad E^\circ \leq +0.6V$$

$$SO_4^{-\bullet} + e^- \longrightarrow SO_4^{2-} \qquad E^\circ \geq +3.4V$$

Recently these results have been used to illustrate electrochemiluminescence by many groups [84]. The species $SO_4^{-\bullet}$ with a negative charge should be a more effective oxidant toward neutral molecules than positively charged ones. The difference in E° values of $SO_4^{-\bullet}$ between acetonitrile or Me_2SO and H_2O may be 0.6-1.0 V [83]. Thus, the E° value of $SO_4^{-\bullet}$ in acetonitrile or Me_2SO is probably about 2.8 V. The Marcus equation for electron transfer equates the rate constant with ΔE° for the reaction but also involves the solvent reorganization parameter, λ,

$$k_{obs} = 10^{11} exp - [\frac{\lambda}{4}(1 + \frac{\Delta G^\circ}{\lambda})^2/RT]$$

Knowing E°(t-BuHgCl/t-BuHgCl$^{+\bullet}$) = + 1.8 V and $E^\circ(SO_4^{-\bullet}/SO_4^{2-})$=2.8 V it follows that

$$\Delta G^\circ = -23.06(E^\circ_A - E^\circ_D) = -23.06(2.8 - 1.8) = -23.06$$

Taking $\lambda = 40$, it follows that

$$\Delta G^\ddagger = \frac{\lambda}{4}(1 + \frac{\Delta G^\circ}{\lambda})^2 = \frac{40}{4}(1 - \frac{23.06}{40})^2 = 1.79$$

and

$$\log k = 11 - \frac{1.79}{1.36} = 9.68 \qquad \text{at} \quad 25\,^\circ C$$

$$k = 4.8 \times 10^9 \mathrm{M}^{-1} s^{-1}$$

In a similar fashion for MeHgCl,

$$\log k = 5.31$$

$$k = 2 \times 10^5 \mathrm{M}^{-1}s^{-1}$$

If E° ($SO_4^{-\bullet}/SO_4^-$) in CH_3CN or Me_2SO is taken to be +2.4 V, the value of k calculated for *t*-BuHgCl would decrease to 7×10^7 $M^{-1}s^{-1}$.

Reactions of RHgX with α, β-Unsaturated Carbonyl Compounds in the Presence of $S_2O_8^{2-}/I^-$

Brown and Kabalka [85] [86] have shown that 1,4 addition of aklkylboranes to enones is a radical chain process. Acrolein, methyl vinyl ketone and their α-substituted derivatives react with trialkylboranes at 25 °C by 1,4 addition. These reactions can be inhibited by galvinoxyl. The corresponding β-substituted carbonyl compounds, RCH=CHCOR', do not react spontaneously, but their reaction can be initiated by benzoyl peroxide, acetyl peroxide, or oxygen. The following mechanism is suggested.

Scheme 35

$$R\bullet + CH_2{=}CHCOR' \longrightarrow RCH_2CH{=}CR'O\bullet$$

$$RCH_2CH{=}CR'O\bullet + BR_3 \longrightarrow RCH_2CH{=}CR'OBR_2 + R\bullet$$

$$RCH_2CH{=}CR'OBR_2 + H_2O \longrightarrow RCH_2CH_2COR'$$

The radical 1,4- addition of organoboranes to an α,β-unsaturated ketone or aldehyde followed by hydrolysis yields a longer chain ketone or aldehyde. On the basis of these results, it was suggested that R_2Hg could be used instead of R_3B. The photostimulated reaction of dicyclohexylmercury with 2-cyclohexen-1-one leads to the formation of adduct in low yield. With *c*-C_5H_9HgCl, however, the photostimulated

reaction of 2-cyclohexen-1-one gave isolated products in 30% yield. *t*-BuHgCl underwent a photostimulated free radical reaction with 2-cyclopentenone to give a 55% yield (by GLC) of products.

1,4-addition of R_2Hg or RHgX to an α, β- unsaturated carbonyl compound may occur by a free radical chain mechanism (Scheme 36).

Scheme 36

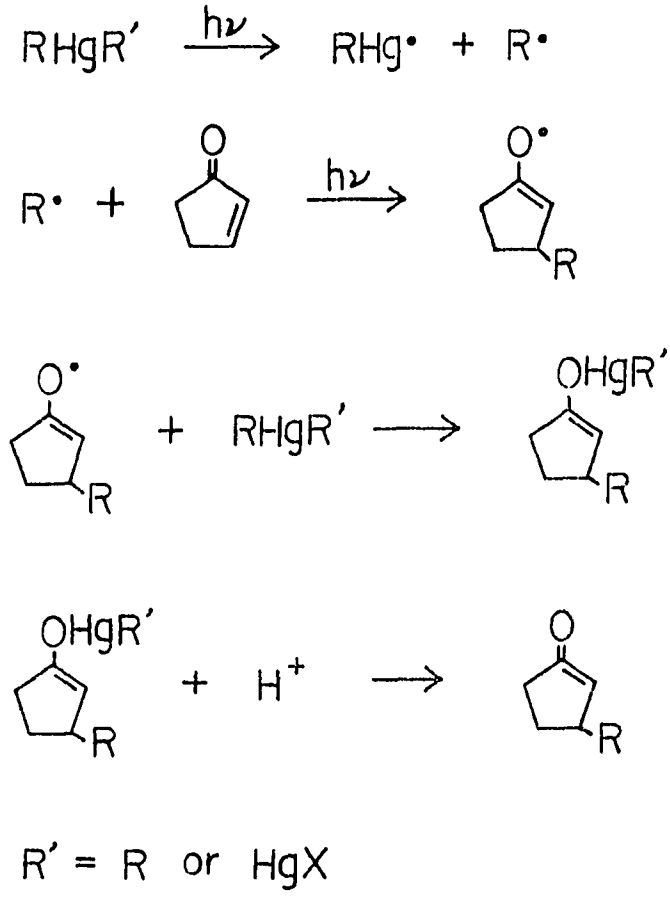

R' = R or HgX

Since the bond of O-Hg is weak, the chain transfer for $RCH_2CH{=}CR'O\bullet$ to RHgX or R_2Hg will be a slow reaction resulting in the formation of $RCH_2CH{=}CR'OHgR$ or $RCH_2CH{=}CR'OHgCl$ in low yield and the formation of the photo-dimer the enone. In presence of NaI, the photoreaction of $(Me)_3CHgCl$ with 2-cyclohexen-1-one gives an 85% yield of product in 6 h [74]. However, in the presence of $S_2O_8^{2-}$ and I^-, the reaction of $(Me)_3CHgCl$ with α,β-unsaturated ketones gave products in higher yield and shorter time (0.5-2 h).

In the presence of $S_2O_8^{2-}$/NaI, the addition of $(Me)_3C\bullet$ to α, β-unsaturated ketones gave the following products (α,β-unsaturated substrate, product, % yield by NMR); 2-cyclopentenone, 3-*tert*-butyl-cyclopentanone, 100; 2-cyclohexen-1-one, 3-*tert*-butyl-cyclohexanone, 90; 3-buten-2-one, 5,5-dimethyl-2-hexanone, 85. Furthermore, in the presence of $S_2O_8^{2-}$/CuCl (exess), $(Me)_3C\bullet$ reacts with 2-cyclopentenone to give a 50% yield of the addition product (3-*tert*-butyl-cyclopentanone) and a small amount of 3-*tert*-butyl-2-cyclopentenone. On the basis of these results, the mechanism may be assumed as the following Scheme 37.

In the presence of $S_2O_8^{2-}$/NaI, the addition of *t*-Bu to diethyl vinylphosphonate or acrylamide gave a 100% yield (by NMR) of *t*-$Bu(CH_2)_2P(O)(OEt)_2$ and an 85% yield (by NMR) of *t*-$BuCH_2C(O)NH_2$ upon reaction at room temperature for 1−1.5 h.

Scheme 37 ($R = t\text{-}Bu$)

$$S_2O_8^2 + I^-(Cu^+ or Cu^{2+}) \longrightarrow SO_4^{2-} + I\bullet(Cu^{2+} or Cu^{3+}) + SO_4^{-\bullet}$$

$$2RHgX + I\bullet(SO_4^{-\bullet}) \longrightarrow 2R\bullet + 2HgXI(HgXSO_4^-)$$

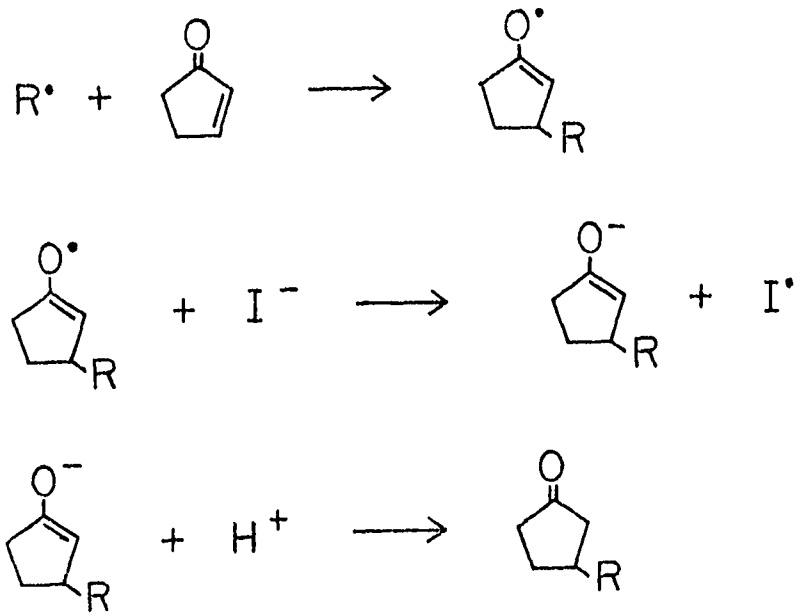

Alkylation of Uracil

Uracil is an important biologically active compound. It is incorporated as the base complementary to adenine in RNA. The susceptibility of uracil to radical attack at the C_6 and C_5 position has been reported in few papers [87] [88]. The attack of $CH_3CH(OH)\bullet$ at the C_6 position of thymine to form isomers of the addition product of thymine and ethanol has been found by Brown and co-workers [87]. Recently, the mechanisms of OH radical reactions with uracil and thymine derivatives have been

studied by Jovanovic and Simic [88]. They found that the addition of OH radical to the 5,6 double bond of pyrimidines gives a reducing radical (5-OH-6-yl-Py, 80%) and an oxidizing radical (6-OH-5-yl-Py, 20%), respectively. The MF-FSGO calculations [89] suggest that the experimentally observed site specificity of the nucleophilic attack on the neutral species (viz. attack preferentially at C_6) as well as the site specificity of the π-electrophilic attack on the anionic species (viz. attack preferentially at C_5) are electronically controlled.

It is interesting that that susceptibility of uracil to nucleophilic radical attack is at the C_6 position but electrophilic radical attack occurs at the C_5 position. The strong nucleophilic *tert*-butyl radical, generated from the reaction of $(Me)_3CHgCl$ and $S_2O_8^{2-}$ in presence of NaI in Me_2SO at room temperature, reacts with uracil to give a 62% yield of 6-*tert*-butyl-5,6-dihydrouracil. The structure was assigned based on its ^1H NMR, GCMS, CI and high resolution MS. The ^1H NMR spectrum (300 MHz, $CDCl_3$) of 6-*tert*-butyl-5,6-dihydrouracil showed peaks at δ 0.976 (s, 9H, $(C\underline{H}_3)_3C$), 2.48-2.66(m, 2H, $-CH_2-$(5)), 3.26-3.41(m, 1H, =CH-(6)), 5.68 (s, 1H, =NH), 8.069(s, 1H, =NH).

The mass spectrum for 6-*tert*-butyl-5,6-dihydrouracil was m/z (relative intensity) 170 (M^+, 2.2), 153.1 (4.9), 114(100), 86(2.7), 70(29), 57(39). The CI spectrum with *i*-C_4H_{10} CI was m/z 171 (M+H, 100). The accurate mass spectrum was m/z 170.10545 ($C_8H_{14}N_2O_2$ requires 170.10553).

On the basis of these results, the mechanism of the reaction is assumed to follow Scheme 38.

Scheme 38

$$S_2O_8^{2} + 2I^{-} \longrightarrow 2I\bullet + 2SO_4^{2-}$$

$$RHgCl + I\bullet \longrightarrow R\bullet + HgClI$$

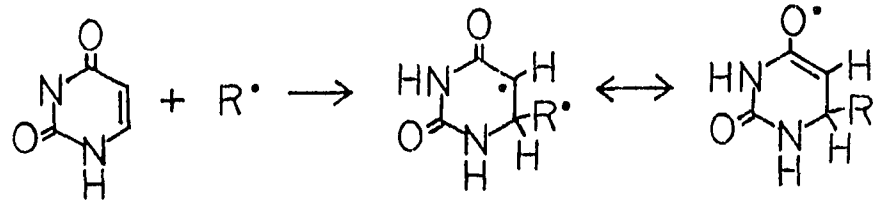

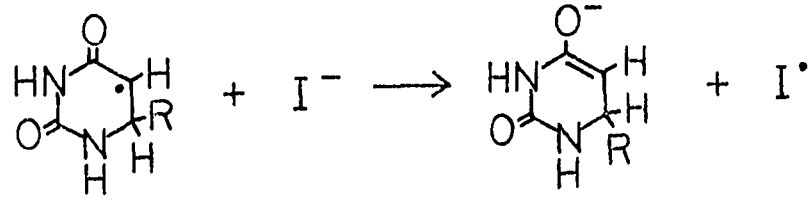

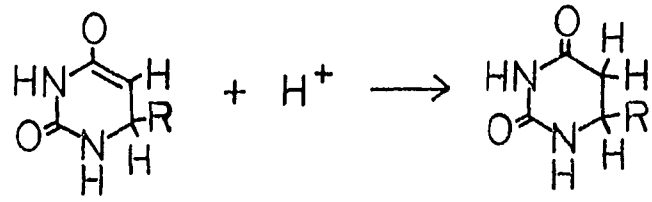

$$R\bullet = (Me)_3C\bullet$$

In principle, $(Me)_3C\bullet$ could react with uracil by addition to C-5 or C-6. However,

the more favored reaction is addition of $(Me)_3C\bullet$ to the 6 position of uracil to form an adduct radical which is an oxidizing radical since its mesomeric form is an oxyradical. Reduction of the adduct radical with I^- yields $I\bullet$ and the enolate precursor of the product. With $(Me)_3C\bullet$, the reaction of 5-F-uracil gave the corresponding addition and substitution products in low yield.

Alkylation of Quinone

The use of quinone as a free radical scavenger or as an inhibitor of free-radical chain processed is well known. Quinone reacts rapidly with alkyl radicals. The rate constants ($k=2.1 \times 10^7 M^{-1}s^{-1}$) for alkyl radicals addition to quinone has been determined by Citterio [90].

Jacobsen and Torssell [91] [92] have reported that radicals generated by decarboxylation of carboxylic acids with silver ions and peroxydisulfate can be used for the alkylation of quinones.

Charge transfer and electron transfer interactions of quinones leading to ring substitution are well known in organic chemistry. The alkylation of quinones with organoboranes [93] and silanes [94] has been shown to proceed via semi-quinone anion-radicals. Similarly, when π-allylnickel bromide is treated with various quinones, charge transfer complexes are formed. Dissolution in DMF leads to various alkyl substituted quinones [95].

The arylation of quinones by diazonium salts in the presence of a small amount of hydroquinone was found by Matnishan et al. [96]. Aryl radicals generated by decomposition of arenediazonium tetrafluroborates induced by copper or $NaHCO_3$

in Me_2SO were known to add to quinones . The absolute rate constant ($8.8 \times 10^8 M^{-1}s^{-1}$ at 20 °) for the addition of phenyl radicals to 1,4-benzoquinone was obtained [97].

Photoreaction of quinones (1,4 benzoquinone or 1,4-naphthaquinone) with $(Me)_3CHgCl$ leads to alkylquinones in low yield, but in presence of $S_2O_8^{2-}/I^-$ or $S_2O_8^{2-}/CuBr$ or $S_2O_8^{2-}/Ag^+$ or Ag^{2+}, the quinones reacted with RHgX or $RHgNO_3$ gave a high yield of alkylquinone products (Table 2.2).

Alkyl radicals generated by the reaction of RHgX and $S_2O_8^{2-}$ with NaI at room temperature react with 1,4-benzoquinone or 1,4-naphthoquinone to give the corresponding alkylquinones in moderate yield. However, in presence of 1,4-diazabicyclo [2.2.2]octane (Dabco), the addition of $Me_3C\bullet$ to quinones leads to the formation of corresponding substitution product in good yield and in a short time (75 min) at room temperature. These products were known compounds which had NMR and MS spectra to consistent with their structures and literature reports.

On the basis of these results, the reaction mechanism of Scheme 39 is proposed.

An alkylquinone radical anion might be formed by the addition of R• to the quinone followed by the loss of a proton, especially in presence of Dabco. A chain reaction could propagate by the transfer of an electron to $S_2O_8^{2-}$ to form the product and $SO_4^{-\bullet}$.

Scheme 39 ($R = t\text{-}Bu$)

$$S_2O_8^{2-} + 2I^- \longrightarrow 2SO_4^{2-} + 2I\bullet$$

Table 2.2: Alkylquinone formed by the alkylation of quinones with RHgX

Quinones (m mol)	RHgX (m mol)	$S_2O_8^{2-}$ (m mol)	MX (m mol)	Time (h)	yield[a] (%)
BZQN[b](1)	$(Me)_3CHgCl$ (1.5)	1.0	1.0[c]	7.0	62(G)
BZQN(1)	$(Me)_3CHgCl$ (0.5)	0.5	0.6[d]	15.0	57(N)
BZQN(1)	$(Me)_2CHHgNO_3$(1.5)	2.0	0.7[e]	4.0	87(N)
NPQN[f](1)	$(Me)_3CHgCl$ (2.4)	2.6	0.8[c]	8.0	67(N), 58(G)
NPQN(1)	$(Me)_3CHgCl$ (1.7)	1.1	—[g]	1.25	80(N), 90(G)
NPQN(1)	$(Me)_3CHgCl$ (1.0)	—	1.5[h]	1.5	72(N)[i], 80(G)[i]
NPQN(1)	$(Me)_2CHHgNO_3$(0.8)	2.0	0.3[e]	5.0	86(N)
NPQN(1)	$(Me)_2CHHgNO_3$(2.3)	4.0	0.6[e]	5.0	55(N)
NPQN(1)	$(Me)_2CHHgNO_3$(2)	—	4[h]	1.5	90(N)
NPQN(1)	c-C_3H_5HgCl(0.5)	0.5	0.6[e]	5.0	40(N)
MNPQN[j](1)	$(Me)_2CHHgNO_3$(1.6)	2.0	0.5[e]	5.0	88(N)

[a] In reaction consisting of quinones (0.1 m mol), RHgX and $(NH_4)_2S_2O_8$/NaI or $(NH_4)_2S_2O_8/AgNO_3$, AgL in d_6-Me_2SO (0.5 mL) at 25 °C; N, by ^1H NMR; G, by GLC.

[b] 1,4-benzoquinone (BZQN).

[c] NaI.

[d] $CuBr_2$.

[e] $AgNO_3$.

[f] 1,4-naphthoquinone (NPQN).

[g] NaI/Dabco = 2/0.3.

[h] AgL, L=quinolinate.

[i] Conversion.

[j] 2-methylnaphthoquinone (MNPQN).

$$RHgX + I\bullet \longrightarrow R\bullet + HgXI$$

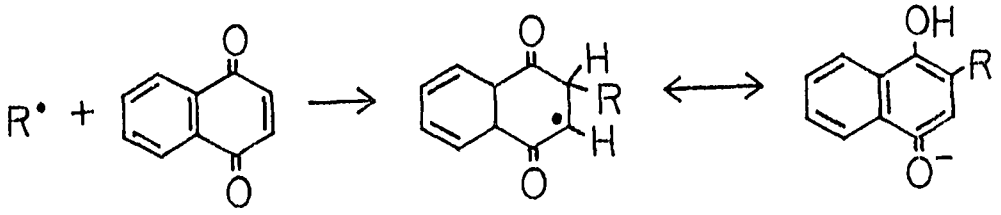

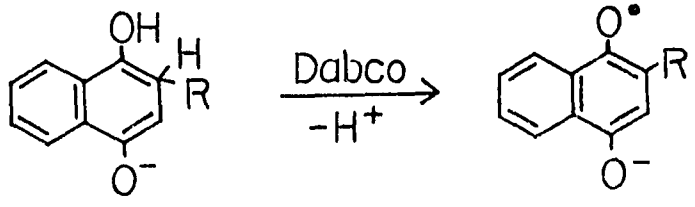

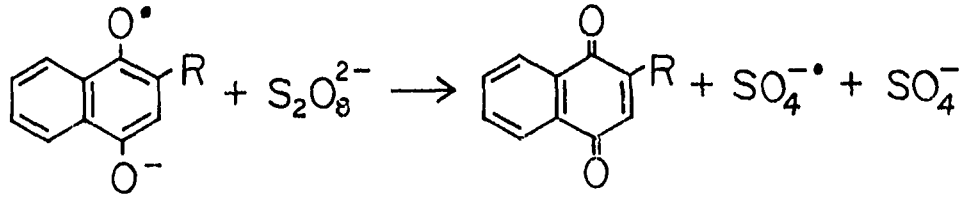

$$SO_4^{-\bullet} + I^- \longrightarrow SO_4^{2-} + I\bullet$$

The quinones underwent a ring substitution with RHgX in presence of $S_2O_8^{2-}$ and $AgNO_3$ or Ag^{2+}. The reaction was fast and mild. The yields were good.

The alkyl radical, generated by the electron-transfer reaction from RHgX to Ag^{2+}, reacts with quinones to yield the adduct radical and radical anion which

undergoes an electron transfer to $S_2O_8^{2-}$ to form $SO_4^{-\bullet}$ and products.

Scheme 40

$$Ag^+ + S_2O_8^{2-} \longrightarrow Ag^{2+} + SO_4^{-\bullet} + SO_4^{2-}$$

$$SO_4^{-\bullet} + Ag^+ \longrightarrow Ag^{2+} + SO_4^{2-}$$

$$RHgX + Ag^{2+} \longrightarrow R\bullet + Ag^+ + HgX^+$$

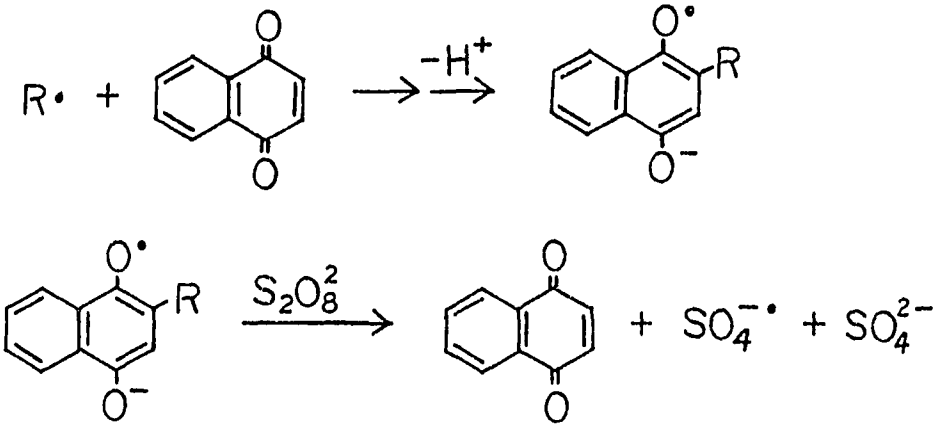

The effect of Ag^{2+} have been confirmed by use of $Ag^{2+}L_2$ (L=quinonlinate) instead of $S_2O_8^{2-}/Ag^+$.

Alkylation of Maleic Anhydride

Maleic anhydride is very reactive toward $(Me)_3C\bullet$. The adduct radical from the addition of $(Me)_3C\bullet$ to maleic anhydride has dual properties. The radical can be an oxidizing radical since its mesomeric form is an oxyradical and it can easily lose a proton to form a reducing radical (captodative radical).

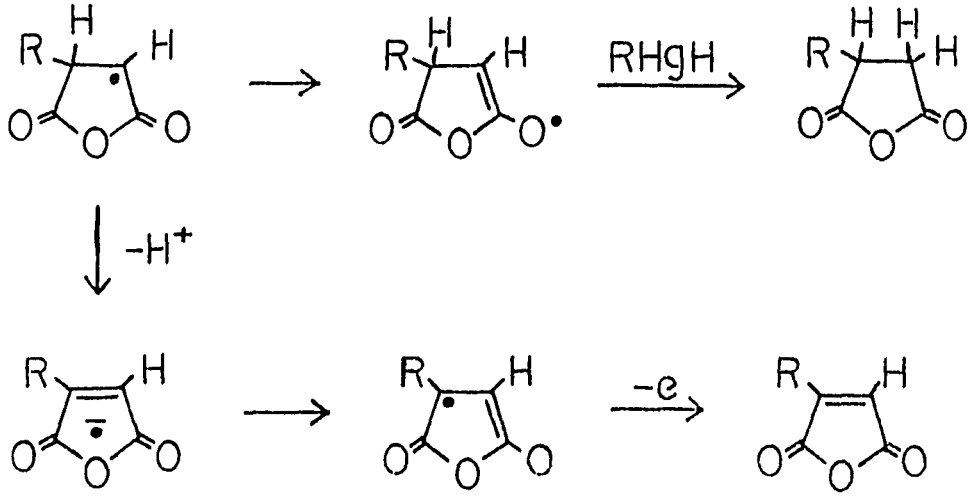

R = $Me_3C^{\bullet}$

The reduction of RHgX with sodium borohydride ion in presence of maleic anhydride leads to formation of the addition product only [98]. The photostimulation of RHgX with maleic anhydride in the presence of NaI gave both addition and

Table 2.3: Alkylmaleic anhydrides formed by the alkylation of maleic anhydride (MA) with RHgX

RHgCl (equiv.)	$S_2O_8^{2-}$ (equiv.)	$AgNO_3$ (equiv.)	% RMA[a]
t-BuHgCl (2.4)	2.6	-	63[b]
(2.0)	1.9	-	58[c]
(2.0)	1.6	0.8	64
i-PrHgCl (0.7)	0.8	0.7	90

[a]In reaction consisting of MA (0.1 m mol), RHgCl and $(NH_4)_2S_2O_8$, $(NH_4)_2S_2O_8/AgNO_3$ in d_6-Me_2SO (0.5 mL) at 25 °C; yield by NMR.
[b]Irradiated with sunlamp.
[c]At 50 °C for 15 min.

substituted products but in the presence of $S_2O_8^{2-}$ the photostimulated reaction of $(Me)_3CHgCl$ with maleic hydride leads to formation of the substituted product only (Table 2.3).

The oxidation of RHgX with $S_2O_8^{2-}$/Ag+ in the presence of maleic anhydride also gives the substituted products in high yield (60-90%) at room temperature.

The ^1H NMR spectrum of 3-*tert*-butylfurandione (in $CDCl_3$) showed the singlet due to $(CH_3)_3C$ at 1.340 ppm and a singlet at 6.688 ppm which is in accord with ^1H NMR data literature [99].

On the basis of these results, a possible reaction is shown in the following Scheme.

Scheme 41

$$S_2O_8^{2-} + 2Ag^+ \longrightarrow 2Ag^{2+}$$

$$RHgNO_3 + Ag^{2+} \longrightarrow R\bullet + Hg^{2+} + Ag^+ + NO_3^-$$

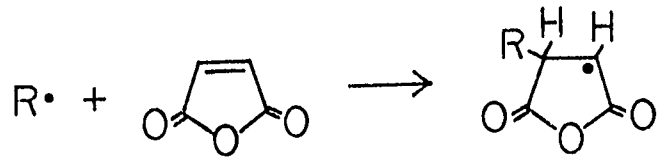

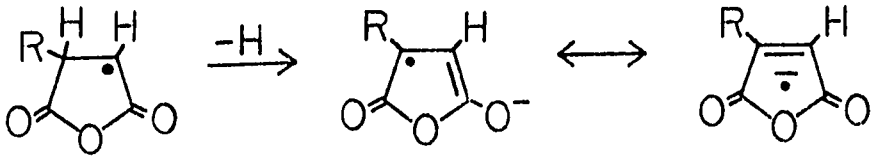

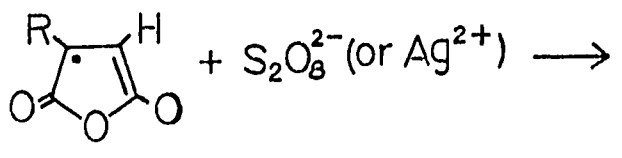

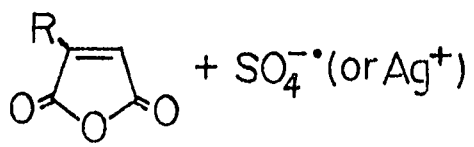

Reaction of *t*-BuHgCl and Pyridine or $PyHgCl_2$ with Oxidizing Reagents

The following radical sources have been utilized to generate *t*-Bu• by the S_H2 or ET reactions from RHgX: $S_2O_8^{2-}$, $S_2O_8^{2-}/I^-$, $S_2O_8^{2-}/Ag^+$. The radicals are trapped by Py, $PyHgCl_2$ and PyHI. Some results summarized in Table 2.4.

No reaction of *t*-BuHgCl with pyridine occurs in absence of light. However, in the presence of $S_2O_8^{2-}$, the addition of *t*-Bu• to pyridine was observed, especially, in the presence of $S_2O_8^{2-}$/NaI. Under these condition *t*-BuHgCl reacts very rapidly with pyridine to give good yields of 2-and 4-*tert*-butylpyridines. The possible mechanism of these reaction is shown by the following Scheme.

Scheme 42 (*R=t-Bu*)

$$S_2O_8^{2-} \rightleftharpoons 2SO_4^{2-\bullet}$$

$$S_2O_8^{2-} + I^- \longrightarrow SO_4^{-\bullet} + I\bullet + SO_4^{2-}$$

$$RHgCl + I^-(SO_4^{-\bullet}) \longrightarrow R\bullet + HgClI(SO_4^-)$$

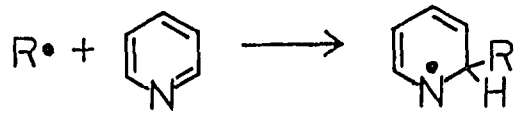

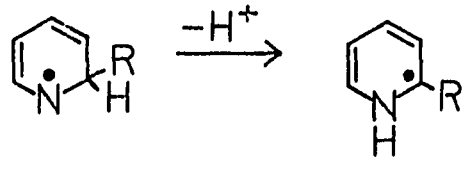

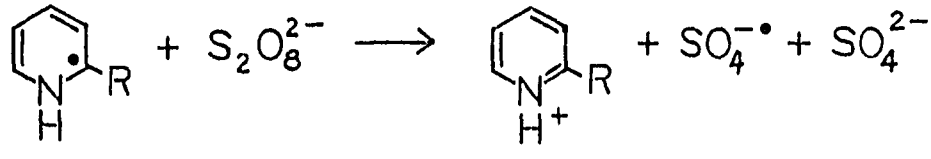

The addition of *t*-Bu• to the pyridine ring leads to formation of an adduct radical. The fast rearomatization of the pyridinyl radical by induced decomposition of peroxydisulfate ion plays an important role in the substitution.

The reaction of *t*-BuHgCl/$S_2O_8^{2-}$ with $PyHgCl_2$ is faster than with Py. A plausible explanation is the fact that $PyHgCl_2$ is much more reactive than Py toward *t*-Bu• and the adduct radical undergoes an internal electron transfer, yielding product and •HgCl (Scheme 43).

Scheme 43

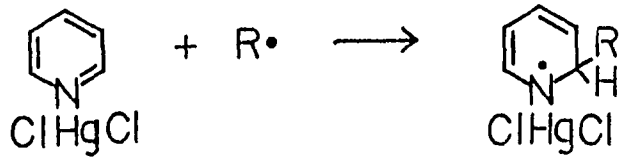

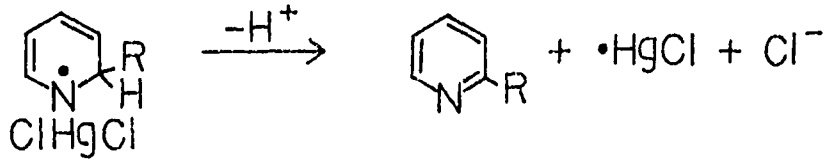

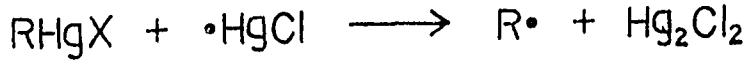

Table 2.4: Reaction of *t*-BuHgCl and substrate with oxidant in pyridine at 30 °C

Substrate	Oxidant	Time	% *t*-BuPy [a]	*o*/*p*
Py[b]	$S_2O_8^{2-}$ [c]	3 h	75	
		4 h	100	1.7
Py	$S_2O_8^{2-}$/NaI	5 min	100	1.5
$PyHgCl_2$	$S_2O_8^{2-}$	15 min	100	1.1
PyHI	$S_2O_8^{2-}$	5 min		1.5
PyTFA[d]	$AgNO_3$	5 min	58	
		32 min	75	1.2
		1 h	80	1.2
PyTFA	$S_2O_8^{2}$/$AgNO_3$	5 min	90	1.0
Py	$S_2O_8^{2}$/$AgNO_3$	8 min	90	1.3

[a]In reaction consisting of *t*-BuHgCl (0.03 mmol), substrate (0.09 mmol) and oxidant (0.06 mmol) in pyridine (0.5 mL); *t*-BuPy = *tert*-butyl pyridine; yield by ^{1}H NMR.

[b]Py=Pyridine.

[c]$S_2O_8^{2-} = (NH_4)_2S_2O_8$.

[d]TFA= trifluoroacetic acid.

Reaction of *t*-BuHgCl and PyHI with Oxidizing Reagents

PyH^+ is much more reactive than Py toward *t*-BuHgCl at room temperature in the presence of light. Attack of *t*-Bu• upon PyH^+ and Py takes place with rate constants of 3.3×10^4 $M^{-1}s^{-1}$ and $\sim 3 \times 10^3$ $M^{-1}s^{-1}$, respectively. The rate of thermal formation of radicals from *t*-BuHgCl rapidly increased in the presence of I^- due to the addition of I^- to *t*-BuHgCl to form the complex *t*-$BuHgClI^-$ or *t*-$BuHgClI_2^{2-}$ which easily decomposed into Hg, Cl^- and I•.

$$t\text{-}BuHgCl + I^- \rightleftharpoons t\text{-}BuHg(Cl)I^-$$

$$t\text{-}BuHg(Cl)I^- \longrightarrow t\text{-}Bu\bullet + Hg + Cl^- + I\bullet$$

Alternatively, the oxidation of I^-(E, 0.7v NHE) by *t*-BuHgCl (E, 1.80v NHE) can occur by the following reaction.

$$t\text{-}BuHgCl + I^- \longrightarrow t\text{-}Bu\bullet + Hg + Cl^- + I\bullet$$

Obviously, in the presence of oxidizing reagents, such as $S_2O_8^{2-}$, $S_2O_8^{2-}/Ag^+$, Ce^{4+}, $PhC(O)OOC(Me)_3$, and $(PhC(O)O)_2$, the rate for the reaction of *t*-BuHgCl with PyHI rapidly increases. A reasonable explanation is that the oxidation of I^- by the oxidizing agent leads to formation of I• which undergoes an S_H2 reaction with *t*-BuHgCl (Table 2.5) (Scheme 44).

Scheme 44

$$S_2O_8^{2-} + I^- \longrightarrow SO_4^{-\bullet} + SO_4^{2-} + I\bullet$$

$$SO_4^{-\bullet} + I^- \longrightarrow SO_4^{2-} + I\bullet$$

Table 2.5: Reaction of *t*-BuHgCl and PyHI with oxidant in d_6-Me_2SO at 30 °C

Oxidant	Time	% *t*-Bu-Py [a]	*o/p*
SeO_2	2 h	64	1.8
	5 h	100	1.8
$(NH_4)_2Ce(NO_3)_6$	5 min	60	3.0
	15 min	80	3.0
	21 min	90	2.0
	2 h	100	1.9
$KClO_4$	2 h	55	0.8
	5 h	100	1.6
$NaClO_3$	2 h	82	2.0
	5 h	100	2.0
$NaIO_4$	1 h	50	1.0
	5 h	100	1.5
$PhCO_3C(Me)_3$	3 min	79	—
	15 min	100	—
$(PhCO_3)_2$	3 min	70	1.4
	18 min	80	1.4
$S_2O_8^{2-}$	5 min	100	2.0
AIBN	48 min	100	
$S_2O_8^{2-}$/Ag+	5–10 min	100	1.3
None	2 h	25	1.7
	3 h	50	—

[a] In reaction consisting of *t*-BuHgCl (0.03 mmol), PyHI (0.06 mmol) and oxidant (0.06 mmol) in d_6-Me_2SO (0.5 mL); Yield by NMR.

$$RHgX + I\bullet \longrightarrow R\bullet + HgXI$$

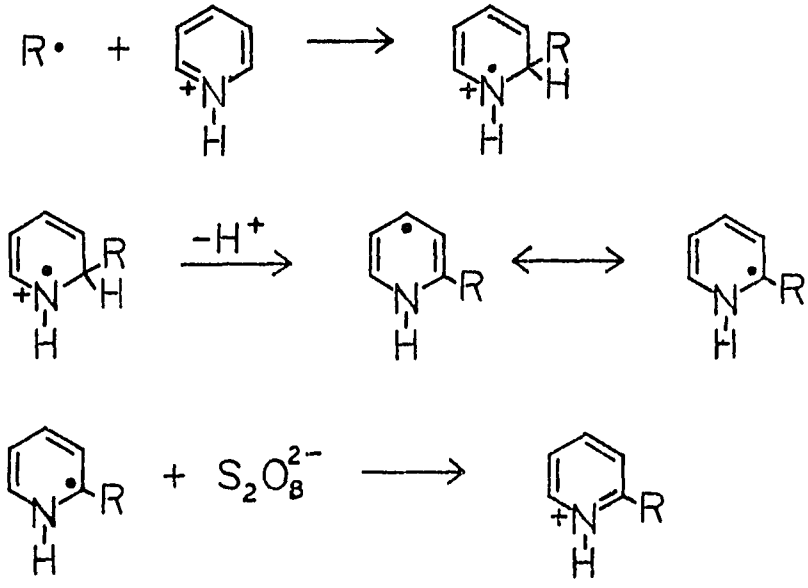

The rate of the overall reaction should increase with an increase in the rate of the oxidation (chain transfer) of the adduct radical ion from *t*-Bu• and PyH^+ by the oxidizing reagent.

Phenylation of Organic Compounds with Ph_2Hg

The phenyl radical [100], a very reactive σ radical, can undergo the Meerwein reaction [101], the $S_{RN}1$ reaction [102], the Sandmeyer reaction [103] and phenyla- tion of aromatic compounds [104]. A phenyl radical can be generated from the following compounds: benzenediazonium ion [105], phenyl iodide [106], phenylazotriphenyl-methane [107], benzoyl peroxide [108], benzoate anion [109], phenylthallium bis(tri-

fluoroacetates) [110]. We have proved that Ph_2Hg reacts with $S_2O_8^{2-}$ to yield Ph• by using the CIDNP technique. Here, we will report that phenyl radical, generated from the reaction of diphenylmercury with peroxydisulfate ion, reacts with quinones, diethyl vinylphosphonate, α, β- unsaturated ketones or α-methylstyrene.

Diphenylmercury in the presence of $S_2O_8^{2-}/AgNO_3$ reacts with 1,4-benzoquinone, 1.4-naphtoquinone and 2-methyl-1.4-naphthoquinone to form 50-60 % of phenylated quinones. A plausible mechanism is shown in the following Scheme.

Scheme 45

$$S_2O_8^{2-} + Ag^+ \longrightarrow SO_4^{-\bullet} + Ag^{2+} + SO_4^{2-}$$

$$SO_4^{-\bullet} + Ag^+ \longrightarrow Ag^{2+}$$

$$Ph_2Hg + Ag^{2+} \longrightarrow Ph\bullet + PhHg^+ + Ag^+$$

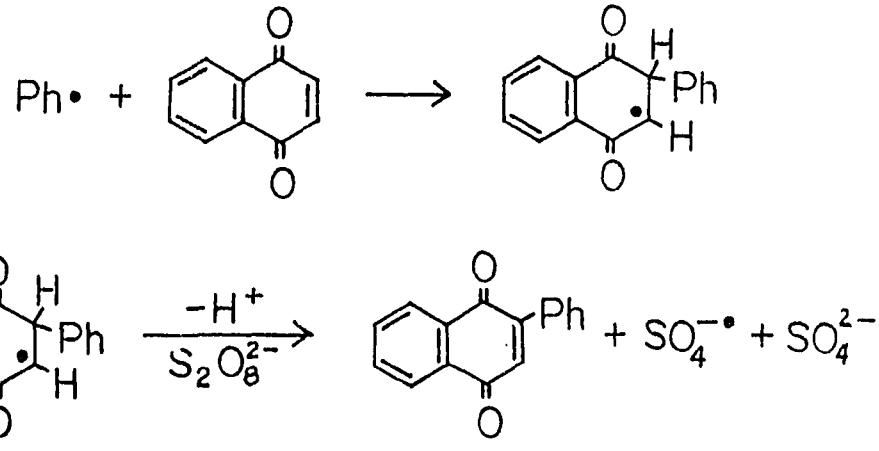

Reaction of diphenylmercury with diethyl vinylphosphonate in the presence of $S_2O_8^{2-}/Ag^+$ leads to the formation of $PhCH_2CH_2P(O)(OC_2H_5)_2$ in 40% yield by GLC. The phenyl radical, generated from the reaction of Ph_2Hg with Ag^{2+}, reacts according to the following Scheme.

Scheme 46

$$S_2O_8^{2+} + 2Ag^+ \longrightarrow 2SO_4^{2+} + 2Ag^{2+}$$

$$Ph_2Hg + Ag^{2+} \longrightarrow Ph\bullet + PhHg^+ + Ag^+$$

$$Ph\bullet + CH_2{=}CHP(O)(OEt)_2 \longrightarrow PhCH_2C(\bullet)HP(O)(OEt)_2$$

$$PhCH_2CH{=}P(O\bullet)(OEt)_2 + Ph_2Hg \longrightarrow PhCH_2CH{=}P(OHgPh)(OEt)_2 + Ph\bullet$$

$$PhCH_2CH{=}P(OHgPh)(OEt)_2 + H^+ \longrightarrow PhCH_2CH_2P(O)(OEt)_2$$

The adduct of phenyl radical and diethyl vinylphosphonate is a acceptor radical which reacts readily with Ph_2Hg to form phenylated product and phenyl radical. In the presence of $S_2O_8^{2-}/CuCl_2$, the Ph_2Hg reacts with diethyl vinylphosphonate to give a low yield of $PhCH_2CH(Cl)P(O)(OEt)_2$.

The reaction of Ph_2Hg in the presence of $S_2O_8^{2-}/CuCl$ with 2-cyclopentenone leads to the formation of a 35% yield (GLC) of 3-phenyl-2-chlorocyclopentanone and biphenyl. The ratio of the arylated product to biphenyl is 1:1.5. The addition of the phenyl radical to 2-cyclopentenone gives rise to an adduct radical which reacts readily with $CuCl_2$ to afford the product and CuCl.

In the presence of $S_2O_8^{2-}/AgNO_3$, diphenylmercury reacts with α-methylstyrene to form a 20 % yield of $PhCH{=}C(Ph)CH_3$. The adduct of the phenyl radical and

α-methylstyrene may be oxidized by Ag^{2+} to form the product.

$$PhCH_2C(\bullet)(Ph)CH_3 + Ag^{2+} \longrightarrow PhCH = C(Ph)CH_3 + H^+ + Ag^+$$

Evidence for [$RHgX^{-\bullet}$]

The organomercuric cations, $RHgX^{+\bullet}$ and RHg^+ have been generated and studied [79] [80]. However the formation of the negative ion of RHgX has not been reported. $RHgX^{-\bullet}$ is a possible intermediate in the $S_{RN}1$ reaction utilizing alkylmercurials.

$$RHgX + e \longrightarrow RHgX^{-\bullet}$$

$$RHgX^{-\bullet} \longrightarrow R\bullet + Hg + X^-$$

Formation of negative ions of RHgX by the interaction of RHgX with negative CI / argon can occur by the following reaction.

$$RHgX + Ar^{-\bullet} \longrightarrow RHgX^{-\bullet} + Ar$$

$$RHgX^{-\bullet} \longrightarrow R\bullet + Hg + X^-$$

A variety of organomercurials, such as MeHgCl EtHgCl, EtHgI, BuHgCl, CH_2=$CH(CH_2)_2CH_2HgCl$, CH_2=$CH(CH_2)_3HgBr$, t-C_3H_7HgCl, c-$C_5H_{11}HgCl$, t-BuHgCl, c-C_3H_5HgBr, CF_3HgCl, CCl_3HgCl, $PhCH_2HgCl$, PhHgCl and Ph_2Hg, have been examined with negative CI / Ar. Distinctive mass and relative abundance are listed in Table 2.6. The spectra were devoid of $RHgX^{-\bullet}$. However, $PhHgCl^{-\bullet}$ was detected. The measured isotope distribution of $PhHgCl^{-\bullet}$ was the same as

Table 2.6: Relative intensity (%) of negative ion peak in RHgX mass spectra

RHgX	$RHgX_2^-$	HgX^-	X^-
MeHgCl	75	100	28
EtHgI	33	10	100
EtHgCl	49	100	22
BuHgCl	80	100	27
CH_2=CH$(CH_2)_4$HgCl	9	53	11
CH_2=CH$(CH_4)_4$HgBr	97	100	78
i-C_3H_7HgCl	37	100	30
c-C_5H_{11}HgCl	100	73	40
t-BuHgCl	34	100	35
c-C_3H_5HgBr	59	100	35
CF_3HgCl[a]	100	25	4
CCl_3HgCl	6	10	15
$PhCH_2$HgCl	44	100	40
PhHgCl[b]	76	100	26
Ph_2Hg	—	—	—

[a] For CF_3^-, m/e(relative intensity) = 69(0.2).

[b] For $PhHgCl^{-\bullet}$, m/e(relative, intensity)= 314(13).

the theoretical isotope distribution (Figure 2.3). With R alkyl, a large ion abundance of $RHgX_2^-$, HgX^-, X^- were produced. From these data, it appears that the organomercurials have undergone an addition reaction with X^- generated from the decomposition of $RHgX^{-\bullet}$.

$$RHgX + Ar^{-\bullet} \longrightarrow [RHgX^{-\bullet}] + Ar$$

$$[RHgX^{-\bullet}] \longrightarrow R\bullet + HgX^-$$

$$HgX^- \longrightarrow Hg + X^-$$

$$RHgX + X^- \longrightarrow RHgX_2^-$$

$$RHgX_2^- + X^- \longrightarrow RHgX_3^{2-}$$

A small ion abundance of CF_3^- was observed and m/e 306.8 was identified as $HgCl_3^-$ by measured isotope distribution.

Reactivity of the 5-Hexenyl Radical toward the Anion of 2-Nitropropane and Borohydride Anion

The addition of radicals to anions plays a key role in $S_{RN}1$ substitution. However, little is known about the rates of these processes in aliphatic systems. We have used the cyclization of the 5-hexenyl radical generated by electron transfer to 5-hexenylmercury chloride to measure the rate constant for the reactions of a 1°-alkyl radical with $Me_2C{=}NO_2^-$ (Scheme 47)

Scheme 47

$$CH_2{=}CH(CH_2)_3CH_2HgCl + e \longrightarrow CH_2{=}CH(CH_2)_3CH_2\bullet$$

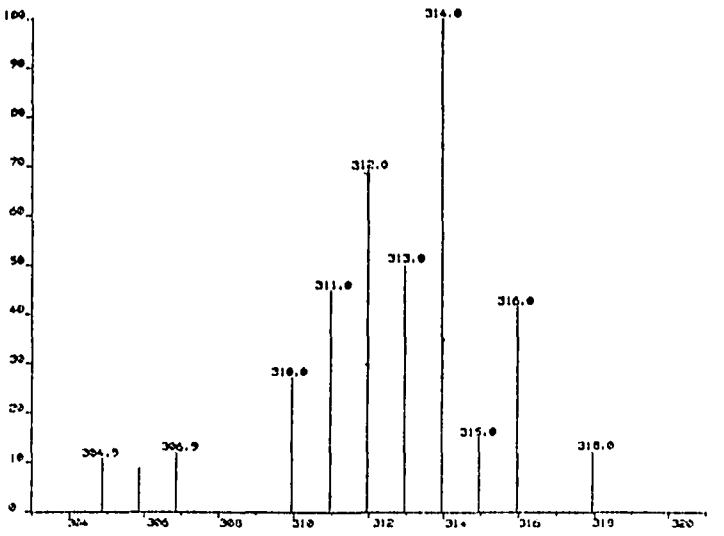

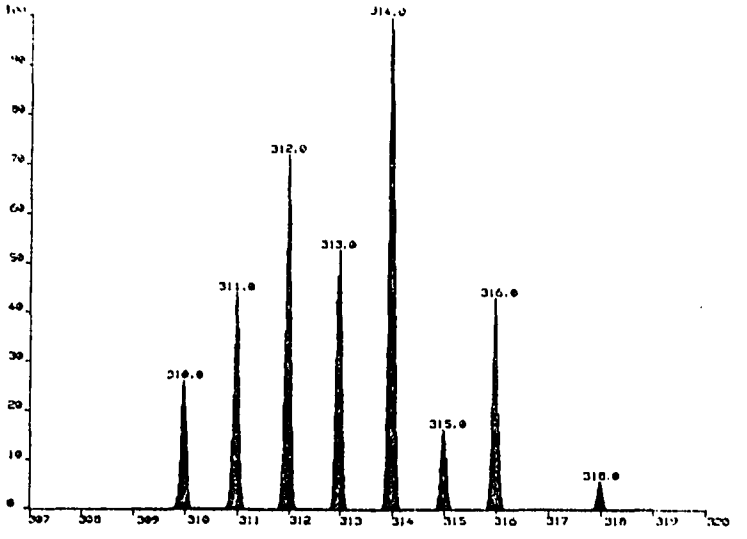

Figure 2.3: (a) PhHgCl negative CI Ar mass spectrum showing the experimentally observed isotopic pattern (b) Calculated isotopic pattern for PhHgCl molecular ion

Table 2.7: Rate constants for trapping the 5-hexenyl radical by $Me_2CNO_2^-M^+$ at 40 °C

M^+	Solvent	k_N (L/mol-s)
Li^+	Me_2SO	0.3×10^5
Bu_4N^+	Me_2SO	0.9×10^5
Li^+	HMPA	0.36×10^5
Bu_4N^+	HMPA	0.75×10^5

$$CH_2{=}CH(CH_2)_3CH_2\bullet \xrightarrow{k_C} c\text{-}C_5H_5CH_2\bullet$$

$$CH_2{=}CH(CH_2)_3CH_2\bullet + Me_2C{=}NO_2^- \xrightarrow{k_N} CH_2{=}CH(CH_2)_3CH_2(Me)_2NO_2^{-\bullet}$$

$$c\text{-}C_5H_5CH_2\bullet + Me_2C{=}NO_2^- \longrightarrow c\text{-}C_5H_5CH_2(Me)_2NO_2^{-\bullet}$$

$$RHgX + RNO_2^{-\bullet} \longrightarrow R\bullet + Hg^\circ + X^-$$

In the $S_{RN}1$ chain reaction of $H_2C{=}CH(CH_2)_3CH_2\bullet$ with $Me_2C{=}NO_2^-M^+$ [111], the ratio of $H_2C{=}CH(CH_2)_3CH_2CMe_2NO_2^-\bullet$ / $c\text{-}C_5H_9CH_2CMe_2NO_2^-\bullet$ increased linearly with $[Me_2C{=}NO_2^-]$. Using the value of k_C of 1.7×10^5 s^{-1} at 40 °C [112] yields the data of Table 2.7.

As expected, ion-pairing with Li^+ decreases the reactivity of $Me_2C{=}NO_2^-$ towards radical attack [113].

Singh and Khanna have suggested that reduction of alkylmercury halides by $LiAlH_4$ involves an electron transfer chain mechanism of the $S_{RN}1$-type involving

attack of R• upon AlH_4^- (Equation 2.1 and Equation 2.2) [114].

$$R\bullet + AlH_4^- \longrightarrow RH + AlH_3\bullet^- \tag{2.1}$$

$$AlH_3\bullet^- + RHgX \longrightarrow AlH_3 + R\bullet + X^- \tag{2.2}$$

A similar process is possible for the reaction with BH_4^- since the presence of alkyl radicals in this reduction have been thoroughly established [115][116]. However, we have found that the homogeneous reduction of CH_2=CH$(CH_2)_3CH_2HgCl$ by BH_4^- in MeOH/1 bf M NaOH yields a ratio of 1-hexene/methylcyclopentane which is independent of the concentration of BH_4^- (Figure 2.4). The occurrence of a reaction between H_2C=CH$(CH_2)_3CH_2$• with BH_4^- would require that this ratio should increase with the concentration of BH_4^- which it does not. The ratio of 1-hexene/methylcyclopentane does increase with the concentration of H_2C=CH$(CH_2)_3CH_2HgCl$ as shown in Figure 2.5. This observation eliminates the $S_{RN}1$ chain in the reaction of RHgX with BH_4^- and is consistent with a mechanism involving the intermediacy of RHgH (Equation 2.3 and Equation 2.4).

$$RHgCl + NaBH_4 \longrightarrow RHgH + NaBH_3Cl \tag{2.3}$$

$$R\bullet + RHgH \longrightarrow RH + RHg\bullet \longrightarrow R\bullet + Hg\bullet \tag{2.4}$$

From the slope of Figure 2.5 and with a value of k_c of 1.25×10^5 s^{-1} at 30 °C, a value of k_H of 2.6×10^6 L/mol-s is required. The absence of any effect of $[BH_4^-]$ on the ratio of 1-hexene/methylcyclopentane requires that reaction (Equation 2.3) must be fast and complete. The rate constant for the reaction of 5-hexenyl radical with BH_4^- cannot be greater than 10^4 and is probably less than 10^3 L/mol-s.

$$CH_2{=}CH(CH_2)_2CH_2HgCl + NaBH_4 \longrightarrow$$

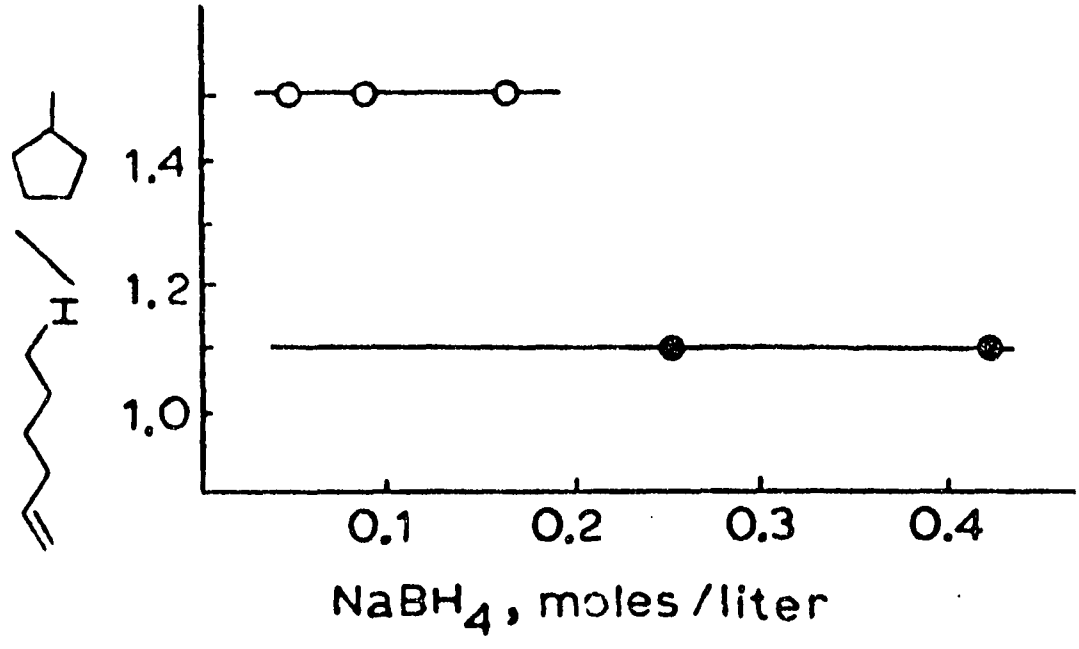

Figure 2.4: Ratio of 1-hexene/methylcyclopentane formed in the sodium borohydride reduction of 5-hexenylmercury chloride (initially 0.05 M (•) and 0.09 M (○) in MeOH/1 M NaOH at 30 °C)

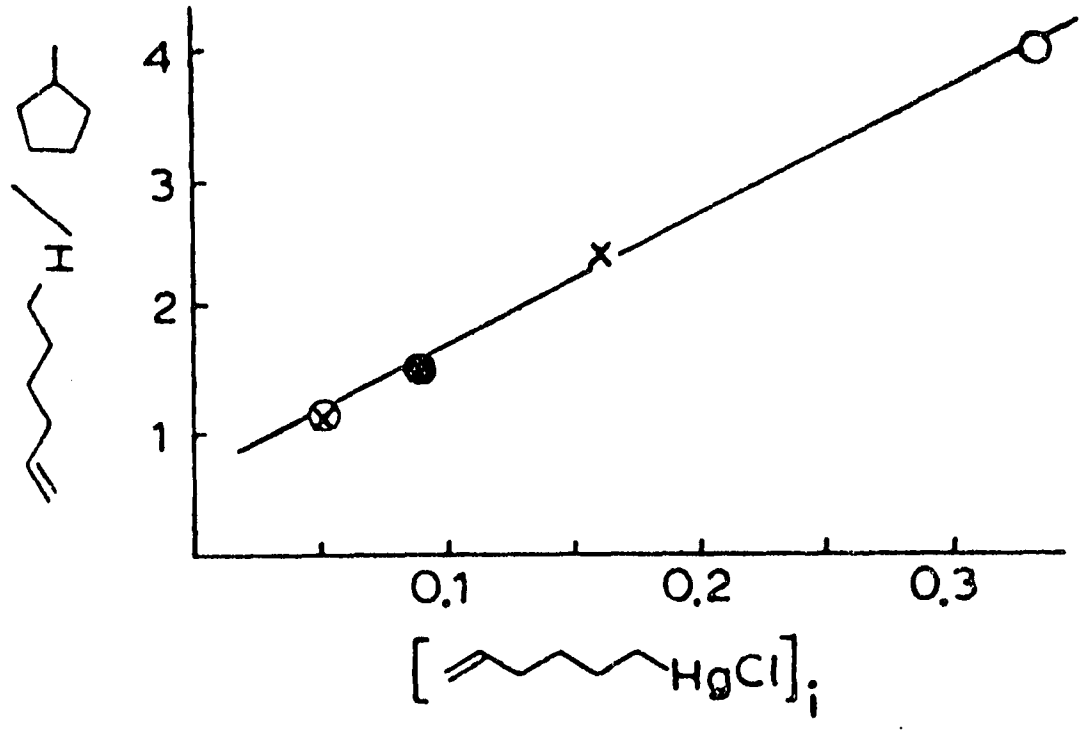

Figure 2.5: Ratio of 1-hexene to methylcyclopentane formed in the reaction of 5-hexenylmercury chloride with sodium borohydride at 30 °C in methanol (containing 1 M sodium hydroxide: ○ , 0.5 M $NaBH_4$; ×, 0.26 M $NaBH_4$; • , 0.05, 0.10, 0.17 M $NaBH_4$)

$$[CH_2 = CH(CH_2)_2CH_2 \bullet + c\text{-}C_5H_9CH_2\bullet]$$

The intercept of Figure 2.5 gives a measure of the hydrogen donor ability of the solvent system (MeOH/1 M NaOH). A pseudounimolcular rate constant of 7 $\times$ 10^4 s^{-1} and an approximate rate constant for hydrogen atom abstraction from CH_3O^- of no more than 1 $\times$ 10^6 L/mol-s at 30 °C is indicated. Although alkyl radicals can abstract a hydrogen atom from $NaBH_4$ [117], it appears that this reaction is ineffective in competition with hydrogen abstraction from RHgH or MeOH/1 M NaOH and perhaps occurs much less readily than attack upon AlH_4^- [114][118].

CHAPTER 3. CONCLUSION

Alkyl radicals, generated from the chemical oxidations of RHgX react with unsaturated organic compounds to form addition or substitution products at room temperature via free radical chain processes. The reaction of *t*-BuHgCl with α,β-unsaturated ketones, diethyl vinylphosphonate, acrylamide and uracil in presence of $S_2O_8^{2-}/I^-$ gave rise to the corresponding *tert*-butylation-addition products in good yields. The reaction of RHgCl, such as *t*-BuHgCl, *i*-PrHgCl or *c*-C_3H_5HgCl with 1,4-benzoquinone, 1,4-naphthoquinone, 2-methyl-1,4-naphthoquinone and maleic anhydride in the presence of $S_2O_8^{2}/I^-$/Dabco or $S_2O_8^{2}/Ag^+$ or $S_2O_8^{2}/Cu^+$ formed the corresponding alkylated-substitution products in good yields. The *tert*-butylation of Py, $PyHgCl_2$ and PyHI with *t*-BuHgCl in presence of oxidation-reduction systems, such as $S_2O_8^{2-}$, $S_2O_8^{2-}/I^-$, $S_2O_8^{2-}/Ag^+$, Ce^{4+}/I^-, $PhC(O)OOC(Me)_3/I^-$ or $(PhC(O)OO)_2/I^-$, have afforded good yields of *tert*-butylated pyridines. The phenylation of quinones, diethyl vinylphosphonate and 2-cyclopentenone with Ph_2Hg, in the presence of $S_2O_8^{2-}$ gave the corresponding substitution products in moderate to low yields. *tert*-Butyl radical, generated from the reaction of *t*-BuHgCl and $S_2O_8^{2-}$, has been identified by an ESR spin trapping experiment. The electron transfer rate from *t*-BuHgCl to $SO_4^{-\bullet}$ has been calculated to be 10^7-10^9 $M^{-1}s^{-1}$ using the Marcus theory.

CHAPTER 4. EXPERIMENTAL

General Considerations

^{1}H NMR spectra were recorded on a Nicolet NT 300 (300 MHz) NMR spectrometer, a JEOL FX-90Q (90 MHz) spectrometer and a Varian EM 360 (60 MHz). ^{1}H decoupling and ^{13}C NMR spectra were also determined on NT 300 instrument. Infrared spectra (IR) were determined on a Beckman 4250 spectrophotometer. Infrared spectra (GCIR) were obtained on an IBM IR/98 spectrometer. Mass spectra (GCMS) are recorded on a Finnegan 4000 spectrometer. High resolution mass spectra (MS) were recorded on an AEI MS 902 mass spectrometer. Analytical gas chromatograph (GLC) was performed on a Varian 3700 gas chromatograph equipped with a Hewlett-Packard 3390 A integrator. Melting points were determined on a Fisher-Johns melting point apparatus and are uncorrected. ESR spectra were obtained on a Varian E-3 spectrometer.

GLC yields were determined by use of internal standards (naphthalene or biphenyl). ^{1}H NMR yields were determined by integration with a known amount of an internal standard (dibromomethane or acetonitrile).

Dimethyl sulfoxide (Me_2SO), dimethylformamide (DMF) and hexamethylphosphoramide (HMPA) were distilled from calcium hydride and stored over 4A molecular

sieves under nitrogen. Tetrahydrofuran (THF) was distilled from lithium aluminum hydride before use and stored over 4A molecular sieves under nitrogen. Davidson 4A molecular sieves were activated by drying in vacuo at 230 °C for 16 hours. Deuterated dimethyl sulfoxide was dried with activated 4A molecular sieves and purged with argon to remove traces of oxygen.

Literature procedures [71] were employed for the preparations of *tert*-butylmercury chloride, benzylmercury chloride, ethylmercury chloride, *n*-butylmercury nitrate, allylmercury chloride, cyclohexylmercury chloride, 5-hexenylmercury chloride, isopropylmercury chloride and 5-methoxy-3-nortricyclylmercury chloride.

Reaction of *t*-BuHgCl with Uracil in Presence of $S_2O_8^{2-}$/NaI

Uracil (1 mmol), *t*-BuHgCl (1.6 mmol) and NaI (2 mmol) were dissolved in 5 mL of a argon-purged Me_2SO. After the argon purge, ammonium persulfate (1 mmol) was added to the mixture at room temperature. After 15 h, the reaction mixture was poured into water and extracted with 10 mL of methylene chloride. The extract was washed with water, dried over anhydrous magnesium sulfate and concentrated in vacuo. The crude mixture was analyzed by GLC, GCMS, CI and high resolution MS which revealed the presence of the addition product, 6-*tert*-butyl-5,6-dihydrouracil in 62% yield (by NMR). The addition product had ^1H NMR spectrum (300 MHz, $CDCl_3$) δ 0.976 (s, 9H), 2.48-2.66 (m, 2H), 3.26-3.41 (m, 1H), 5.68 (s, 1H, NH), 8.069 (s, 1H); GCMS *m/e* (relative intensity) 170 (M^+, 2.2), 153.1 (4.4), 114 (100), 86 (2.6), 70 (2.6), 57 (39); HRGS *m/e* calculated for $C_8H_{14}N_2O_2$ 170.10553, found 170.10545. The CI spectrum with *i*-C_4H_{10} CI was *m/z* 171 (M+H, 100).

Reaction of *t*-BuHgCl with Acrylamide in Presence of $S_2O_8^{2-}$/NaI

Acrylamide (0.7 mmol), *t*-BuHgCl (1.36 mmol) and NaI (0.7 mmol) were dissolved in 5 mL of argon-purged Me_2SO. After the argon purge, ammonium persulfate (0.2 mmol) was added to the mixture at room temperature. After 3 h, the reaction mixture was poured into water and extracted with 10 mL of methylene chloride. The extract was washed with water, dried over anhydrous magnesium sulfate and concentrated in vacuo. The crude mixture was analyzed by GLC, GCMS, CI and high resolution MS which revealed the presence of the addition product, $(Me)_3C(CH_2)_2C(O)NH_2$ in 83% yield (by NMR). The addition product had ^1H NMR spectrum (300 MHz $CDCl_3$) δ 0.910 (s, 9H), 1.147-1.589 (m, 2H), 2.043-2.200 (m, 2H), 5.59 (m, 2H, NH_2); GCMS *m/e* (relative intensity) 129 (M^+, 1.1), 114 (25), 100 (6.6), 97 (14.8), 72 (100), 69 (20), 57 (40), 41 (47).

Reaction of *t*-BuHgCl with NPQN in Presence of $S_2O_8^{2-}$ / NaI / Dabco

1,4-Naphthoquinone (0.09 mmol), *t*-BuHgCl (0.16 mmol), NaI(0.2 mmol) and Dabco (0.03 mmol) were dissolved in 0.5 mL of argon-purged d_6-Me_2SO. After the argon purge, ammonium persulfate(0.11 mmol) was added to the mixture at room temperature. After 75 min, the reaction mixture was poured into water and extracted with 10 mL of methylene chloride. The extract was washed with water and dried over anhydrous magnesium sulfate. Evaporation of CH_2Cl_2 gave a residue shown by GLC to contain 90% of 2-*tert*-butyl-1,4-napthoquione. The product had ^1H NMR (90 MHz $CDCl_3$) δ 1.376 (s, 9H), 6.86 (s, 1H), 7.71-7.83 (m, 2H), 8.03-8.17 (m, 2H); GCMS *m/e* (relative intensity) 214 (M^+, 100), 199 (50), 171 (40), 160 (42), 144 (20), 128

(55), 115 (30), 105 (30), 76 (65), 57 (30), 41 (48).

Reaction of *i*-PrHgNO$_3$ with 1,4-Naphthoquinone in Presence of $S_2O_8^{2-}/Ag^+$

1,4-Naphthoquione(1 mmol), *i*-PrHgNO$_3$(0.8 mmol) and AgNO$_3$(0.3 mmol) in 5 mL of Me$_2$SO were deoxygenated by an argon stream. After 5 h, workup provided an 86% yield (by NMR) of 2-iso-propyl-1,4-naphthoquinone. The product gave ^{1}H NMR (90 MHz $CDCl_3$) δ 1.358 (d, J = 7.0 Hz, 6H), 3.319 (septet, J = 7.0 Hz, 1H), 6.760 (s, 1H), 7.49-7.71 (m, 2H), 7.90-8.10 (m, 2H); GCMS m/e (relative intensity) 200 (M^+, 100), 185 (31), 172 (29), 157 (54), 144 (20), 129 (68), 115 (20), 105 (40), 89 (10), 76 (82), 64 (20), 54 (42), 39 (24).

Reaction of *i*-PrHgNO$_3$ with 2-Methyl-1,4-naphthoquinone in Presence of $S_2O_8^{2-}$ / Ag^+

2-methyl-1,4-naphthoquione (0.1 mmol), *i*-PrHgNO$_3$ (0.16 mmol) and AgNO$_3$ (0.05 mmol) in 0.5 mL of d_6-Me$_2$SO were deoxygenated by an argon stream. After 5 h, workup provided an 86% yield (by NMR) of 3-iso-propyl-2-methyl-1,4-naphthoquinone. The product gave ^{1}H NMR (90 MHz $CDCl_3$) δ 1.338 (d, J = 7.0 Hz, 6H), 2.188 (s, 3H), 3.270 (septet, J = 7.0 Hz, 1H), 7.678-7.784 (m, 2H), 8.008-8.127 (m, 2H); GCMS m/e (relative intensity) 214 (M^+, 52), 199 (28), 171 (30), 57 (30), 143 (20), 120 (40), 115 (50), 105 (60), 76 (100), 63 (28), 50 (52), 39 (75).

General Procedure for the Chemical Oxidation of RHgX with π Compounds in Presence of $S_2O_8^{2-}$ / NaI or $AgNO_3$

π compounds(0.1-0.2 mmol), RHgCl or $RHgNO_3$(0.1-0.2 mmol) and $S_2O_8^{2-}$/NaI (0.1-0.2 mmol) or $AgNO_3$(0.01-0.03 mmol) in Me_2SO were deoxygenated by an argon stream at room temperature. After 2-20 h, the usual workup afford a crude mixture which was analyzed by GLC, GCMS and NMR. Yield of the products from the reaction of RHgX with α,β-unsaturated ketones, acrylamide, quinones, maleic anhydride, pyridine and PyHI were determined by ^1H NMR or GLC. Identification of the products was confirmed by the ^1H NMR and GCMS spectra of the substitution or addition products as given in Table 4.1, Table 4.2, Table 4.3 and Table 4.4.

Table 4.1: GCMS data for the products of the reaction of *t*-BuHgCl with π compounds in the presence of $S_2O_8^{2-}$/NaI

π Compound	Products	*m/e* (relative intensity)
2-Cyclopentenone	3-*tert*-Butyl-cyclopentanone	140(17), 125(4), 84(36), 57(100).
2-Cyclohexenone	3-*tert*-Butyl-cyclohexanone	154(M^+,20), 98(91), 83(26), 69(30), 57(100), 41(59).
2-Cyclohexenone	3-Norbornyl-cyclohexanone	192(M^+, 10), 149(35), 134(50), 95(100), 79(13), 67(28), 55(15).
Acrylamide	*t*-$BuCH_2CH_2C(O)NH_2$	129.1(M^+, 1.1), 114(25), 100(6.6), 97(14.8), 72(100), 69(20), 57(40), 41(47).
Uracil	6-*tert*-Butyl-5,6-dihydrouracil	170(M^+, 2.2), 153.1(4.4), 114(100), 86(2.6), 70(2.6), 57(39).
5-Fluorouracil	5-Fluoro-6-em tert-butyl-5,6-dihydrouracil	188(M^+, 10), 186(16), 168(32) 153(20), 145(43), 131(37), 126(47), 57(100)

Table 4.2: GCMS data for the products of the reaction of *t*-BuHgCl with quinone in the presence of $S_2O_8^{2-}$/NaI or $S_2O_8^{2-}/Ag^+$

π Compound	Product	m/e (relative intensity)
1,4-Benzoquinone	2-*tert*-Butyl-1,4-benzoquinone	164(M^+, 20), 149(40), 136(20), 121(65), 108(20), 103(10), 93(70), 77(80), 67(40), 54(65), 41(100).
1,4-Benzoquinone	2-Isopropyl-1,4-benzoquinone	150(M^+, 90), 135(28), 122(80), 107(68), 94(28), 82(35), 79(100), 67(20), 54(52), 39(50).
1,4-Benzoquinone	2-Benzyl-1,4-benzoquinone	198(M^+, 100), 181(50), 169(20), 152(15), 141(38), 115(50), 89(20), 65(18), 55(20), 39(20).
1,4-Naphthoquinone	2-*tert*-Butyl-1,4-naphthoquinone	214(M^+, 100), 199(50), 171(40), 160(42), 144(20), 128(55), 115(30), 105(30), 76(65), 57(30), 41(48).
1,4-Naphthoquinone	2-Isopropyl-1,4-naphthoquinone	200(M^+, 100), 185(31), 172(29), 157(54), 144(20), 129(68), 115(20), 105(40), 89(10), 76(82), 64(20), 54(42), 39(24).

Table 4.2 (Continued)

π Compound	Product	m/e (relative intensity)
1,4-Naphthoquinone	2-Cyclopropyl-1,4-naphthoquinone	198(M^+, 100), 181(30), 169(20), 141(50), 127(10), 115(28), 104(49), 76(86), 50(43), 39(30).
2-Methyl-1,4-naphthoquinone	2-Methyl-3-propyl-1,4-naphthoquinone	214(M^+, 52), 199(28), 171(30), 157(30), 143(20), 120(40), 115(50), 105(60), 76(100), 63(28), 50(52), 39(75).
2-Methyl-1,4-naphthoquinone	2-Methyl-3-cyclopropyl-1,4-naphthoquinone	212(M^+, 100), 197(90), 183(25), 169(25), 152(10), 141(30), 128(12), 115(16), 105(48), 76(58), 63(15), 50(25), 39(20).

Table 4.3: GCMS data for the products of the reaction between Ph_2Hg and π compounds in the presence of $S_2O_8^{2-}/Ag^+$

π Compound	Product	m/e (relative intensity)
1,4-Benzoquinone	2-Phenyl-1,4-benzoquinone	184(M^+,60), 156(40), 128(40), 102(45), 82(100), 76(20), 54(70), 39(20).
1,4-Naphthoquinone	2-Phenyl-1,4-naphthoquinone	234(M^+, 28), 206(25), 178(15), 104(70), 76(100), 50(30).
1,4-Naphthoquinone	2,3-Diphenyl-1,4-naphthoquinone	310(M^+, 30), 281(20), 252(10), 104(70), 76(100), 50(50).
2-Methyl-1,4-naphthoquinone	2-Methyl-3-phenyl-1,4-naphtoquinone	248(M^+, 100), 231(45), 219(40), 191(20), 165(10), 115(20), 104(50), 76(50), 50(20).

Table 4.3 (Continued)

π Compound	product	m/e (relative intensity)
Diethyl vinyl-phosphonate	$PhCH_2CH_2P(O)(OEt)_2$	242(M^+, 32), 169(12), 138(100), 111(90), 104(66), 82(52), 77(22).
α-Methylstyrene	$PhCH{=}C(Ph)CH_3$	194(M^+, 52), 179(43), 116(54), 103(100), 91(26), 77(54), 65(16), 51(27).
2-Cyclopentenone	3-Phenyl-2-chloro -cyclopentanone	196(M^++2,32), 194(M^+, 98), 159(100), 141(17), 129(25), 117(72), 105(62), 91(40), 77(48), 64(26), 56(40), 51(52).
Diethyl vinyl-phosphonate	$PhCH_2CH(Cl)P(O)(OEt)_2$	275(M^+−H, 0.19), 241(M−Cl, 100), 185(69), 167(11), 131(28), 103(24), 91(37), 77(19); CI 277.1(M+H, 100), 305 (M+C_2H_5, 17),

Table 4.4: ^{1}H NMR data for the products of the reaction between *t*-BuHgCl and π compounds in presence of $S_2O_8^{2-}$/NaI or Ag^+

π Compound	Product	δ ^{1}H NMR(90 MHz $CDCl_3$)
1,4-Benzoquinone	2-*tert*-Butyl-1,4-benzoquinone	1.264(s, 9H), 6.549(s, 1H), 6.6673(s, 2H).
1,4-Benzoquinone	2-*iso*-Propyl-1,4-benzoquinone	1.07(d, J=7.0 Hz, 6H), 2.89(septet, J=7.0 Hz, 1H), 6.865(s, 1H), 6.844(s, 2H).
1,4-Naphthoquinone	2-*tert*-Butyl-1,4-naphthoquinone	1.376(s, 9H), 6.86(s, 1H), 7.71-7.83(m, 2H), 8.03-8.17(m, 2H).
1,4-Naphthoquinone	2-*iso*-Propyl-1,4-naphthoquinone	1.358(d, J=7.0 Hz, 6H), 3.319(septet, J=3.3 Hz, 1H), 6.760(s, 1H), 7.49-7.71(m, 2H), 7.90-8.10(m, 2H).
Maleic anhydride	2-*tert*-Butyl maleic anhydride	1.344(s, 9H), 6.548(s, 1H).
Acrylamide	$(CH_3)_3C(CH_2)_2C(O)NH_2$	0.910(s, 9H), 1.147-1.589(m, 2H), 2.043-2.200(m, 2H), 5.59(m, 2H, NH_2)
Uracil	6-*tert*-Butyl-5,6-dihydrouracil	0.976(s, 9H), 2.48-2.66(m, 2H), 3.26-3.41(m, 1H), 5.68(s, 1H, NH), 8.069(s, 1H).
Methyl vinyl ketone	$(CH_3)_3C(CH_2)_2C(O)CH_3$	0.872(s, 9H), 1.382(~t, J=8 Hz, 2H), 2.072(s, 3H), 2.362(~t, J=8 Hz, 2H).

GENERAL SUMMARY

Part I of this dissertation presents data on the chemically induced dynamic polarization (CIDNP) proton NMR signals during oxidation of organomercurials. The strong CIDNP multiplet signals(A/E) for RH, R(-H) and R-R were observed from the diffusive encounter of primary, secondary or tertiary alkyl radicals, during the reaction of RHgX with $S_2O_8^{2-}$, $S_2O_8^{2-}/I^-$,or $S_2O_8^{2-}/Ag^+$, involving S_H2 and ET processes. Strong E net polarization effect signals (E/A) for R(-H), were observed from the pair, $\overline{R \bullet\bullet SO_4^-}$, during the reaction of R_2Hg with $S_2O_8^{2-}$, or $HgNO_3$, or during the reaction of RCOOH or RCHO with $S_2O_8^{2-}$ involving electron transfer process.

Part II of this dissertation presents the study of photostimulated free radical chain (reduction) reaction of alkylmercury halides or carboxylates with heteroaromatic compounds such as quinoines, isoquinolines, benzothiazole, pyridine and N,N,N',N'-tetramethyl-p-phenylenediamine.

Solvomecuration products of alkenes ($R^1CH(Y)CH(R^2)HgX$ with Y=HO, RO and X=CH_3CO_2, CF_3CO_2) can be used without isolation for the alkylation reaction.

Part III of this dissertation presents data on alkyl or phenyl radicals, generated from chemical oxidation of RHgX with oxidants, such as $S_2O_8^{2-}$, $S_2O_8^{2-}/I^-$ or $S_2O_8^{2-}/Ag^+$. Reaction of the radicals with organic compounds, such as α, β

unsaturated ketones, diethyl vinylphosphonete, acrylamide, uracil and quinones or heteroaromatic compounds forms addition and substitution products involving free radical chain processes. The species $RHgX^{+\bullet}$ and $R^{\bullet}$ have been probed by MS and ESR techniques, respectively. No evidence has been found in negative ion CI(Ar) mass spectrometry for alkyl $HgX\bullet^{-}$. The 5-hexenyl radical adds to the anion of 2-nitropropane with a rate constant of $\sim 1 \times 10^6$ L/mol-s at 40 °C.

BIBLIOGRAPHY

[1] Bargon, J.; Fischer, H.; Johnsen, U. *Z. Naturforsch.* **1967**, *22a*, 1551.

[2] Ward, H. R.; Lawler, R. G. *J. Am. Chem. Soc.* **1967**, *89*, 5517.

[3] Ward, H. R.; Lawler, R. G.; Marzilli, T. A. *Tetrahedron Lett.* **1970**, 521.

[4] Savin, V. I. *Zh. Org. Khim.* **1978**, *14*, 2090.

[5] Garst, J. F.; Cox, R. H. *J. Am. Chem. Soc.* **1970**, 6389.

[6] Garst, J. F.; Barton, F. E.; Morris, J. I. *J. Am. Chem. Soc.* **1971**, *93*, 4310.

[7] Nugent, W. A.; Bertini, F.; Kochi, J. K. *J. Am. Chem. Soc.* **1974**, *96*, 4945.

[8] Benn, R. *Chem. Phys.* **1976**, *15*, 369.

[9] Lehr, G. F.; Lawler, R. G. *J. Am. Chem. Soc.* **1984**, *106*, 4048.

[10] Kaptein, R.; Van Leevwen, P. W. N. M.; Huis, R. *J. Chem. Soc., Chem. Comm.* **1975**, 568.

[11] Mitchell, T. N. *Tetrahedron Lett.* **1972**, 228.

[12] Beletskaya, I. P.; Rykov, S. V.; Buchachenko, A. L. *Org. Magn. Reson.* **1973**, 595.

[13] Kanter, F. J. J. de *Org. Magn. Reson.* **1967**, *8*, 129.

[14] Van Leeuven, P. W. N. M.; Roobeek, C. F.; Huis, R. *J. Organomet. Chem.* **1977**, *142*, 243.

[15] Closs, G. L. *J. Am. Chem. Soc.* **1969**, *91*, 4552.

[16] Kaptein, R.; Oosterhoff, J. L. *Chem. Phys. Lett.* **1969**, *4*, 195.

[17] Kaptein, R. *J. Am. Chem. Soc.* **1972**, *94*, 6251.

[18] House, D. A. *Chem. Rev.* **1962**, *62*, 185.

[19] Taube, H. *J. Am. Chem. Soc.* **1942**, *64*, 161.

[20] Jensen, F. R.; Rickborn, B. *Electrophilic Substitution of Organomercurials;* McGraw Hill: New York, **1968**.

[21] Ingold, K. U.; Roberts, B. P. *Free-Radical Substitution Reactions;* Wiley-Interscience: New York, **1970**; 29.

[22] Huyser, E. S. *Free-Radical Chain Reactions;* Wiley-Interscience: New York, **1970**; 287.

[23] Fronaens, S.; Ostman, C. O. *Acta Chem. Scand.* **1955**, *9*, 902.

[24] Memming, R. *J. Electrochem. Soc.* **1969**, *116*, 785.

[25] Anderson, J. M.; Kochi, J. K. *J. Org. Chem.* **1970**, *35*, 986.

[26] Charman, H. B.; Hughes, E. D.; Ingold, C. K. *J. Chem. Soc.* **1959**, 2530.

[27] Minisci, F. *Topics Curr. Chem.* **1976**, *62*, 1.

[28] Davies, M. J.; Gilbert, B. C.; Norman, R. O. C. *J. Chem. Soc., Perkin Trans.* II **1985**, 1199.

[29] Breitmaier, E.; Voelter, W. *Carbon-13 NMR Spectroscopy*; VCH: New York, **1987**; 192.

[30] Giese, B. *Radicals in Organic Synthesis Formation of Carbon-Carbon Bonds*; Pergamon Press: Oxford, **1986**.

[31] Russell, G. A.; Hershberger, J.; Owens, K. *J. Am. Chem. Soc.* **1979**, *101*, 1312; *J. Organomet. Chem.* **1982**, *224*, 43.

[32] Kochi, K. J. *Organometallic Mechanisms and Catalysis*; Academic Press: New York, **1978**; 238.

[33] Lowary, T. H.; Richardson, K. S. *Mechanism and Theory in Organic Chemistry*; Harper & Row Publishers: New York, **1984**; 161.

[34] Rossi, R. A.; de Rossi, R. H. *Aromatic Substitution by the $S_{RN}1$ Mechanism*; American Chemical Society: Washington D.C., **1981**; 220.

[35] Kubota, T. *J. Am. Chem. Soc.* **1965**, *87*, 458.

[36] Russell, G. A.; Guo, D.-L.; Khanna, R. K. *J. Org. Chem.* **1985**, *50*, 3423; Russell, G. A.; Guo, D.-L.; Baik, W.; Herron, S. J. *Heterocycles* **1989**, *29*, 143; Russell, G. A.; Khanna, R. K.; Guo, D.-L. *J. Chem. Soc., Chem. Comm.* **1986**, 632.

[37] Ingold, K. U. In *Organic Free Radicals,* ACS Symposium Series, Vol. 69, Pryor, W.S., Ed.; American Chemical Society: Washington, D. C. **1978.**

[38] Carlsson, D. J.; Ingold, K. U. *J. Am. Chem. Soc.* **1968**, *90*, 7047.

[39] Lai, D.; Griller, D.; Husband, S.; Ingold, K. U. *J. Am. Chem. Soc.* **1974**, *96*, 6355.

[40] Espenson, J. H. *Chemical Kinetics and Reaction Mechanisms*; McGraw-Hill: New York, **1981.**

[41] Citterio, A.; Minisci, F.; Franchi, V. *J. Org. Chem.* **1980**, *45*, 4752.

[42] Minisci, F.; Vismara, E.; Fontana, F.; Morini, G.; Serravalle, M.; Giordano, C. *J. Org. Chem.* **1987**, *52*, 730.

[43] Ingold, K. U. In *Free Radicals*; Kochi, J. Ed.; John Wiley and Sons: New York, **1973**; Vol 1, Chapter 2, P93.

[44] Minisci, F.; Vismara, E.; Fontane, F.; Morini, G.; Serravalle, M. *J. Org. Chem.* **1987**, *52*, 730.

[45] Graddon, D. P.; Mondal, J. *J. Organomet. Chem.* **1978**, *160*, 377.

[46] Klopman, G. *Chemical Reactivity and Reaction Paths*; John Wiley : New York, **1974.**

[47] Arnaud, R.; Court, J.; Bonnier, J. M.; Fossey, J. *Nov. J. Chem.* **1980**, *4*, 299.

[48] McLafferty, F. W. *Interpretation of Mass Spectra*; University Science Books: Mill Valley, Calif., **1980**; Table A.3.

[49] Sergeev, Yu. L.; Akipyan, M. E.; Vilesov, F. I. *Opt. Spectrosc.* **1971**, *30*, 121.

[50] Nenner, I.; Schulz, G. J. *J. Chem. Phys.* **1975**, *62*, 1747.

[51] Jordan, F. *J. Am. Chem. Soc.* **1975**, *97*, 3330.

[52] Seeman, J. I.; Chavdavian, C. G.; Kornfild, R. A.; Naworal, D. J. *Tetrahedron* **1985**, *41*, 595.

[53] Kucherov, M. G. *Zh. Russ. Fiz-Khim. Obshch.* **1892**, *24*, 33.

[54] Hofman, K. A.; Sand, J. *Ber. Dt. Chem. Ges.* **1900**, *33*, 1340.

[55] Larock, R. C. *Solvomercuration/Demercuration Reactions in Organic Synthesis*, Springer-Verlag: Heidelberg and New York, **1986**.

[56] Brown, H. C.; Kawakami, J. H.; Ikegami, S. *J. Am. Chem. Soc.* **1967**, *89*, 1526.

[57] Brown, H. C.; Geoghegan, P. *J. Am. Chem. Soc.* **1967**, *89*, 1525.

[58] Bohm, B. A.; Abll, P. T. *Chem. Rev.* **1962**, *62*, 599.

[59] Dowbenko, R. *J. Am. Chem. Soc.* **1965**, *86*, 946.

[60] Dowbenko, R. *Tetrahedron* **1964**, *20*, 1843.

[61] Wilt, J. W. In *Free Radicals*; Kochi, J. Ed.; John Wiley and Sons: New York, **1973**; Vol 1, Chapter 8, P333.

[62] Davies, D. I.; Parrott, M. J. *Free Radicals in Organic Synthesis*; Springer-Verlag: Berlin, Heidelberg and New York, **1978**; 10.

[63] Chamber, V. M. A.; Jackson, W. R.; Young, G. W. *Chem. Commum.* **1970**, 1275.

[64] Wong, P. C.; Griller, D. *J. Org. Chem.* **1981**, *46*, 2327.

[65] Gray, G. A.; Jackson, W. R.; Chambers, V. M. A. *J. Chem. Soc.(C)* **1971**, 200.

[66] Russell, G. A.; Guo, D.-L. *Tetrahedron Lett.* **1984**, *25*, 5239.

[67] Dvorak, V.; Nemec, I.; Zyka, A. J. *Microchem. J.* **1967**, *12*, 324.

[68] Forrester, A. R.; Hay, J. M.; Thomson, R. H. *Organic Chemistry of Stable Free Radicals*; Academic Press: London and New York, **1968**; 225.

[69] Audrews, L. J.; Keefer, R. M. *Molecular Complexes in Organic Chemistry*; Holden-Day: London, **1964**.

[70] Scott, G. *Atmospheric Oxidation and Antioxidants*; Elsevier: Amsterdam, **1965**.

[71] Makarova, L. G.; Nesmeyanov, A. N. *The Organic Compounds of Mercury, Methods of Elemento—Organic Chemistry*; Vol. 4, North Holland Publishing Co.: Amsterdam, **1967**.

[72] Alexander, R. A.; Baenziger, N. C.; Carpenter, C.; Doyle, J. R. *J. Am. Chem. Soc.* **1960**, *82*, 535.

[73] Larock, R. C. *Organomercury Compounds in Organic Synthesis*; Springer-Verlag: Heidelberg and New York, **1985**.

[74] Russell, G. A. *Acc. Chem. Res.* **1989**, *22*, 1.

[75] Giese, B. *Angew. Chem., Int. Ed. Engl.* **1985**, *24*, 553.

[76] Robson, J. H.; Wright, G. *Can. J. Chem.* **1960**, *38*, 1.

[77] Kochi, K. J. *Angew. Chem., Int. Ed. Engl.* **1988**, *27*, 1227.

[78] Baidin, V. N.; Timoshenko, M. M.; Chizhov, Yu. V. *J. Organomet. Chem.* **1985**, *292*, 55.

[79] Bryant, W. F.; Kinstle, T. H. *J. Organomet. Chem.* **1970**, *24*, 573.

[80] Zagorevskii, D. V.; Mikeladze, M. Sh.; Nekrasov, Yu. S.; Rayevsky, N. I.; Sukharev, Yu. N.; Borisov, Yu. A. *J. Organomet. Chem.* **1988**, *348*, 285.

[81] Kilngler, R. J.; Kochi, J. K. *J. Am. Chem. Soc.* **1980**, *102*, 4790.

[82] Fukuzumi, S.; Wong, C. L.; Kochi, J. K. *J. Am. Chem. Soc.* **1980**, *102*, 2928.

[83] Eberson, L. *Adv. Phys. Org. Chem.* **1982**, *18*, 79.

[84] Bolletta, F.; Ciano, M.; Balzani, V.; Serpone, N. *Inorg. Chim. Acta.* **1982**, *62*, 207; Rubinstein, I.; Bard, A. J. *J. Am. Chem. Soc.* **1981**, *103*, 5007.

[85] Brown, H. C.; Kabalka, G. W. *J. Am. Chem Soc.* **1970**, *92*, 712.

[86] Brown, H. C.; Kabalka, G. W. *J. Am. Chem Soc.* **1970**, *94*, 714.

[87] Brown, P. E.; Calvin, M.; Newmark, L. F. *Science* **1966**, *150*, 68.

[88] Jovanovic, S. V.; Simic, M. G. *J. Am. Chem. Soc.* **1986**, *108*, 5968.

[89] Lin, L.-H.; LeBreton, P. R.; Shipman, L. L. *J. Phys. Chem.* **1980**, *84*, 431.

[90] Citterio, A. *Tetrahedron Lett.* **1978**, *39*, 2701.

[91] Jacobsen, N.; Torssell, K. *Ann. Chem.* **1972**, *763*, 135.

[92] Jacobsen, N.; Torssell, K. *Acta Chem. Scand.* **1973**, *9*, 27.

[93] Kabalka, G. W. *J. Organomet. Chem.* **1971**, *33*, C25.

[94] Hosomi, A.; Sakurai, H. *Tetrahedron Lett.* **1977**, 4041.

[95] Hegedus, L. S.; Evans, B. R.; Korte, D. E.; Waterman, E. L.; Sjoberg, K. *J. Am. Chem. Soc.* **1976**, *98*, 3901.

[96] Matnishan, A. A.; Fomin, G. V.; Prut, E. V.; Liogon, B. I.; Berlin, A. A. *Russ. J. Phys. Chem.* **1971**, *45*, 745.

[97] Citterio, A.; Vismara, E.; Bernardi, R. *J. Chem. Res.* **1983**, 88.

[98] Giese, B.; Kretzachmar, G. *Chem. Ber.* **1982**, *115*, 2012.

[99] Funabiki, F. *J. Am. Chem. Soc.* **1986**, *108*, 2921.

[100] Galli, C. *Chem. Rev.* **1988**, *88*, 765.

[101] Rondestvedt, C. S. Jr. *Org. Reactions* **1976**, *24*, 225; Rossi, R. A.; de Rossi, C. H. *Aromatic Substitution by the* $S_{RN}1$ *Mechanism*; ACS Monograph 178; American Chemical Society: Washington, D. C. **1983**.

[102] Bunnett, J. F. *Acc. Chem. Res.* **1978**, *11*, 413.

[103] Kochi, J. K.; Subramaniam, R. V. *J. Am. Chem. Soc.* **1965**, *87*, 1508.

[104] Leake, P. H. *Chem. Rev.* **1956**, *56*, 27.

[105] Kochi, J. K. *J. Am. Chem. Soc.* **1957**, *79*, 2942.

[106] Bolton, R.; Williams, G. H. *Chem. Soc. Rev.* **1986**, *15*, 261.

[107] Williams, G. H. *Homolytic Aromatic Substitution*; Pergamon: London, **1960**.

[108] DeTar, D. F. *J. Am. Chem. Soc.* **1967**, *89*, 4058.

[109] Norman, R. O. C. *Chem. Soc. Rev.* **1979**, *8*, 1.

[110] Taylor, E. C.; Kienzle, F.; Robey, R. L.; McKillop, A.; Hunt, J. D. *J. Am. Chem. Soc.* **1971**, *93*, 4845.

[111] Russell, G. A.; Hershberger, J.; Owens, K. *J. Am. Chem. Soc.* **1979**, *101*, 1312.

[112] Griller, D.; Ingold, K. U. *Acc. Chem. Res.* **1980**, *13*, 317.

[113] Russell, G. A.; Ros, F.; Mudryk, B. *J. Am. Chem. Soc.* **1980**, *102*, 7601.

[114] Singh, P. R.; Khanna, R. K. *Tetrahedron Lett.* **1983**, 1411.

[115] Whitesides, G. M.; San Filippo, J. Jr. *J. Am. Chem. Soc.* **1970**, *92*, 6611; Hill, C. L.; Whitesides, G. M. *J. Am. Chem. Soc.* **1974**, *96*, 870.

[116] Quirk, R. P.; Lea, R. E. *Tetrahedron Lett.* **1974**, 1925.

[117] Barltrop, J. A.; Bradbury, D. *J. Am. Chem. Soc.* **1973**, *95*, 5085. Groves, J. T.; Ma, K. W. *J. Am. Chem. Soc.* **1974**, *96*, 6527.

[118] Chung, S.-K.; Chung, F.-F. *Tetrahedron Lett.* **1979**, 2473; Chung, S.-K. *J. Org. Chem.* **1980**, *45*, 3513; Chung, S.-K.; Filmore, K. L. *J. Chem. Soc., Chem. Commun.* **1983**, 358; Singh, P. R.; Nigam, A.; Khurana, J. M. *Tetrahedron Lett.* **1980**, *21*, 4753; Singh, P. R.; Khurana, J. M.; Nigam, A. *Tetrahedron Lett.* **1981**, *22*, 2901.

ACKNOWLEDGEMENTS

I would like to thank my major professor, Dr. Glen A. Russell, for his guidance, assistance, and financial support given throughout the course of my studies. His kindness and understanding are deeply appreciated.

I am also grateful to all the past and present members of Russell's group, especially Jim Anderson and Mark Nebgen for their friendship and valuable assistance.

I also would like to thank Dr. Wu Hsuech-Chou for his kindness and encouragement to make this degree possible.

Finally, I would like to thank Jialing, my wife, whose contribution to and importance in my life cannot be expressed in words.